Pathways to deeper roots: Anatomical phenes of maize under impedance

Dorien J. Vanhees, Msc.

Thesis submitted to the University of Nottingham
for the degree of Doctor of Philosophy

October 2019

Acknowledgements

First of all I wish to express my gratitude to my supervisory team. I am greatly indebted to Jonathan Lynch for his advice and stimulating discussions over the past years. My sincerest thank you as you helped me to become a better scientist. I also wish to thank Sacha Mooney for introducing me to the fascinating world of soil and guiding me through my PhD. I wish to thank Glyn Bengough and Kenneth Loades for reviewing this work and making suggestions along the way on how to improve it.

I could not have concluded this work without the help of the roots lab at PSU. Therefore I would like to thank Hannah Schneider, Stephanie Klein, Molly Hanlon, Chris Strock, Jimmy Burridge, Anica Sanders, Kemo Jin and last but not least Bob Snyder. These people have shown me the ropes when conducting field trials and helped maintain sanity when things got hard (literally and figuratively).

I can build an extended list of people I met through my PhD that I can now count as my friends. But I would like to express special thanks to Rosie Brian – for always listening and being there for a cup of tea, Heather Sanders – for giving some needed tough love, Hannah Cooper – for always encouraging me and Daisy Dobrijević – for always bringing a smile to my face. Special thanks as well to Emma Hooley, all those PhD students would be nowhere without coffee club, tea break and a good chat.

I would also like to thank my family, who have always supported me whatever I ended up doing. This now includes moving countries and pursuing a PhD. I know I can always count on my sister. I would like to thank my parents especially for believing in me and giving me plentiful opportunities during my life.

Finally I would like to thank John Vaughan-Hirsch, who I met 'in the field' and soon after became my biggest supporter during this PhD. Thank you for all the love and understanding. I could not have done it without you.

Abstract

When roots grow through soil they experience mechanical impedance to varying extents. When levels of mechanical impedance become greater, for instance when soils become compacted or soil moisture decreases, roots can become obstructed. As a consequence the uptake of nutrients and water from the soil reduces, which can reduce plant growth and ultimately negatively impact yield. In this work field trials were conducted at two different field sites (one at the Apache Root Biology Centre in Willcox, Arizona and one at the Russell E. Larson Agricultural Research Center in Rock Springs, Pennsylvania) to study the differential distribution of maize roots following the interaction with a compacted soil profile. In soils with compacted plots the rooting depth of coarse roots was not correlated with coarse root length, which indicated that nodal roots of some genotypes were able to grow under impeding conditions while other genotypes were not capable of growing through impeding conditions. Furthermore genotypes were identified which had similar rooting depths but contrasting coarse root lengths, these genotypes were equally able to reach to deeper depths. The amount of roots formed by the root system therefore does not determine the ability of roots to grow deeper under impeded conditions. Root thickening, a response of roots often seen when submitted to mechanical impedance, varied among genotypes. The same field trial were also used to investigate the role of root anatomy and adaptation to soil mechanical impedance. Root anatomy varied according to genotype and nodal position. Deeper rooting was facilitated by root anatomical phenes such as reduced cortical cell file number in combination with greater middle cortical cell area for node 3 and increased aerenchyma for node 4.

In a separate pot trial the hypothesis that radial expansion was related to the ability of roots to cross a compacted layer in four different genotypes was tested. Radial expansion of roots was mainly attributed to the cortex. Cortical expansion of a single root axis was caused by cellular expansion and not an increase in cell file number. The ability of roots to reach the compacted layer was dependent on the root growth angle. Genotypic variability was present for the ability to cross the compacted layer, and genotypes that did not radially expand in response to

impedance had more roots crossing the layer and reached deeper past the layer. The same genotypes were tested in a hydroponics experiment, which showed that genotypes that did not thicken in response to ethylene were the same as those that were able to overcome impedance.

It can be concluded that radial thickening should be seen as a response to mechanical impedance rather than a positive adaptation. Genotypic variation was related to rooting depth, and anatomical adaptation was more important for thinner than thicker root classes. Understanding the functional utility of root anatomical phenotypes under abiotic stress, such as impedance, is important for the breeding of new crop cultivars with superior adaptation to edaphic stress. Furthermore this work illustrates that root systems are highly adaptive across genotypes but also within an individual plant. The understanding of such adaptability is important, as edaphic stresses such as impedance influence global agriculture.

Publications arising from this work

Vanhees, D.J., Loades, K.W., Bengough, A.G., Mooney, S.J., Lynch, J.P. 2019. The ability of maize roots to grow through compacted soil is not dependent on the amount of roots formed. In preparation.

Vanhees, D.J., Loades, K.W., Bengough, A.G., Mooney, S.J., Lynch, J.P. 2019. Root anatomical traits contribute to deeper rooting of maize (*Zea mays* L.) under compacted field conditions. Under review.

Vanhees, D.J., Schneider, H.M., Loades, K.W., Bengough, A.G., Bennett, M.J., Brown, K.M., Mooney, S.J., Lynch J.P. 2019. Genotypic variation in maize nodal root penetration of a compacted layer is negatively related to impedance and ethylene-induced thickening. In preparation.

Table of contents

Abbreviations and acronyms

1-MCP	1-methylcyclopropene
2D	2 dimensional
3D	3 dimensional
AA	Aerenchyma area
AA/RCSA	Ratio aerenchyma area to root cross sectional area
AA/TCA	Ratio aerenchyma area to total cortical area
AIC	Akaike Information Criterion
ANOVA	Analysis of Variance
ARBC	Apache Root Biology Centre
C	Compacted
CF	Cell file number
CT	Computed Tomography
D_{75}	in Chapter 4: Root depth above which 75% of the total root length is located
D_{75}	in Chapter 5: Root depth above which 75% of the total coarse root length is located
D_{75c}	Root depth above which 75% of the total coarse root length is located
D_{95}	Root depth above which 95% of the total root length is located
D_{95c}	Root depth above which 95% of the total coarse root length is located
FAO	Food and Agriculture Organisation of the United Nations
Fig.	Figure
Figs.	Figures
IN	Cell area – inner cortical region
kV	kilovolts
LAT	Laser Ablation Tomography
MID	Cell area – middle cortical region
MRI	Magnetic resonance imaging
NC	Non-compacted
nonAA	Non-aerenchyma cortical area
NT	Non-thickening
OUT	Cell area – outer cortical region
P_c	Coarse root proportion

P_f	Fine root proportion
PAM	Polyline Analysis Measurements software
PC	Principle component
PCA	Principle component analysis
PSU	Pennsylvania State University
pxls	pixels
RCSA	Root cross sectional area
SE	Standard error
T	Thickening
TCA	Total cortical area
TCA/RCSA	Ratio cortex to root cross sectional area
TCA/TSA	Ratio cortex to stele
TRL	Total root length
TRL_c	Total coarse root length
TRL_f	Total fine root length
TSA	Total stele area
TSA/RCSA	Ratio stele to root cross sectional area
v/v	volume/volume
µA	micro-ampere

List of tables

Chapter 4

Chapter 5

Chapter 6

Supplementary tables

List of figures

Chapter 2

Chapter 3

Chapter 5

Supplementary figures

Chapter 1 – General introduction

Chapter 1 consists of a general introduction that aims to consider the wider context of this thesis. This chapter also provides an overview of the thesis structure including the overarching hypothesis, aims and objectives.

1.1 General introduction

1.1.1 Maize as a major crop

Maize (*Zea mays* L.) is an important crop as, together with wheat and rice, it contributes to 42.5% of the global food calorie supply (FAO, 2016). Conventional hybrid breeding has significantly increased maize yield and quality (Gong *et al.*, 2015) but in order to adjust to specific environments and/or environmental changes in combination with an increase in the global population further advancements need to be made.

1.1.2 Global context

The increase in the world population is predicted to reach 9 billion people as of 2050 (Godfray *et al.*, 2010). The relative production of grain crops has already increased almost three-fold in 2010 versus 1960 (Godfray *et al.*, 2010). By 2050 the demand for cereal crops such as maize, rice and wheat will amount to an estimated 3.3 billion tonnes, which is larger than recent yields (FAO, 2016). Clearly a further increase in crop production will be needed to sustain the demand for food. Additionally climate change is already occurring and is projected to intensify (Padgham, 2009) and has detrimental effects on crop production. Between 1980 and 2008 maize achieved 3.8% less yield worldwide due to climate change compared to if the climate would have remained stable during that period (Lobell *et al.*, 2011). Adaptation of crops is needed as yields are likely to suffer from further temperature increases, water shortages, more pests and diseases, and a plethora of other climate change driven effects (FAO, 2016). There is an urgent need for improved crops and varieties adapted to adverse stresses, with higher yield potentials.

1.1.2.1 Better root systems for food security

Many plant breeding efforts have focussed on shoot traits but root traits cannot be ignored. Plant roots have a multitude of functions, for example they anchor the plant in the ground and forage for water and nutrients. Both root architectural, as well as root anatomical traits have been proven to contribute to maize yields. For instance, low crown root number had greater relative grain yield then high crown root number genotypes under low N conditions (Saengwilai *et al.*, 2014a). Relevant examples of the effect of root anatomy are greater yields achieved under water stress by genotypes that had lower cortical cell file number or larger cortical cell size (Chimungu *et al.*, 2014a, 2014b) or that roots with reduced living cortical area improve yield (Galindo-Castañeda *et al.*, 2018). Root anatomical phenes, i.e. the specific root traits that constitute a phenotype, that contribute to growth under stress conditions have been underexplored. Furthermore these phenes can be integrated in a root ideotype and linked to certain soil environments. For instance the steep, cheap and deep ideotype for maize incorporates architectural, anatomical and physiological phenes in order to optimize root growth for acquisition of water and nitrogen (Lynch, 2013). Other ideotypes exist for topsoil foraging of roots for P (Lynch and Brown, 2001) or an intermediate response for roots in quest for K (White *et al.*, 2013). Plants can therefore be specifically selected according to their root ideotype.

1.1.2.2 Impedance as a global issue

The soil physical environment experienced by roots can also limit their growth. Impedance is the mechanical stress imposed on a root *(*Bennie, *1996;* Whalley *et al.,* 2005) and will slow root growth, resulting in reduced elongation rates which can result in reduced soil exploration and plant growth (Rich and Watt, 2013).

Soil drying can cause impedance as the soil strength increases with decreasing water content in the soil (Gao *et al.*, 2012; Whalley *et al.*, 2005). Roots also experience higher levels of impedance deeper down the soil profile due to overburden pressure (Sands *et al.*, 1979). Another cause of increased levels of mechanical impedance can be due to compaction, or the densification of soils.

Denser subsoil and their associated subsoil constraints can occur naturally, such as poorly structured clay subsoils or alkaline duplex soils (Adcock *et al.*, 2007) or hard-setting soils found in Australia (Mullins *et al.*, 1987). On the other hand, compaction can be human-derived by the use of heavy traffic vehicles or the introduction of plough pans due to tillage (Tracy *et al.*, 2011). Globally 68 million hectares of arable land are estimated to be compacted (Oldeman *et al.*, 1991), half of which can be found in Europe (van Ouwerkerk and Soane, 1994).

One needs to carefully distinguish between different stresses associated with impedance. Impedance due to soil drying might coincide with drought stress, while impedance due to denser soil might occur simultaneously with waterlogging or hypoxic soil conditions. In this thesis mechanical impedance was applied to the root system by soil compaction, not drought.

1.2 Aims and objectives of this thesis

The aim of this research was to investigate how different root system phenes respond to impedance through the application of compacted soil. This project used the combination of different imaging techniques such as Laser Ablation Tomography (LAT), confocal microscopy in combination with X-ray Computed Tomography (CT) scanning in different test settings (field and pot studies). Further multiple contrasting genotypes were included to assess genotypic diversity on different scales from root system distribution down to the anatomical level.

The project aimed to address the following overarching research questions:

- Which are the most successful growing strategies used by roots to grow under impeded conditions in the field? (**Chapter 4 and 5**)
- Are there genotypic differences in the ability of maize to grow and overcome impeded conditions? (**Chapter 4, 5 and 6**)
- Can anatomical phenes that contribute to deeper rooting be identified? (**Chapter 5 and 6**)
- Are there nodal differences in the reaction to impeded conditions? (**Chapter 5 and 6**)

- ❖ Is ethylene involved in the root thickening process? (**Chapter 6**)

Each of the experimental chapters will put forward its own more detailed hypothesis and research questions.

In order to answer these questions the following different research objectives were to:

1. Establish successful field trials in different environments, including different genotypes with the aim of assessing root system distribution and size under compacted versus non-compacted conditions.
2. Use field data to evaluate which anatomical traits are related to deeper rooting in order to identify new phenes.
3. Conduct a X-ray CT experiment via a pot trial including a compacted soil layer in order to assess the change in anatomy on a single root axis encountering a denser soil layer and potentially link it to ethylene.
4. To investigate if there are nodal differences in root anatomy.

1.3 Thesis structure

The experimental chapters featured in these thesis are presented in a 'paper format'. This means these experimental chapters are either submitted papers or presented as papers in preparation for submission. Each paper/experimental chapter contains all the associated information relevant for the experiments conducted within that paper/chapter. The other chapters follow a more traditional thesis structure.

Chapter 1 gives a short overview of the research topic and places it in a wider context. This chapter also provides an overview of the research questions, aims and objectives of the thesis. The thesis structure is also presented. **Chapter 2** is a more extensive literature review and presented as a traditional thesis chapter. This chapter will review the current stage of research regarding the research questions listed above. **Chapter 3** describes the experimental methods that were not presented in the submitted paper or papers in preparation. **Chapter 4** describes a field experiment conducted to assess different growing strategies of

root systems under compacted versus non-compacted conditions. The relationship between root depth and root length will be explored as to build a theory around root system size and root penetration ability. This work is in preparation for submission to *Field Crops Research* and is presented in 'paper format'. **Chapter 5** investigates which anatomical traits contribute to the deeper rooting of maize under compacted field conditions. Differences between nodal anatomy were also investigated. This chapter is presented in 'paper format' and is currently under review at the *Journal of Experimental Botany*. **Chapter 6** assesses the anatomical changes of root axis of different genotypes encountering a denser soil layer and links it to the plant hormone ethylene. This chapter is presented in 'paper format' and is in preparation for submission to *Plant, Cell and Environment*. **Chapter 7** offers a general discussion of the key results and findings and suggests further work for research continuation. This chapter is presented as a traditional thesis chapter.

Chapter 2 – Literature review

Chapter 2 is a detailed literature review and presented as a traditional thesis chapter.

2.1 What is impedance?

Mechanical impedance is the physical resistance a plant root experiences when growing through soil (Bennie, 1996; Whalley *et al.*, 2005). It is dependent on the physical state of the soil as water content, soil texture, bulk density, soil depth all influence resistance to penetration (Aggarwal *et al.*, 2006; Gao *et al.*, 2012; Lin *et al.*, 2016). For most soils, soil strength increases with decreasing soil moisture, thereby increasing mechanical impedance (Whalley *et al.*, 2005). Soil compaction increases mechanical impedance by increasing soil bulk density while reducing porosity and pore connectivity (Chen *et al.*, 2014b; Kuncoro *et al.*, 2014). Thus, soil compaction also increases the risk of hypoxia by reducing hydraulic conductivity and air permeability (Bengough *et al.*, 2006; Chen *et al.*, 2014b; Laboski *et al.*, 1998; Simojoki *et al.*, 1991). Generally accepted limits of penetration resistance and air filled porosity that limit root growth are shown in Fig. 2.1. Soil bulk density, and hence impedance, generally increase with depth (Merotto and Mundstock, 1999; Whalley *et al*., 2008). Deeper rooting crops therefore will be affected more readily by impedance.

Furthermore, soils are rarely uniform and mechanical impedance is typically highly variable throughout the soil profile (Clark *et al.*, 2003; Usowicz and Lipiec, 2017). One example is the occurrence of a plough pan, which can arise when soil is compacted at the ploughing depth beneath the plough furrow (Gao *et al.*, 2016). Plough pans will cause roots to experience a sudden change in impedance when encountered (Whalley *et al*., 2008). Mechanical impedance can also be present at different spatial scales. As soil structure is non-uniform (Jin *et al*., 2013) roots will often encounter different soil structures, aggregate sizes and shapes. Roots that penetrate a soil clod (Konôpka *et al*., 2009) or biopore wall (Helliwell *et al*., 2019) will have to overcome greater levels of impedance. The interactions with stones

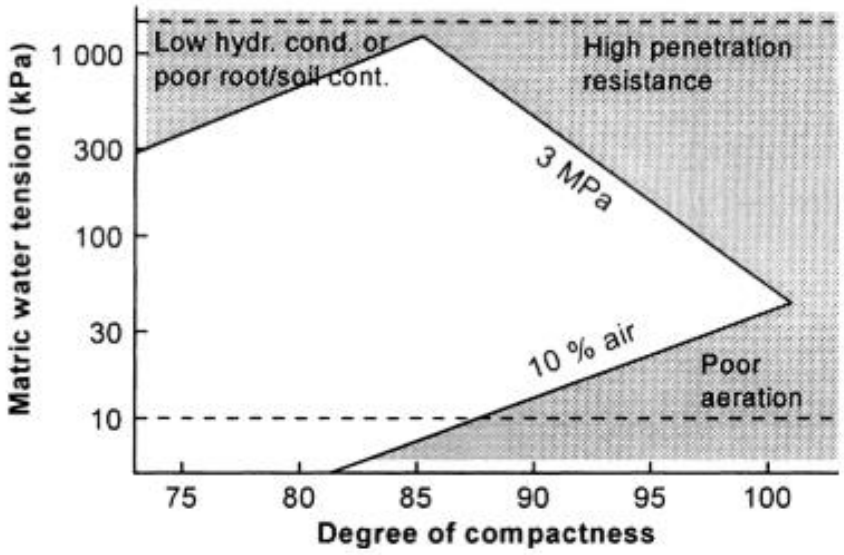

Figure 2.1 – Diagram illustrating the relationship of soil compactness and matric water tension (kPa) with air filled porosity level of 10% (v/v) and a penetration resistance of 3 MPa as critical limits to plant growth. Growth is only considered possible in the centre white area of the graph (Håkansson and Lipiec, 2000)

makes maize roots react as if mechanically impeded (Babalola and Lal, 1977). In addition mechanical impedance does not only vary spatially but also with time (Whalley *et al*., 2008). Under field conditions levels of mechanical impedance will vary depending on soil moisture content which itself is dependent on other factors such as rainfall (Martino and Shaykewich, 2011) and the depth of the water table (Rizzo *et al.*, 2018) which are highly variable not just year to year but also within a growing season. This illustrates that impedance is not just spatial but also temporal.

2.2 The effect of impedance on the root system of maize

Penetration resistance is used as a measure of mechanical impedance and is negatively correlated with root growth (Bengough and Mullins, 1991). Different levels of penetration resistance have been identified to limit root growth. Wheat grown at soil strength of 3.5 MPa became impeded with shoot growth severely affected at a soil strength of 5.5 MPa (Merotto and Mundstock, 1999). Passioura (2002) states that root growth is affected at resistances as low as 1 MPa with growth linearly declining up to 5 MPa, resistance beyond which no root growth is possible. Adcock *et al*. (2007) claim that root growth of annual crops is reduced

by more than 50% (dependent on species, soil type and temperature) between soil strengths of between 1.6 and 2.5 MPa. Species dependent variability in penetrating physically limiting soils is widespread with some species, such as peanuts, continuing to grow at penetrometer resistances of up to 6 MPa (Atwell, 1993).

Impedance has a major impact on root development, influences root architecture, morphology, and anatomy and can lead to a reduction in yield. Root phenotypes of various species or genotypes within a species change in different ways under compaction and multiple traits can be affected simultaneously.

2.2.1 The maize root system

Many classification systems, and nomenclature, exists to distinguish between root classes dependent on taxa (monocot versus dicot) or can be based on the time of emergence (embryonic versus postembryonic) (Atkinson *et al.*, 2014). In this thesis the following classification between root classes has been made (Fig. 2.2): the maize root system consists of primary, seminal, nodal roots and their laterals. Nodal roots can either be formed belowground (referred to as crown roots) or aboveground (referred to as brace roots). Nodal roots are acropetally ordered with all classes forming lateral roots. Root elongation rates have been found to differ between different root classes of maize; Cahn *et al.* (1989) found that laterals elongate at a rate of 2.2 cm day^{-1} and stopped elongating after 2.5 days, while nodal roots elongated faster (3.2 cm day^{-1}) for the duration of the experiment, 5 weeks. Veen and Boone (1990) found elongation rates of primary and seminal roots were 4.8 and 3.2 cm day^{-1} respectively.

Differential effects of impedance exist for the different root classes. Overall, axial root growth is inhibited in wheat (Coelho Filho *et al.*, 2013), triticale (Grzesiak *et al.,* 2013) and maize (Grzesiak *et al.*, 2013; Panayiotopoulos *et al.*, 1994) under compaction. In contrast, increased production of lateral roots in response to strong soil has been observed in tomato (*Solanum lycopersicum*) (Tracy *et al.*, 2012). Loades *et al*. (2013) found reduced seminal root length under compaction, while nodal and lateral roots had non-distinguishable lengths for 21 day old plants. Bingham and Bengough (2003) found that spring barley lateral roots were

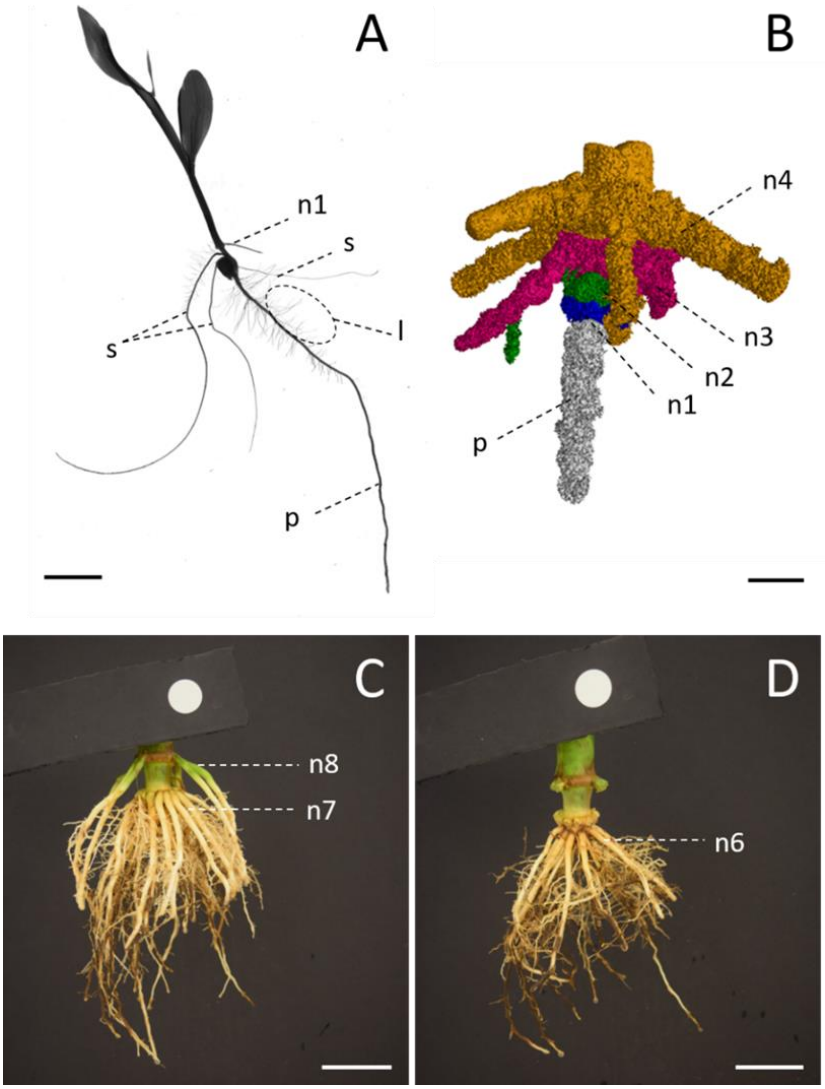

Figure 2.2 – The maize root system visualised at different growth stages and with different techniques. (A) A 5-day old maize seedling scanned on a flatbed scanner with winRHIZO software. Scale bar at 2.5 cm. (B) A segmentation result obtained from an X-ray CT scan of a 30-day old maize crown for visualising the different nodes. Scale bar at 0.5 cm. (C) A picture of a 60-day old root crown with brace roots that emerged above ground. Scale bar at 5 cm. (D) The same root crown as visualised in panel C, but with excised brace roots to uncover the crown roots. Scale bar at 5 cm. The different root classes are p – primary root, s – seminal roots, l – lateral roots, n-nodal roots followed with the number indicating the nodal position

affected less than nodal roots in compacted soil. The latter was attributed to the accessibility of small pores by lateral roots which are smaller in diameter. When laterals roots become sufficiently impeded, for instance if these pores become smaller, or disappear altogether, lateral root length density has been observed to

decrease (Goss, 1977). Ideally biopores should be part of a continuous network so that roots can continuously follow them (Gregory, 2006; Tracy *et al.*, 2011) and have an ideal size, close to their root diameter, in order to facilitate root growth. For instance barley roots growing in pores that are too large, will have reduced root soil contact in comparison to growing in narrower biopores, or pores filled with peat (Stirzaker *et al.*, 1996). In contrast if a biopore is too narrow, the root will need to displace soil particles during growth (Jin *et al.*, 2017; Bengough and Mullins, 1990; Vollsnes *et al.*, 2010).

2.2.2 The effect of impedance on root distributions

Root distribution affects nutrient and water capture in both time and space. As root systems grow, they explore increasingly more of the soil allowing greater access to resources for the plant. Spatially, root system distribution differs among architectural ideotypes which have been proven to forage for nutrients and water in different ways. For instance, topsoil foraging root systems are able to put their roots in the upper soil strata, which is beneficial under low phosphorus conditions (Lynch, 2011). On the other hand, deeper rooting ideotypes are able to extract water from the subsoil, which is beneficial under drought (Lynch and Wojciechowski, 2015). The effect of mechanical impedance can result in both reduced total root length as well as different root distributions through the soil profile (Pfeifer *et al.* 2014a; Shierlaw and Alston, 1984). When root growth is physically hindered, root elongation and rooting depth are reduced (see 2.2.3 and 2.2.4).

Root systems can compensate for loss of root length due to mechanical impedance by increasing growth in lesser impeded soil regions (Pfeifer *et al.*, 2014a). As such, compensatory root growth can introduce altered root distributions under impeded conditions. Compensatory root growth has been observed on soybean encountering a plough pan (Dong *et al.*, 2017), winter wheat grown in a soil with subsoil pan (Barraclough and Weir, 1988), barley planted in vertically split pots or split-root chambers (Bingham and Bengough, 2003; Pfeifer *et al.*, 2014a), broccoli studied in layered pot systems (Montagu *et al.*, 2001) or ryegrass with a mesh screen (Scholefield and Hall, 1985). Increased root length

density in lesser impeded soil regions could stimulate resource competition between roots which is estimated to occur at root length densities of 0.1 to 2 cm cm^{-3} (Postma and Lynch, 2012; Yamaguchi and Tanaka, 199; Ge *et al.*, 2000; Rubio *et al.*, 2001) with shallow rooting introducing greater levels of inter-plant competition (Rubio *et al.*, 2001).

Root branching densities can become altered under impedance. This has been illustrated by Goss (1977) on barley grown in ballotini where, irrespective of pore size, laterals emerged closer to the root tip when experiencing 50 kPa of applied pressure. Laterals did not just move closer to the tip in this study, they also extended further when they could grow without experiencing impedance. As such lateral root length is part of compensatory growth (discussed earlier). As laterals have smaller diameters than the main root axis they emerge from, they could explore the smaller pore structure of a compacted medium (also see 2.2.1).

2.2.3 Root elongation is reduced by impedance

Mechanical impedance retards root elongation (Fig. 2.3) (Bengough and Mullins, 1991; Croser *et al.*, 2000; Materechera *et al.*, 1991, Schmidt *et al.*, 2013) with energy costs associated with root elongation increasing with greater penetration resistances (Colombi *et al.*, 2019). Generally mechanical impedance greater than 2 MPa is considered to reduce the root elongation of most species by 50% (Atwell, 1993) but should not be considered a threshold value (Whitmore and Whalley, 2009). For maize, elongation rates slow to 10% of the elongation rate in non-impeded conditions when penetration resistance increased from 1 MPa to 2MPa in a sandy loam soil (Fig. 2.3) (Schmidt *et al.*, 2013). Reduced elongation rates imply reduced root length as observed for fine tobacco roots (diameter classes smaller than 0.5 mm) growing in compacted soil (Alameda *et al.*, 2012). Increased penetration resistance (from 0.90 MPa to 2.24 MPa) reduced root length by more than 50% for barley, rye, wheat, maize and triticale (Lipiec *et al*., 2012).

Root elongation is dependent on soil conditions. Soils are characterised by a certain texture, ranging from fine and medium textures soils such as clays, clay loam, silty clay and clay loams to coarse sandy soils (White, 2006). Different soil textures can introduce differences in elongation rates with roots elongating faster

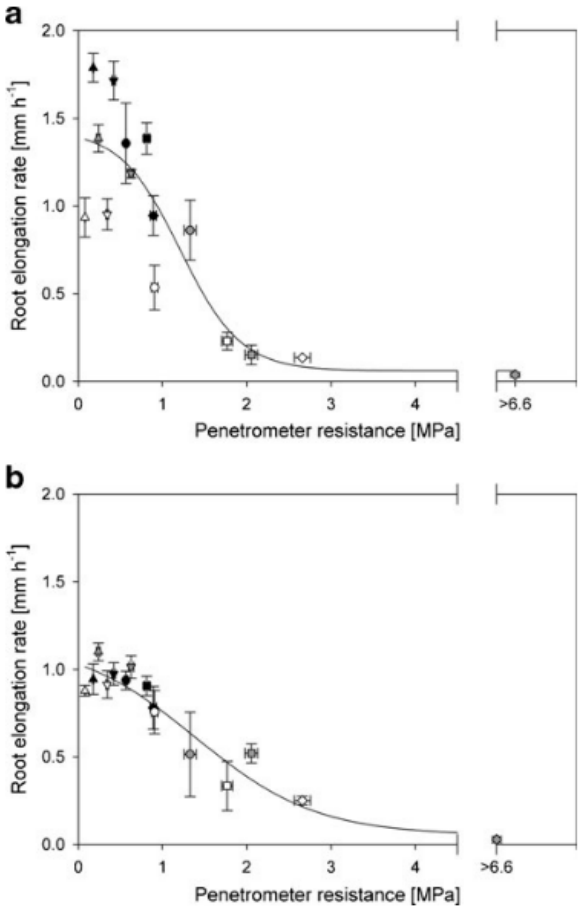

Figure 2.3 – Root elongation rates of (a) maize and (b) lupin over a 96 hour period in a sandy loam soil packed to different bulk densities of 1.1 (▲), 1.2 (▼), 1.3 (●), 1.4 (■) and 1.5 (◆) g cm^{-3} at matric potentials of -0.01 MPa (closed symbols), -0.4 MPa (grey symbols) and -1.2 MPa (open symbols). Mean data (n=5) with standard error. A sigmoidal curve was fit ($f=y_0+a/(1+\exp(-(x-x_0/b))$). r^2 values were 0.67 ($p<0.001$) and 0.81 ($p<0.001$) for maize and lupin respectively (Schmidt *et al.*, 2013)

in soils with finer soil texture (Kirby and Bengough, 2002; Tracy *et al.*, 2013). Coarser soils, with greater sand fractions, expand less and therefor hinder root elongation more than finer soil textures (Batey and McKenzie, 2006). Furthermore, better root-soil contact of finer textured soil will improve root elongation as long as soil strength does not limit root elongation (Schmidt, 2011). Soil structure will also be of influence, as illustrated by Valentine *et al.* (2012), who found there is a strong correlation between the volume of large pores (6 - 600µm) and root elongation. Artificial macropores in pot experiments with high and low bulk densities have shown that shoot dry weight increases when artificial pores are introduced under high bulk densities (Colombi *et al.*, 2017a). Thus, the

presence of pores can positively influence elongation rates as pores can (1) offer an alternative route of less resistance to roots exploring the soil and/or (2) reduce hypoxic conditions which can reduce elongation rates (Valentine *et al.*, 2012).

2.2.4 Reduced rooting depths under mechanical impedance

Mechanical impedance can constrain the maximum rooting depth in various ways. Roots can be become spatially obstructed by a plough pan (as mentioned earlier), where levels of impedance become so high that roots are unable to penetrate through and reach deeper (Batey, 2009; Laboski *et al*., 1998). Or greater levels of impedance throughout the soil profile can slow down root proliferation. Roots are still able to grow through the soil but at a reduced elongation rate.

Reduced elongation rates as well as altered root distribution can lead to differences in rooting depth. Root systems that are capable of growing deeper are better adapted to drought with rooting depth linked to water acquisition (Gao and Lynch, 2016; Hund *et al*., 2009; Lynch, 2013, 2018; Chimungu *et al*., 2014a; 2014b; Zhan *et al*., 2015). The effects of drought get more severe when compaction is present (Grzesiak *et al*., 2014). When compensatory growth occurs in the upper region within compacted soil, penetration resistance can further increase due to water uptake by roots, in turn reducing root access to the deeper soil strata more (Colombi *et al*., 2018). The ability of a root system to maintain its elongation rate and growth through impeded conditions will maintain water and nutrient uptake in comparison to non-impeded conditions.

2.2.5 Non-anatomical root phenes that contribute to growth under impeded conditions

2.2.5.1 Root angle

Roots with greater angles from the horizonal plane will penetrate deeper, more easily, if able to overcome impedance. Root angle becomes steeper with each subsequent node for maize (Araki *et al*., 2000; Tardieu and Pellerin, 1990), which means that with each nodal tier roots will encounter impeding conditions more

easily. Intrinsic relationships exist between rooting angle under impeded conditions. For instance root growth angle of triticale has been observed to decrease by 15-30° becoming shallower within compacted soil (Colombi and Walter, 2016). Primary lateral roots of narrow-leaved lupin can grow more horizontally and even slightly upward in the topsoil when a hard layer (20-30 cm) and hardpan (> 30 cm) were present (Chen *et al*., 2014b). Root angle when encountering a strong soil layer also plays a role. Steeper angles could be beneficial to plants growing through compacted soil (Jin *et al*., 2013). The proportion of wheat roots penetrating a strong medium from a weaker medium is dependent on media strength and root angle, with a steeper angle of incidence allowing improved capability in penetrating the stronger medium (Dexter and Hewitt, 1978).

2.2.5.2 Root tip shape

Root tip geometry influences soil deformation ahead of the root tip. Blunting of root tips, by removal of the root cap, slows down root elongation in maize and increases the root diameter and penetration resistance of the decapped roots when grown in compacted soil (Iijima *et al*., 2003b). To accommodate axial extension of roots in bulk soil or when pores are too small, roots must be capable of displacing the soil locally. At the forefront of decapped roots, this will cause a local maximum density, while capped roots distribute the local displacement of soil around their root tip (Vollsnes *et al*., 2010). Colombi *et al*. (2017b) shows genotypic variability for root tip shape of wheat (considered as the whole of the apex with the cap) correlates with root elongation rates under increased soil strengths. Root tips with small radius to length ratio had increased elongation rates in medium and high bulk densities.

2.2.5.3 Mucilage and cell sloughing

The outer two cell layers of the root cap produce mucilage, a polysaccharide solution which retains water, facilitates the root passage through soil and plays a role in soil aggregation through its adhesive characteristics (Gregory, 2006; McCully, 1999). The frictional component and external pressure imposed by mechanical impedance can be decreased by the amount of mucilage produced at

the root tip. Root cap width decreases due to the formation of lesser and shorter cells for maize grown in compacted conditions. The resulting smaller root cap facilitates an increase in the cell division rate in the cap meristem, making it possible for the entire cap to be covered by a layer of loosened sloughed border cells (103% coverage in compaction versus 11% coverage in non-compacted conditions), increasing the release of cells into the direct environment of the root by 49% (Iijima *et al*., 2000, 2003a). Mucilage in combination with a greater amount of sloughed border cells form a low-friction sleeve around the root cap (Bengough and McKenzie, 1997; Iijima *et al*., 2000, 2003b, 2004). Mucilage and cell sloughing characteristics are species specific. Lupin roots are enclosed with filaments of border-like cells and mucilage accumulates around the flanks of the roots, whilst maize mucilage is only found locally at the tip of a root, potentially making lupin roots better at overcoming resistance in comparison to maize (Schmidt *et al*., 2013).

2.2.5.4 Root hairs

Root hairs can improve root penetrability under impeded conditions. Barley genotypes lacking root hairs had lower percentages of seminal roots penetrating higher bulk density soil layers in comparison with genotypes that had root hairs which resulted in an overall reduced seminal root length (Haling *et al*., 2013). Experiments with hairless maize mutants identified that the presence of root hairs facilitated improved penetration in loose soils (1.0-1.2 g cm^{-3}) due to improvements in root anchorage. However, for denser soil (1.5 g cm^{-3}) increased anchorage was no longer sufficient in improving penetrability (Bengough *et al*., 2016). Barley roots exhibited reduced root hair length when grown at greater soil strength (> 1.43 MPa) or when in wetter soil (4% versus 6% v/v) (Haling *et al*., 2014). This shows that the relationships between root hairs and root penetrability is not explicit but also dependent on soil conditions.

2.2.6 Root thickening

Root thickening is often observed under impedance for different species (Atwell, 1993; Colombi and Walter, 2016; Iijima *et al*., 2000; Pfeifer *et al*., 2014a; Pritchard, 1994; Tracy *et al*., 2012; Alameda *et al*., 2012, Croser *et al*., 2000).

Diameter increases of 30-120% have been reported for various plant species at high penetration resistances (4.2 MPa) (Materechera *et al*., 1991). A more moderate increase in bulk density (1.3 to 1.45 g/m^3, corresponding with an increase of 0.34 MPa to 0.44 MPa) caused wheat seedlings to increase their diameters by 16%, while a more pronounced shift in bulk density (1.3 to 1.6 g/cm^3, corresponding with 0.34 MPa to 1.06 MPa) made diameters increase by 44 % (Colombi *et al*., 2017b).

Soil texture influences root thickening. Kirby and Bengough (2002) observed pea roots (*Pisum sativum)*, grown in a sandy loam soil, increase their diameter by 60% when grown at a mechanical impedance of 2 MPa versus the reference diameter at 0.7 MPa. Smaller increases in diameter were observed in clay loam soil packed to similar bulk densities, illustrating the importance of soil type on the stress response (Fig. 2.4).

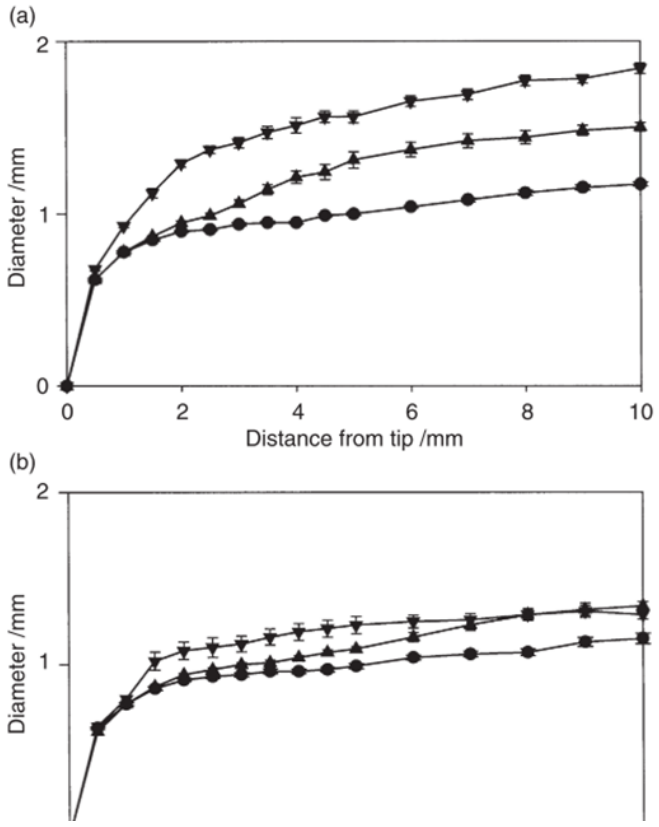

Figure 2.4 – Mean diameter and standard errors for pea roots grown in (a) sandy loam and (b) clay loam soil. Bulk densities are 1.4 (●), 1.5 (▲) and 1.6 (▼) g cm^{-3} for sandy loam and 1.3 (●), 1.4 (▲) and 1.5 (▼) g cm^{-3} for clay loam (Kirby and Bengough, 2002)

Root thickening can relieve stress from the root tip while being able to deform the soil and facilitate further penetration (Atwell, 1993; Bengough *et al*., 2006; Gregory, 2006; Hettiaratchi, 1990; Kirby and Bengough, 2002; Pritchard, 1994). Thicker roots have been suggested to reduce buckling (Chimungu *et al*., 2015a; Clark *et al*., 2003). Root diameters increase immediately behind the root tip. Impeded roots diameter continues increasing in diameter for a longer distance behind a root tip compared to an unimpeded root (Bengough *et al*., 1997, Kirby and Bengough, 2002) (Fig. 2.4). Under impeded conditions the elongation zone becomes shorter and moves closer to the root tip (Croser *et al*., 1999; Bengough *et al*., 2006) which can reduce the friction on this zone (Atwell, 1993). Root thickening coincides with reduction of elongation rate (see 2.2.3), due to reduced cell lengths and a reduced cell production from the meristem (see 2.3.4). Radial expansion is related to anatomical changes which are discussed in the next section.

2.3 Root anatomy under impedance

Root anatomical traits refer to cell and tissue organisation within a root (Lynch, 1995) and differs among plant species. A schematic organisation of maize root anatomy can be found in Fig. 2.5. Within a species, root anatomy can vary from root to root, along the axis of an individual root and with root age (Colombi and Walter, 2016; Gregory, 2006, Yang *et al*., 2019).

2.3.1 The effect of impedance on the anatomy of the root tip

The stresses a growing root needs to endure are concentrated around the root tip and root cap (Kirby and Bengough, 2002). The root cap protects the root tip against mechanical damage and senses the immediate soil environment when growing through soil (Gregory, 2006; Iijima *et al*., 2003b). Maize has a closed meristem which under mechanical impedance changes to an open type meristem, which could induce cell pattern changes (Iijima *et al*., 2003b; Potocka *et al*., 2011). What the changes to meristematic tissue mean are still unclear, one hypothesis is that it could be that they are part of a stress sensing mechanism or they could be related to the further differentiation of cell layers higher up the root. Another

effect of impedance is the reduction of cell division within the meristem (Clark *et al*., 2003) which could contribute to the reduced root elongation rates.

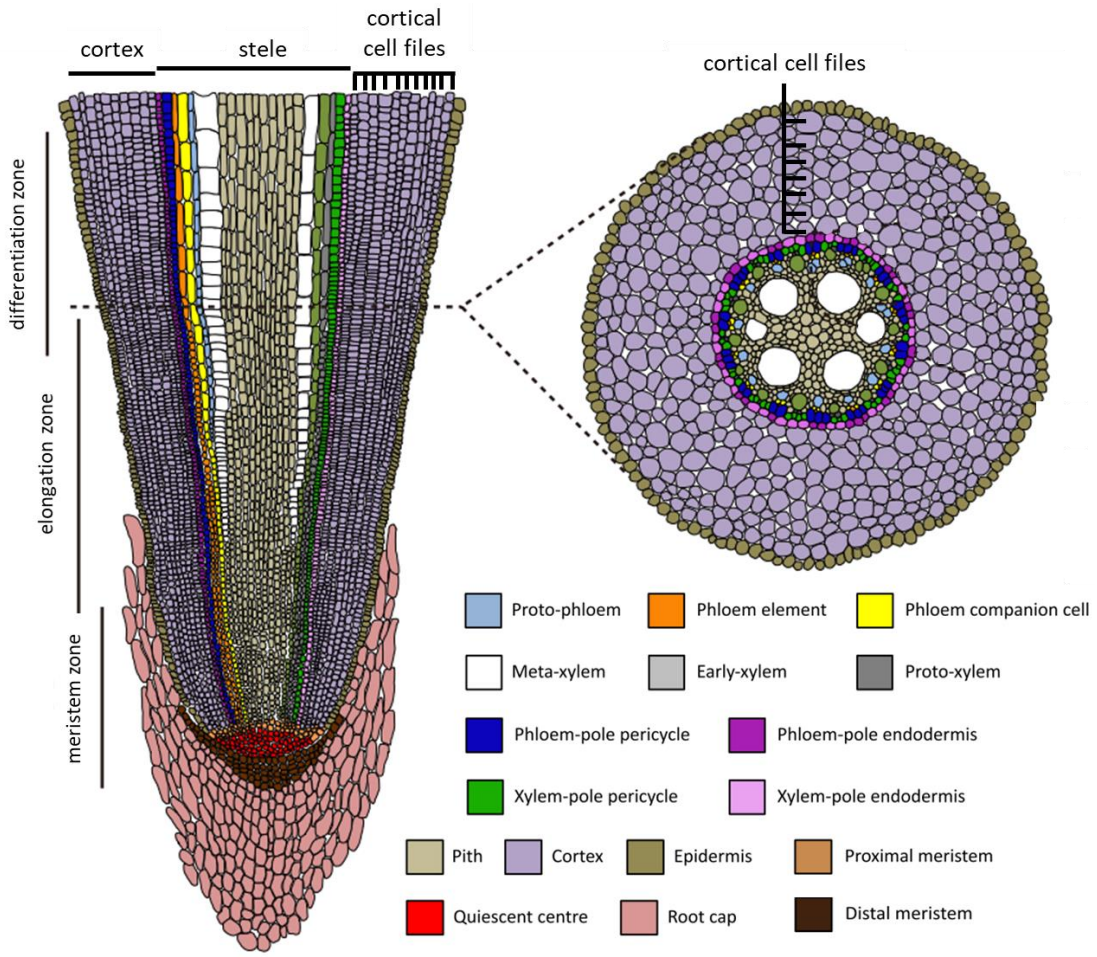

Figure 2.5 – Illustration of maize root anatomy for a longitudinal and transversal plane. The different cell types are color-coded as indicated in the key. Illustration adapted from Yu *et al.* (2016).

2.3.2 The effect of impedance on the root elongation zone

Root elongation happens in the elongation zone of the root, which is about 5-12 mm long under unimpeded conditions but becomes shorter and shifts towards the root tip when the roots are impeded (Atwell, 1990, 1993). When elongation halts, the maturation zone will move closer towards the root tip (McCully, 1999).

Cell wall characteristics and microfibrils orientation change under compaction (Veen, 1982). A change to transversely oriented microfibrils is induced by cellulase, of which the activity is upregulated by ethylene (He *et al*., 1996a),

making it possible for cells to radially expand (Kawai *et al*, 1998). Ethylene production itself is upregulated when roots experience mechanical impedance (Moss *et al*., 1988; Sarquis *et al*., 1991), ethylene reduces the root elongation rate (Sarquis *et al.,* 1991). One hypothesis that remains to be investigated is that through cellulase, ethylene could stimulate an increase in root diameter.

2.3.3 The effect of impedance on stele anatomy

Contrasting observations have been made for the anatomy of the stele under impeding conditions. Increased stele area was recorded for primary roots of maize, barley, rye, and triticale, while stele dimensions decreased for wheat under impeded conditions (Lipiec *et al*., 2012). Atwell (1990) found that the dimensions of the stele of wheat remained stable when mechanically impeded. In a study on barley, observed stele diameters were greater nearer to the root tip (< 1 mm from the tip) under impedance, but at a distance of 40 mm from the root tip stele diameters were similar to those observed in unimpeded roots (Wilson *et al*., 1977). More recently, Colombi *et al*. (2017b) reported that in wheat, stele cross-sectional areas increased under soil compaction for embryonic roots, while stele cross-sectional area for post-embryonic roots decreased. However Colombi and Walter (2016) found that stele dimensions of triticale remained constant under compacted versus control conditions. Alameda *et al*. (2012) found that xylem traits of tobacco such as vessel cross-sectional area, vessel frequency and mean radius of xylem vessels were not changed significantly under impeding conditions.

2.3.4 The effect of impedance on cortical anatomy

The cortical area increases for wheat, triticale, barley, rye, pea, cotton and maize under impedance (Colombi and Walter, 2016; Iijima *et al*., 2007; Lipiec *et al*., 2012). This is due to either an increase in cortical cell area (Atwell, 1988; Hanbury and Atwell, 2005; Veen, 1982), an increase in cell file number (Croser, 1999; Wilson *et al*., 1977) or a combination of both (Colombi *et al*., 2017; Iijima *et al*., 2007; Croser *et al*., 1999). An example of the thickening caused by increased cortical dimensions of different species (soybean and triticale) is given in Fig. 2.6 (Colombi and Walter, 2016). Interspecies variation for cell file number is evident

as shown by Bramley *et al*. (2009) for lupin in comparison with wheat roots, but within a plant, cell file number can differ depending on root type. Lateral roots will have less cortical cell layers than the axial roots from which they emerged and cell file number is correlated with diameter of those lateral roots (Pauluzzi *et al*., 2012). For nodal maize roots, each new node formed will have more cell files, while cell file number is negatively correlated with the cortex to stele region for nodal roots (Yang *et al*., 2019). Differences in cell file number increases were observed for wheat: embryonic roots show increased cell file numbers under impedance while post-embryonic roots do not, whereas cortical cell diameters increased regardless of root type (Colombi *et al*., 2017b). Another recent study of Colombi (2019) showed that cortical cell diameter increases significantly for wheat roots under high penetration resistance and that genotypes that had greater root cortical cell diameter had reduced energy cost to root growth. The different cell layers within the cortex react differently to impedance. In barley, cell diameters of the outer cortical cells increase under mechanical impedance, while inner cell diameters became smaller (Wilson *et al*., 1977). Smaller cells are deemed to be more rigid and strong (Chimungu *et al*., 2015a). Cortical cell lengths have been observed to decrease under impeding conditions (Croser *et al*., 1999; Veen, 1982). Indirect methods for estimating cell dimensions (cross-sectional area and length) have been used to calculate cell volumes for impeded roots (Atwell, 1990; Wilson *et al*., 1977). However, calculated volumes have shown contrasting results as cell volumes increase under compaction for wheat (Atwell, 1990) and decrease for barley (Wilson *et al*., 1977). Cell volumes have however not been directly measured. Furthermore, cell position within the cortex will determine cell volume, as observed in rice seedlings in which the middle cortical cells appear to be shorter and wider than those in the inner and outer cortical regions (Kawai *et al*., 1998). The latter is in contrast with observations by Deacon *et al*. (1986) who observed no significant difference in cell length across the maize cortex.

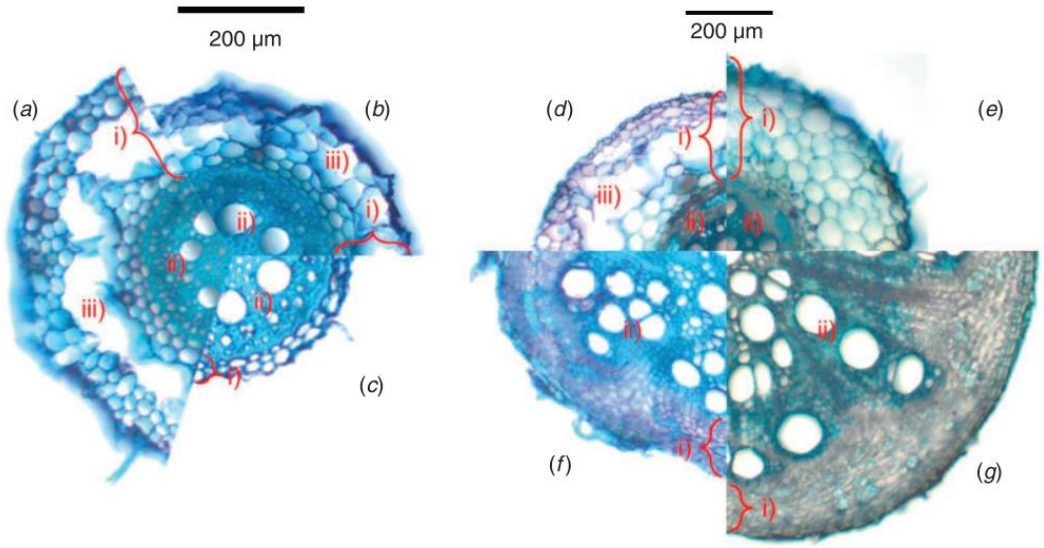

Figure 2.6 – Root anatomy of nodal roots of triticale (left) and adventitious (d,e) and taproots (f,g) roots of soybean (right). Different anatomical adjustments of the cortex can be seen due to (a) top soil compaction, (b) subsoil compaction and (c) uncompacted soil for triticale. The anatomical adjustments of soybean when under compaction (e,g) and loose soil (d,f). Root cortex is indicated by (i), stele (ii) and (iii) aerenchyma. Roots were sectioned 2 and 10 cm from the root base for triticale and soybean respectively (Colombi and Walter, 2016)

2.3.5 Impedance and the presence of aerenchyma

Within the cortex, gas-filled spaces known as root cortical aerenchyma can be formed by separation of cells (schizogenous) or cell collapse (lysigenous) (Evans, 2004; Kawai *et al*., 1998). Aerenchyma varies between species, genotypes, root types and within a root (Colmer, 2003). More aerenchyma area was found in wheat and triticale under impeded conditions (Colombi *et al*., 2017b; Colombi and Walter, 2016).

It should also be noted that aerenchyma is formed a certain distance away from the root tip, past the elongation zone (Lenochová *et al*., 2009). This means that no aerenchyma is present when a root elongates and pushes through the harder soil and therefore does not directly influence a roots ability to penetrate harder soils. The presence of aerenchyma can counter the effects of drought, hypoxia or nutrient deficiencies by improving soil exploration through the reduction of metabolic costs of cortical cell maintenance (Chimungu *et al*., 2015b; Postma and

Lynch, 2011; Zhu *et al*., 2010; Coudert *et al*., 2010; Kawai *et al*., 1998). Longitudinal oxygen flow through the roots is helped by the presence of large lacunae and aerenchyma enables CO_2 venting out (Colmer, 2003; Drew *et al*., 2000; Karahara *et al*., 2012). Considering that oxygen becomes more limited in a compacted soil, as soil porosity decreases, the formation of aerenchyma could be of a benefit to roots in hard soil (Lynch and Wojciechowski, 2015). But aerenchyma will also limit the transport of water and nutrients (Hu *et al*., 2014).

Aerenchyma might influence root mechanical strength as root porosity can weaken the root structure, but when a dense multiseriate, sclerenchymatic ring of cells is present in the outer cortex, the effect can be reduced (Striker *et al*., 2007; Striker *et al*., 2006). Considering cortical attributes, Chimungu *et al*. (2015a) proposed a root anatomical ideotype that would facilitate penetration of hard subsoils. The outer protective layer of the cortex should consist of small cells to counteract bending and buckling, while aerenchyma which is formed in the inner and middle cortical regions (Deacon *et al*., 1986) reduces metabolic costs of thick axial roots (Chimungu *et al*., 2015a). Colombi and Walter (2016) proposed that diameter enlargement, by increasing the relative cortical area of a cross-section, followed by aerenchyma formation is important in order to allow oxygen flow within a root and is not necessarily for reducing metabolic costs per se. Either of these interpretations can hold true and would need to be confirmed in future studies.

2.4 Other effects induced by impedance

2.4.1 Ethylene

Greater levels of ethylene due to impedance can be measured in primary maize roots (Moss *et al*., 1988, Sarquis *et al*., 1991). *Vicia faba* roots produce more ethylene when roots hit a physical barrier and mechanical impedance is increased (Kays *et al*., 1974). Production can be attributed to an increased ACC synthase activity, malonyl-ACC and the ethylene-forming-enzyme complex (Clark *et al*., 2003; He *et al*., 1996a). These enhanced levels of ethylene production are measured prior to anatomical adjustments (Kays *et al*., 1974; Sarquis *et al*., 1991, He *et al*., 1996a).

Ethylene modulates both anatomical and architectural traits. For instance the production of aerenchyma is upregulated with increased ethylene concentrations due to mechanical impedance (He *et al*., 1996a). Root hairs are affected by ethylene as more root hairs are present in *Arabidopsis thaliana* under ACC treatment (Tanimoto *et al*., 1995). Ethylene stimulates lateral root development (Borch *et al*., 1999). Ethylene causes root thickening while reducing elongation rates (Moss *et al*., 1988; Sarquis *et al*., 1991). Ethylene has also been found to change the orientation of microtubules within cortical cells (Baluška *et al*., 1994), an observation that also has been made under mechanical impedance (Veen, 1982).

Ethylene is linked to mechanical impedance as it causes a similar root response in response to impedance. However, whether the effect of ethylene is either positive or negative for root growth remains unclear. Zacarias and Reid (1992) found that roots which had ethylene production inhibited by silver thiosulfate were unable to penetrate the growing medium, which points to the necessity of ethylene in growth under impeding conditions. In contrast, ethylene induced radial expansion (plus 200 µm) also massively impacts root elongation rates (an elongation rate of 1 mm h^{-1} gets reduced to 0,3 mm h^{-1} elongation under exogenous application of ethylene on maize primary roots) at the same time (Sarquis *et al.*, 1991), which ultimately will reduce soil exploration. Atwell (1993) makes a case for the involvement of auxin in the root response to mechanical impedance with auxin distribution influenced by enhanced ethylene synthesis in *Arabidopsis* roots.

2.4.2 Root deformations

Considerable plasticity among monocotyledonous species was found for root deformations. Roots of barley and triticale appeared flattened when grown on compacted field soils, while those of wheat, rye and maize remained close to circular (Lipiec *et al*., 2012). In order to grow into pores smaller than the root diameter, root diameter can adjust itself through radial deformation. Scholefield and Hall (1985) found that radial deformation is limited by the size of the root cap and the stele. For maize it was found that this kind of radial constriction was

also present within the stele for both primary and nodal roots (Bengough *et al*., 1997). Whether root deformations aid soil exploration, or are in reality a reaction to the imposed impeding stresses, remains unclear.

2.4.3 Root surface properties

Szatanik-Kloc *et al*. (2018) recently showed changes to the surface properties of the roots (increased apparent surface area, root cation exchange capacity, total surface charge, number of strongly acidic groups, and surface charge density) by compaction. This should be taken into account, although minor, when considering the reduced nutrient uptake by plants on a compacted soil, next to the fact that impeded roots are less able to exploit the soil fully and reach deeper for nutrients (Ishaq *et al*., 2001; Szatanik-Kloc *et al*., 2018).

2.5 Conclusions

Mechanical impedance imposes physical resistance to root growth. Roots in turn adapt or react to these conditions on different levels. Root systems can redistribute roots over the soil profile to seek lesser impeded regions, thus compensating the reduction of root length in the impeded areas. Mechanically impeded roots show reduced root elongation, which limits soil exploration by reducing root length and rooting depth. Whether rooting depth and root length are correlated under mechanical impedance has so far not been investigated. This will be discussed in **Chapter 4**, where we investigated the differential root distributions of twelve different maize genotypes in a field trial.

In order to overcome the adverse effects of mechanical impedance roots will have traits such as a sharp root tip, increased mucilage production or the presence of root hairs. Anatomical traits have been studied far less, effects of impedance have shown that the root tip meristem changes to an open type meristem, while the length of the elongation zone becomes shorter. Observations on stele and cortical anatomy have been inconclusive. Therefore we conducted a field study in order to identify root anatomical phenotypes which could contribute to growth under impeded conditions (**Chapter 5**). In this experimental chapter we also hypothesised that the radial thickening response varied among the genotypes

tested, between root classes and soil types. We further will discuss why a distinction between thicker and thickening roots should be made.

Furthermore the involvement of ethylene has not been completely understood. In **Chapter 6** we show the results of a pot experiment, where we tested the hypothesis that radial expansion is not related to the ability of a root to cross a compacted soil layer. The results for the changes of the anatomical traits of four different genotypes crossing this denser layer were compared to results from exogenous ethylene application on the anatomical traits of these genotypes. We will discuss why ethylene insensitive roots would have a competitive advantage as they are more capable of overcoming mechanical stress. We also suggest that prolonged ethylene exposure can function as a stop signal for growth through reduced root elongation.

Chapter 3 – Materials and methods

Each of the following experimental chapters (**Chapter 4**, **Chapter 5**, **Chapter 6**) have their own specific materials and methods section. **Chapter 3** contains experimental methods not presented elsewhere in the thesis and gives more details on certain methods to clarify the experimental chapters further.

3.1 Field trial plot design

Chapter 4 and **Chapter 5** handle field trials and materials and methods can be found in these respective chapters. The following is to provide further information about the plot design.

Field trials were planted at two different field sites. The first field site was planted at the Apache Root Biology Centre (ARBC), Willcox Arizona, USA (32°01'N, 109°41'W) in 2016. The second field site was planted at the Russel E. Larson Agricultural Research Center in Rock Springs (referred to as PSU), Pennsylvania, USA (40°42'N, 77°57'W). Both field sites were divided into 8 wholeplots on which 12 genotypes were randomly planted within 4 row subplots (3.05 x 4.57 m). The subplots were separated from each other by an alley between the ranges, which makes subplot identification possible by row and range. Treatments (compacted and non-compacted) were allocated on wholeplot level, four replicates for compaction and four replicates for non-compacted wholeplots.

3.1.1 Field lay-out at ARBC

The field site at ARBC had a pivot lay-out for irrigation purposes. One quadrant was allocated for use by the University of Pennsylvania. One third of the area within the quadrant was used for maize trials, while the other parts were used for other experiments or were left fallow for rotation reasons. The compaction trials were located in the inner rings B and C (Fig. 3.1). Ring B and C were irrigated simultaneously during the growing season.

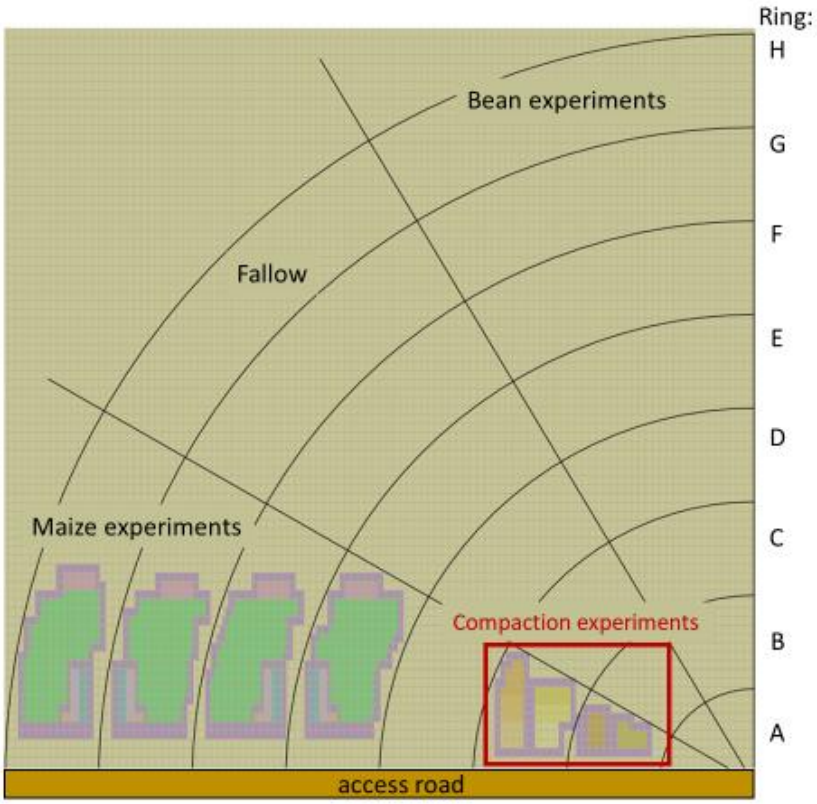

Figure 3.1 – Location of the compaction trial within the pivot at ARBC

At ARBC eight wholeplots for the field trial were locacted within ring B and C (Fig. 3.1). The outer edges of the experimental wholeplots were surrounded by a 4-row border plots (commercial hybrid maize variety), but no borders were present between wholeplots. Fig. 3.2 is a field map of the wholeplots with treatments; compacted and non-compacted on wholeplot level and genotype on subplot level. Planting was performed with a 4-row planter.

3.1.2 Field lay-out at PSU

The field site at PSU had a rectangular lay-out (Fig. 3.3). Other parts of compacted field site were used for different experiments. The outer edges of the experimental wholeplots were surrounded by a 2-row border (planted with a commercial hybrid maize variety). A one row border was planted around the inner edges of the wholeplots. While an alley (brown on Fig. 3.3) was left to allow for easy access to wholeplots, as well as for turning of heavy machinery during the compaction. Planting was performed manually with a jab planter.

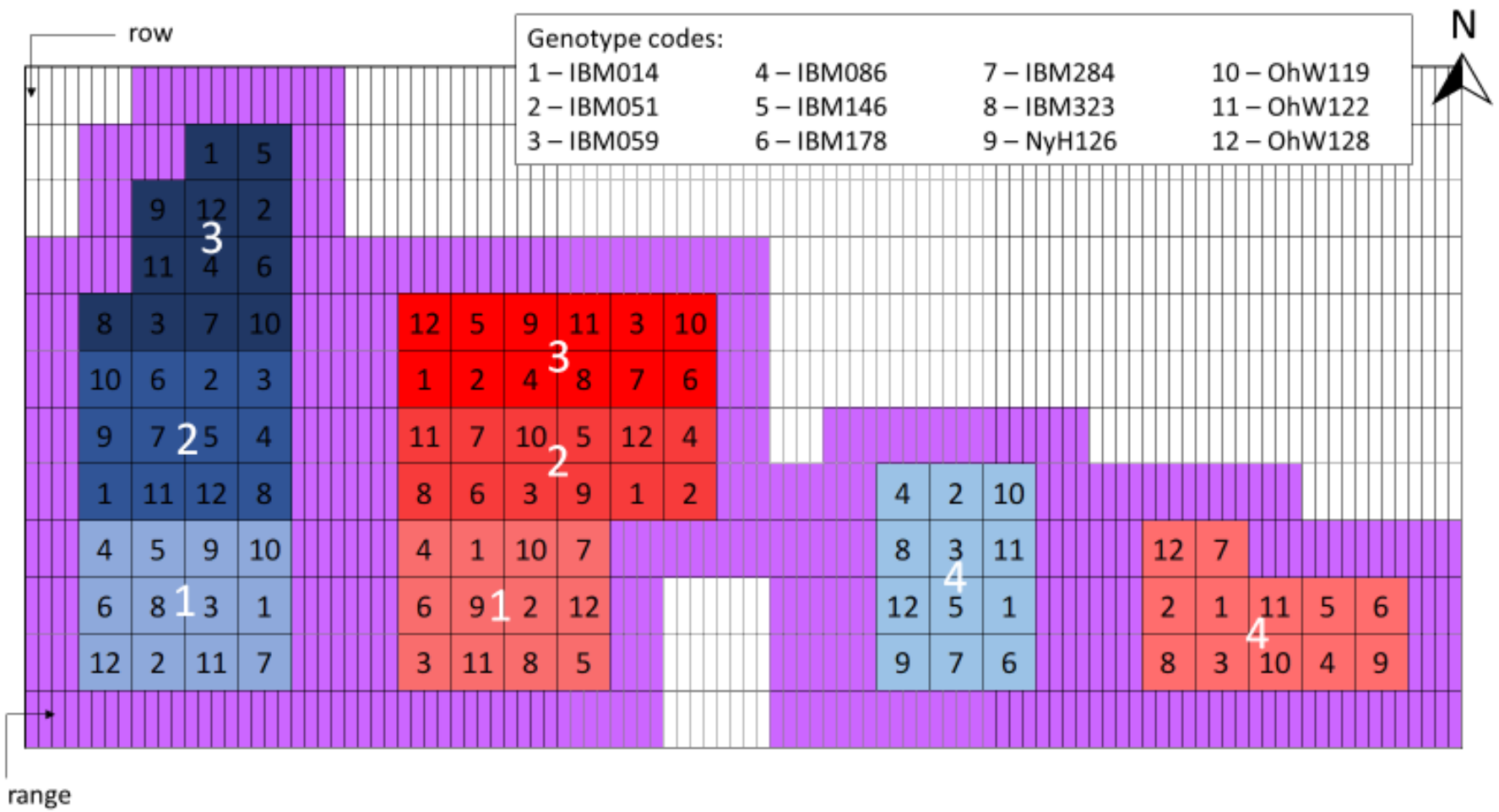

Figure 3.2 – Field lay-out of compaction trial at ARBC with allocated genotypes (number from 1 – 12) on subplot level and compaction treatment (non-compacted wholeplots in blue and compacted plots in red (numbered per replicate per treatment)) on wholeplot level. Border plantings in purple.

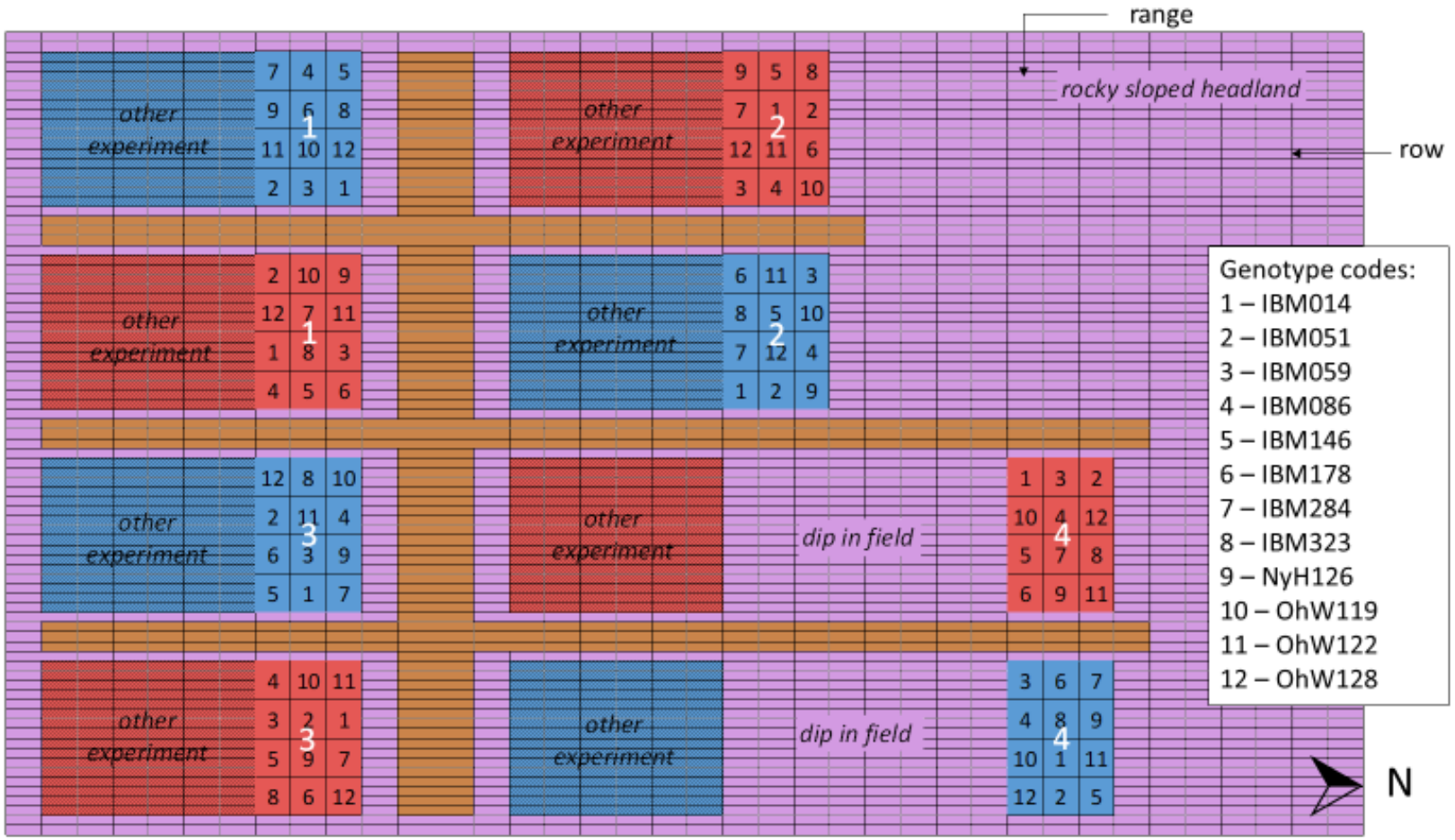

Figure 3.3 - Field lay-out of compaction trial at PSU with allocated genotypes (number from 1 – 12) on subplot level and compaction treatment (non-compacted wholeplots in blue and compacted plots in red (numbered per replicate per treatment)) on wholeplot level. Border plantings in purple

3.2 Genotype selection

3.2.1 Genotypes used in field trials

Genotypes were selected from a set of genotypes previously used by Chimungu *et al.* (2015a) in a pot experiment with a wax layer that identified different root penetration ratios for 24 genotypes (Figure 3.4). Twelve genotypes were selected as the available field area only allowed for a maximum of 12 genotypes to be planted at ARBC. For PSU the same genotypes were used to ascertain consistency between the field sites. Genotypes that differed in root anatomical traits as well as penetration rates were selected from this set, furthermore enough seeds needed to be available with high germination rates (Figure 3.4). These genotypes are used in **Chapter 4** and **Chapter 5**.

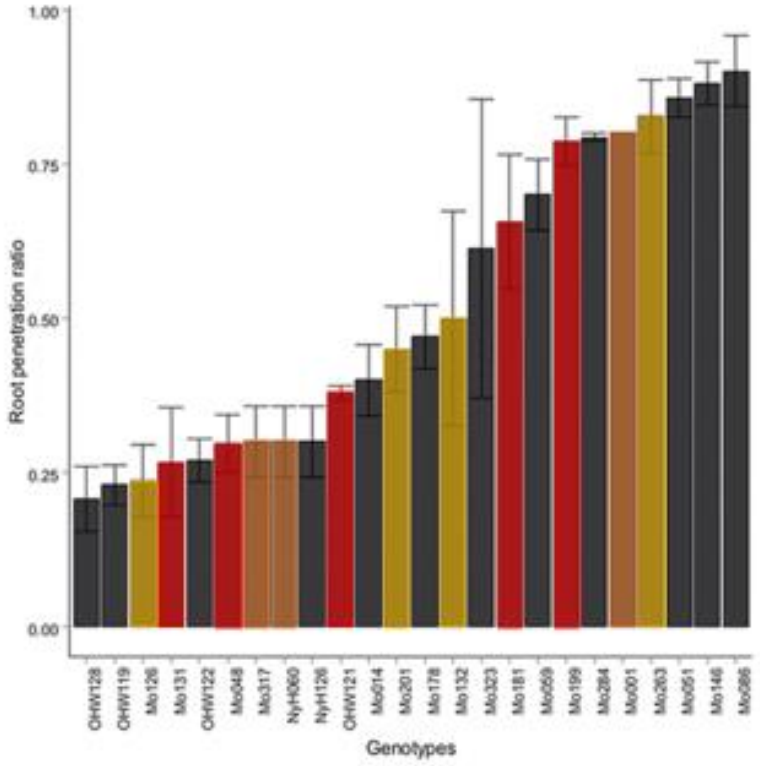

Figure 3.4 – Selected genotypes from the subset of 24 genotypes used by Chimungu *et al.* (2015a). The grey bars show the selected genotypes included in the field trials. The bars in red represent the genotypes with an insufficient number of seeds, the bars in yellow represent the genotypes with insufficient germination rates and the bars in orange represent the genotypes discarded due to anatomical traits or root penetration ratio. Bar chart adapted from Chimungu *et al.* (2015a)

3.2.2 Genotypes used in pot trials

For **Chapter 6** the genotypes OhW128, IBM146, IBM086 and IBM014 were selected based on observations from a preliminary trial set-up that firstly was set up to set CT scanning parameters (see 3.3.2) and column packing method (see 3.3.3). These genotypes were able to reach the pot layer for roots of node 3 and node 4, and showed differences in penetration ability. Furthermore they showed differences in anatomical changes when interacting with the denser soil layer.

3.3 Pot trial materials and methods

Chapter 6 describes a pot trial. Materials and methods are included in the chapter, the following gives more background information about these materials and methods.

3.3.1 Soil texture

The soil texture was determined by mechanical analysis by hydrometer (Day, 1965; Rowell, 1994). 50 g of sieved (< 2 mm) air-dried soil was dried overnight in an oven at 105 °C and oven-dry weight was weighed. 100 ml of 6% H_2O_2 was added to the oven-dried soil and left to stand overnight, after which 100 ml of $(NaPO_3)_6$ was mixed with this solution and left for 12 hours. Distilled water was added as to make up a total volume of 1L in a sedimentation cylinder. The temperature of the soil suspension was recorded. The suspension was mixed with a plunger before lowering the hydrometer into the solution. The hydrometer was read after 32 seconds (silt/clay reading) and the solution was mixed again and allowed to stand for 8 hours until the next reading (clay content reading).

A calibration reading for the hydrometer was taken in a similar way, the used solution had 100 ml of $(NaPO_3)_6$ topped up to 1 L with distilled water, but without the added soil and H_2O_2. A correction for density is carried out by subtracting the density of the calibration reading from the soil sample readings.

The following equations can be used to calculate the soil texture:

$$\%\ clay = \frac{corrected\ hydrometer\ reading\ at\ 8\ hours}{oven\ dry\ weight\ of\ soil} x100$$

$$\%\ silt = \left(\frac{corrected\ hydrometer\ reading\ at\ 32\ seconds}{oven\ dry\ weight\ of\ soil} x100\right) - \%\ clay$$

$$\%\ sand = 100\% - \%\ silt - \%\ clay$$

3.3.2 X-ray Computed Tomography

X-ray Computed Tomography (CT) has been used as a non-destructive method to image growing root systems, soil pore networks, mineral components and water distributions in 3D without disturbing the soil environment (Tracy *et al.*, 2010; Mooney, 2002, 2012; Helliwel *et al*., 2013). Together with magnetic resonance imaging (MRI), X-ray CT scanning is a technique that can extract root architectural traits without disturbing the soil. But both techniques differ as MRI can be hindered by the occurrence of iron and manganese in soil (Tracy *et al.*, 2010; Mooney *et al.*, 2012).

2D cross-sectional slices of the soil cores with a root system are made based on the attenuation of the X-rays (a form of electromagnetic waves) that pass through the sample, with X-ray beams passing more easily through lower density materials in comparison to denser materials (Pajor *et al.*, 2013; Tracy *et al*., 2010; Mooney *et al.*, 2012; Helliwel *et al*., 2013). Hence attenuations gives information about sample density (Tracy *et al.*, 2010). A digital detector records the reduction in the X-ray intensity that reaches the detector after X-rays have passed through a sample in a radiograph (Pajor *et al.*, 2013; Mooney *et al*., 2012). These radiographs are then used with together with their X-ray attenuation coefficient (voxel) to reconstruct to reconstruct a 2D cross-sectional slice of the 3D volume (Pajor *et al.*, 2013; Tracy *et al.*, 2010; Mooney *et al.*, 2012).

As attenuation values of soil water, roots and organic matter are similar, acquisition settings and experimental conditions need to be closely tailored to each other as to assure the best resolution (Pajor *et al.*, 2013; Helliwel *et al.*, 2013). Exact used settings for X-ray CT scanning and subsequent image analysis are described in **Chapter 6**. In order to improve the contrast between soil and roots the pots from experiment **Chapter 6** were left to dry 48 hours prior to scanning. Depending on attenuation density different voxels are either bright (dense material for example mineral grains) or dark (low density for example air-filled pores). These voxels can be segmented either by 'overall thresholding' or 'localised thresholding' in order to distinguish roots from their direct environment (Helliwel *et al.*, 2013)

3.3.3 Column packing with a compacted layer

Three different soil packing options were assessed before opting for a compacted layer used in **Chapter 6**. Columns (30 cm high, internal diameter of 14.8cm) were packed using a sandy loam topsoil (Newport series, obtained from the University of Nottingham farm, Melton Lane 52.83°N, 1.25°W), air-dried and sieved to <4 mm and rewetted to a moisture content of 17%. Option 1 had a 15 cm tall bottom layer compacted in three increments of 5 cm to a bulk density of 1.5 g cm^{-3}. The layers were scarified to ensure homogeneity after which the top half of the column was filled with soil up to a bulk density of 1.2 gcm^{-3}. For option 2, the bottom 15 cm was compacted at once to 1.5 g cm^{-3} cm, topped with a soil of bulk density 1.2 g cm^{-3}. The compacted layer was scarified before adding the top layer. Option 3 consisted of preparing a soil 'disk' (3 cm thick) in a compaction mould with bulk density of 1.5 g cm^{-3}. The top and bottom of the disk were scarified before the layer was placed between the top and bottom parts of the column. A smaller column of 15 cm was packed with soil to a bulk density of 1.2 g cm^{-3}. The soil disk was carefully placing on top and a second column (15 cm high) was stacked on top of the bottom column to form one larger column. Columns were taped together and the top column was filled to a bulk density of 1.2 g cm^{-3}.

Afterwards these columns were imaged with an X-ray CT-scanner (V |tome|x m) set at 180kV and 180 µA and a pixel/voxel resolution of 55 µm. Scan duration was set at 1h 13min. Greyscale images obtained from the CT scans show the different packing results (Fig. 3.4). Method 3 was selected for the experiments of **Chapter 6** as the compacted layer provided the sharpest change in bulk density and allowed for assessment of root anatomy once they have past the compacted layer. Due to restrictions in top soil quantities the sandy loam soil was replaced with a brown earth soil with a sandy loam texture procured from local beet farms through British Sugar in Newark (UK) for the pot experiment described in **Chapter 6**.

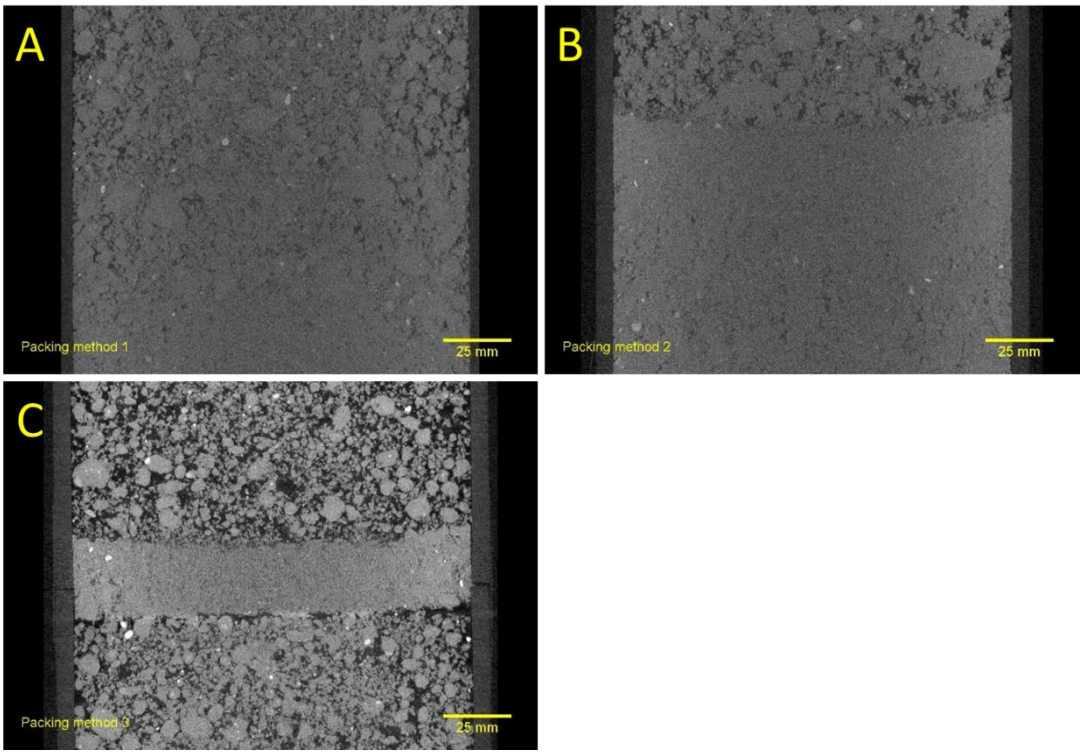

Figure 3.5 -Scanning results for the three tested packing methods. (A) Packing with different scarified layers, (B) packing with just one layer and (C) packing with a single soil disk

3.4 Sectioning techniques

Tedious hand sectioning methods have long been a standard practice in anatomical research. The technique limits the amount of samples that can be taken as it is slow and requires patience. Using a vibrating microtome (7000 smz-

2) (Campden Instruments Ltd., Loughborough, UK), sectioning becomes less labour intensive and more accurate samples can be taken as the thickness of a section can be controlled. In combination with 3D printed moulds, sectioning can be sped up somewhat (Atkinson and Wells, 2017). However, roots need to be embedded in a fixing medium, hence adding a step before sections can be analysed under a microscope.

Standard light microscopy (Fig. 3.5A) can be used to analyse sections, but advancements in imaging technology enable better visualisation by scanning confocal microscopy (Fig. 3.5B) or Laser Ablation Tomography (LAT) (Fig. 3.5C). Confocal microscopy has an increased resolution and the advantage of staining which can help identify tissues. Laser Ablation Tomography accelerates taking cross-sectional images significantly. Furthermore the technique combines the precision that can be achieved with a microtome, with the 3-dimensional capabilities (Hall *et al.*, 2019; Strock *et al.*, 2019). More details about the confocal and LAT imaging methods can be found in **Chapter 6**.

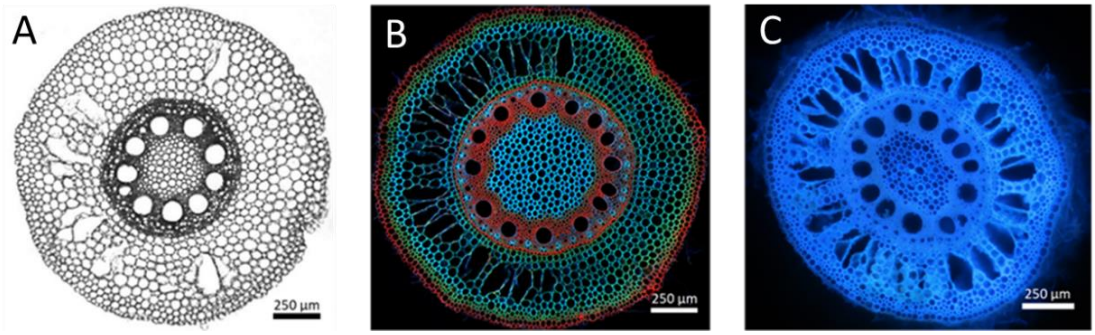

Figure 3.6 – Root cross-sections of maize roots obtained by (A) hand sectioning followed by light microscopy, (B) sectioning by vibrating microtome followed by confocal microscopy and (C) sectioning and imaging by Laser Ablation Tomography

3.5 Image processing

During the field and pot experiments different images were collected, most of the image processing methods can be found in the respective chapters. An overview of the different images and measurements is given in the diagram in Figure 3.7.

Figure 3.7 – Diagram of images and measurements obtained from those images (1/2)

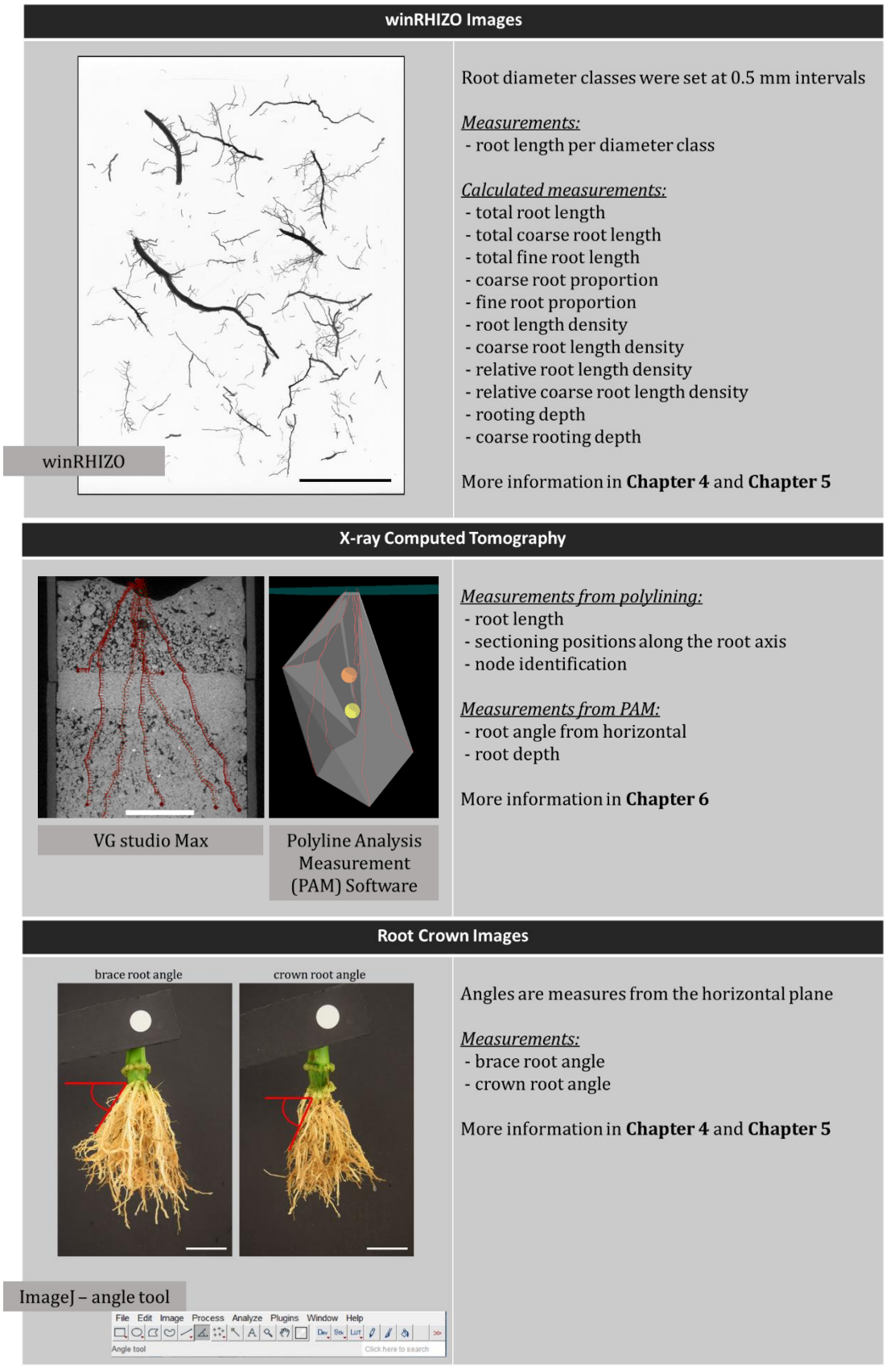

Figure 3.7 – Diagram of images and measurements obtained from those images (2/2)

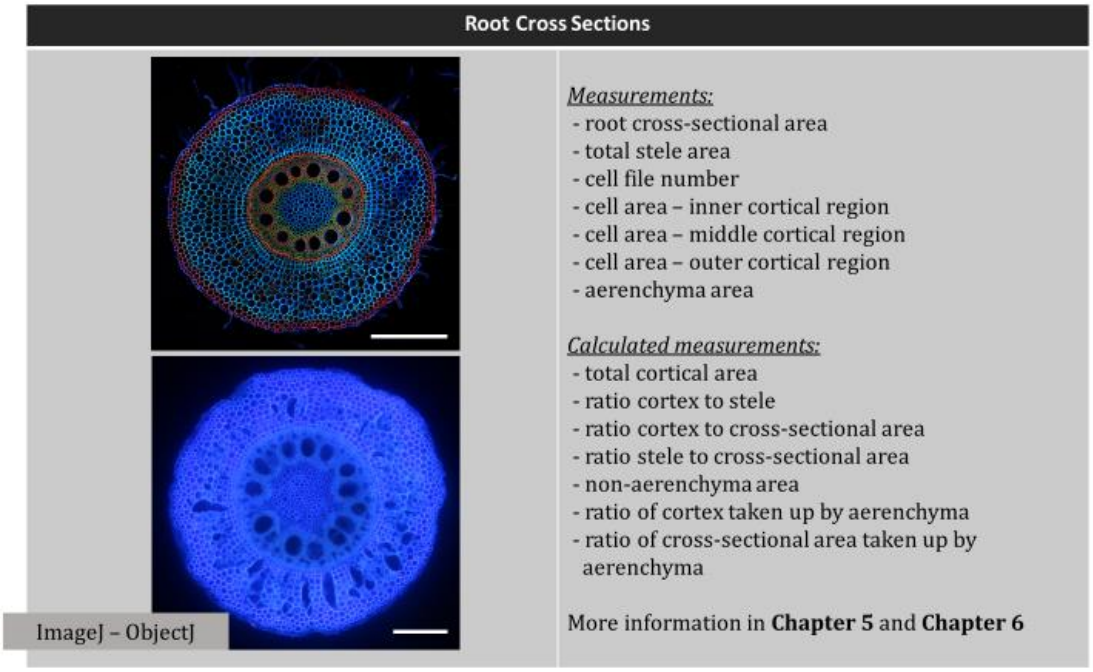

Chapter 4 – The ability of maize roots to grow through compacted soil is not dependent on the amount of roots formed

Paper in preparation for *Field Crops Research*

Chapter 4 investigates the effect of impedance through soil compaction on root length and depth distributions. The hypothesis set was that rooting depth and root length were not related on compacted plots. Root length was differentiated into coarse or fine root length as to account for lateral or nodal growth. Root systems either avoid stress by redistributing their root length or are capable of growing deeper. This paper is currently in preparation for submission to *Field Crops Research.*

Author contributions

Project supervision and paper editing provided by K.W. Loades, A.G. Bengough, S.J. Mooney and J.P. Lynch. Experiments, analysis and paper preparation by D.J. Vanhees.

4.1 Abstract

Mechanical impedance is a primary constraint to root growth and hence the capture of soil resources. To investigate whether rooting depth and root length under mechanical impedance are correlated 12 maize lines were evaluated at two field sites. To distinguish between lateral and nodal roots, roots were sorted into different diameter classes. Coarse roots had diameters >1 mm and represent nodal roots. Total root length, total coarse root length and total fine root length were greater at one field site than the other. Greater proportions of coarse roots on compacted plots were found at both field sites however results were driven by genotypic variation. Soil compaction reduced total rooting depth (rooting depth including all diameter classes) and coarse rooting depth (rooting depth of coarse roots) at both sites compared to non-compacted plots. Root distribution was influenced by compaction with greater root length densities closer to the soil surface. Root length and rooting depth were not related to each other under impeded conditions. Coarse roots of some genotypes became obstructed on the compacted plots, while other genotypes were capable of growing through the impeding soil and reached deeper soil strata. This resulted in differential distribution of roots down the soil profile. On compacted plots genotypes with similar rooting depths but with contrasting coarse root lengths were identified. The ability of roots to grow through compacted soils is therefore not dependent solely on the coarse root length formed by the root system.

4.2 Introduction

The ability of plants to acquire nutrients and water is dependent on soil exploration. Mechanical impedance can lead to reduced total root length and/or a redistribution of root length within the soil profile (Pfeifer *et al.*, 2014a; Shierlaw and Alston, 1984), which could affect the acquisition of water and nutrients. Root length densities of 1.0 cm cm^{-3} have been suggested to be sufficient for water extraction (Gregory *et al.*, 2009). However, this estimation does not take into account differences in the capacity of roots to acquire water or nutrients according to their class, age or anatomical phenotype (Ahmed *et al.*, 2017; Hu *et al.*, 2014; Schneider *et al.*, 2017; York *et al.*, 2016). Root length

densities of 0.1 to 2 cm cm^{-3} have been suggested to cause competition for mobile resources among roots (Postma and Lynch, 2012; Yamaguchi and Tanaka, 1990; Ge *et al.*, 2000; Rubio *et al.*, 2001). Inter-plant competition is greatest for roots with similar root architectures, specifically for plants with shallow roots (Rubio *et al.*, 2001). But both inter- as well as intra-plant competition could become greater in cases of reduced soil exploration caused by impedance.

Root distribution affects resource capture in time and space as roots need to be located close to soil resources. Topsoil foraging phenotypes perform better in phosphorus scarce conditions while water and N acquisition are linked to the development of deep roots in most environments (Lynch, 2011, 2013, 2019). Architectural traits such as steep root angles, fewer nodal roots, less lateral branching and low plasticity in the local soil environment contribute to reaching deeper into the soil strata (Lynch, 2019). As soils get denser and stronger with depth due to overburden pressure (Gao *et al.*, 2012, Gao and Lynch, 2016), mechanical impedance will be imposed more deeper rooting phenotypes than on topsoil foraging root phenotypes. Periodic droughts are common in many ecosystems and drier soils are generally harder (Gao *et al.*, 2012; To and Kay, 2005; Vaz *et al.*, 2011; Whalley *et al.*, 2005). However, plants with root systems that grow deeper are in general better adapted to drought (Chimungu *et al.*, 2014b; Lilley and Kirkegaard, 2016; Lynch, 2013; Zhan *et al.*, 2015). Certain soils offer very large mechanical impedance to roots like naturally hard-setting soils in Australia (Mullins *et al.*, 1987). Agricultural management can introduce compaction and plough pans by wheeled traffic or trampling (Batey, 2009; Hamza and Anderson, 2005). Depending on the soil textural characteristics, suboptimal soil conditions during trafficking (such as high moisture contents) will exacerbate compaction (Horn *et al*., 1995; Raper, 2005). Roots can become confined to surface soil strata when not capable of penetrating through a hard soil layer such as a plough pan (Barraclough and Weir, 1988; Ehlers *et al.*, 1983). Root systems are able to compensate root growth by exploiting the lesser impeded regions of the soil, as illustrated by split pot experiments (Bingham and Bengough, 2003; Pfeifer *et al.*, 2014a) or layered pot systems (Shierlaw and Alston, 1984). Roots of maize (Chimungu *et al.*, 2015a), rice (Chandra Babu *et al.*.,

2001; Clark *et al.*, 2000, 2002; Yu *et al.*, 1995), wheat (Botwright Acuña and Wade, 2005; Kubo *et al.*, 2006) and common bean (Rivera *et al.*, 2019) show substantial genotypic variability for penetrating strong wax layers simulating mechanical impedance.

Root systems consist of distinct root classes which vary by taxa, for example many dicot taxa have a dominant taproot, while monocots such as cereals form nodal roots from shoot nodes (Hochholdinger *et al.*, 2004; Lynch and Brown, 2012; Rich and Watt, 2013). Adult maize root systems consist of primary, seminal, crown (belowground nodal) and brace (aboveground nodal) roots. All these classes form lateral roots. For monocotyledons, nodal roots are the main parent axes of lateral roots present at depth as these laterals proliferate from nodal roots (Cairns *et al.*, 2004; Nagel *et al.*, 2012).

Genotypic variation for lateral root phenotypes has functional consequences in maize. Long laterals in combination with low lateral branching density are better for water and N acquisition, while short laterals in combination with high lateral branching improve P acquisition (Postma *et al.*, 2014; Zhan *et al.*, 2015; Zhan and Lynch, 2015; Jin *et al.*, 2018). Root classes have different elongation rates that differ greatly as a function of time. For maize, lateral roots have been found to elongate at 2.2 cm day^{-1} for 2.5 days, while nodal roots elongated at a rate of 3 cm day^{-1} over a 5 week period (Cahn *et al.*, 1989). Under non-impeded conditions primary roots of maize elongated at 4.8 cm day^{-1}, while seminals only elongated at 3.2 cm day^{-1} (Veen and Boone, 1990). Differences in elongation rates between root types can lead to soils being differentially explored with time by each root type and could affect the volume and depth of bulk soil that can be explored within a certain time by different root types. Biomechanical properties also vary according to root class, with seminal roots being stronger than lateral roots (Loades *et al.*, 2013). Whether this translates to specific penetration ability under impeded soil conditions according to root class remains to be investigated. It has been hypothesised that the contrasting phenotypes of distinct root classes adds to a plants' plasticity and flexibility when interacting with different environments (Chochois *et al.*, 2015; Wu *et al.*, 2016) but the functional implications of the

differential effects of mechanical impedance on distinct root classes are poorly understood.

Root system size differs among genotypes and different soil conditions (Gao and Lynch, 2016; Nakhforoosh *et al.*, 2014). Root system size, expressed as total root length or root length density, can be split between coarse and fine roots (Cahn *et al.*, 1989; Steinemann *et al.*, 2015; Varney *et al.*, 1991). Small grain cereals such as wheat or barley are characterised by fine axial roots, maize has thicker axial roots, while dicots and perennials have very coarse axial roots. But for all these species, a distinction between a main root axes and a smaller diameter laterals root can be made. Coarser roots are needed in order to deploy finer roots within the soil profile. Studies on wheat suggest that wheat genotypes with more root axes had greater penetration of wax layers (Whalley *et al.*, 2013).

Better root growth under mechanical impedance can be attributed to different traits. For instance the frictional component of impedance is reduced when roots produce mucilage or border cell sloughing (Iijima *et al.* 2000, 2004; Bengough and McKenzie, 1997). Smaller root tip radius to length ratios are linked to greater elongation rates under impedance. Another beneficial trait is the presence of root hairs which can provide anchorage for roots to cross from loose to harder soil layers (Bengough *et al.*, 2011; Haling *et al.,* 2013). Root hairs also maintain water uptake when soils dry (Carminati *et al.*, 2017). Root anatomical traits such as greater cortical cell diameter have been linked to reduced energy costs under impeded conditions (Colombi *et al.*, 2019). It has been suggested that smaller outer cortical cells prevent buckling, which facilitate penetration of harder layers (Chimungu *et al.,* 2015a).

Genotypes can adjust their root distribution with depth in response to compaction (Barraclough and Weir, 1988) however few studies have compared different genotypes and their redistribution of roots under compaction. Little is known about root system size for those root systems that do manage to grow deeper in compacted soils. The hypothesis that rooting depth and root length are not related to each other on compacted plots is tested for deeper rooting genotypes.

4.3 Materials and methods

4.3.1 Plant material and growing conditions

Twelve maize (*Zea mays* L.) recombinant inbred lines, selected (see **Chapter 3** for additional details) from a study by Chimungu *et al.* (2015a) were planted in a split-plot design in order to study their root growth in compacted conditions at two field sites. Seeds were obtained from Dr. Shawn Kaeppler (University of Wisconsin, Madison WI, USA – Genetics Cooperations Stock Center, Urbana, IL, USA). Genotypes were grown at the Apache Root Biology Centre (ARBC), Willcox Arizona, USA (32º01'N, 109º41'W), planted on June 16, 2016, and the Russell E. Larson Agricultural Research Center in Rock Springs (further referred to as PSU), Pennsylvania, USA (40º42'N, 77º57'W), planted on July 10, 2017. Field sites differed in soil texture, the ARBC site has a soil classified as a Grabe series (coarse-loamy, mixed, superactive, calcareous thermic Torrifluvent) and has a clay loam texture, while the PSU site is classified as a Hagerstown series (silt loam, fine, mixed, semiactive, mesic Typic Hapludalf) and has a silt loam texture. Compaction was introduced by passing over the treated plots with heavy machinery. At ARBC a 4 wheel tractor (4 tonnes with 8 passes) and at PSU a 3-axle truck (20 tonnes with 4 passes) were used. At ARBC the soil was irrigated before compacting to provide a high enough water content. Penetrometer resistance (Fig. 4.1) as well as an increase of bulk density (Table S4.1) were measured over the soil profile in order to verify increased soil strength and soil density. Irrigation was managed on the basis of soil moisture content to avoid water deficit stress (PR2/6-tubes at ARBC (Delta-T Devices Ltd, Cambridge UK) and multiplexed TDR-100 probes at PSU (Campbell Scientific Inc., Logan, UT, USA). Nutrients and pesticides were applied based on standard agronomic practices (Table S4.3).

4.3.2 Root sampling

During tasselling (55 and 51 days after planting for ARBC and PSU respectively) one soil core was taken from each subplot. Coring tubes (60 cm deep, 5.1 cm diameter) fitted with a plastic sleeve (4.5 cm diameter) were driven into the soil between 2 plants in a row (Trachsel *et al.*, 2013). Cores were stored at 4º C until

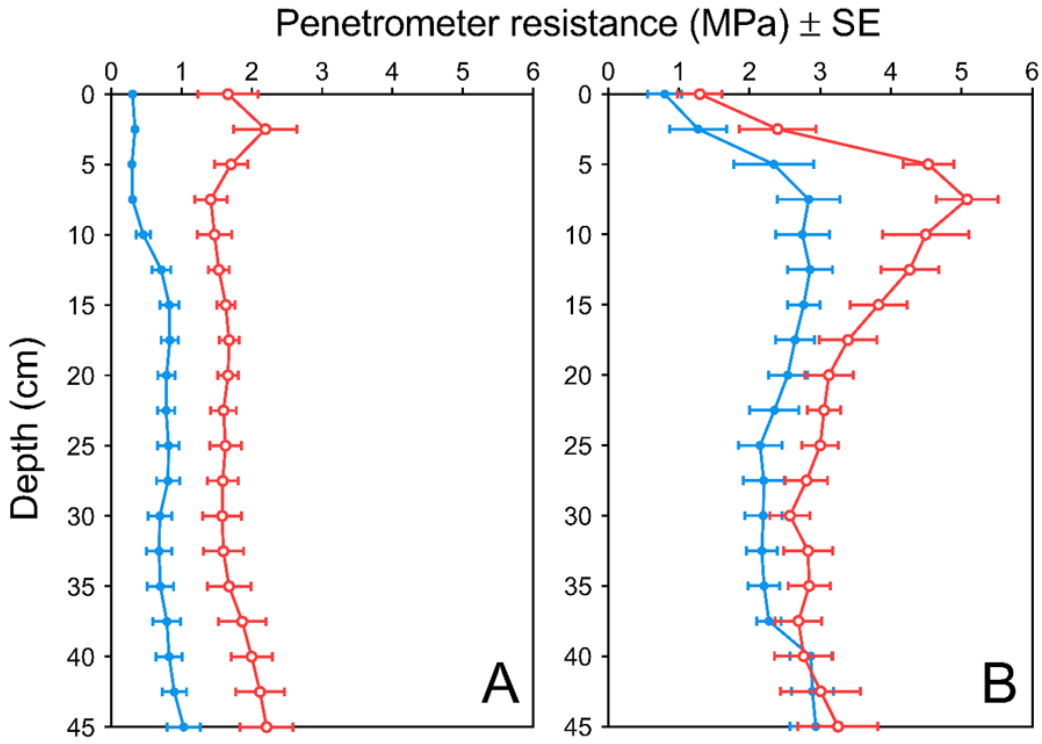

Figure 4.1 - Average penetrometer resistances ± SE for compacted (red) and non-compacted (blue) treatments at (A) the ARBC field site and (B) the PSU field site before planting. Mean soil moisture content was measured at 28.8% and 22.5% (v/v) for the compacted plots at ARBC and PSU respectively. For non-compacted plots the moisture content was 29.4% and 21.9% (v/v) for ARBC and PSU respectively. For the upper 7.5 cm of the non-compacted plots at ARBC the SE is too small to be visible. Average bulk density and volumetric moisture content over the profile can be found in Table S4.1, S4.2 respectively.

root washing could be carried out, up to a maximum of 2 weeks. Cores were divided into six 10 cm increments and roots were washed out of the soil over a 850 µm sieve for each depth profile. Roots were temporarily stored in 75% ethanol in water (v/v). Root length per section was measured by scanning roots on a flatbed scanner (Epson Perfection V700 photo, Epson America, Inc., Long Beach, USA) and analysis was carried out with WinRHIZO Pro 2013e system (Regent Systems Inc., Quebec, Canada). Each core increment was captured by images taken at a resolution of 400 dpi (15.75 pxls/mm), speed priority setting off and dust removal on high. Axial roots (nodal, primary, seminals) and lateral roots have been identified as having a diameter >0.6 cm and <1.0 cm for maize respectively (Cahn *et al.*, 1989; Varney *et al.,* 1991, Hund *et al.,* 2009). Using root diameter classes of 0 – 0.5, 0.5 – 1.0, 1 – 1.5, 1.5 – 2.0, 2.0 – 2.5, 2.5 – 3.0, 3.0 – 3.5, 3.5 -4.0, >4 mm permitted discrimination of coarse (> 1 mm diameter) and fine

(< 1 mm diameter) roots and attributed coarse roots to nodal root classes from the third node and upward. However individual nodal root classes could not be distinguished from cores as there is no reference to root crown position. Root length measurements (total, coarse and fine) and proportions (coarse and fine) were made for the entire soil core. Root distributions were compared on the basis of root length densities measurements within 10 cm increments. D_{95} and D_{75} are the rooting depth above which 95 and 75% of the total root length within a core were located. These rooting depth measurements were calculated by linear interpolation (Schenk and Jackson, 2002). When applied to the coarse root fraction in the core, in order to calculate the coarse rooting depth, these measurements are indicated as D_{95c}, D_{75c}. An overview of the different measurements directly measured or calculated from the winRHIZO scans and their definition can be found in Table 4.1.

4.3.3 Plant sampling

Two plants per subplot (4 replicate subplots per compaction treatment) were sampled at tasselling using the 'shovelomics' method (Trachsel *et al.*, 2011). Subsequent measurements per subplot were obtained by averaging between the two harvested plants per subplot. Root crowns were carefully washed and removed from the stem above the brace roots, brace roots not reaching the soil were clipped off at the base of the stem to expose the crown roots. Root crowns were then imaged to obtain information about the root angle from the horizontal in order to establish that root angle did not influence rooting depth (Fig. S4.1). Above ground plant parts were dried at 60° C for 3 days and dry weight of the biomass recorded (Fig. S4.2).

4.3.4 Statistical analysis

Genotypes were planted in a completely randomised split-plot design with compaction treatment at the whole-plot level (167.26 m^2) and twelve genotypes as subplots, replicated four times in each field site. Each subplot was 3.05 m x 4.57 m meters and ordering of genotypes (subplots) was randomised within each whole-plot. Every subplot was then planted with 4 rows of the appropriate

Table 4.1 – Definitions of the different measurements obtained after winRHIZO analysis of soil cores

Measurement	Abbreviation	Definition	Unit
Total root length	TRL	The summation of all individual root sections per 10 cm increment of the entire soil core	cm
Total coarse root length	TRL_c	The summation of all individual root sections per 10 cm increment with a diameter greater than 1 mm over the entire soil core	cm
Total fine root length	TRL_f	The summation of all individual root sections per 10 cm increment with a diameter smaller than 1 mm over the entire soil core	cm
Coarse root proportion	P_c	The ratio of total coarse root length versus total root length	%
Fine root proportion	P_f	The ratio of total fine root length versus total root length	%
Root length density	-	The root length found in the soil volume of a 10 cm increment of the soil core and this including all root diameter classes	$cm\ cm^{-3}$
Coarse root length density	-	The total coarse root length found in the soil volume of a 10 cm increment of the soil core	$cm\ cm^{-3}$
Relative root length density	-	The ratio of total root length density of a single 10 cm increment versus the sum of the total root length density found over the entire core	%
Relative coarse root length density	-	The ratio of coarse root length density of a single 10 cm increment versus the sum of the coarse root length density found over the entire core	%
Rooting depth	D_{95}	The rooting depth above which 95% of the total root length is located	cm
	D_{75}	The rooting depth above which 75% of the total root length is located	cm
Coarse rooting depth	D_{95c}	The rooting depth above which 95% of the total coarse root length is located	cm
	D_{75c}	The rooting depth above which 75% of the total coarse root length is located	cm

genotype, with 23 cm within row spacing and 75 cm between row spacing reaching a planting density of approximately 57500 plants per hectare. All coring variables (1 soil core per subplot) were transformed using a Box-Cox transformation to achieve normality before analysing the data in a split plot ANOVA. Total root length per genotype was plotted against averaged penetration resistance across both field sites. Root proportions per genotype were plotted per field site and post-hoc comparisons between compacted and non-compacted treatments were carried out using a Tukey. The same was done for coarse and total rooting depth, where additionally a linear regression was tested between these measurements. A generalised linear model was applied to assess the effect of field site, compaction and genotype and coarse and total root lengths on rooting depth. Relationships between variables were first assessed by correlation plots on pooled data across all genotypes. For the relationship between D_{75} and D_{75c} an analysis of covariance (ANCOVA) analysis was performed, followed by linear regression. As genotypic effects were identified by the split plot analysis on certain variables, individual linear regressions were made on the averaged genotypic values. Rooting depth data (coarse and total) and total root length averaged per genotype were normally distributed within impedance level and field site datasets. Root proportional data was analysed by using a beta regression (Cribari-Neto and Zeileis, 2015). To further analyse the variable relationships among each other, a principal component analysis (PCA) was conducted within field site – compaction treatment combinations. Principal components were retained based of eigenvalues greater than 1. In order to investigate different types of root distributions under compacted conditions rooting depth data was plotted against total root length data and genotypes with either similar root length and contrasting depth or with similar depth and contrasting root length were identified. Graphpad Prism (Graphpad Software, 2017) was used for visualising data and R version 3.5.0 (R Core Team, 2018) was used for data analysis.

4.4 Results

4.4.1 Root length reduction on compacted soil depends on field site

Total root length (TRL) from ARBC soil cores was greater than the total root length in PSU cores in both compacted and non-compacted plots (Figs. 4.2, S4.3). At ARBC total root length was reduced by 47.4% on average across all genotypes when grown on the compacted plots and total root length was clearly reduced for each genotype (Fig. 4.2, Table 4.2). As total coarse root length represents only a small part of the total root length (Figs. 4.2, 4.3), total root length reduction at ARBC is mainly due to reduced total fine root length (Fig. 4.3, Table 4.2). In contrast, at PSU, compaction did not significantly alter total root length but only adjusted it slightly (1.2%, $p < 0.10$) (Fig S4.3, Table 4.2). When the penetrometer resistance is considered across the two field trials the reduction in total root length for each genotype seems to reach an exponential threshold beyond 2 MPa (Fig S4.3).

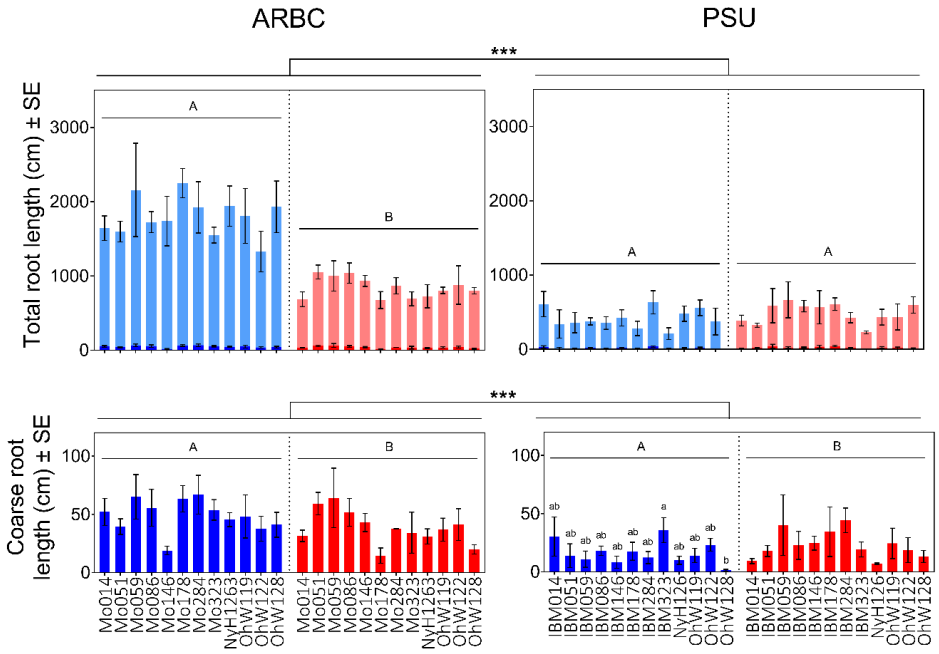

Figure 4.2 - Average total root length (cm) ± SE split into coarse (dark blue, dark red) and fine (light blue and light red) root length (cm) for maize genotypes tested at the two different field sites. Coarse roots are defined as having diameters larger than 1 mm, while fine roots are those with diameter smaller than 1 mm. Compacted measurements in red, non-compacted measurement in blue. Error bars represent standard deviations. ARBC stands for the Apache Root Biology Center field site, PSU stands for the Pennsylvania State University field site. If differences between the field sites (***, $p \leq 0.001$), treatments (A/B, $p \leq 0.05$) and genotypes (a/ab/b, $p \leq 0.05$) were present.

Table 4.2 - F-values for split plot analysis results of the different coring variables at the two field sites. P-values tested at the following levels of significance: † p ≤ 0.10, * p ≤ 0.05, ** p ≤ 0.01, *** p ≤ 0.001. Subscript c stands for coarse and f stands for fine when measurements are made on a separate root class. TRL stands for total root length, P stands for proportion of coarse or fine roots. D_{75} and D_{95} stand for rooting depth at which 75 and 95 percent of the total root length can be found.

		ARBC		PSU	
TRL	Compaction	77.12	***	1.37	
	Genotype	0.67		0.54	
	Compaction x Genotype	0.87		0.85	
TRL_c	Compaction	4.59	†	3.61	†
	Genotype	1.58		1.12	
	Compaction x Genotype	2.11	*	1.35	
TRL_f	Compaction	78.81	***	1.25	
	Genotype	0.67		0.56	
	Compaction x Genotype	0.81		0.83	
P_c	Compaction	18.29	**	3.43	
	Genotype	2.60	**	1.97	*
	Compaction x Genotype	2.12	*	1.34	
P_f	Compaction	18.62	**	2.63	
	Genotype	2.46	*	1.77	†
	Compaction x Genotype	1.93	†	1.30	
D_{75c}	Compaction	76.53	***	4.65	†
	Genotype	3.15	**	1.67	
	Compaction x Genotype	0.71		0.55	
D_{95c}	Compaction	42.29	***	0.78	
	Genotype	3.86	***	0.65	
	Compaction x Genotype	1.33		0.60	
D_{75}	Compaction	17.31	**	6.78	*
	Genotype	2.74	**	1.08	
	Compaction x Genotype	0.87		0.36	
D_{95}	Compaction	25.02	***	1.56	
	Genotype	2.70	**	1.11	
	Compaction x Genotype	1.33		0.33	

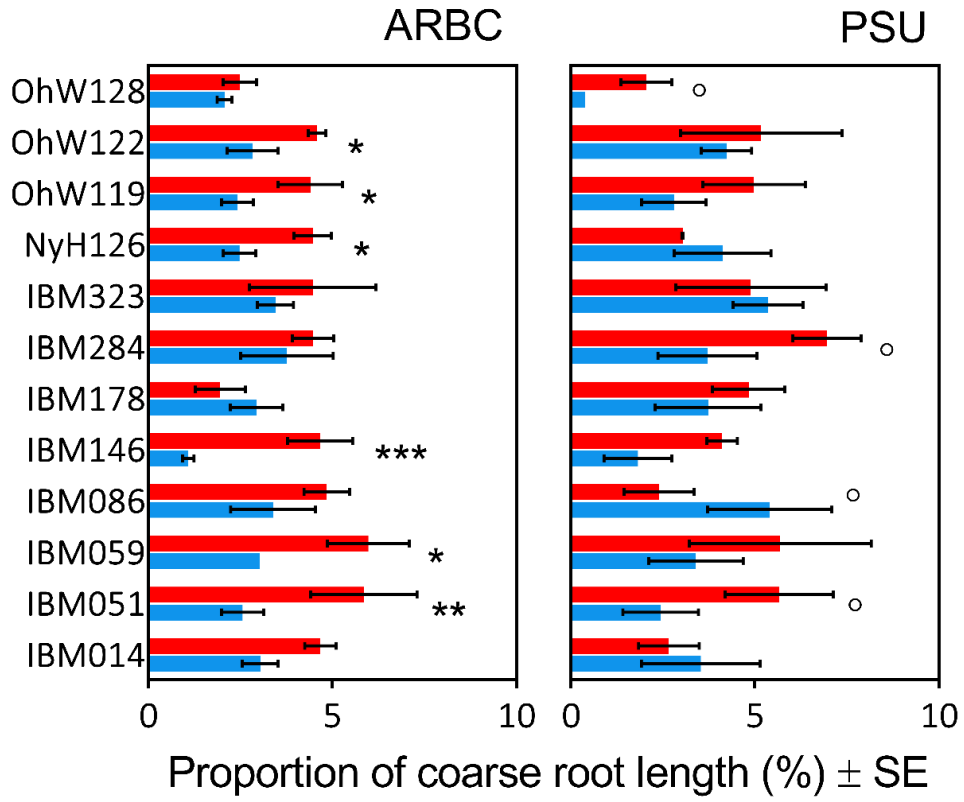

Figure 4.3 - Proportions of coarse (>1.0 mm diameter) root length (%) ± SE found in cores of different genotypes in two field sites. Non-compacted data in blue, compacted data in red. IBM059 (ARBC) and OhW128 (PSU) have such small standard errors they could not be visualised. Post-hoc Tukey comparisons within field site indicate when treatment effect was significant for each genotype at significance level ^{0} P ≤ 0.10, * P ≤ 0.05-0.01, ** P ≤ 0.01-0.001, *** P ≤ 0.001.

Total coarse root length (TRL_c) was differentially affected by the compaction treatment at both field sites (Fig. 4.2, Table 4.2). An impedance x genotype interaction was present at ARBC, but not PSU (Table 4.2). The overall average of total coarse root length decreased from 48.86 cm ± 3.35 (SE) to 38.95 cm ± 3.25 (SE) under compaction at ARBC, while it increased from 16.28 cm ± 2.18 (SE) to 23.65 cm ± 3.24 (SE) under compaction at PSU. Total fine root length (TRL_f) was negatively affected by the compaction treatment at ARBC (decreasing from 1755.92 cm ± 77.94 (SE) to 809.11 cm ± 37.33 (SE)), but was not affected at PSU (Table 4.2). At both field sites no genotypic differences were present for total fine root length (Table 2). A positive effect of compaction was noted on overall coarse root proportion (P_c) at ARBC with an increase from 2.8% to 4.4% under compacted soil conditions (Table 4.2, Fig. 4.3). At PSU an increase from 3.4% to

4.4% for P_c was observed (Fig. 4.3) although no compaction treatment effect was noted (Table 4.2). Genotype had significant effect on the proportion of coarse roots (P_c) and fine roots (P_f) at both field sites and for ARBC there was an interaction between compaction treatment and genotype present (Table 4.2). Compaction increased the proportion of coarse roots for most genotypes (Fig. 4.3). The only genotype that had greater P_c under impeded conditions at both field sites was IBM051. Other genotypes manifesting increased P_c under impeded conditions were OhW122, OhW119, NyH126, IBM146 and IBM059 at ARBC, but these did not show increased P_c at PSU. At PSU other genotypes such as OhW128 and IBM284 increased their P_c, while they did not at ARBC. A genotype that did not have greater coarse root proportions in response to compaction in either location was IBM086, this genotype had similar coarse root proportions at ARBC, while at PSU the coarse root proportions appeared smaller under compaction.

4.4.2 Total rooting depth versus coarse rooting depth

Absolute and relative measures of root length density per depth increment provided insight into how roots were growing within the soil profile and how root distributions change in response to compaction (Fig. 4.4). Root distribution changes became clearer when relative root length density measures were considered (Fig. 4.4B-D). Distributions of coarse root length density and root length density differed (Fig. 4.4) illustrated by differences in values of D_{95} and D_{75} (rooting depth considering all roots diameter classes) versus D_{95c} and D_{75c} (rooting depth considering coarse roots) (D_{75} and D_{75c} shown in Figs. 4.4, 4.5). Total rooting depth and coarse rooting depth measurements were correlated (Fig. 4.5E-F). The ANCOVA analysis showed that linear regression between D_{75} and D_{75c} were not different according to compaction (Fig 4.5, Table S4.4). D_{75} and D_{75c} were significantly reduced by compaction at both locations, while D_{95} and D_{95c} were only reduced at ARBC (Table 4.2). A genotypic effect on rooting depth was present at ARBC, but absent at PSU (Table 2). At ARBC some genotypes had significantly shallower total and coarse rooting depths under impeded conditions (IBM014, IBM059, IBM146, OhW119, OhW122) (Fig. 4.5A-C). Other genotypes such as OhW128 had shallower total root length under impeded conditions, but coarse rooting depth was not significantly reduced (Fig. 4.5C). In contrast,

IBM323, IBM178, IBM284 and IBM086 had shallower coarse rooting depth under compaction, but total rooting depth was not reduced (Fig. 4.5A-C). At PSU an effect of compaction was present on D_{75c} and D_{75} (Table 4.2). however only genotype, IBM059, showed significantly shallower coarse root distributions (Fig. 4.5B).

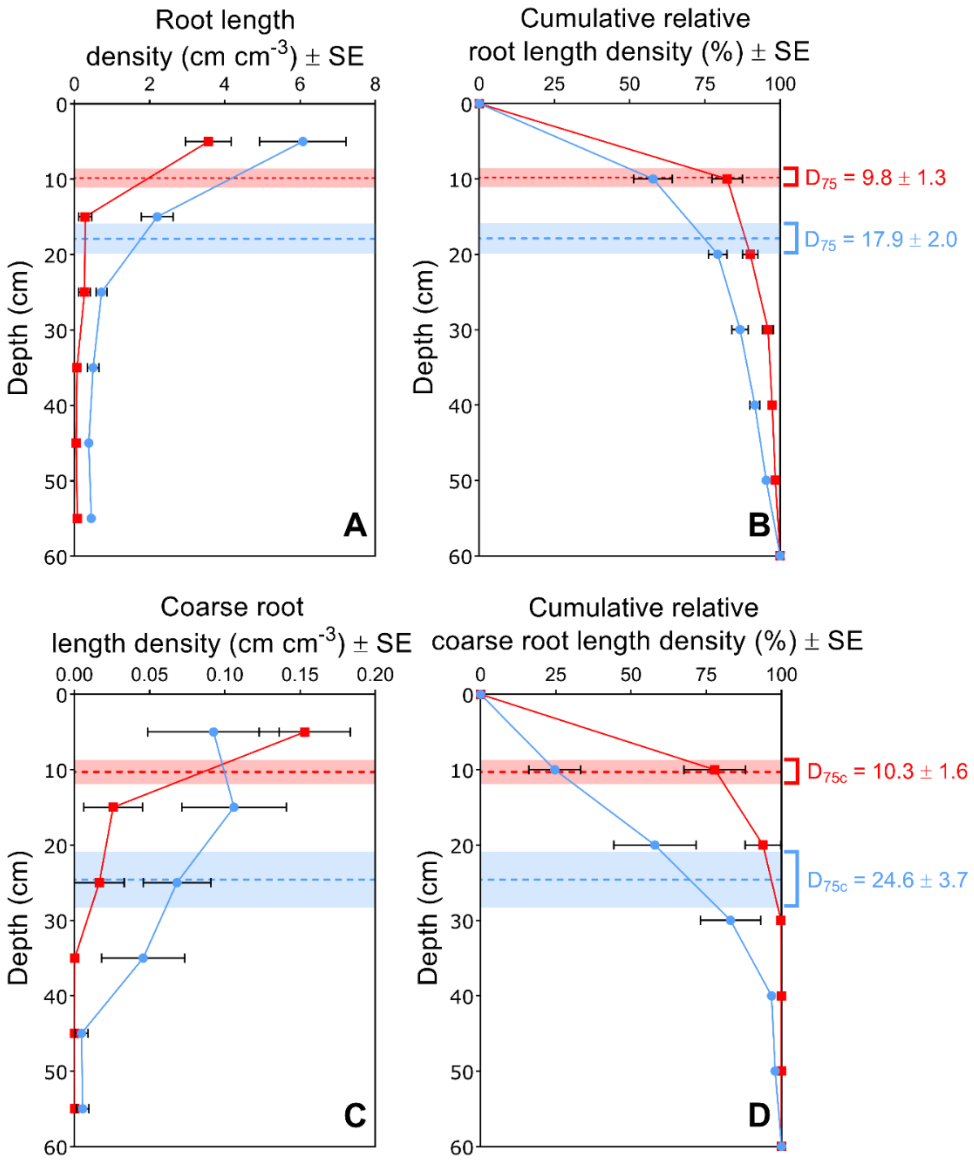

Figure 4.4 – Illustration of difference between absolute versus relative root length density distributions for genotype IBM014 considering total root length and coarse root length at the ARBC field site. (A) + (C) Absolute distributions of root length densities, (B) + (D) Relative distributions of root length densities. Compacted data in red and non-compacted data in blue. Error bars represent standard errors. The rooting depth (cm) ± SE where 75% of the total root length (D75) or coarse root length (D75c) was visualised by the striped line, coloured region represents SE for the depth measurements. No error bars shown when standard error was too small to visualise.

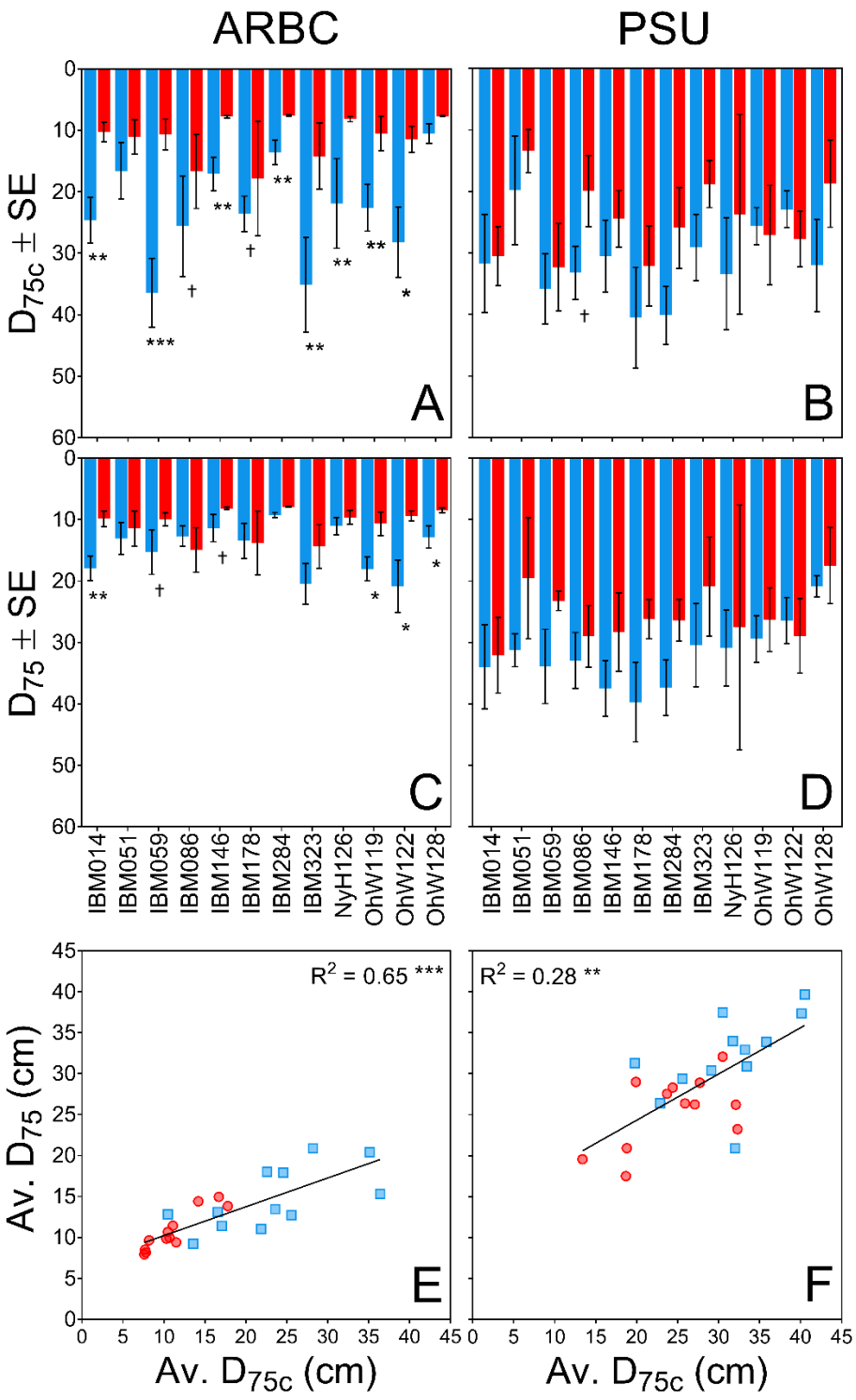

Figure 4.5 – Coarse and total rooting depth and their correlation for both field sites. (A) + (B) Average coarse rooting depth (D_{75c}), (C) + (D) Average total rooting depth, (E) + (F) Correlation between D_{75} and D_{75c}. Compacted data in red, non-compacted data in blue. Error bars represent standard errors. (A) + (C) + (E): ARBC field site and (B) + (D) + (F): PSU field site. Post hoc Tukey comparisons between compaction and noncompaction within each field site for each genotype were carried out on rooting depth data (panels A-D). Coarse and total rooting depth are linearly correlated (E-F). Levels of significance ** $P \leq 0.01$, *** $P \leq 0.001$.

4.4.3 Relationships between coring variables

Relationships between the different variables can be further explored through the correlation plot across all genotypes (Fig. S4.4), as well as the PCA plots per field site with treatment combination (Fig. S4.5). Individual linear regressions between coring variables depicting the different genotypes can be found in Figs. 4.6, S4.6, S4.7. Across all field sites and levels of impedance rooting depth variables (D_{95}, D_{75}, D_{95c} and D_{75c}) positively correlated to each other (Fig. S4.5). Likewise root length variables total root length (TRL), total fine root length (TRL_f) and total coarse root length (TRL_c) correlated strongly with each other (Fig. S4.5). Relationships between rooting depth and the other coring variables are discussed below.

4.4.3.1 The relationship between total rooting depth and other coring variables

A negative relationship between total root length and total rooting depth was found under ARBC non-compacted conditions (Figs. 4.6A, S4.6). General linear modelling indicated integrative effects of field site and compaction on the relationship between total root length and total rooting depth (Table 4.3). As total root length mainly consists of fine roots, a relationship persists between total fine root length and total rooting depth (Figs. S4.5, S4.6A). No such relationship was seen at PSU or under compaction (Figs. 4.6B, S4.5, S4.6B). No relationship was found for total rooting depth and total coarse root length (Fig. S4.6C-D) and coarse root proportion (Fig. S4.6E-F) under any scenario.

4.4.3.2 The relationship between coarse rooting depth and other coring variables

A positive relationship between coarse root proportion and coarse rooting depth (D_{75c}) was present under non-compacted conditions at the ARBC field site (Fig. 4.6C). This correlation was not observed under compacted conditions, nor at the other field site (Fig. 4.6C-D). Coarse rooting depth was also not correlated with total root length, total coarse root length or total fine root length under any of the field site with compaction treatment combinations (Figs. 4.6E-F, S4.7). This could

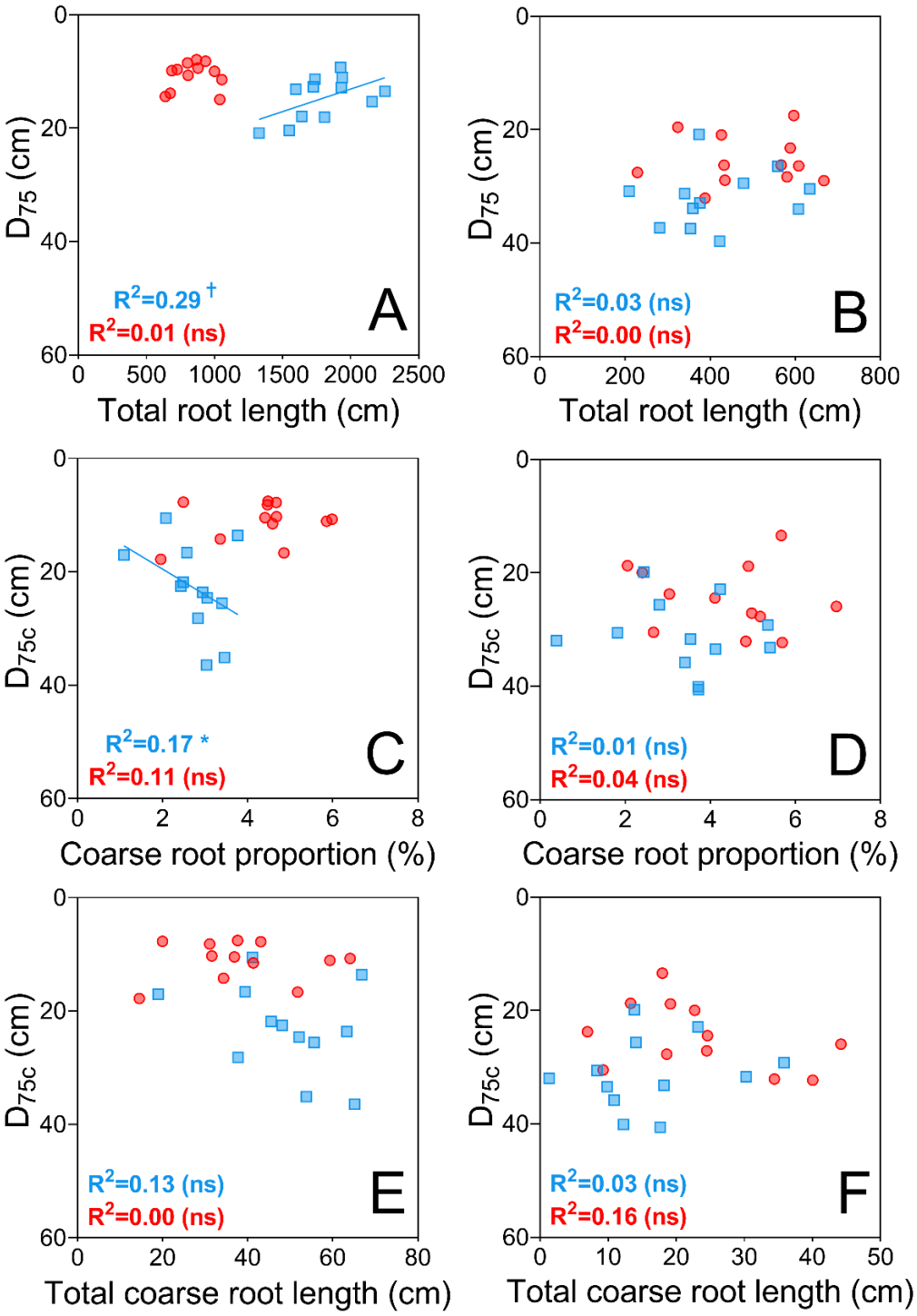

Figure 4.6 – Linear regressions between coring variables at the two different field sites. Field site ARBC visualised in A, C, E and field site PSU visualised in B, D, F. Compacted data (red) and non-compacted data (blue). Each datapoint represents the averaged value across the replicates for each genotype tested. Normal linear regression was used for A–B and E-F, and betaregression with a beta regression as data was proportional for C-D. Levels of significance † ≤ 0.10, * P ≤ 0.05, ** P ≤ 0.01, *** P ≤ 0.001.

Table 4.3 – Summary of general linear model results for the linear regression of total or coarse rooting depth (D_{75} or D_{75c}) with total root length (TRL) or total coarse root length (TRL_c). P-values tested at the following levels of significance: † p ≤ 0.10, * p ≤ 0.05, ** p ≤ 0.01 and *** p ≤ 0.001.

D_{75} ~ TRL + Field site + Compaction + Genotype

	F-value	p-value
Field site	57.36	***
Compaction	12.21	*
Genotype	1.22	
Total root length	3.09	†

D_{75} ~ TRL_c + Field site + Compaction + Genotype

	F-value	p-value
Field site	106.37	***
Compaction	10.2	*
Genotype	1.17	
Total root length	0.34	

D_{75c} ~ TRL + Field site + Compaction + Genotype

	F-value	p-value
Field site	35.83	***
Compaction	25.51	***
Genotype	2.12	*
Total root length	2.73	

D_{75c} ~ TRL_c + Field site + Compaction + Genotype

	F-value	p-value
Field site	41.39	***
Compaction	34.77	***
Genotype	1.99	*
Total root length	1.39	

also be deduced from the general linear model (Table 4.3).

4.4.4 Root length density distributions show field-site dependent genotypic adjustments to compacted conditions

Genotype had an effect on coarse rooting depth for ARBC but not PSU (Table 4.2). Coarse (Fig. 4.7) and total (Fig. S4.8) root length distributions over the soil profile at PSU had smaller root length densities at PSU than at ARBC. Distribution differences with depth were more evident at PSU, even though no significant statistical effect of genotype was noted on D_{75} or D_{75c}. Based on total coarse root length (TRL_c) and coarse rooting depth measurements in compacted soils, different genotypes were selected for each field site (Fig. S4.9). A similar analysis was carried out based on total root length and depth (Figs. S4.10, S4.11). For coarse measurements there were genotypes with similar total coarse root length, but with different rooting depths, representing shallow and deeper root systems with similar root system sizes (IBM284 versus IBM323 for ARBC and IBM051 and OhW122 for PSU) (Fig. 4.8A).

4.5 Discussion

In this study, on two different soils with compacted and non-compacted plots, total root length reduction by mechanical impedance was field site dependent (Figs. 4.2, S4.8, Table 4.2). Coarse root proportions were influenced by genotype at both field sites (Fig. 4.3, Table 4.2). Rooting depths of coarse and total roots were strongly correlated (Fig. 4.5). Root length and rooting depth variables were not correlated when plants were grown on compacted plots (Figs. 4.6, S4.5, S4.6, S4.7). These results support the hypothesis that the ability of roots to grow to depth through compacted soils is not dependent on the amount of roots formed by the root system. Furthermore, the hypothesis that root length density distributions are either characterised by avoidance or by adaptive strategies for different genotypes when grown in compaction is discussed.

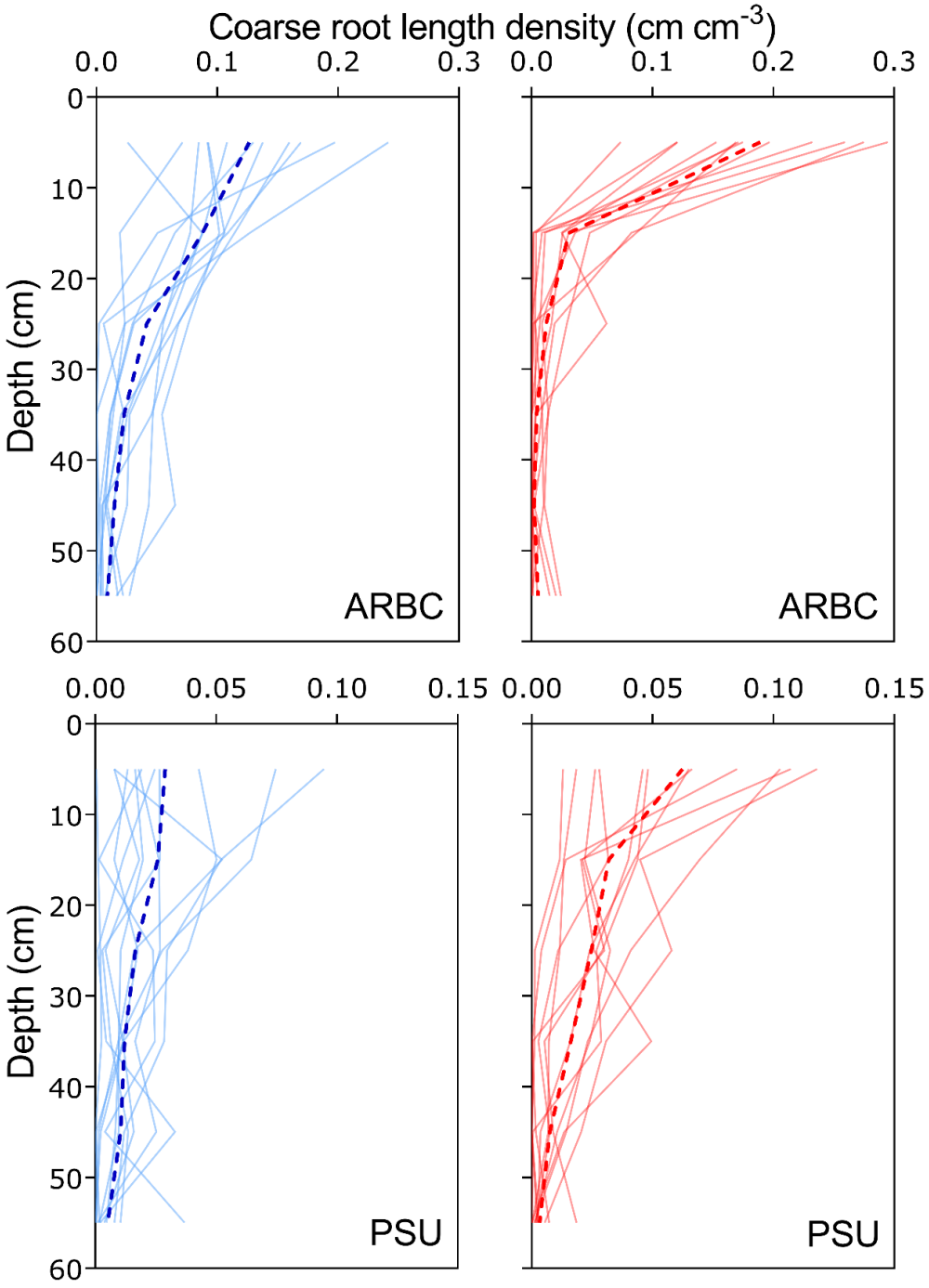

Figure 4.7 - Genotypic variation in the coarse root length density (cm cm^{-3}) per depth increment across two field sites and two compaction treatments. Non-compacted data in blue and compacted data in red. The striped lines are the averages across all genotypes, lighter coloured lines are the average for individual genotypes tested. Similar plots for total root length density distributions can be found in Fig. S4.8

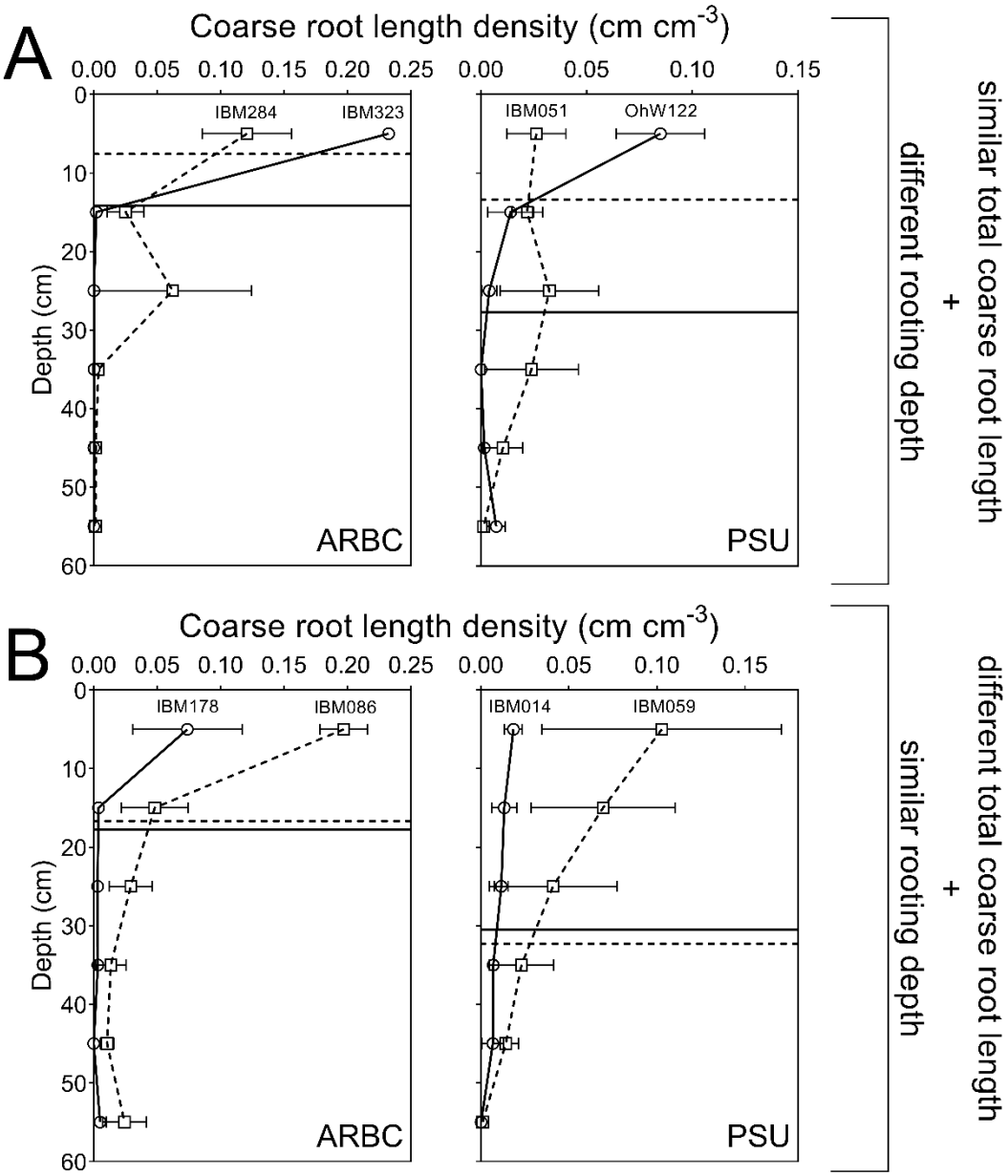

Figure 4.8 – Coarse root length densities (cm cm^{-3}) ± SE distributions with soil depth on compacted plots comparing (A) two genotypes per field season with similar total coarse root length but with different associated rooting depths and (B) two genotypes with similar rooting depths but with different total coarse root lengths. For (A) striped lines stands for the deeper rooting genotype and associated D_{75c}, while the solid line stands for the shallower rooting genotypes and associated D_{75c}. For (B), the solid line is used for the genotype that produces less roots but reaches equally deep as the genotype that produces more roots (striped lines). No error bars shown when standard error was too small to visualise. Selection comparison can be found in Fig. S4.9. Similar plots for total root length density distributions can be found in Fig. S4.11

4.5.1 Root phenotypes show high levels of plasticity

4.5.1.1 Field site effects on root systems

Total root lengths (TRL), total fine root lengths (TRL_f) and total coarse root lengths (TRL_c) were greater at ARBC then at PSU (Figs. 4.2, S4.3, S4.6). The significant reduction of the fine root length due to impedance at ARBC could influence the proportions of fine and coarse roots. Greater root proportional changes were observed at ARBC versus PSU, which could potentially be driven by a disproportionally greater reduction of total fine root length versus that of total coarse root length (causing a shift towards greater coarse root proportions). Rooting depths D_{75} and D_{75c} were different at the two field sites (Figs. 4.5, Table 4.3). Differences between field sites for observations considering root length, root proportions and rooting depth could be related to differences in soil parameters. Maize seedlings had significantly longer seminal roots in a sandy loam versus a sandy clay loam (Panayiotopoulos *et al.*, 1994) while rooting depths of grapevines were deeper in coarse textured soils than fine textured soils (Nagarajah, 1987). Greater root length was possibly attained at ARBC because of the greater sand fraction in the soil versus PSU. Another possible explanation for the root length differences between ARBC and PSU could be a difference in root-soil contact between the field sites. On the non-compacted plots of PSU, smaller bulk densities could mean reduced levels of root-soil contact, which in turn reduces water and nutrient uptake (Veen *et al.*, 1992). The ARBC field site consisted of a more uniform, less structured soil, while the PSU field site had more pronounced soil structure in terms of aggregation observed in the field. Roots can take advantage of cracks or bio-pores from earthworms or old root channels present to bypass compacted layers (Atwell, 1993; Hatano *et al.*, 1988; Stirzaker *et al.*, 1996). Cracks and pores will impose lower axial pressures on roots than bulk soil (Jin *et al.*, 2013). It is likely that the presence of such low-resistance channels in the soil structure at PSU could have permitted deeper rooting than at ARBC.

4.5.1.2 Compaction influences root system distribution

Compaction influenced root growth at both field sites, but more significantly at ARBC, where all rooting variables were significantly affected (Table 4.2). At both field sites the compaction treatment influenced the average total coarse root length across genotypes in different ways (Fig. 4.3, Table 4.2). Total coarse root length decreased at ARBC, which could be due to the effect compaction had on root system size in general. Total and fine root length were more significantly reduced than total coarse root length under compaction (Table 4.2, Fig. 4.2). Reductions in root length in compacted soil has been reported for different species including maize (Grzesiak, 2009; Iijima and Kono, 1991). At PSU total and fine root length were not significantly affected by compaction (Table 4.2) and total coarse root length increased (Fig. 4.3, Table 4.2). Increased total coarse root length could potentially be caused by radial expansion as roots generally increase in diameter when experiencing mechanical impedance. Elongation is slowed compared to elongation rates at lower levels of impedance, which in turn decreases root length (Bengough *et al.*, 2006; Bengough and Mullins, 1991; Bengough and Young, 1993). While all root length measures decreased at ARBC, these observations on root length were different at PSU. Under different field conditions fine and coarse roots were differentially affected by the compaction treatment. Coarser roots such as seminal or nodal root axes were more impeded then lateral roots possibly reflecting the fewer macropores present under compacted conditions. Such effects have been found in barley growing in glass ballotini of different sizes, with larger pores only restricting seminal growth and smaller pores restricting both laterals and seminal growth of barley (Goss, 1977). Laterals capable of growing in pores larger than their own diameters would encounter less impedance than those laterals forced to grow through bulk soil or smaller pores (Iijima and Kono, 1991).

Under compaction both rooting depth (D_{75}) and rooting depth of coarse roots (D_{75c}) decreased at both field sites (Tables 4.1, 4.2; Figs. 4.5, 4.6, S4.6, S4.7). Shallower rooting depth probably reflect slower root elongation rates, so it will take longer for a root to reach deep soil strata. Smaller differences in rooting depth of compacted and non-compacted plots at PSU (Fig. 4.5) could be due to the

smaller differences in penetration resistance with increasing depth versus ARBC (Fig. 4.1). Roots at PSU would initially experience greater levels of impedance, but once they pass this zone should be able to elongate more normally. The reduction in rooting depth under compaction is in agreement with observations with wheat (Barraclough and Weir, 1988; Chen *et al.*, 2014a). Compaction altered root distribution, generally shifting root distribution to shallower strata (Figs. 4.4, 4.5, 4.7, S4.8). Multiple studies have described similar redistributions of roots under impeded field conditions for various crops (Barraclough and Weir, 1988; Brereton *et al.*, 1986; Chen and Weil, 2011; Chen *et al.*, 2014a). For maize specifically, roots of 2-3 week old plants were confined to surface layers under compaction (Veen and Boone, 1990). A similar observation was made during a 4 week growing period for maize grown in root boxes (Iijima *et al.*, 1991) and in the field up to tasselling (Laboski *et al.*, 1998).

4.5.1.3 Impedance influenced genotypes differently

Under compaction at both field sites most genotypes had a greater proportion of coarse roots (Fig. 4.3) and genotypes differed in this response (Table 4.3). An increased proportion of coarse roots could either be attributed to (1) the reduction of the fine root proportion, (2) the increase in diameter of roots grown under impeded conditions due to thickening or (3) a combination of the two. At ARBC, total fine root length was significantly reduced (Table 4.3, Fig. 4.2), which in turn would influence root proportions. However, as there was no such reduction of total fine root length at PSU, root thickening is probably the main cause of a shift in root proportions at PSU.

Genotypic differences were found for total and coarse rooting depth variables (Figs. 4.5, 4.7, 4.8, S4.6, S4.7, Tables 4.2, 4.3). As no relationship between root length variables existed (with the exception of negative relationship between total root length and total rooting depth under non-compacted conditions at ARBC), in addition with the finding that deeper rooting was not associated with root system size, other mechanisms that promote root growth under impeded conditions must be at play. Root phenes that have been found to contribute to overcoming impedance under these specific conditions include anatomical traits

such as reduced cell file number and increased levels of aerenchyma (Lynch and Wojciechowski, 2015). It has also been suggested that anatomical traits such as smaller outer cortical region cells will stabilize a root during the penetration of a harder soil layers (Chimungu *et al.,* 2015a). Other phenes are sharper root tip shape, the presence of root hairs, the production of mucilage, root cap sloughing and steeper growth angles (Iijima *et al.*, 2000, 2004; Bengough *et al.*, 2011; Haling *et al.*, 2013; Jin *et al.*, 2013; Lynch and Wojciechowski, 2015; Colombi *et al.*, 2017b). How all these phenes can synergistically work together is worthy of further investigation.

4.5.2 The relationship between root length and rooting depth varies among genotypes

Root length and rooting depth are not related under impeded conditions (Figs. 4.6, S4.4, S4.6, S4.7). Coarse rooting depth, representing nodal roots, responded differently to compaction among genotypes. Genotypes such as IBM059 or IBM323 at ARBC or IBM086 at PSU grew deeper under non-compacted conditions but reduced their coarse root length under compaction (Fig. 4.5A-B). IBM178 grew intermediately deep (at ARBC), and deep (at PSU) but did not reduce its coarse rooting depth to the same extent as the aforementioned genotypes (Fig. 4.5A-B). This suggests that nodal roots of some genotypes were obstructed by the compaction treatment while nodal roots of other genotypes were capable of growing through.

Genotypes with similar root system size that reached different rooting depths were found (Figs. 4.8A, S4.9) as well as genotypes with similar deeper coarse rooting depth but with different total coarse root length (Figs. 4.8B, S4.10). Coarse rooting depths can thus be reached in different ways as the root system with smaller values for coarse root length densities were able to grow as deep as the root systems that have greater coarse root length density at depth. Shoots can be sustained by different root system sizes and rooting depths as long as water and nutrients are available. Therefore rooting depth under compaction is not simply related to the amount of roots formed. How each type of root distribution with depth could sustain plant growth is discussed in the following section.

4.5.2.1 Root systems with equal coarse root length reach different depths

Coarse roots of some genotypes were obstructed, while others managed to grow through impeded soil domains and reached deeper strata (Fig. 4.8A). If nodal roots are sufficiently impeded, these and any laterals roots emerging from them will automatically be located within the upper soil strata. However laterals may grow downwards from a shallow starting point when they experience less impedance than nodal roots by, for instance, making use of smaller pores (Goss, 1977). Increased lateral branching has been observed in the non-impeded parts of the soil (Montagu *et al.*, 2001) and will enable a plant to extract water and nutrients when root length is maintained and sufficient soil resources are available in the unimpeded soil (Barraclough and Weir, 1988). Compensatory root growth introduces more roots in the less impeded domains, often in the upper soil strata (Barraclough and Weir, 1988; Materechera *et al.*, 1993; Nosalewicz and Lipiec, 2014; Pfeifer *et al.*, 2014a). A similar redistribution can be seen in the compacted plots (Figs. 4.7, S4.8). Compensatory mechanisms may influence nutrient and water acquisition. Greater root densities near the surface will deplete the resource supply in the upper soil strata, including P, K, shallow water, and freshly mineralized N, while reduced access to deeper soil strata will reduce the access to mobile resources such as leached N and water.

Rooting depth has been linked to water acquisition, especially under drought conditions were deeper rooting increases yield (Gao and Lynch, 2016; Hund *et al.*, 2009; Lynch, 2013, 2018; Chimungu *et al.*, 2014a, 2014b; Lynch *et al.,* 2014; Zhan *et al*., 2015). In this study water deficit was not applied, but it has been shown that compaction can make water deficit stress more severe (Grzesiak *et al.*, 2014). Even without the presence of water deficit stress, increased water uptake from the topsoil can be present on compacted soils. This in turn will increase the penetration resistance within the topsoil and further limit access to the deeper soil layers (Colombi *et al.*, 2018). A root system that is limited to shallow soil strata will thus be more at risk for water deficit both in terms of reduced access, as well as increased water depletion in its local soil environment. Clear shifts in root distribution occurred on the field sites and changes in root proportion, changes in rooting depth, and changes in root distribution were

present (Figs. 4.3, 4.5, 4.7, S4.8). How these shifts influence resource acquisition under impeded field conditions merits further investigation. It would also be interesting to test phenotypes that contrast in their ability to grow deeper under impeded soil conditions for differences in nutrient and water acquisition.

Stresses such as waterlogging have been found to have a more severe impact in impeded soils (Grzesiak *et al.*, 2014). Environmental effects such as temperature fluctuations or soil drying by direct evaporation pose additional threats to more shallow root systems (Lynch, 2018). Overall compensatory root growth can be seen as a stress avoidance strategy as plants come less into direct contact with the impeded soil regions and grow where impedance is lower. This can be considered as an indirect adaptation or response to the impeding conditions. Roots adapted to impedance are characterised by traits that help them overcome impedance, enabling them to grow better in harder soils. Those genotypes capable of rooting deeper and of overcoming impedance stress are at less at risk of nutrient deficiencies, of lack of access to water and of other environmental stresses.

4.5.2.2 Equal depths can be reached by root systems of different sizes

Genotypes that contrasted in root system size (measured as total coarse root length) were able to reach similar depths on compacted plots (Figs. 4.8B, S4.9). Greater amounts of coarse roots (measured as greater TRL_c) would be found when a maize plant forms more root axes per nodal position, additionally greater amounts of coarse roots may also be caused by root thickening. None of the rooting depth measurements correlated with TRL_c (Figs. 4.6E-F, S4.4A-D, S4.7). The ability of a root system to grow deeper in compacted soils is therefore not dependent on the amount of roots formed as both large and parsimonious root systems can reach similar depths on compacted plots at both field sites. This is in contrast with observations on wheat, where penetrability of a harder wax layer was related to amount of root axis formed (Whalley *et al.*, 2013), or that denser root systems of lupin are deeper rooting (Chen *et al.*, 2014a). On the other hand, comparisons between species show that species with a larger number of roots in the top layers of a layered medium did not automatically have greater

penetration rates through the compacted layer (Materechera *et al.*, 1993). A field study with two rice varieties showed that varieties with a greater root density were able to root deeper under control conditions, but under greater penetrometer resistances became more strongly affected than others with lower rooting densities (Cairns *et al.*, 2004).

The formation of more roots can have benefits such as increased foraging for water and nutrients or reduced risk of root loss due to pests and diseases (Lynch, 2003, 2018, Postma *et al.*, 2013). Increased root formation can however come at a substantial costs (York *et al.*, 2013, Lynch, 2003). Greater elongation rate, greater root diameter, increased branching or greater formation of axial roots increase the metabolic cost of the root system (York *et al.*, 2013, Lynch, 2018). Second, the formation of too many roots will introduce competition for internal and external resources (Lynch, 2018). Excessive root formation not only induces within plant competition for resources, it also increases the maintenance and formation costs. Other traits, such as increased aerenchyma formation, large cortical cell size, reduced cortical cell file number or reduced crown root number bring costs down (Lynch, 2003, 2018) which would enable these plants to allocate resources elsewhere. For instance, it has been shown that maize with fewer crown roots are able to allocate roots deeper (Saengwilai *et al.,* 2014a; Gao and Lynch, 2016, Lynch 2018). Recent experiments by Guo and York (2019) showed excising nodal roots stimulated greater shoot biomass and root length at depth under low N conditions as biomass was reallocated to lateral and early nodal roots. Under impeded conditions, metabolic cost reduction might be significant. A recent study by Colombi (2019) found energy costs were linked to cortical cell diameters, with greater cell diameters reducing the metabolic cost under impeded conditions. As both large as well as parsimonious root systems were able to reach similar coarse rooting depth (Figs. 4.9B, S4.11B) therefore it is suggested that parsimonious phenotypes could potentially allocate more resources to shoot growth. This effect could be apparent under high input systems, where improved conversion of soil resources to yield would be greater for parsiminous phenotypes (Lynch and Brown, 2012; Lynch, 2018).

4.6 Conclusions

Rooting depth and root length were not correlated under impeded conditions. Different coarse rooting depths were reached by genotypes characterised by similar root system sizes. We found that the amount of roots formed by the root system does not determine the ability of those roots to grow deeper under impeded conditions. It can be suggested that genotypes better adapted to impedance (and therefore rooting deeper) are less at risk of additional stresses such as nutrient deficiency, soil drying, lack of access to water and other environmental conditions. One can hypothesise that excessive root formation will introduce greater competition for internal and external resources, furthermore larger root systems have greater metabolic costs associated with them. If parsimonious phenotypes will be able to steer resource allocation to shoot growth better than larger root systems this could lead to improved yields.

Chapter 5 – Root anatomical traits contribute to deeper rooting of maize (*Zea mays* L.) under compacted soil conditions

Paper as submitted to *Journal of Experimental Botany*

Chapter 5 explores the hypothesis that deeper rooting under impeded conditions is not explained by root thickening. Additionally this chapter provides new insights into the anatomical basis of root responses to mechanical impedance. Genotypic variation in root anatomy was found to be related to rooting depth, with anatomical adaptations being more important for thinner versus thicker root classes.

This paper is currently in review for *Journal of Experimental Botany.*

Author contribution

Project supervision and paper editing provided by K.W. Loades, A.G. Bengough, S.J. Mooney and J.P. Lynch. Experiments, analysis and paper preparation by D.J. Vanhees.

5.1 Abstract

To better understand the role of root anatomy in regulating plant adaptation to soil mechanical impedance, 12 maize lines were evaluated in two soils with and without compaction treatments under field conditions. Penetrometer resistance was 1 to 2 MPa greater in the surface 30 cm of the compacted plots at water content of 17-20% (v/v). Root thickening in response to compaction varied among genotypes and was negatively associated with rooting depth at one field site under non-compacted plots. Thickening was not associated with rooting depth on compacted plots. Genotypic variation in root anatomy was related with rooting depth. Deeper-rooting plants were associated with reduced cortical cell file number in combination with greater mid cortical cell area for node 3 roots. For node 4, roots with increased aerenchyma had deeper roots. A greater influence of anatomy on rooting depth was observed for the thinner root classes. No evidence that root thickening is related to deeper rooting in compacted soil was found. However anatomical traits are important, especially for thinner root classes.

5.2 Introduction

Mechanical impedance has important effects on root development and plant growth as it restricts soil exploration and therefore nutrient and water capture (Batey, 2009; Lipiec and Hatano, 2003; Merotto and Mundstock, 1999; Yamaguchi and Tanaka, 1990). Improved understanding of root adaptations to mechanical impedance could contribute to the development of crops with improved exploration of hard soils, commonly encountered in deep soil horizons, with improved water and nutrient acquisition (Lynch and Wojciechowski, 2015).

Root diameter often increases in response to mechanical impedance (Atwell, 1993; Colombi and Walter, 2016; Iijima *et al*., 2000; Pfeifer *et al*., 2014; Pritchard, 1994; Tracy *et al*., 2012) as cell division decreases (Clark *et al*., 2003) and root elongation slows (Atwell, 1993; Gregory, 2006). Mechanical impedance greater than 2 MPa reduces root elongation for most plants (Atwell, 1993). The energy cost of root elongation increases with increasing penetration resistance (Colombi

et al., 2019). Radial thickening is thought to relieve stress from the root tip while deforming the soil near the root tip, allowing the root to penetrate deeper into the compacted soil (Atwell, 1993; Bengough *et al*., 2006; Gregory, 2006; Hettiaratchi, 1990; Kirby and Bengough, 2002; Pritchard, 1994). Furthermore, thicker roots have been linked to increased buckling resistance (Chimungu *et al*., 2015a; Clark *et al*., 2003). Radial thickening occurs within the elongation zone immediately basal to the root tip. The elongation zone itself becomes shorter when under mechanical impedance (Croser *et al*., 1999; Bengough *et al*., 2006) which can reduce the friction upon this zone as the zone has become smaller (Atwell, 1993). Theoretical simulations of roots growing through a strong sandy loam soil showed that larger roots were associated with smaller shear stresses over the root surface and lower axial stress at the root tip, and that thickening as such could be of advantage to roots that experience impedance (Kirby and Bengough, 2002). Thicker roots might be beneficial while thickening itself would only contribute to reduce stress on a localised scale at the root tip. The difference between a thicker root and a thickening root should be noted as thickening is also associated with reduced elongation rates due to anatomical changes. Mechanical impedance will induce shorter and fatter cells to be formed (Bengough *et al*., 2006), which contribute to reduced elongation. Mechanical impedance also causes slower cell flux out of the meristem (Croser *et al*., 1999). Reduced root elongation reduces soil exploration, while those roots that do not thicken and are able to elongate normally would be capable of acquiring more water and nutrients. Reports regarding the thickening response of specific root classes are scarce as most studies consider seedling roots. Root diameter and cross-sectional area of 2-day old wheat seed-borne roots increased under increased soil strength up to a maximum diameter of 0.78 mm, while diameters of nodal roots (first node) increased less while still reaching a similar maximum (Colombi *et al*., 2017b). In another recent study (Colombi and Walter, 2016) root diameter under compaction increased in young soybean adventitious roots, however, as the plants aged root diameter was similar between compacted and non-compacted conditions. The adaptive utility of root thickening, as opposed to the possibility that it represents reduced cell formation and elongation, remains unclear.

Root anatomical phenotypes can improve adaptation to abiotic stresses including suboptimal nitrogen (Lynch, 2013; Saengwilai *et al*., 2014b; Schneider *et al*., 2017), phosphorus (Schneider *et al.*, 2017, Galindo-Castañeda *et al.*, 2018, Schneider and Lynch, 2018, Strock *et al.*, 2018), water deficit (Jaramillo *et al.*, 2013; Lynch, 2013; Chimungu *et al.*, 2014a, 2014b, Lynch, 2018), as well as flooding (hypoxia; Yamauchi, 2013). Root anatomy correlated with penetration of strong wax layers in maize (Chimungu *et al*., 2015a). Thickening under impedance has been related to the changes in the underlying tissues and cellular structures. Both the cortex, as well as the stele, react to mechanical impedance. Cortical changes such as the addition of cell layers (Wilson *et al*., 1977, Colombi *et al.*, 2019) or the expansion of cortical cells have been observed (Atwell, 1988; Colombi *et al*., 2017b, 2019; Hanbury and Atwell, 2005). For instance, in lupin, which is usually able to penetrate strong soil (Materechera *et al*., 1991), radial thickening is caused by the swelling of cortical cells, rather than the addition of cell files (Atwell, 1988; Hanbury and Atwell, 2005). However, diverse observations have been made for different species and under a range of experimental conditions. A good overview of different cortical changes associated with impedance, as well as changes to vascular tissues and meristems has been discussed recently by Potocka and Szymanowska-Pułka (2018). Additionally, increased aerenchyma area has been observed under impeded conditions (Colombi *et al*.,2017b; Colombi and Walter, 2016), which may have adaptive value (Lynch and Wojciechoski, 2015). Recent developments such as Laser Ablation Tomography (LAT) accompanied by image analysis have enabled more rapid anatomical phenotyping (Hall and Lanba, 2019, Strock *et al.*, 2019), facilitating the analysis of multiple root classes, genotypes, and environments, to discern relationships between root anatomical phenotypes and responses to mechanical impedance.

Comparisons among species suggest that plants with thicker seedling roots are better able to penetrate hard soils (Materechera *et al*., 1991). For pea, a threefold increase in maximum growth force was associated with primary versus lateral roots with primary roots exerting 6 - 32% more pressure (Misra, 1997). A study of 14 wheat genotypes revealed that traits such as root cross-sectional area, stele

area, cortical area, root cortical aerenchyma, cell size and cell file number were affected by increased soil strength, and that responses were both genotype-dependent as well as between primary and first node roots (Colombi *et al*., 2017b). How different axial root classes of maize adapt to impedance under field conditions has so far not been considered. A single root system of maize consists of nodal root axes characterised by increasing diameters and associated changed anatomy per node (Fig. 5.1) that potentially could react differently to mechanical impedance. Diameter changes associated with underlying changes in anatomy have so far not been studied across different maize genotypes under impedance. Different soil types, in this instance soil texture, can influence the root diameter of tomato plants as shown by Tracy *et al*. (2012). Field studies carried out on different soil types have identified differences in root distributions under impeded conditions, but anatomical differences between fields have so far not been accounted for.

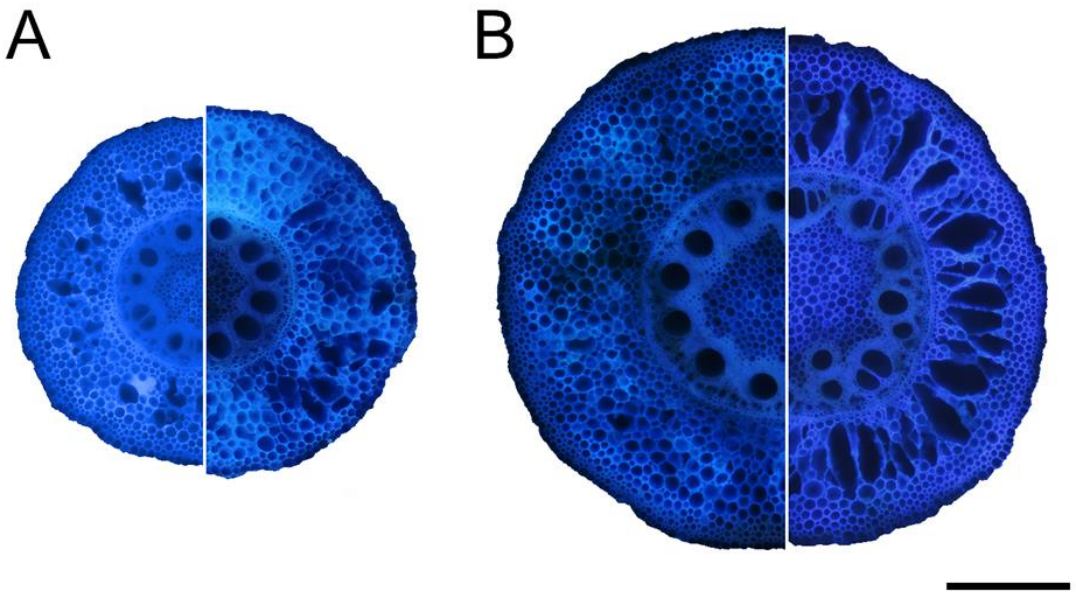

Figure 5.1 – Cross-sectional images obtained by Laser Ablation Ablation Tomography depicting the anatomical differences within each node. (A) Node 3 cross-sections with greater cell file number, smaller cells on the left and smaller cell file number and bigger cells on the right. (B) Node 4 cross-sections with lower aerenchyma area on the left and greater aerenchyma area on the right. Scale bar at 500 μm for all images

One suggestion is that thickening *per se* does not explain differential rooting capabilities among maize genotypes. The hypothesis that radial thickening in response to mechanical impedance will vary among genotypes, root classes, and soil types was tested. Further it was investigated if older, thinner nodes will thicken more than younger, thicker nodal roots. The hypothesis is that node-specific root anatomical phenotypes influence growth through compacted soils, especially in thinner roots from older nodes, as opposed to thicker roots from younger nodes. Roots of younger nodes, that are thicker from the start, do not have a need for extensive thickening and hence less cellular adjustments would be needed. However younger, thicker roots can benefit from tissue adjustments, such as the formation of aerenchyma. This can further aide root growth in compacted soils as these soils are often not just a source of impedance but are also associated with lower level of oxygen (Lynch and Wojciechowski, 2015).

The purpose of this study was to identify if radial thickening is related to root penetration of hard soils or rather is an indication of non-penetration, in contrasting soils, genotypes and root classes. Secondly, the hypothesis that root anatomical phenotypes contribute to growth in hard soil was tested.

5.3 Materials and methods

5.3.1 Growth conditions and plant material

The first field site was planted June 16, 2016 at the Apache Root Biology Center (hereafter referred to as ARBC), Willcox Arizona, USA (32º01'N, 109º41'W) where the soil is a Grabe series (coarse-loamy, mixed, superactive, calcareous thermic Torrifluvent) clay loam. The second field site was planted on July 10, 2017 at the Russell E. Larson Agricultural Research Center in Rock Springs (hereafter referred to as PSU), Pennsylvania, USA (40º42'N, 77º57'W) on a Hagerstown series silt loam soil (fine, mixed, semiactive, mesic Typic Hapludalf). To increase mechanical impedance heavy machinery (4 wheel tractor, 4 tonnes at ARBC and 3-axle truck, 20 tonnes at PSU) was passed over the treated plots (8 passes at ARBC and 4 passes at PSU). Penetrometer resistance (Fieldscout SC900 Compaction Meter, ½ inch cone, Spectrum Technologies Inc., Aurora, Illinois) (Fig. 4.1), bulk density (Table S4.1) and volumetric moisture content (Table S4.2)

through the soil to a depth of 50 cm were measured. Soil moisture content was monitored at the whole plot level using PR2/6-tubes (Delta-T Devices Ltd, Cambridge, UK) with measurement at 10, 20, 30, 40, 60 and 100 cm depth at ARBC and multi-plexed TDR-100 (Time Domain Reflectometer) system (Campbell Scientific Inc., Logan, UT, USA) installed at 15 and 30 cm depth at PSU. Irrigation, nutrients and pesticides were applied as needed (Table S4.3). Twelve maize (Zea mays L.) recombinant inbred lines were selected from a pre-screen (for more details see 3.1.3) of genotypes by Chimungu *et al.* (2015a) and planted in a completely randomised split plot design, with treatments (compaction and non-compaction) at whole plot levels and genotypes on subplot levels for both field sites. Each genotype was planted within 4 row subplots (3.05 m x 4.57 m) within each whole plot and individual plants were spaced 23 cm apart within row and 76 cm between rows.

5.3.2 Rooting depth

Soils were cored at tasselling which was 55 and 51 days after planting for ARBC and PSU, respectively. A coring tube fitted with a 4.5 cm diameter, 60 cm long plastic sleeve was driven into the soil (Trachsel *et al.*, 2013) for assessment of rooting depth. In combination with the increased penetrometer resistance in the 10 – 35 cm depth (or 0 – 45 cm in the case of ARBC) for compacted fields, the root system was considered sufficiently sampled by the maximal achievable sampling depth of 60 cm. Cores were stored at 4 ºC, divided into 10 cm increments and roots were washed from the soil over a 800 µm soil sieve. Washed roots were spread on a glass tray filled with water and analyzed with WinRHIZO Pro 2013e software (Regent Systems Inc., Quebec, Canada). All images were taken at 400 dpi (15.75 pixels/mm) resolution, dust removal set at high and no speed priority selected. To assess the capability of roots to grow through an impeded zone, the focus was on the coarse root fraction (> 1 mm diameter) rather than fine roots (<1 mm diameter). Root diameter classes were set at 0.5 mm increments up to 4.5 mm in order to allow for coarse root length (>1.0 mm diameter) calculations. Rooting depth (D_{75}) above which 75% of the coarse root length can be found within the core was estimated by linear interpolation (Schenk and Jackson, 2002).

5.3.3 Plant harvest, anatomical sampling and image analysis

Two plants per subplot (4 replicate subplots per compaction treatment), were selected and sampled by 'shovelomics' (Trachsel *et al*., 2011) and measurements within each subplot averaged yielding 4 replicates per genotype/compaction treatment combination. Shoots were dried for several days at 60°C. Crown and brace roots were imaged to verify root angles between genotypes within field site and treatment (York *et al.*, 2015), as root angle could influence D_{75}. Images were analysed with ImageJ and root angles were recorded (Table S5.4). Roots of node 3 and 4 were selected for anatomical analysis and sampled 30 mm from the crown base. Approximately 30 mm long sections of roots were stored in 75% ethanol in water (v/v).

Laser Ablation Tomography (LAT) (Hall and Lanba, 2019, Strock *et al.*, 2019) was used to obtain cross-sectional images (Figs. 5.1). LAT uses a nanosecond pulsed laser beam (Avia 7000, 355nm pulse, Coherent, Santa Clara, CA) focused into a single-line scanning beam with a HurryScan 10 galvanometer (Scanlab, Puchheim, Germany) to vaporize and sublimate tissue in front of a Canon T3i camera fitted with a 5x micro lens (MP-E 65mm) focussed on the ablation plane. Samples were guided into the ablation plane by a three-axis motorized stage (ATS100-100, Aerotech Inc, Pittsburgh, PA) at a speed of 30 μm per second. Images for anatomical assessment were obtained from the central region of the 30 mm sampled sections between laterals.

A root cross-section is constructed of diverse tissues and each tissue trait can be explained as a combination of cellular traits and/or other tissue related traits (Fig. 5.2). For instance, cellular traits such as cell file number (CF) and inner (IN), middle (MID) and outer (OUT) cortical cell area build up the cortical tissue. Aerenchyma related traits can be considered a tissue trait as their dimensions are closer related to tissues then that of cells, moreover aerenchyma has tissue functions related to it as well. To measure or calculate these cellular and tissue related traits four different object directories were created in objectJ (Vischer and Nastase, 2009), a plugin for Fiji/ImageJ (Schindelin *et al.*, 2012) (Table 5.1) over a root cross-section image.

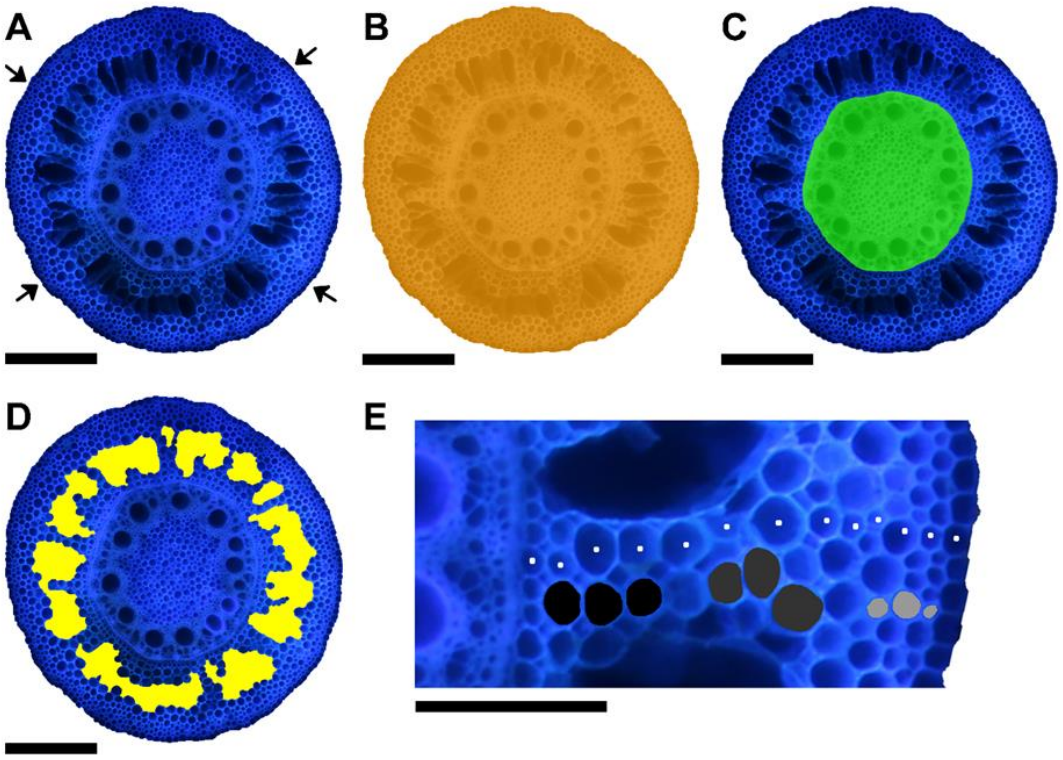

Figure 5.2 - Illustration of the different anatomical traits that were directly measured. (A) Original cross-sectional image of a root obtained by Laser Ablation Tomography (LAT). (B) Root cross-sectional area indicated in orange and (C) total stele area indicated in green. (D) Aerenchyma area indicated in yellow. (E) Shows one of four places where inner (black), middle (dark grey) and outer (light grey) cell area was measured as well as cell file number (white dots). Arrows in (A) indicate that measurements of (E) were taken from 4 different places around the cross-section. From (B) and (C) total cortical area can be calculated and from this as non-aerenchyma area in the cortex. From (B-D) all relative measures found in Table 1 can be calculated. Scale bars (A-D) at 500 µm, scale bar (E) at 200 µm.

Table 5.1 – Different anatomical traits measured

Abbreviation	Root anatomical trait	Unit	Measured / calculated
RCSA	Root cross-sectional area	mm^2	measured - traced
TSA	Total stele area	mm^2	measured - traced
TCA	Total cortical area	mm^2	calculated (RCSA - TCA)
TCA/TSA	Ratio cortex to stele	-	calculated (TCA/TSA)
TCA/RCSA	Ratio cortex to cross-sectional area	%	calculated (TCA/RCSA)
TSA/RCSA	Ratio stele to cross-sectional area	%	calculated (TSA/RCSA)
CF	Cell file number	-	counted
IN	Cell area - inner cortical region	μm^2	measured - traced
MID	Cell area - middle cortical region	μm^2	measured - traced
OUT	Cell area - outer cortical region	μm^2	measured - traced
AA	Aerenchyma area	mm^2	measured - traced
nonAA	Non-aerenchyma cortical area	mm^2	calculated (RCSA-AA)
AA/TCA	Ratio of cortex taken up by aerenchyma	%	calculated (AA/TCA)
AA/RCSA	Ratio of cross-sectional area taken up by aerenchyma	%	calculated (AA/RCSA)

5.3.4 Statistical analysis

Statistical analysis and visualisations were carried out in Graphpad Prism version 7.04 (Graphpad Software, La Jolla California, USA) or R version 3.5.0 (R Core Team, 2018). A bivariate approach was used to identify outliers on the basis of the RCSA data within their respective compaction treatment x genotype x node combinations, as outliers for other anatomical data were linked to outliers for

RCSA data. Outliers were replaced by a single observation per subplot instead of the average observation of two plants per subplot (this related to about 1% of the data). Principal component analysis (PCA) was carried out to elucidate the anatomical trait relationships over different nodes, treatments and field sites. Principal components were retained on the basis of eigenvalues greater than 1. Split-plot analysis with treatment on whole plot level and genotype on subplot level was carried out within node and field site combinations to assess the effects of compaction treatment and genotype on RCSA and TCA/RCSA. Allometric relationships were assessed by fitting a linear regression model on the natural log of the anatomical trait against the natural log of shoot biomass. Based on TCA/RCSA, RCSA and allometry observations, genotypes were classified as thickening and non-thickening for node 3. A generalised linear model was used to investigate the effect of genotype, field site, root class, treatment and thickening on D_{75}. Thickening was represented by TCA/RCSA data that was box-cox transformed for normality prior to running a general linear model with gamma distribution for D_{75}. An ANCOVA was used to investigate the interaction effects between factors thickening, field site and compaction treatment. A second set of PCAs on anatomy variables in relationship with D_{75} within each node and within compacted treatment were performed. Pearson correlations between D_{75} and anatomical traits for each node were used to select independent variables for building multiple regression models. Stepwise multiple regression was carried out to describe a model based on all the anatomical traits. To further understand if either cellular or tissue related traits contribute to rooting depth D_{75}, additional models were constructed by selecting traits on either tissue level or cellular level. After which models were compared with each other. Variance inflation factors were calculated to inspect multicollinearity (Miles and Shevlin, 2001) and the Akaike information criterion identified the best fitting model (Konishi and Kitagawa, 2008).

5.4 Results

5.4.1 Cellular and tissue related trait relationships

Trait variation was observed within and across nodes as well as field sites (Fig. S5.1) and among genotypes (Table 5.2). In the PCA (Fig. 5.3), the three retained

dimensions explained 88% of the total variation in root anatomy. Root tissue traits, total cortical aerenchyma, non-aerenchyma cortical area and total stele area, were more closely related to root cross-sectional area than cellular traits. Non-aerenchyma cortical area and total cortical area explained the root cross-sectional area better than the total stele area. Cellular traits of middle (MID), inner (IN) and outer (OUT) cortical cell area correlated to each other, while IN and MID were more closely related to each other than with OUT. All cell area traits were orthogonally oriented from cell file number, indicating no correlation between cell area and the number of cell layers. Total cortical area and root cross-sectional area were correlated to both dimensions and that due to the fact that traits such as cell file layer versus IN and MID were found on different principal components. Although cell file layer was not correlated with IN and MID, all these traits were correlated with the cortex, which in turn was related to root cross-sectional area. Interestingly the cellular area trait OUT was orthogonally oriented versus root cross-sectional area, this meant that OUT was not related to root cross-sectional area or total cortical area. OUT cells were smaller than MID cells, but IN cells were similarly small (Fig S5.1) and still contributed to root cross-sectional area. Aerenchyma traits were closely correlated with principal component 3, with the exception of non-aerenchyma cortical area, and therefore independent from the other cellular or tissue traits.

5.4.2 Anatomical traits are dynamic and dependent on field site, node and compaction

The effects of field site, node and compaction were visualised by colouring the PCA scores (Fig. 5.4). Visualisation of the first and second principal components shows that field sites and nodal data cause separation, while treatment had more overlap. More overlap of the point clouds was seen in the second versus third dimension projections as compared to the first versus second dimension projection. This means that for traits such as aerenchyma, effects of field site and node were smaller than the effects of node and field site on cell file number.

Table 5.2 – Summary of split plot ANOVA (F-values) on the root cross-sectional area (RCSA) and ratio cortex to cross-sectional area (TCA/RCSA). With treatment (compaced versus non-compacted plots) on wholeplot level and genotype (12 genotypes) on subplot level for root sections. Data across two different nodes and from two different field sites: the Apache Root Biology Center (ARBC) and Pennsylvania State University (PSU). ° significance level at p≤ 0.1, * significance level at p ≤ 0.05, ** significance level at p ≤ 0.01, *** significance level at p ≤ 0.001

Effect	RCSA								TCA/RCSA							
	Node 3				Node 4				Node 3				Node 4			
	ARBC		PSU		ARBC		PSU		ARBC		PSU		ARBC		PSU	
Compaction Treatment	8.54	*	2.52		4.43	°	2.70		19.54	**	12.29	***	9.29	**	2.31	
Genotype	1.62		3.42	***	1.93	*	6.01	***	8.87	***	2.13	*	7.87	***	5.21	***
Compaction Treatment x Genotype	1.27		1.60		1.59		2.38	*	1.84	°	0.95		1.03		1.08	

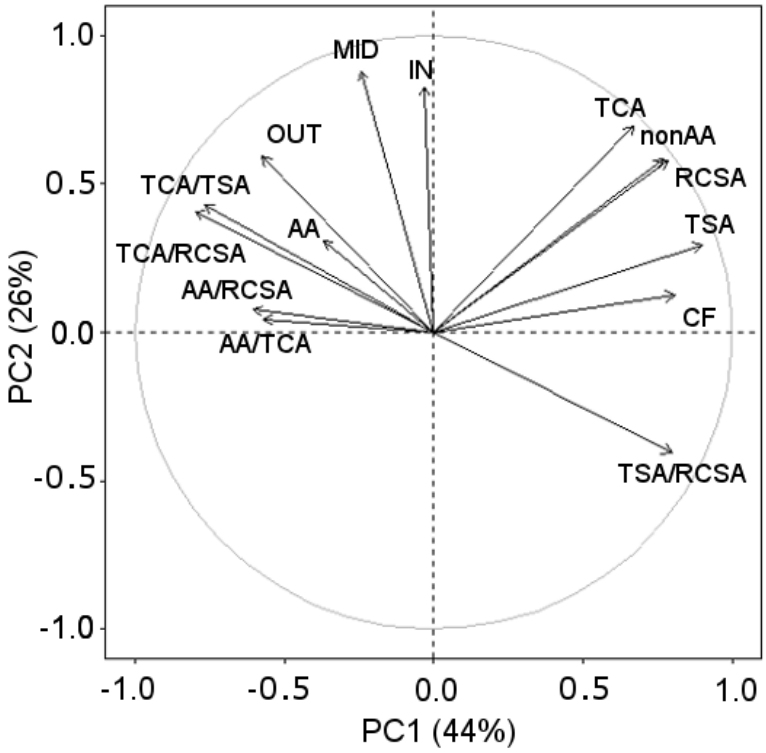

Figure 5.3 - Principal component analysis (PCA) of 14 anatomical traits from root cross-sections across different fields, compaction treatments and nodes. PCA loadings of the different variables illustrate how different anatomical traits relate to each other. Traits with arrows that group together are correlated to each other, traits with arrows in opposite direction are negatively correlated with each other. When variables appear orthogonally from each other, associated traits do not correlate. Length of the arrow illustrates how strongly the trait is associated with each principal component. Abbreviations for each trait can be found in Table 5.1

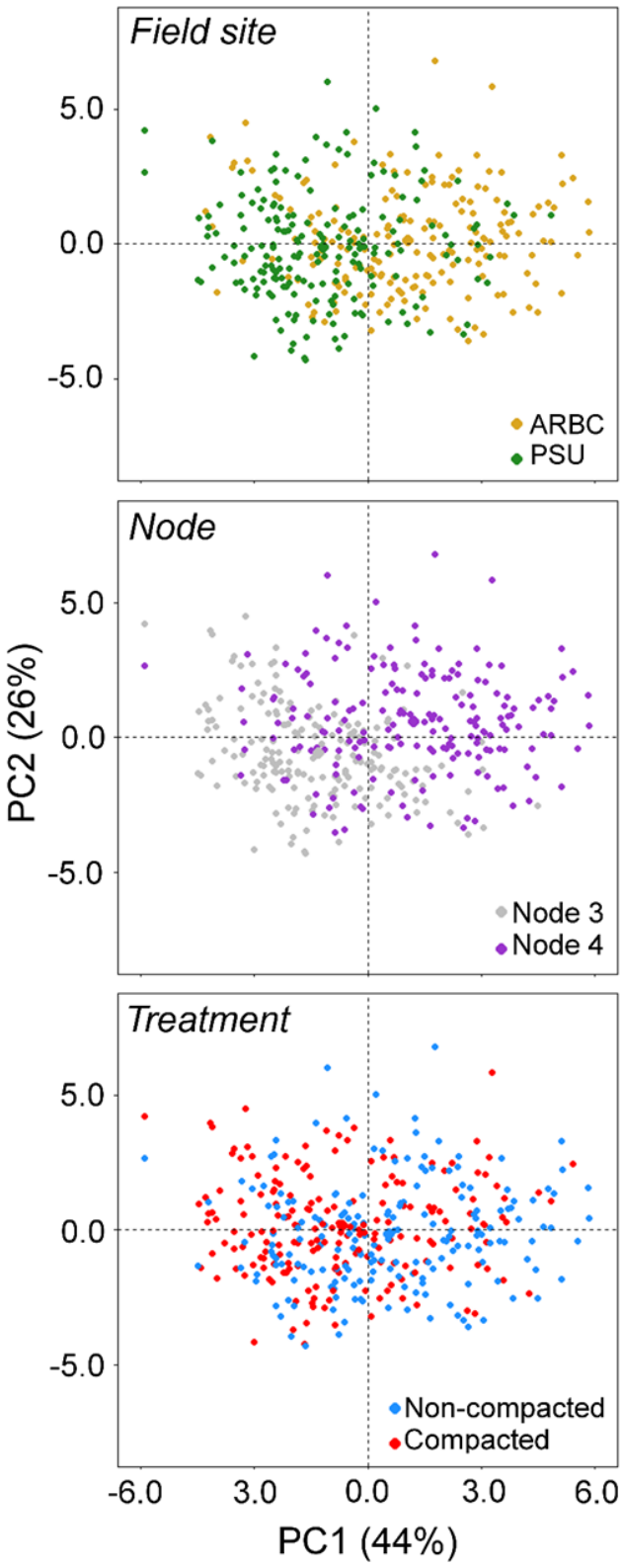

Figure 5.4 - Principal component scores of anatomical data on principal component 1 (PC1) and principal component 2 (PC2). Data can be visualised per field site, node and treatment showing that anatomical traits are dependent on field site, node and compaction.

5.4.3 Genotypic and treatment effects on root cross-sectional area and cortical tissue ratios

Genotype had a significant effect on both RCSA and TCA/RCSA across both nodes, with the exception of RCSA for node 3 at ARBC (Table 5.2, Fig. 5.5). No thickening as an increase of RCSA under compaction was observed, moreover RCSA was significantly negatively affected by treatment at ARBC (Table 5.2, Fig. 5.5A). Thickening of cortical tissue measured as TCA/RCSA, was responsive to the compaction treatment as well as to genotype (Table 5.2, Fig. 5.5B) as TCA/RCSA increased under all but one node-field combination (node 4 – PSU) (Table 5.2). Under compaction the mean TCA/RCSA value was greater but non-significantly different from non-compacted conditions for most genotypes at both sites (Fig. 5.5B). Roots had greater cortical expansion in response to the compaction treatment in node 3 versus node 4 in general (Fig 5.6B).

5.4.4 Node-specific allometry affects root anatomy

Soil compaction reduced shoot biomass (Fig. 5.6), therefore allometry or proportional growth should be factored into the analysis. For RCSA allometric relationships were dependent on nodal position as allometric effects were only observed for node 3 and across both field sites (Fig. 5.6). Node 3 RCSA was hypoallometric, as the scaling component α was smaller than 1. Under compaction, plants that had a greater biomass formed greater RCSA for node 3 roots.

5.4.5 Non-thickening versus thickening genotypes and their relation to rooting depth

For node 3, non-thickening roots were characterised by greater TCA/RCSA in general, while thickening roots had lower TCA/RCSA under non-compacted conditions and increased in TCA/RCSA under compaction (Fig. 5.7A-B). Differences between thickening and non-thickening roots for TCA/RCSA were less clear for node 4 (Fig. 5.7C-D). The general linear model on rooting depth (D_{75}) indicated that field site had an effect on rooting depth and compaction reduced rooting depth (Table S5.2). Interaction effects were present between field site

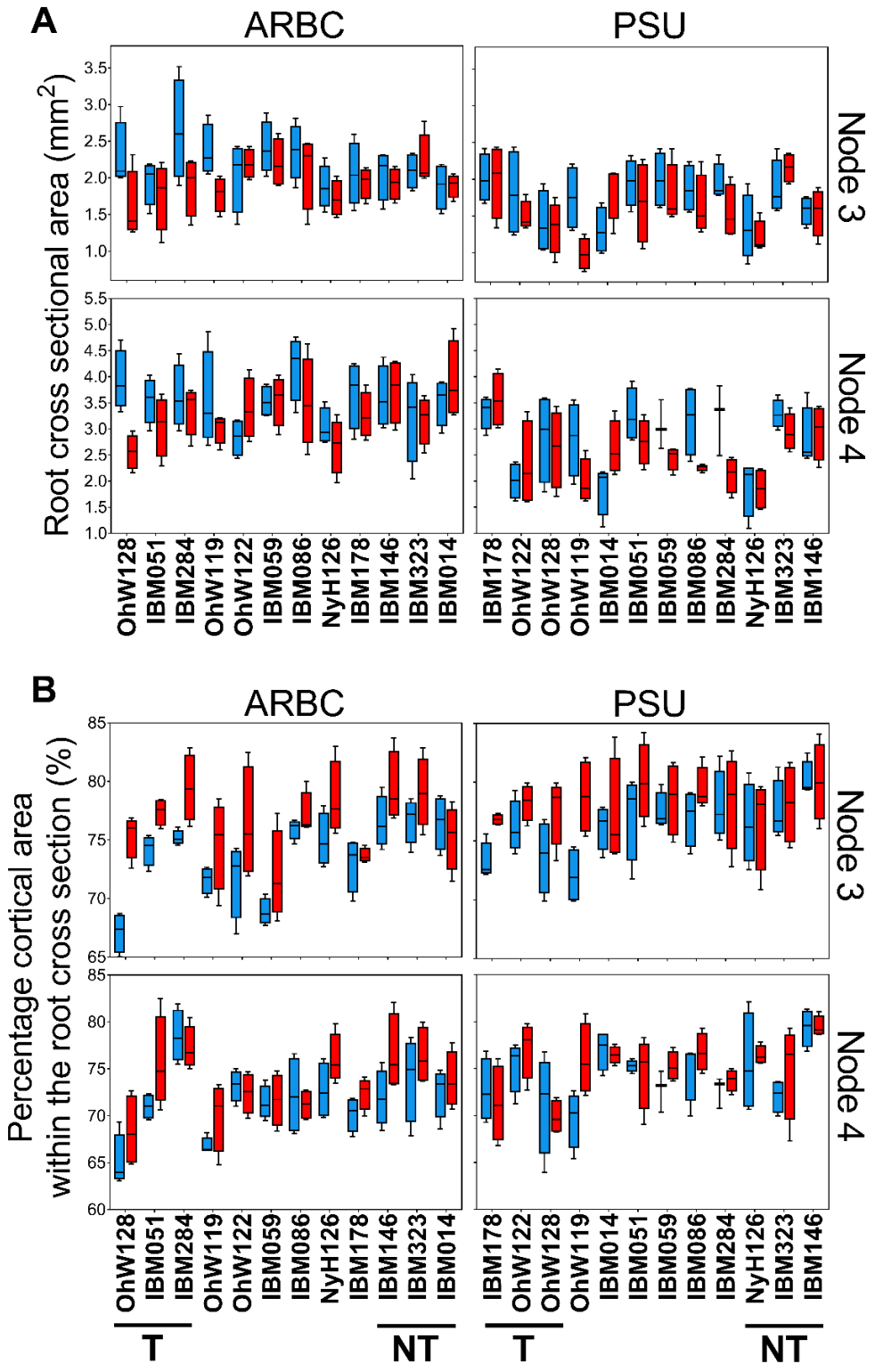

Figure 5.5 - Effects of impedance on root anatomical traits. (A) Boxplots showing the root cross-sectional area (mm^2) and (B) the percentage of root cross-section that is cortical area (%). Data per graph is split up over different nodes and over different field sites (ARBC or PSU) and visualised per genotype. Compacted data in red, non-compacted data in blue. Thickening and non-thickening selected genotypes are identified by T and NT respectively.

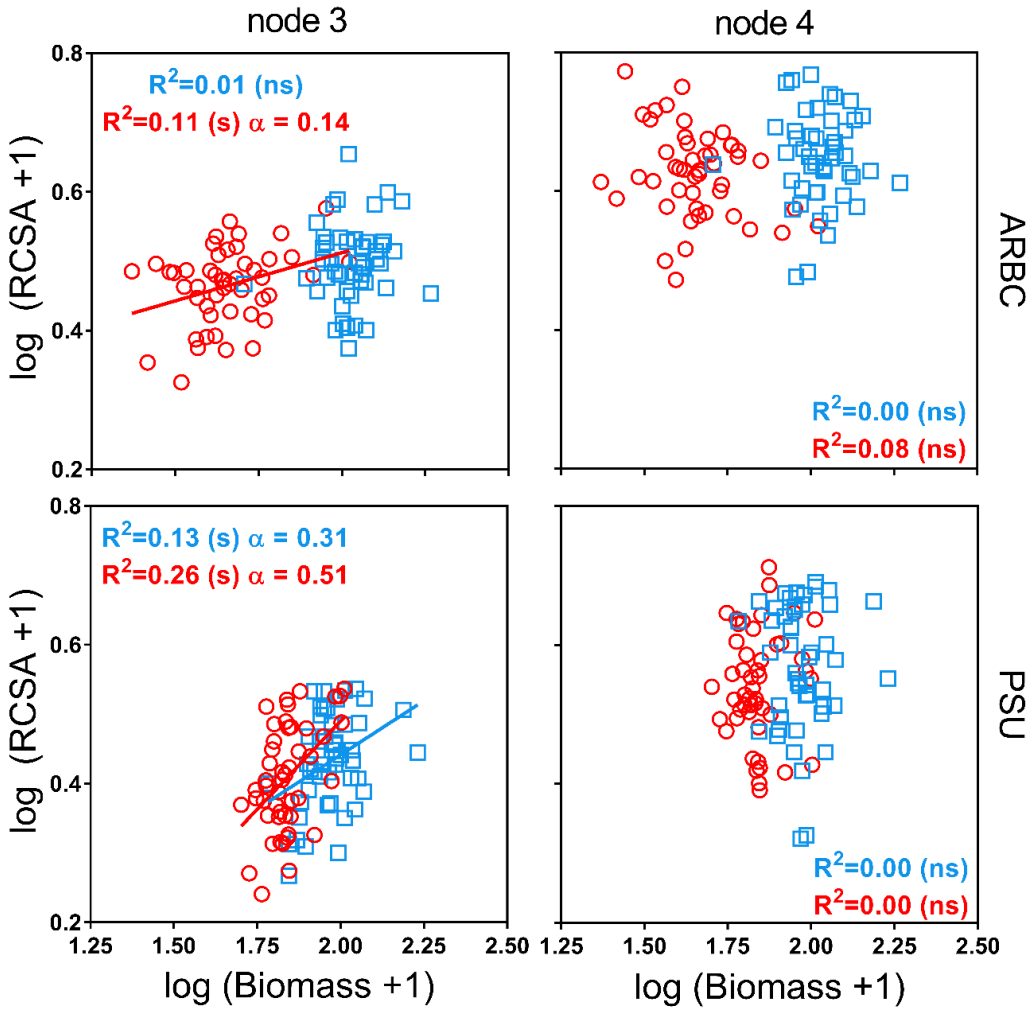

Figure 5.6 - Allometric relationships within node 3 and 4 under compacted (red circles) and non-compacted (blue squared) conditions. Full lines: allometry present, striped lines: no allometric relationship present. No significant allometric relationship is found under node 4, while node 3 root cross-sectional area scales allometrically across field sites for compacted roots. The allometric scaling component (α) depicts allometry when the relationship is significant (* $p < 0.05$, *** $p < 0.001$), ns stands for non-significant.

and thickening and field site and compaction treatment (Table S5.3). Compaction had a greater effect on rooting depth at ARBC then at PSU (Fig. 5.8E-F). Root thickening was associated with rooting depth in one field site location (ARBC) under non-compacted conditions (Fig. 5.7E-F, Table S5.3). At ARBC non-thickening genotypes grew deeper than thickening genotypes under non-compacted conditions, but under compaction no differences in D_{75} between thickening and non-thickening genotypes were present (Fig. 5.7E). At PSU

rooting depth was reduced in all but one case (genotype OhW122) by compaction, but no differences between thickening and non-thickening genotypes in either compacted or noncompaction treatments (Fig. 5.7F).

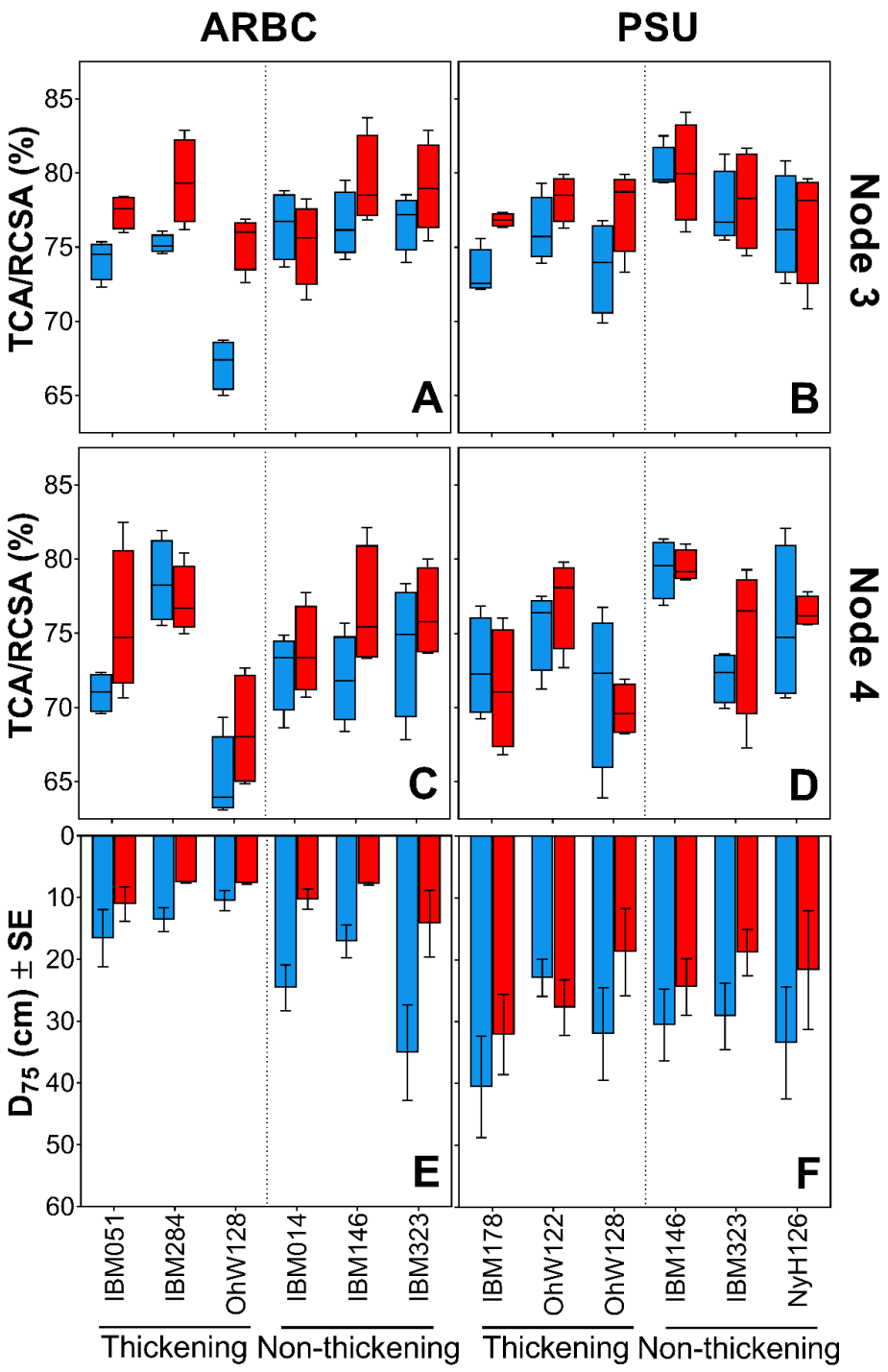

Figure 5.7 – Changes of the percentage of cortical area (TCA/RCSA) and related rooting depth (D_{75}) of thickening and non-thickening genotypes across nodes and field sites. Compacted data in red, non-compacted data in blue.

5.4.6 Node-dependent anatomical traits associated with deeper rooting in compacted soil

For each node, within compaction, a PCA was performed on the anatomical data and D_{75} (Fig. 5.8). For node 3, five principal components were retained, explaining 90% of the data variation. Rooting depth (D_{75}) was most associated with principal component 4. D_{75} was negatively correlated with CF in all principal component projections, while other traits were harder to interpret as they contributed to other principal components. For node 4 three principal components were retained, which explained 83% of the data variation. Rooting depth for node 4 was not associated with any of the retained principal components, suggesting it must have a weaker relationship with anatomy than in node 3.

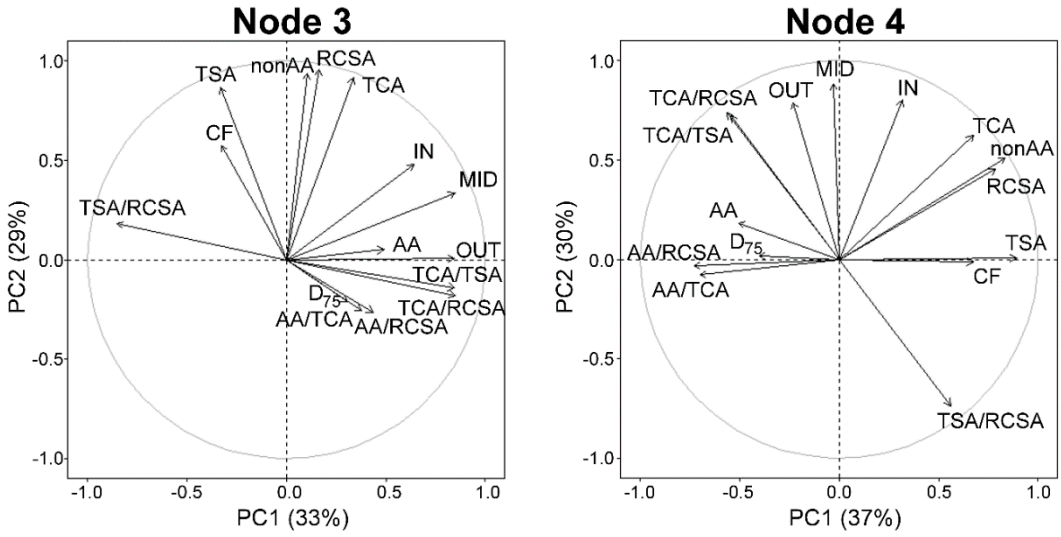

Figure 5.8 - Relationships between anatomical traits and rooting depth D75 for two different nodes as analysed by principal component analysis under compaction. Abbreviations for traits can be found in Table 1. The angle between variables represents the correlation between those variables, when the angle is 90 degrees the variables are not correlated in this dimensional projection.

D_{75} was negatively correlated with CF and positively correlated with MID, OUT, AA and AA/RCSA for node 3 (Table S5.4). For node 4, D_{75} was negatively correlated with RCSA, TSA, nonAA and CF and positively correlated with AA, AA/TCA and AA/RCSA. Summaries for each individual multiple regression are shown in Table S5.5 (node 3) and Table S5.6 (node 4). Multiple regression models

are compared in Table 5.3. Cellular traits (model 5; adjusted R^2 = 0.19) were better predictors for D_{75} then tissue-related traits (model 3; adjusted R^2 = 0.04) for node 3 (Table 5.3 – A). The best fitting model (lowest Aikake Information Criterion) was model 2, which included two cellular variables CF and MID explaining 20% of the variability in D_{75} (Tables 5.3A, 5.4A; $p<0.001$). Therefore, the contribution of cellular traits in node 3 to deeper rooting was significant. Node 3 root sections that contained fewer cellular layers in combination with greater MID cellular area rooted deeper. For node 4, tissue traits (model 2; adjusted R^2 = 0.12) were better predictors for D_{75} than cellular traits (model 5; adjusted R^2 = 0.06) (Table 5.3B). D_{75} for node 4 roots was negatively influenced by TSA and positively by AA/RCSA. The model with the lowest Aikake Information Criterion was model 2, explaining 14% of the variability in D_{75} (Table 5.3, 5.4 – B; $p<0.01$). These traits therefore made a small but significant contribution to deeper rooting under impeded conditions, but less so than for node 3. Fig. 5.1 illustrates these differences in anatomical traits across nodes.

5.5 Discussion

Root anatomical phenotypes are dynamic, responding to genotype, field site and soil compaction. Root anatomy contributes to the ability of root penetration through compacted soil but allometry needs to be taken into account for smaller, older roots. Roots that are thicker from the outset, such as those of the younger node 4, had less anatomical response to hard soil then those of node 3. Moreover, although individual anatomical traits play a role in the ability to penetrate hard soil, radial thickening was not one of them. Within node 3, cellular traits such as cell file number and middle cortical cell area play an important role, while for node 4, increased cortical aerenchyma and a smaller stele area were associated with deeper rooting in compacted soils.

5.5.1 Traits are highly interactive and adaptive to their local environments

When comparing between field sites, different root cross-sectional areas (Fig. 5.6A) are observed for the same genotype. Differences for RCSA between field

Table 5.3 – Comparison of different multiple regression models ran on (A) node 3 and (B) node 4 data, traits selected on the basis of Pearson correlation with the response variable D_{75}. AIC stands for the Akaike Information Criterion, with in bold the model with the lowest value for AIC which represents the best model fitted out of models tested. Abbreviations for the anatomical traits are found in Table 1. D_{75} stands for the rooting depth were 75% of the total coarse root length within a core can be found. (m) indicates that the model has a multi-collinear component. ns stands for non-significant, * significance level at $p \leq 0.05$, ** significance level at $p \leq 0.01$, *** significance level at $p \leq 0.001$.

A

Model		R^2	Adj. R^2	p-value		AIC
1	D_{75} ~ CF + MID + OUT + AA + AA/RCSA	0.24	0.19	4.85E-03	**	662.55
2	**D_{75} ~ CF + MID**	**0.20**	**0.19**	**6.65E-05**	**	**660.02**
3	D_{75} ~AA + AA/RCSA	0.06	0.03	0.09	ns	675.00
4	D_{75}~ AA	0.06	0.04	2.84E-02	*	673.01
5	D_{75}~ CF + MID + OUT	0.22	0.19	1.08E-04	***	660.11
6	= model 2					

B

Model		R^2	Adj. R^2	p-value		AIC	
1	D_{75} ~ RCSA + TSA + CF + AA + AA/TCA + AA/RCSA + nonAA	0.18	0.10	0.03	*	673.10	(m)
2	**D_{75}~ TSA + AA/RCSA**	**0.14**	**0.12**	**1.83E-03**	*	**666.89**	
3	D_{75} ~ RCSA + TSA + AA + AA/TCA + AA/RCSA + nonAA	0.17	0.10	0.02	*	672.08	(m)
4	= model 2						
5	D_{75} ~ CF	0.07	0.06	1.44E-02	*	671.78	

Table 5.4 - Summary of multiple regression with lowest Akaike Information Criterion values for (A) node 3 and (B) node 4. *** level of significance at p ≤ 0.001 and ** level of significance at p ≤ 0.01. Abbreviations for the anatomical traits are found in Table 1. D_{75} stands for the rooting depth were 75% of the total coarse root length within a core can be found.

A **Model 2 - D_{75} ~ CF + MID**

	Estimate	SE	t-value	p-value	
(Intercept)	43.96	11.36	3.87	2.14E-04	***
CF	-3.13	0.89	-3.52	6.93E-03	***
MID	4.67E-03	2.22E-03	2.10	3.88E-02	*
Multiple R^2	0.205				
Adjusted R^2	0.186				
p-value	6.65E-05	***			

B **Model 2 - D_{75} ~ TSA + AA/TCA**

	Estimate	SE	t-value	p-value	
(Intercept)	20.11	4.95	4.06	1.09E-04	***
TSA	-9.00	5.18	-1.74	8.61E-02	
AA/TCA	27.46	11.12	2.47	1.56E-02	*
Multiple R^2	0.14				
Adjusted R^2	0.12				
p-value	1.83E-03	**			

sites could be caused by a difference in soil texture as larger root diameters have been observed in soils with greater aggregate size (Logsdon *et al.*, 1987). Greater root diameters would be capable of displacing larger particles and aggregates (Whiteley and Dexter, 1984). As roots are deflected around larger aggregates that cannot be displaced or penetrated, alternating thin and thicker root diameters can be found along a root axis as the level of impedance changes along the root trajectory (Logsdon *et al.*, 1987) confirming that the arrangement of the soil pore network plays a role in root anatomy. Kirby and Bengough (2002) observed pea roots, grown in a sandy loam soil, can increase their diameter by 60% when grown at a mechanical impedance of 2 MPa versus 0.7 MPa. When grown in clay loam instead of sandy loam soil root diameter increased less. Tomato root diameter increased in hard loamy sand more than in hard clay loam, illustrating the importance of soil texture (Tracy *et al.*, 2013). The greater sand fraction, less structured soil in combination with greater differences in penetrometer resistance between compaction and non-compaction treatment at the ARBC field

site could explain why larger diameter under non-compacted conditions are seen in both nodes versus at the PSU field site. As root diameters respond to their local environments, so must the underlying anatomy. Differences in penetrometer resistance were recorded at both PSU and ARBC fields (Fig. 4.1) and differences in soil structure were observed. However under compaction more tortuous, bent, roots with irregularly shaped root sections were observed (Fig. S5.2). Plasticity for root cross-sectional shape falls outside of the scope of this study but root deformation in response to the local soil structure warrants further investigation.

Anatomical traits are strongly intercorrelated in similar ways across nodes (Figs. 5.3, 5.8) as seen by Yang *et al.* (2019). Nonetheless anatomy makes a significant contribution to deeper rooting (Tables 5.3, 5.4). Under specific field and compaction conditions root anatomy changes (Figs. 5.4, 5.5, 5.6). Most interesting are the shifts in tissue ratios between cortex and stele and changes in aerenchyma, which points to an effect of compaction treatment on the cortex. Here it is illustrated that cortical tissues expand (Fig. 5.5) under compacted conditions. Greater anatomical changes were observed when the differences in penetrometer resistance were greater between non-compacted and compacted plots, as was the case at ARBC (Figs. S5.1, 5.5, 5.7). Different phenotypic adaptations were observed with node and genotypic dependence. Node 3 roots of some genotypes (IBM051, IBM178, IBM284, OhW122, OhW128) thicken while node 3 roots of other genotypes do not (IBM014, IBM146, IBM323, NyH126) (Fig. 5.7), while some genotypes remain stable in this phenotype at both sites (OhW128, IBM146, IBM323) and others are not (IBM051, IBM284, IBM014, NyH126). This shows that root systems are highly adaptable across genotypes but also within individual plants. The response to impedance of different nodes and genotypes was non-uniform. Future work might consider these patterns on a larger set of genotypes and under varying levels of mechanical impedance.

5.5.2 Thickening is node-dependent and obscured by allometry

Root thickening is commonly observed in response to mechanical impedance for different plant species and root types in different experimental conditions (Atwell, 1993; Barraclough and Weir, 1988; Colombi and Walter, 2016; Iijima *et*

al., 2000; Kirby and Bengough, 2002; Materechera *et al.*, 1991). Root thickening is often considered beneficial since thicker roots would be less likely to buckle (Whiteley *et al.*, 1982) and would reduce stress at the root tip (Abdalla *et al.*, 1969). Additionally the elongation zone of impeded roots becomes shorter and moves closer to the root tip and as such the friction upon this zone is reduced (Atwell, 1993). On the other hand greater penetration resistances increased root diameters and energy costs for root elongation for wheat primary roots (Colombi *et al.*, 2019). No direct thickening was observed in this field study. This could partly be due to the remote measurement of the RCSA near the root crown in the shallower part of the soil. RCSA was not significantly greater in compacted plots (Fig. 5.5A), but TCA/RCSA was greater under compaction of node 3 and to a lesser extent in node 4. Together with the results found in Table 5.2 it can be concluded that root cortical tissues do react when impeded and that this is genotype-dependent.

Soil compaction reduced plant biomass in both field sites (Fig. 5.6). Shoot growth is coordinated with root growth and nodes develop in acropetal tiers, becoming progressively thicker in younger nodes. Impedance causes allometric effects in node 3 across field sites but not for node 4, RCSA is therefore more strongly linked to plant size in the early growth. Allometric effects on maize root anatomy have been reported previously (Burton *et al.*, 2013). The cortex reacts to compaction and increases in relative size. The thickening effect had been obscured by an allometric effect in node 3. For node 4, no allometric effect was present (Fig. 5.6) additionally no differences in RCSA were caused by compaction (Fig. 5.5A) and only a significant increase in TCA/RCSA at ARBC was observed (Fig. 5.5B, Table 5.2). Therefore, it can be concluded that thickening does not occur in the younger node 4 roots. As greater diameter roots have previously been found to be more capable of growing under compacted conditions (monocotyledons versus dicotyledons (Materechera *et al.*, 1991)) and pea versus barley (Stirzaker *et al.*, 1996), this could be also the case for the younger, thicker roots of maize within the same root system. Most studies observing root thickening, have done so on seedling roots which are generally small, while crops such as maize, have larger roots than small grains (e.g. wheat, barley). Thinner

roots or seedling roots might thicken to a larger extent in comparison with roots from older maize plants (younger, thicker nodes) that already have a certain diameter. Thickening might not be present for node 4 roots, due to roots developing as the plant matures being more structural in the support of aboveground biomass, while node 3 roots would be more dependent on anatomical changes at cellular level in order to grow through impeded zones.

Cortical expansion has been linked to thickening through the increase of either cell file number and/or cell expansion in the radial plane, however the literature is inconsistent in reports on what the main driver of radial expansion would be. Maize has been observed to increase cortical cell area, which in turn increases root diameter, when grown in glass beads under pressure but that study did not consider the effect of additional cell file layers (Veen, 1982). Iijima *et al.* (2007) found maize seminal root diameter increased by 80% in response to mechanical impedance, while the cortical thickness increased by 110%. This study also reported a 20% increase in the number of cortical cell tiers under impeded conditions. Cellular area was not measured but a clear increase in cellular area can be observed from their images (Fig 5.3 in Iijima *et al.* (2007)). Additionally, different nodal root classes were considered instead of seminal roots in this study.

Thickening versus non-thickening genotypes were distinguished based on node 3 (Fig. 5.7A-B). Both thickening as well as non-thickening genotypes show similar rooting depths on compacted plots (Fig. 5.7E-F). Root thickening was negatively associated with rooting depth growing in non-compacted ARBC field conditions (Fig 5.7E, Table S5.6). Different nodal tiers are present within the same plant, with increasingly steeper root angle with each node formed (Araki *et al.*, 2000; Wu *et al.*, 2015; York *et al.*, 2015). As younger nodes are thicker it could be that these roots experience less impedance stress then the older nodes. Less thickening would occur for these younger nodes, which supports the view that non-plasticity for thickening would be better for growing through impedance. Rooting depth was also influenced by the field site and compaction (Tables S5.2, S5.3). Site differences include growth conditions, weather and soil physical

characteristics such as soil texture and structure could have influenced root growth.

5.5.3 Reduced cell file number is an important cellular trait under compaction

Cell file number (CF) and cell area (OUT, MID, IN) variables were found on different dimensions in all PCA results (Figs. 5.3, 5.8) and are independent from each other. A similar result has been observed under N stress; under low N, cortical cell area was reduced but CF number changed little (Yang *et al.*, 2019). This evidence suggests that CF number and cell area traits are independent. Reduced CF number is an important trait when growing in compacted plots (Tables 5.3, 5.4). For node 3, this manifested in combination with the addition of MID in the model (Table 5.4). Greater MID in combination with reduced CF (Fig. 5.1A) was positively associated with increased rooting depth for node 3 roots.

Within the cortex, different cell layers react differently to mechanical impedance. In barley, cell diameters of the outer cortical cells increase under mechanical impedance, while inner cell diameters become smaller (Wilson *et al.*, 1977) with smaller cells shown to be more rigid and strong in maize (Chimungu *et al.*, 2015a). In this study OUT increased, but in comparison with MID, OUT remains small, as do the inner cell layers (Fig. S5.1). Considering cortical attributes, Chimungu *et al.*, (2015a) proposed a root anatomical ideotype that would facilitate penetration of hard subsoils. The outer protective layer of the cortex should consist of small cells to counteract bending and buckling in combination with larger cortical cells in the inner layers that contribute to a larger diameter and reduced metabolic cost. Barley roots under moderate mechanical impedance increased in diameter while the tensile strength of those roots remained unaffected (Loades *et al.*, 2013). Further research is needed to link the effect of changing root anatomical characteristics to the physical properties of roots.

Assuming root cross-sectional area is either built out of larger cell areas with fewer cell files or smaller cell areas with more cell files, the greater number of CF would entail additional metabolic costs (Lynch, 2015). Respiratory costs to cells could be driven up as bigger cells generally have higher metabolic costs

associated (Glazier, 2009). However a plant cell largely consists of a vacuole, which would not contribute towards the cell metabolism. Therefor the exact relationship between cell size and metabolic costs needs to be further investigated. It has been proposed that metabolic cost reduction assists with deeper rooting (Lynch and Wojciechowskie, 2015; Lynch, 2015). Recently Colombi *et al.* (2019) showed that energy costs for root elongation were increased by mechanical impedance, but that energy costs were reduced for those wheat genotypes with greater cortical cell diameters. The oxygen demand of impeded roots has been observed to be greater than under control conditions with elongating cells showing higher critical levels of O2 pressures of respiration, additionally diffusion pathways became longer due to radial thickening (Hanbury and Atwell, 2005). Extra cell walls, from increased CF number, will contribute to slower O_2 diffusion across the root and will demand more oxygen by the cortical tissue (Hanbury and Atwell, 2005). In order to produce additional CF layers a root will also need to adjust its pattern of cell division within its meristem. Within the meristem, cell divisions will occur anticlinally adding cells to a cell file, while periclinal cell division (adding CF layers) occurs far less (Shishkova *et al.*, 2008, Potocka *et al.*, 2011). This would make the addition of a CF dependent on meristematic changes. A meristematic change, such as the switch from a closed to open meristem has been observed in maize under mechanical stress (Potocka *et al.*, 2011), though what this means and how often this has an effect on CF changes remains unclear.

5.5.4 Increased aerenchyma is an important tissue trait under compaction

The significant effect of cortical aerenchyma (as AA or AA/RCSA) on rooting depth (Tables 5.3, 5.4, Fig. 5.8) can be interpreted as deriving from its effect on oxygen transport in the root (Colmer, 2003) and in the context of the metabolic costs of soil exploration (Lynch, 2013). When soils become stronger due to drying, and associated changes in impedance rise, it has been shown that aerenchyma formation has a positive effect on overall root growth (Jaramillo *et al.*, 2013; Zhu *et al.*, 2010). Root cortical aerenchyma has also been shown to contribute to deeper rooting (Lynch and Wojciechowski, 2015). Greater ratios of

aerenchyma in roots are associated with reduced respiration rates, lowering the demand for oxygen by the cells (Chimungu *et al.*, 2015a; Fan *et al.*, 2003, Colmer, 2003) . In contrast with harder, and potential drier soils, compacted soils have a lower porosity and have a greater potential to become waterlogged, thus the presence of aerenchyma could counteract hypoxia within the tissue. Large lacunae promote longitudinal oxygen flow through the roots, reduce oxygen metabolism and enable CO2 to vent out of the root tissue (Colmer, 2003; Drew *et al.*, 2000; Karahara *et al.*, 2012) and is adaptive under hypoxic conditions (Coudert *et al*., 2010; Kawai *et al*., 1998; Lynch and Wojciechowski, 2015). On the other hand aerenchyma reduces the radial transport of water and nutrients (Hu et al., 2014). Root porosity, enhanced by aerenchyma formation, can weaken root structure, but when a dense multiseriate, sclerenchymatic ring of cells is present in the outer cortex, the effect can be reduced (Striker *et al.*, 2006, 2007). However, as aerenchyma only develops post root penetration, at a considerable distance from the root tip and elongation zone, it is not likely to have a negative effect on the physical aspect of root penetration into hard soil. As aerenchyma is independent from the other anatomical traits (Figs. 5.3, 5.8) and clear variation exists (Figs. S5.1, 5.1B) it merits attention as a breeding target to improve rooting depth (Lynch and Wojciechowski, 2015).

The focus of this study lay on the role of root anatomical phenes in overcoming the mechanical impedance associated with compacted soils. It should be noted that compaction could induce oxygen limitations as soil porosity and air permeability decrease and hydraulic conductivity is reduced within compacted soil. Soil physical properties are influenced by each other and vary both in space and time. Hypoxia impacts roots when soils have less than 10% air-filled volume (Valentine *et al.*, 2012). Limited oxygen reduces root elongation (Bengough and Mullins, 1990, Valentine *et al.*, 2012) and influences anatomical traits such as aerenchyma (Van Noordwijk and Brouwer, 1993).

This study focused on anatomical traits, however other root traits will also contribute to overcoming impedance as well. The presence of mucilage assists in reducing the friction experienced by the root cap by lubricating the soil-root interface (Iijima *et al.*, 2000, 2004). Another trait decreasing friction is that of root

cap sloughing (Bengough and McKenzie, 1997; Iijima *et al.*, 2000). The root cap itself helps to overcome impedance (Iijima *et al.*, 2003b) whilst root tips characterised by a smaller root tip radius to length ratio will increase root elongation as impedance is overcome more easily by this shape (Colombi *et al.*, 2017b). Root tip anchorage can be provided by changing root trajectories, for instance when hitting a layer, as well as the presence of root hairs that appear closer to the root tip under impeded conditions (Bengough et al., 2011; Haling *et al.*, 2013). Root architectural traits, such as steep root angles, will also increase the probability of roots penetrating through layers (Jin *et al.*, 2013). Future research should look at synergies between these traits and root anatomy.

5.6 Conclusions

Root thickening in maize was obscured by an allometric effect in node 3, but the cortical area clearly expands in reaction to mechanical impedance. However, this effect is lost in subsequent root classes and thickening was not observed in node 4 roots. As node 4 roots were thicker from emergence, they may be less sensitive to impedance. Cellular traits in younger roots might play less of a role here in comparison with the older, thinner, node 3 roots. Genotypes could be classified as thickening or non-thickening in response to soil compaction, but no differences in rooting depth were observed between these groups. Under the imposed experimental conditions no evidence was found that thickening of root axes in response to impeded conditions contributed to rooting depth in compacted soil. We have shown that anatomy contributes to deeper rooting, especially for older nodal roots. Within their respective nodes, root anatomical traits, such as reduced cell file number and increased middle cortical area were associated with deeper rooting. Aerenchyma on the other hand was more important in node 4. Both reduced cell file number and increased cell size as well as aerenchyma are traits that reduce the metabolic costs of roots growing in compacted soils. Therefore a clear distinction between thicker roots, that have the innate capability to grow under mechanical impedance, and thickening roots, as a reaction to impedance, should be made more clearly. Anatomical traits contribute to the ability of a root system to grow under impeded conditions. Root anatomy should be considered and studied more closely to increase our

understanding, and ensure the screening of cultivars is optimised for the exploration of soils in sub-optimal conditions due to the hard soil conditions many plants have to contend with.

Chapter 6 – Genetic variation in maize nodal root penetration of a compacted layer is negatively related to impedance and ethylene-induced thickening

Paper in preparation for *Plant, Cell and Environment*

Chapter 6 investigates whether or not root thickening and root anatomy is related to the penetration percentage of a compacted soil layer by maize roots of different genotypes and different nodes. In a first experiment a compacted soil layer was created and placed within a pot that was subsequently X-ray CT scanned in order to determine specific sectioning locations along a root axis. Roots were sectioned for anatomical analysis. A second experiment tested the same genotypes and their response to ethylene applied in a hydroponic environment. Outcomes of both experiments were compared and the function of ethylene within an impeded root was discussed.

Author contribution

Conceptualisation by D.J. Vanhees, S.J. Mooney, K.W. Loades, A.G. Bengough, M.J. Bennett. Project supervision provided by K.W. Loades, A.G. Bengough, S.J. Mooney and J.P. Lynch. Experiments, analysis and paper preparation by D.J. Vanhees. The ethylene experiment was carried out by H.M. Schneider, under guidance of K.M. Brown. Paper editing by D.J. Vanhees, H.M. Schneider, K.W. Loades, A.G. Bengough, M.J. Bennett, K.M. Brown, S.J. Mooney and J.P Lynch.

6.1 Abstract

Radial expansion is a classic response of roots to mechanical impedance. The response of maize nodal roots to impedance was analysed to test the hypothesis that radial expansion is not related to the ability of roots to cross a compacted soil layer. The ability of nodal roots to reach a compacted soil layer was influenced by the root growth angle. Genotypes varied in their ability to cross the compacted layer. Root radial expansion was due to cortical cell area expansion, while cortical cell file number remained constant. In separate experiments radial expansion under ethylene was correlated with the thickening response to impedance in soil. Strong correlations between the root cellular areas of genotypes between these experiments were identified. Different genotypes and nodal root classes varied in their responses to ethylene applied in hydroponic experiments, and the genotypes that did not increase in nodal root diameter in response to ethylene were the same as those that were able to cross the compacted layer more frequently. Ethylene insensitive roots, that do not thicken while being able to overcome impedance, would have a competitive advantage under mechanically impeded conditions as they can maintain their elongation rates. One could suggest that prolonged exposure to ethylene could function as a stop signal for axial root growth.

6.2 Introduction

Roots interact dynamically with the highly heterogeneous soil environment and commonly need to withstand abiotic and biotic stresses in order to acquire water and nutrients. One major constraint to root growth and function is mechanical impedance, or the physical resistance to root penetration imposed by soil (Bennie, 1996; Whalley *et al.*, 2005). An example of localised mechanically impeding conditions that roots encounter is the presence of harder soil clods or aggregates (Konôpka *et al.*, 2009, 2008). Plough pans created by tillage are spatially abrupt. Roots unable to penetrate through harder soil strata run the risk of being confined to the upper, less dense soil strata while roots adapted to impeded conditions are able to penetrate through harder layers and would be able to maintain normal plant growth (Barraclough and Weir, 1988; Ehlers *et al.*,

1983; Pfeifer *et al.*, 2014). Soil structure itself can facilitate root exploration but could also hinder root growth. Biopores formed by pre-existing roots can be used to bypass harder soil domains (Athmann, 2019; Ehlers *et al.*, 1983; Han *et al.*, 2015; Valentine et al., 2012; Whitmore and Whalley, 2009). However, roots can become confined in soil pores restricting soil exploration of the bulk soil (Pankhurst *et al.,* 2002; White and Kirkegaard, 2010). When leaving a biopore a root will encounter a localised denser region of soil surrounding the biopore (Helliwell *et al.*, 2019). In most soils, mechanical impedance increases with soil drying (Gao *et al.*, 2016; Grzesiak *et al.*, 2013; Whalley *et al.*, 2005; Whitmore and Whalley, 2009). Thus alternating wetting and drying of soil can therefore temporally impede roots depending on soil matric potential.

Root adaptions to mechanical impedance encompass several strategies. Root tip traits such as increased production of mucilage and root cap cell sloughing lubricate the root-soil interface (Boeuf-Tremblay *et al.*, 1995; Iijima *et al.*, 2000, 2004). Sharper root tip shape reduces stress at the root tip via a more cylindrical cavity expansion (Bengough *et al.*, 2011; Colombi *et al.*, 2017a). Architectural traits, such as steeper root angles upon encountering a strong layer might reduce deflection (Dexter and Hewitt, 1978). Other traits such as the presence of root hairs help root tip penetration by anchoring the root into the soil (Bengough *et al.*, 2016). A comprehensive review of root morphological adaptions to mechanical impedance by Potocka and Szymanowska-Pułka (2018) concluded that adaptations are present across different architectural and anatomical scales. However, for root anatomy it is clear that limited research has been carried out discriminating among root types in response to mechanical impedance.

Maize root anatomy has been linked to penetration of strong wax layers (Chimungu *et al.*, 2015a). Mechanical impedance generally causes radial thickening of roots, including that of maize which was studied here (Bengough and Mullins, 1991; Konôpka *et al.*, 2009; Materechera *et al.*, 1991; Moss *et al.*, 1988). This form of radial expansion is different from that resulting from secondary growth (Strock *et al.*, 2018). Thicker roots buckle less (Clark *et al.*, 2008; Whiteley *et al.*, 1982), and modelling has found that radial expansion will reduce the stress from the root tip (Bengough *et al.*, 2006; Kirby and Bengough,

2002) while simultaneously pushing particles out of the way so that the root can extend further (Vollsnes *et al.*, 2010). Root thickening is associated with reduced elongation rates (Bengough and Mullins, 1991; Clark *et al.*, 2001; Colombi *et al.*, 2017b; Iijima *et al.*, 2007; Schmidt *et al.*, 2013), which ultimately can result in reduced soil exploration. Roots that thicken in response to impedance do so by increasing the dimensions of the cortex (Atwell, 1990) or by increasing both stele and cortical dimensions (Atwell, 1988; Colombi *et al.*, 2017b; Hanbury and Atwell, 2005; Iijima *et al.*, 2007; Wilson *et al.*, 1977). These responses vary among plant species, root type, plant developmental stage and experimental conditions (Colombi and Walter, 2016). Cortical dimensions change either by an increase in cell file number (Croser *et al.*, 1999), an increase in cell area of cortical cells (Atwell, 1988; Hanbury and Atwell, 2005; Veen, 1982) or a combination of both (Colombi *et al.*, 2017b; Iijima *et al.*, 2007). Cortical cells increase their area radially, facilitated by the loosening of cell walls by microfibril reorientation (Iijima *et al.*, 2007; Veen, 1982). The increase in cellular area coincides with reduction of cell lengths (Atwell, 1988; Croser *et al.*, 2000). Cortical cell length reduction could partly explain reduced elongation rates observed under mechanical impedance (Atwell, 1988). Further reduction of elongation rate could be caused by reduced cell production in the meristem (Croser *et al.*, 2000). Recently root thickening has been directly linked to increased energy cost for root elongation with increasing soil penetration resistance for different wheat genotypes (Colombi *et al.*, 2019). Root thickening has also been associated with an increase in the demand for oxygen (50% per unit volume growth to 80% per unit extension) for impeded lupin roots (Hanbury and Atwell, 2005). It is clear that root thickening has beneficial, as well as detrimental effects for the plant root system. There is a need to better understand the mechanism controlling radial thickening.

Ethylene biosynthesis and systems modified by ethylene have been demonstrated to be involved in stress responses and may regulate root responses to impedance (Atwell *et al.*, 1988; Sarquis *et al.*, 1991). Mechanical impedance alters maize root growth through ethylene biosynthesis by inhibiting elongation and promoting swelling (Sarquis *et al.*, 1991). Impeded maize primary roots

produced more ethylene and had an increased root diameter compared to nonimpeded roots (Moss *et al.,* 1988; Sarquis *et al.*, 1991). Mechanically impeded *Vicia faba* roots produced more ethylene compared to nonimpeded roots (Kays *et al.*, 1974). While roots of 7-day old never ripe (ethylene-insensitive) tomatoes formed elongated roots and shorter hypocotyls and did not penetrate a sand medium that impeded the roots more in comparison to potting mix (Clark *et al.*, 1999). Ethylene has known roles in modulating root anatomical and architectural traits including cortical aerenchyma, root hairs, lateral root density, and root diameter (Tanimoto *et al.*, 1995; He *et al.*, 1996b; Borch *et al.*, 1999; Fan *et al.*, 2003; Zhang *et al.*, 2003; Dahleen *et al.*, 2012; Moss *et al.,* 1988). Furthermore ethylene is differently involved in the formation of adventitious and normal roots (Clark *et al.*, 1999). However, the correlations between the sensitivity of root responses to ethylene, the responses to mechanical impedance and its effect on anatomical traits have yet to be studied.

Existing studies have generally focused on root length, branching and diameter in response to mechanical impedance (Konôpka *et al.*, 2008). If root anatomy is studied, different root axes are compared while changes within a single root axis have rarely been considered. With few exceptions (Veen, 1982; Colombi *et al.*, 2017a), root anatomy has mainly been studied on primary roots (Hanbury and Atwell, 2005; Croser *et al.,* 1999; Iijima *et al.*, 2007; Colombi *et al.*, 2019). However, different root classes can react differently to impedance (see **Chapter 5**). In this study the hypothesis that root radial expansion is not linked to the penetration rate of roots in compacted soil layers was tested. Secondly, root class and genotypic differences were assessed for the ability of roots to penetrate hard soil and link these results to separate experiments with ethylene. In this context the following proposal; ethylene might function as a signal associated with thickening was discussed. And, it is suggested that prolonged production of ethylene in response to mechanical impedance can function as a stop signal for axial growth of that particular root axis. Genotypes that produce less ethylene, or that are insensitive to ethylene could therefore maintain root elongation rate more easily under impeded conditions.

6.3 Materials and methods

6.3.1 Experiment 1: Anatomical changes to a root axis crossing a compacted layer

6.3.1.1 Experimental set-up

A brown earth soil (FAO classification: Stagno Gleyic Luvisol) with sandy loam texture (2% clay, 21% silt, 77% sand) was procured from local sugar beet farms through British Sugar in Newark (UK). The soil was obtained from sugar beet during the manufacturing process. Before column packing the soil was air-dried and sieved to <2 mm. Dried soil was wet to 17% gravimetric moisture content. Columns (14.8 cm diameter, 23 cm total height) were uniformly packed creating three regions with a compacted layer (1.5 g/cm^3 and thickness of 3 cm) placed between low bulk density layers (1.2 g/cm^3) (Fig. 6.1). The top and bottom areas were 7.5 and 9.5 cm long respectively, making up a total of 20 cm of total height of soil in column. A mould was used to create the compacted layer after which it was transferred onto the bottom half of the column. The soil surface of the compacted layer was abraded at each side to assure the compacted layer and the non-compacted soil above and below the compacted layer were adequately adhered. The pots were lined with a plastic sleeve to facilitate removal of the intact soil column after scanning. A preliminary trial was conducted to optimise the positioning of the compacted layer and to identify the preferred number of growing days (to account for growth up to node 4 reaching below the compacted layer).

Smaller columns (10 cm high, 5 cm diameter) packed at the same moisture content and density as the layered system were used to record penetrometer resistance and measurements were made with an Instron (Instron 5969, 50kN load cell, Instron, Norwood, USA) fitted with a penetrometer needle (0.996 mm cone diameter). The penetrometer tip penetrated the samples for 12 mm at a constant speed of 4 mm sec^{-1}. Measurements were averaged between 5 – 11 mm extension. Smaller (1.2 g/cm^3) and greater (1.5 cm^3) bulk densities had penetrometer resistance of 0.48 ± 0.03 (sd) MPa and 0.83 ± 0.01 (sd) MPa respectively and were significantly different (t-test, p = 0.002).

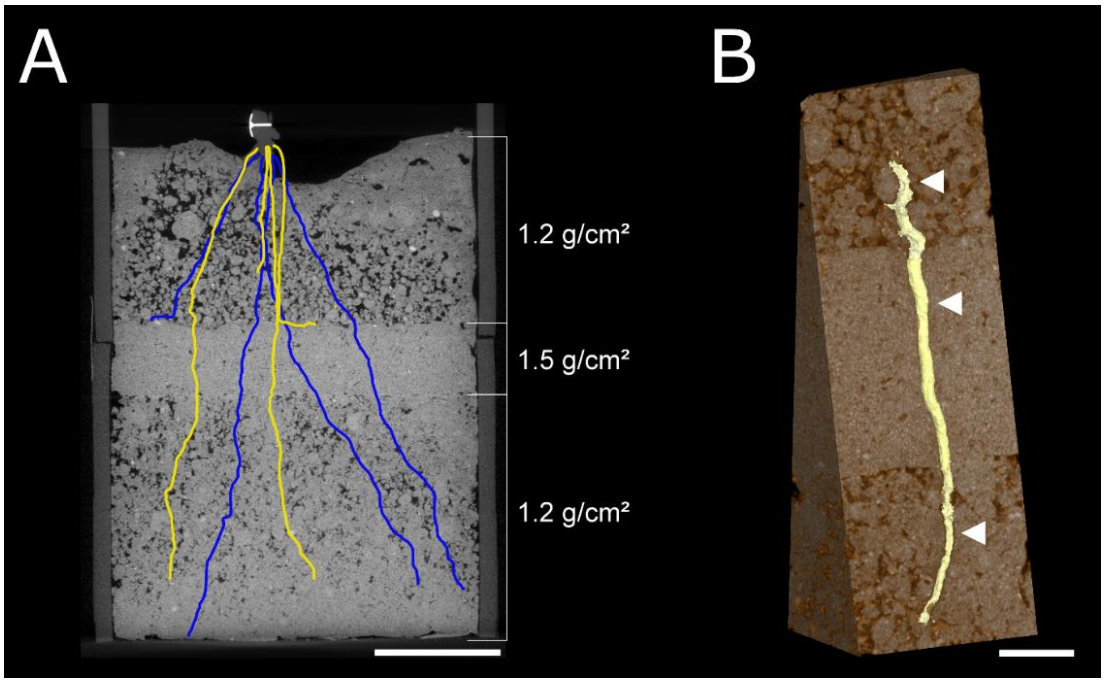

Figure 6.1 - X-ray CT images/reconstruction of (A) a root system encountering a compacted layer and (B) a root growing through the compacted layer. (A) Cross-sectional view of a soil column in the xy-plane with a compacted layer in between less dense layers. Blue and yellow lines represent the projection of the different polylines on the xy-plane. Colours: yellow - node 4 and blue - node 3. Scale bar at 5 cm. (B) A 3D reconstruction of a segmented root growing through the denser layer. The white arrows represent the sectioning positions along the root axis (1 cm before, within and after the compacted layer). Scale bar at 1 cm.

6.3.1.2 Plant material and growing conditions

Four genotypes (recombinant inbred lines; IBM086, IBM146, IBM014 and OhW128) previously studied in the field trials of **Chapter 4** and **Chapter 5** as well as by Chimungu *et al.* (2015a), were selected based on their contrasting ability to penetrate the compacted layer and with sufficiently steep root angle to allow for roots to reach the compacted layer. Seeds were acquired from the University of Wisconsin, Madison WI, USA – Genetics Cooperative Stock Center, Urbana, IL, USA. Seeds were sterilised (6% NaOCl in H_2O) for 30 minutes, imbibed for 24 hours and germinated at 26 °C for 3 days before planting. Germinated seeds with similar primary root length (± 1 cm) were selected for planting. Two seeds per pot were planted 0.5 cm deep for each genotype, plants were thinned to one plant per pot if both of the seeds developed. Five blocks were planted with one replicate for each genotype per block. Blocks were staggered in time and this experimental design was used to allow for scanning time. Plants were grown in a

greenhouse at a 25/18°C day/night temperature. Additional lighting was provided as to ensure a 14h/10h day/night cycle. Once a week a nutrient solution (100 g of HortiMix Standard: NPK ratio 15-7-30 to 1L of solution contains 107 mmole of total water soluble N, 4.5 mmoles P_2O_5 (w/w), 32 mmoles total K_2O (w/w), 4 mmoles MgO (w/w), 0.04 mmoles Fe-EDTA, 0.18 mmoles Mn, 0.28 mmoles B, 0.04 mmoles Zn, 0.03 mmoles Cu, 0.013 mmoles Mo (Hortifeeds, Lincoln, UK) was added when watering. Moisture content of the pots was maintained at 17% gravimetric moisture content by watering a constant amount of water per block based on the overall starting reference weight of the pots. Plants were grown for 49 days to assure sufficient growth of node 3 and node 4 roots. These nodes were selected because node 1 and 2 were too horizontally oriented to sufficiently interact with the compacted layer (more horizontal growth of earliest nodes has also described by Araki *et al.*, 2000; York *et al.*, 2015).

6.3.1.3 X-ray Computed Tomography

Soil columns were not watered 48 hours prior to scanning to allow for enhanced contrast between the root and soil matrix. Each column was imaged using a v|tome|x L (GE Measurement and Control Solutions, Wunstrof, Germany) X-ray CT scanner. Two scans (multiscan option) were taken per column (top and bottom) with a total scanning time of two hours per column. The distance from the centre of the sample to the detector was 2000 mm. X-ray energy was set at 290 kV and the current was 2700 µA. Filters were fitted to the X-ray gun (1.5 mm copper, 0.5 tin) and detector (0.5 mm copper) to enhance the image quality. Image averaging was set at 5 images. The scanning resolution was 96 µm and 2400 image projections were taken for each scan.

6.3.1.4 Image processing and analysis

Images were reconstructed at 32-bit (Phoenix DatoS|x2 reconstruction tool, GE Sensing & Inspection Technologies GmbH, Wünstorf, Germany) with scan optimisation and beam hardening correction set at 8. The 3D image volumes were analysed in VGStudioMax 2.3 (Volume graphics Gmb, Heidelberg, Germany). The greyscale values of the two obtained volumes were equalised and scans were aligned and stitched together. An example of a scan can be found in Fig. 6.1. Nodes

1 to 4 were identified manually from 2D projections of the scans (Fig. S6.1). Each plant was marked at the base of the stem with a thumbnail pressed into the stem prior to scanning which served as a reference point for labelling of each root axis (Fig. 6.1A). For each node, all roots were labelled clockwise (observed from above, yz-projection plane) around the reference point. After labelling each root axis, the polyline tool within VGStudioMAX was used to trace the roots from the root base downwards (Fig. 6.1A). Polylining stopped either at the root tip or alternatively when the column wall or bottom of the column was reached. Whether roots reached and subsequently crossed the compacted layer was recorded. Distances along the root axis were measured during polylining to determine sectioning positions relative to the compacted layer along penetrating roots. Three sectioning points were located along each selected penetrating root axis; 'before', 1 cm above the compacted layer, 'within', 1 cm after penetrating the compacted layer and 'after', 1 cm after crossing the layer (Fig. 6.1B). The polylines were also used for measuring root angle and rooting depth with PAM (Polyline Analysis Measurement Software, University of Nottingham, UK), an in-house software developed for these measurements. The 100% setting of the polylines was used as a reference to calculate root angle from the horizontal. Rooting depth per pot was taken as the average maximum depth of all roots up till their root tip or when they hit the pot wall.

6.3.1.5 Root harvest and sectioning for root anatomical traits

Immediately after scanning all soil columns were lifted out of the plastic columns and roots were washed from the soil. The entire root system was extracted and stored in 75% ethanol (v/v) until sectioning. Penetrating roots of node 3 and node 4 were selected for sectioning based on polylining results and clipped from the entire root system. The length along each individual root axis was measured and sectioning positions were identified along the root axis of interest (Fig. 6.1). Pieces of root containing the sectioning positions were excised out of the root axis and embedded by placing them into 3D printed moulds (Atkinson and Wells, 2017). 6% agarose (Sigma-Aldrich Co. Ltd, Gillingham, UK) at 39°C was used to fixate the roots within the mould. A vibrating microtome (7000 smz-2) (Campden Instruments Ltd., Loughborough, UK) was used to section the roots within the

agarose block at 200-230 μm thickness per slice (blade speed at 1.75-2 mm s^{-1}, blade frequency at 70 μm). Root sections were then incubated in calcofluor white (Sigma-Aldrich, Co. Lt, Gillingham, UK), 0.3 mg ml^{-1} for 90 seconds, rinsed with deionised water and placed on a microscopy slide and covered by a coverslip. Cross-sectional images (Fig. 6.2) were obtained by using an Eclipse Ti CLSM confocal scanning microscope (Nikon Instruments Europe B.V., Amsterdam, The Netherlands) with three excitation lasers. Images were collected using 10x objective, all three image channels were combined. As entire cross-sections did not fit the 10x objective image space, multiple images per root section were obtained, taking care that part of each set of images overlapped. ICE software (Microsoft, Redmond, WA, US) was used to obtain one composite image per root section (camera motion set at planar motion). Image analysis for root anatomical traits was conducted according to the methods described in **Chapter 5**. Measurements of root anatomical traits can be found in Table 6.1.

6.3.2 Experiment 2: Thickening of roots is ethylene driven

6.3.2.1 Plant material and growing conditions

Seeds from four genotypes (IBM086, IBM146, IBM014 and OhW128) were surface sterilized in 3% DI water in sodium hypochlorite (v/v), rolled into tubes of germination paper (76 lb, Anchor Paper, St Paul, MN, USA), and placed in a dark chamber at 28 °C for 4 days in beakers containing 0.5 mM CaSO4. Beakers containing germinating seedlings were placed under a fluorescent light (350 μE $m^{-2}s^{-1}$) at 28 °C for one day before transplanting to an aerated solution culture. Three randomly assigned seedlings from each genotype were transplanted in foam plugs suspended above each 38 L solution culture tank. The solution culture tank contained per litre: 3 mmol KNO_3, 2 mmol $Ca(NO_3)_2$, 1 mmol $(NH_4)_2HPO_4$, 0.5 mmol $MgSO_4$, 50 mmol Fe-EDTA, 50 mmol KCl, 25 mmol H_3BO_3, 2 mmol $MnSO_4$, 2 mmol $ZnSO_4$, 0.5 mmol $CuSO_4$ and 0.5 mmol $(NH_4)_6Mo_7O_{24}$. The pH was adjusted daily to 5.5 using KOH and the solution was completely replaced every 7 days. Plants were grown for 30 days in a climate chamber. During the growth period, the mean minimum and maximum air temperatures were 26 ±

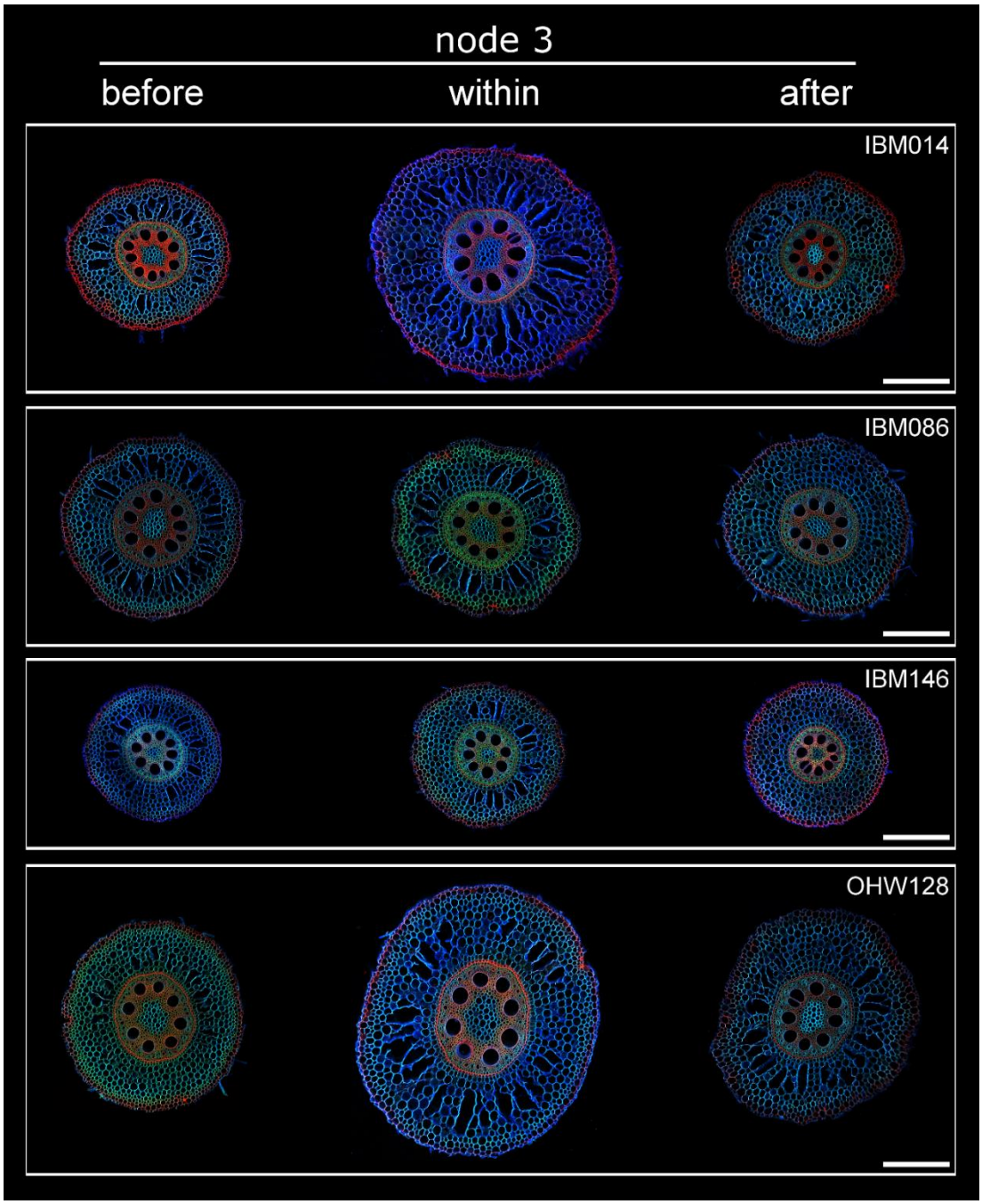

Figure 6.2 – Typical images of sections taken along the same root axis from node 3 and node 4 (see continued figure) for each genotype. Before, within and after indicate the root axis location where the roots were sectioned in relation to the compacted layer. All images are at the same scale, scale bar at 500 μm.

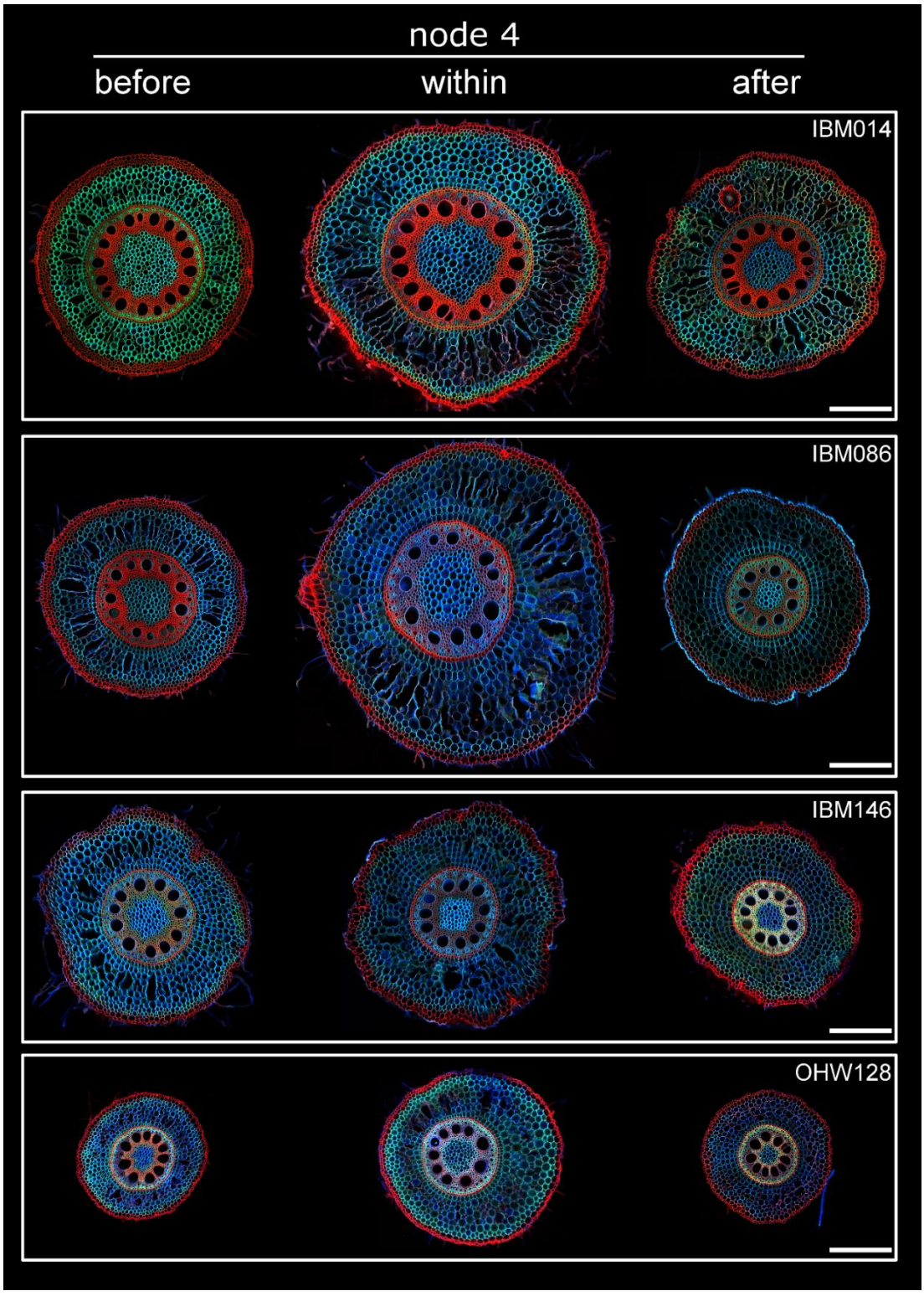

Figure 6.2 – continued

Table 6.1 - Observed root anatomical traits. All traits were directly measured with the exception of total cortical area which was calculated as the difference between root cross-sectional area and stele area.

Abbreviation	Root anatomical trait	Unit
RCSA	Root cross-sectional area	mm^2
TSA	Total stele area	mm^2
TCA	Total cortical area	mm^2
CF	Cell file number	-
IN	Cell area - inner cortical region	μm^2
MID	Cell area - middle cortical region	μm^2
OUT	Cell area - outer cortical region	μm^2

3°C and 30 ± 3°C, respectively with maximum illumination of 800 µmol photons m^{-2} s^{-1} and average relative humidity of 40%.

6.3.2.2 Ethylene application

Three replicates of all four genotypes (i.e. each 38 L tank) were exposed to one of four different treatments (1) root zone air application (control), (2) root zone ethylene application (dose 1), (3) root zone ethylene application (dose 2) and (4) root zone 1-MCP (1-methylcyclopropene, ethylene inhibitor) application, all applied continuously beginning at seedling transfer to solution culture. Solution culture tanks in the control treatment were bubbled at 10 mL min^{-1} with ambient air in 38 L of solution culture. In the ethylene treatment (dose 1), compressed ethylene (1 mL L^{-1} in air, as used by Gunawardena *et al.* (2001)) was bubbled through 38 L of solution culture at 10 mL min^{-1}. In the ethylene treatment (dose 2), compressed ethylene (1 mL L^{-1} in air) was bubbled through 38 L of solution culture at 20 mL min^{-1}. For the 1-MCP treatment, 1-MCP (SmartFresh, ~3.8 % active ingredient, AgroFresh, USA) was volatilized by dissolving 0.17 g in 5 mL water in a glass scintillation vial, and then transferred into a 2L sidearm flask. An open-cell foam plug enclosed the mouth of the flask, and the headspace containing 1-MCP gas was bubbled through 38 L of solution culture at a rate of 10 mL min^{-1}. The air pump ran continuously, and the 1-MCP was replenished daily into the sidearm flask. There was no significant effect of flow rate on headspace

ethylene concentrations, which ranged from 0.78-1.58 μL L^{-1} with a mean of 1.15 μL L^{-1}, therefore the results of ethylene treatments were combined in a single mean.

After 30 days of growth, plants were sampled. Two seminal and first, second, third, and fourth whorl nodal roots from each plant were sampled 5-8 cm from the base of the plant and preserved in 75% EtOH (v/v) for further anatomical analysis. For this experiment only node 3 and node 4 roots were used.

6.3.2.3 Laser Ablation Tomography and evaluation of root anatomy

Root anatomy was imaged using Laser Ablation Tomography (LAT) (Hall *et al.*, 2019; Strock *et al.*, 2019). In brief, a pulsed UV laser is used to vaporize the sample at the camera focal plane and simultaneously imaged. Imaging of root cross-sections was performed using a Canon T3i camera (Canon Inc. Tokyo, Japan) and 5× micro lens (MP-E 65 mm). Two images for each root sampled were collected for phenotypic analysis. Six anatomical phenes (Table 1) on every image were measured using objectJ (Vischer and Nastase, 2009) and a Fiji plug in (Schindelin *et al.*, 2012) according to the method described in **Chapter 5**.

6.3.3 Statistical analysis

6.3.3.1 Experiment 1

The number of replicates obtained per genotype and node varied as one plant (genotype OhW128) died during the 49 day growth period. Hence for node 3 and 4 only four replicates were taken into account for this genotype. For genotype IBM014, node 4 roots were underdeveloped (< 0.5 cm long, observed during washing) at sampling, hence only four replicates for this measurement were obtained. Additionally, not all genotypes were equal in crossing the compacted layer, hence some genotypes have fewer replicates at the within and after the compacted layer sectioning positions. Both the effect of blocking and interaction effects were tested, when not significant they were omitted from the analysis. Factorial regression was used to assess the effect of different factors on root counts. A Poisson distribution was used followed with post-hoc Tukey comparisons to compare factor levels. Correlations between root angle and count

data were calculated using a Spearman-Rank correlation. Penetration rates were calculated per node as the ratio of roots that crossed the layer and reached the layer. Root thickening was defined as the increase of overall root cross-sectional area and an ANOVA was used to identify the effect of factors genotype and node. Anatomical changes were similarly assessed by ANOVA that included factors genotype, node and sectioning position on root cross-sectional area, total stele area, total cortical area and cell file number. The same factors were used with the addition of the cortical region for the ANOVA on cell area. Tukey comparisons were carried out between nodes, between genotypes within nodes and between sectioning positions for root cross-sectional area. For cortical cell areas and cell file number Tukey comparisons were used to identify differences between sectioning positions. Fold-increases for cell area were calculated for the different cortical regions and for the different nodes.

6.3.3.2 Experiment 2

Average cortical area, stele area and cell file number were assessed by ANOVA and Tukey comparison identified differences between ethylene, 1-MCP and control treatments. Root anatomical measurements were compared between the two experiments and differences across treatments were assessed by Tukey comparison. Correlations between cortical cell area obtained from both experiments were calculated.

6.4 Results

6.4.1 Experiment 1: Anatomical changes to a root axis crossing a compacted layer

6.4.1.1 Reaching the compacted layer was root angle dependent

Location and genotype had effects on the number of nodal roots counted (Table 6.2). The same number of roots was formed per node irrespective of genotype or node (Fig. 6.3A, Table 6.2). Within a node, the number of roots reaching the compacted layer was not different for the different genotypes (Fig. 6.3A). However, significantly fewer roots reached the layer for node 3 roots of genotype IBM086 in comparison with node 4 roots of genotype IBM146 (Fig. 6.3A).

Numbers of roots reaching the layer were only significantly different from those crossing for IBM086 (Fig. 6.3B). Younger nodes (node 4) were steeper than older nodes (node 3) (Fig. 6.4A) and root angle was correlated with the number of roots that reach the compacted layer (Spearman's rank correlation r=0.53) (Fig. 6.4B). Root angle itself was node and genotype dependent (Table 6.2B). IBM086 had the most shallow roots (Fig. 6.4A), this led to node 3 roots hitting the pot-wall before reaching the compacted layer and this should be taken into account when root penetration rates are interpreted.

Table 6.2 – (A) Factorial regression for root number and (B) root angle. Significance at ** $p \leq 0.01$ and *** $p \leq 0.001$.

A

Number of roots			
Factor	Deviance	p (> Chi)	
Location	35.75	1.72E-08	***
Genotype	13.52	3.64E-03	**
Node	0.80	0.37	

B

Root angle			
Factor	F-value	p-value	
Genotype	5.39	4.06E-03	***
Node	17.45	2.12E-04	**

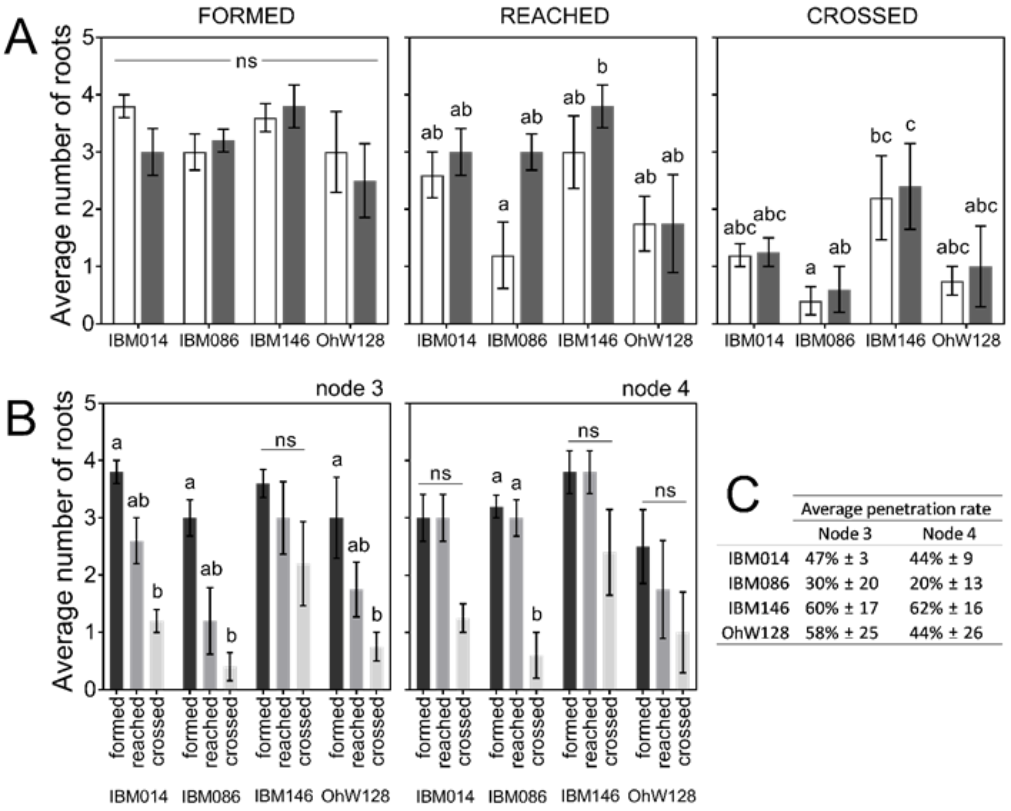

Figure 6.3 – (A) Root counts at different locations with respect to the compacted layer. Bars in white are root counts for node 3, bars in grey are root counts for node 4. Differences in root counts between nodes and genotypes were assessed with Tukey comparisons ($P \leq 0.05$). (B) Root counts per node and genotype on different locations in respect to the compacted layer. Differences between root counts are shown by different letters, based on a Tukey comparison ($p \leq 0.10$) within node and genotype combinations. ns stands for non-significant. (C) Associated average penetration rate ± SE per genotype and node.

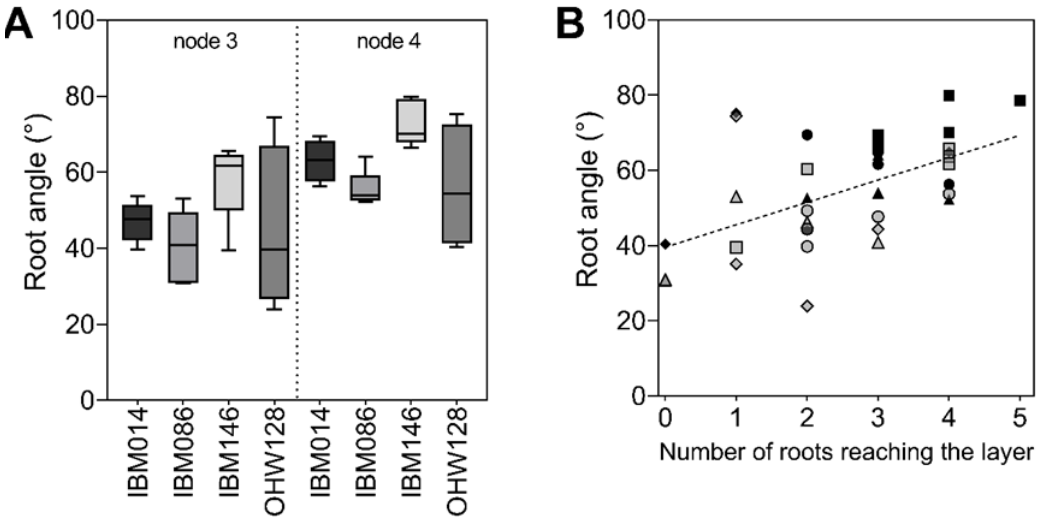

Figure 6.4 - Root angle is different between nodes and determines if roots reach the compacted layer. (A) Boxplots for different genotypes per node. (B) Correlation between root angle and the number of roots reaching the layer. Node 3 data in grey and node 4 data in black. Different shapes relate to the different genotypes (● IBM014, ▲ IBM086, ■ IBM146, ♦ OhW128). Correlations were tested with a Spearman rank correlation (r=0.5318, p=0.0007).

6.4.1.2 Genotypes differed in the ability to penetrate a compacted layer

The number of roots crossing the compacted layer varied among genotypes (Fig 6.3A). For example, IBM146 had more roots crossing the compacted layer (Fig. 6.3A) in comparison with other genotypes, that either did not fully reach the compacted layer (IBM086, node 3) or did not cross the compacted layer (IBM014). When roots did not cross the compacted layer, they either buckled or deflected (Fig. S6.2). Genotypes differed in the number of roots crossing the layer, resulting in different average penetration percentages between genotypes (Fig. 6.3C). The average rooting depth (Fig. 6.5) for both nodes differed, overall roots of node 3 were more shallow than roots of node 4. Roots of genotype IBM146 grew to the greatest depth for both nodes. A limited number of roots were able to grow past the compacted layer for nodal roots of genotypes IBM014 and OhW128.

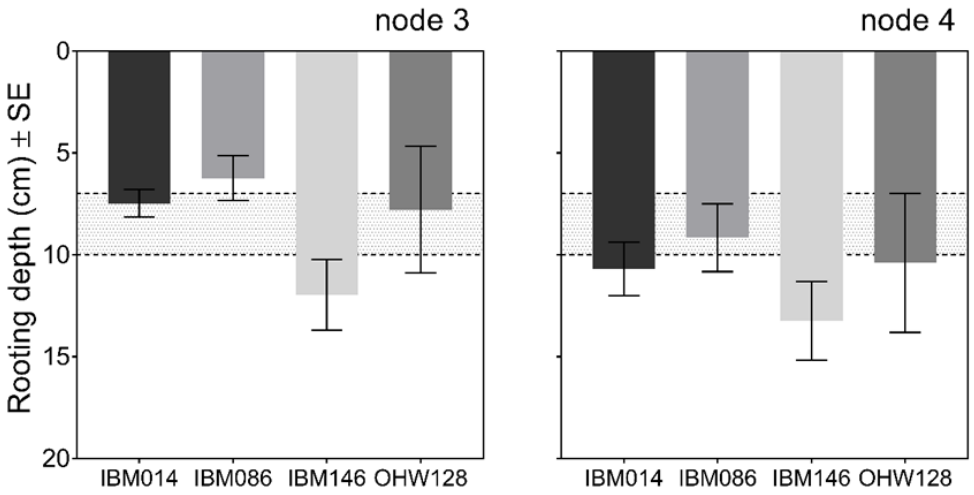

Figure 6.5 - Average rooting depth (cm) ± SE per node and genotype, averaged for each replicate. Depth was calculated including all roots. If roots hit the column wall depth was recorded as the depth of where they hit the column wall. The greater bulk density layer was located at 7 – 10 cm depth and depicted by the dotted lines and grey area on the graph.

6.4.1.3 Root thickening was genotype and node dependent

Root cross-sectional area was affected by node, genotype and sectioning position (Table 6.3, Figs. 6.2, S6.3). The older nodes (node 3) had significantly smaller root cross-sectional areas then the younger nodes (node 4) for sectioning positions before the compacted layer and within the compacted layer (Fig. S6.3, capital letters). However, root cross-sectional areas between the different nodes after the compacted layers were not significantly different (Fig. S6.3). Most genotypes thickened when crossing the compacted layer (Figs. 6.2, 6.6, S6.3). Radial expansion was affected by genotype, node, and their interaction (Table 6.4). The average number of roots capable of crossing the compacted layer for both nodes of IBM086 and OhW128 was less than 1, hence caution should be taken interpreting thickening for these root axes. For node 3 IBM014 thickened to a greater root cross-sectional area than IBM146 (Fig. S6.3). When node 3 roots thickened, they reached root cross-sectional area dimensions close to node 4 roots before they crossed the compacted layer. Not all genotypes thickened, for example, IBM146 did not thicken to the same extent as the other genotypes (Fig. S6.3). For node 4 thickening was absent for IBM146 as root cross-sectional area

of sections from the before and within the compacted layer sectioning positions were not significantly different (Fig. S6.3). After roots crossed the compacted layer, root cross-sectional areas returned to similar dimensions seen at the before the compacted layer sectioning position (Fig. S6.3).

Table 6.3 - (A) ANOVA results for root cross-sectional area (RCSA), total cortical area (TCA), total stele area (TSA) and cell file number (CF). (B) ANOVA results for cortical cell area. Significance levels at *** p≤0.001, ** p≤0.01, * p≤0.05. ns stands for non-significant. For (B) only the significant effects were listed. F-values and p-values can be found in Table S6.1.

A

Factor	RCSA	TCA	TSA	CF
Node	***	***	***	***
Genotype	***	***	***	*
Sectioning position	***	***	***	ns
Node:Sectioning position	***	*	ns	ns
Genotype:Sectioning position	ns	ns	ns	ns
Node:Genotype	ns	ns	ns	ns
Node:Genotype:Sectioning position	ns	ns	ns	ns

B

Factor	Cortical cell area
Node	**
Genotype	***
Sectioning position	***
Cortical region	***
Node:Genotype	**
Node:Sectioning position	**
Genotype:Sectioning position	***
Location: Cortical region	*
Node:Genotype:Sectioning position	*

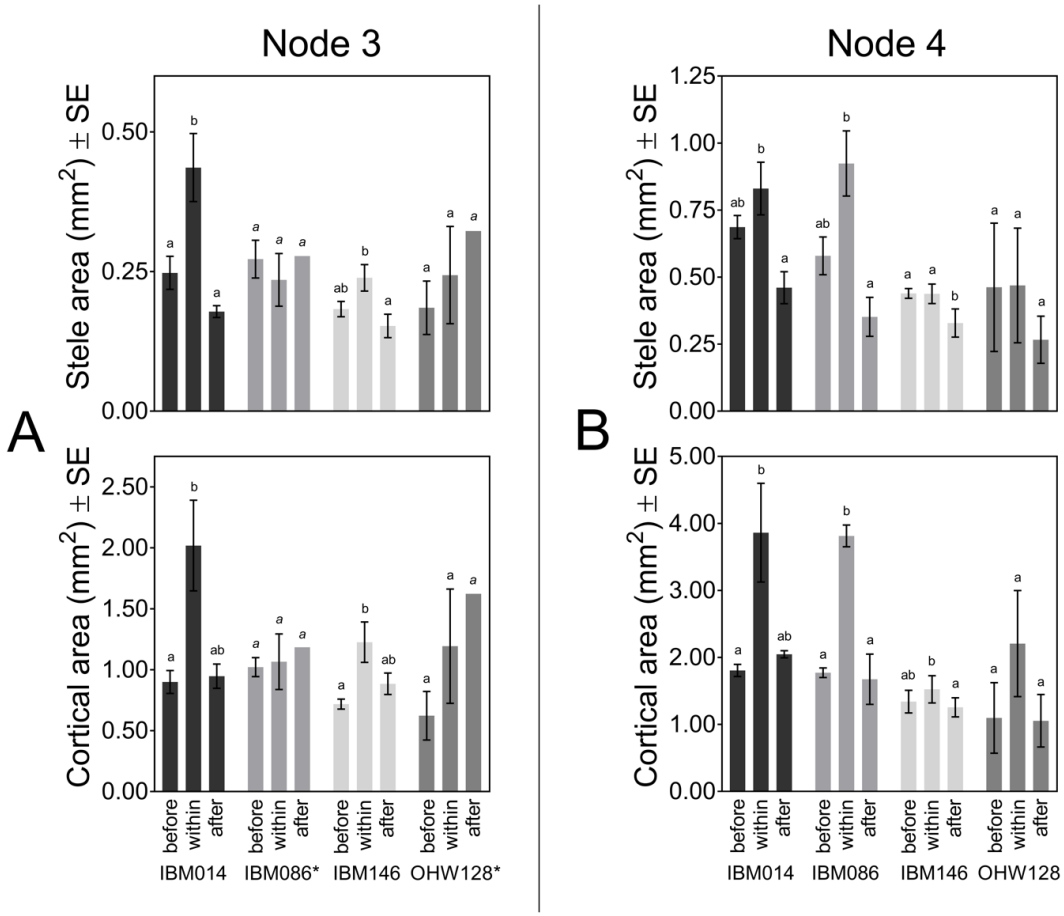

Figure 6.6 – Average stele area and cortical area (± SE) at different sectioning positions (before, within and after a compacted layer) along a root axis. Data for (A) node 3 and (B) node 4. Differences between locations were calculated by Tukey comparisons within node - genotype combinations (P ≤ 0.05).Genotypes with * had few roots capable of crossing the compacted layer leading to a reduced number of roots that could be sectioned. Cursive letters mean separation letters indicate that replicate numbers dropped for IBM086 from n=3 (before), n=2 (within) to n=1 (after) and for OhW128 from n=4 (within) to n=1 (after). When n=1 there are no SE.

Table 6.4 - ANOVA results for radial expansion, measured as an increase in root cross-sectional area, in response to mechanical impedance. Significance levels at *** p≤0.001, ** p≤0.01, * p≤0.05.

Radial expansion			
Factor	F-value	p-value	
Node	9.23	5.36E-03	**
Genotype	4.67	9.70E-03	**
Node:Genotype	3.02	4.80E-02	*

6.4.1.4 Root thickening is more related to expansion of the cortex than the stele

Root cross-sectional area, total cortical area and total stele area were dependent on node, genotype and sectioning position (Table 6.3A). Thickening was due to increased cortical area and/or increased stele area (Fig. 6.6). Radial thickening was not always associated with increased stele area, for instance no significant increase in stele area was observed for node 4 roots of IBM014 while this genotype clearly thickened upon encountering the compacted layer due to cortical area increase (Fig. 6.6B). Overall the cortical tissues expanded more than the stele (Fig. 6.6) and the cortex has more area overall.

6.4.1.5 Cortical expansion is due to cellular area changes and not cell file changes

Cell areas across the different cortical regions were of unequal size (Table 6.3B). The middle cortical (MID) cells had the largest cell areas, surrounded by OUT and IN cells with smaller cell areas (Fig. 6.7). Cell area was also dependent on node, genotype and location (Table 6.3B, Fig. 6.7). All cortical cells areas from all cortical regions increased for thickening genotypes within the compacted layer (Fig. 6.7). While for IBM146 (node 4), that did not thicken, cell areas remained constant (Fig. 6.7). For OhW128 cell areas did not increase and had large variability (Fig. 6.7). Cell areas below the compacted layer were similar to above the layer (Fig. 6.7). Across the cortex, for thickening genotypes, the outer cortical cells had a greater relative cortical cell area increase then the inner and middle cortical cells (Table 6.5). Regardless of this greater relative increase in cell area, the outer cortical cells remained smaller than the middle cortical cells at all sectioning positions (Fig. 6.8).

Cell file number was significantly different for the different nodes and genotypes (Table 6.3A). Each genotype had a smaller cell file number for node 3 than for node 4 (Fig. 6.8). Cell file numbers were however not significantly different for the different sectioning positions along the root axis with respect to the compacted layer (Table 6.4C). For all genotypes the cell file number remained

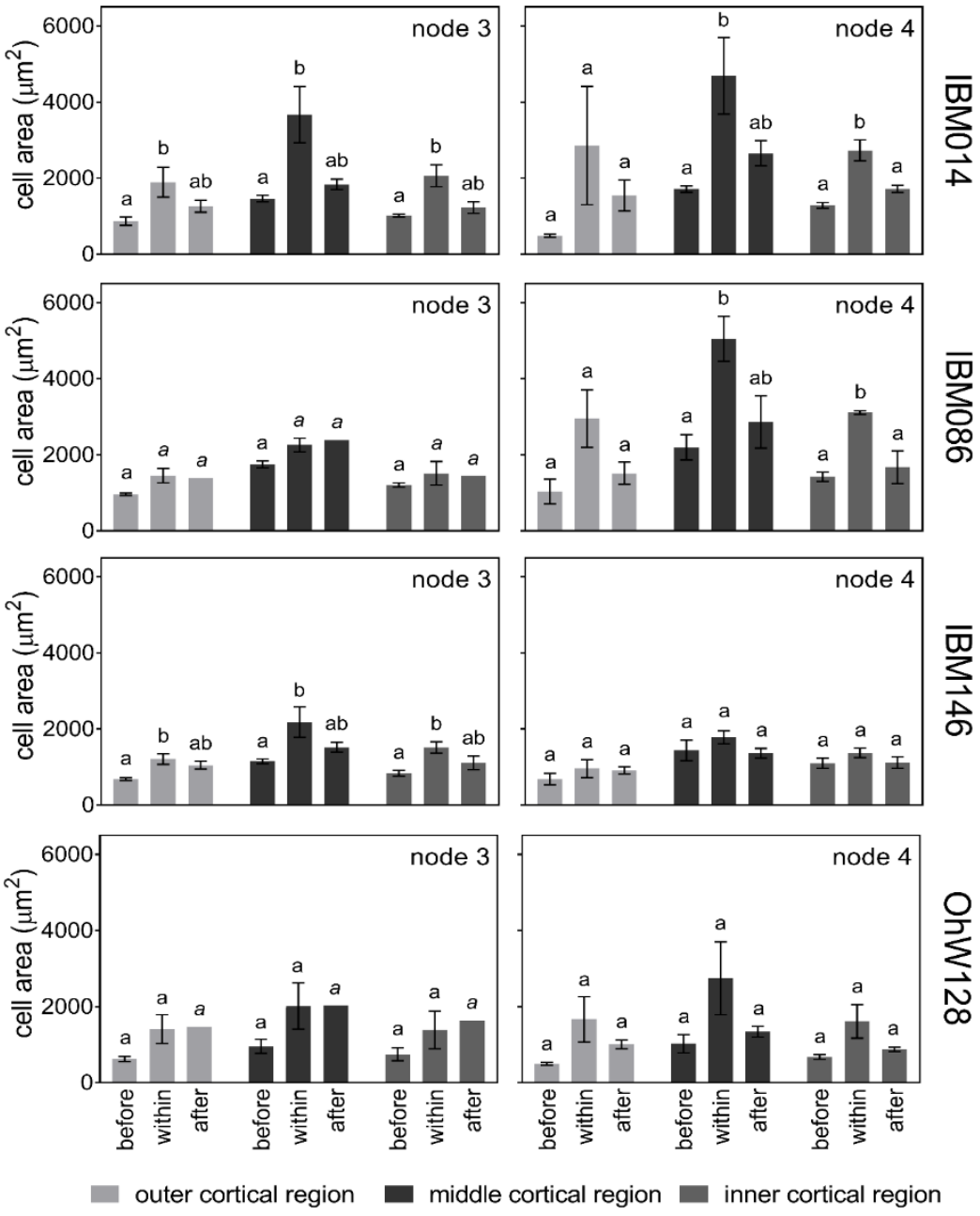

Figure 6.7 - Cortical cell areas (μm^2) ± SE for different cortical cell positions within the root cross-section. Cell areas were measured along node 3 and node 4 root axes before, within and after passing the compacted layer. Differences between locations were calculated by Tukey comparisons within node - genotype combinations ($P \leq 0.05$). Cursive mean separation letters indicate that replicate numbers dropped for IBM086 from n=3 (before) to n=2 (within) to n=1 (after) and for OhW128 from n=4 (within) to n=1 (after). There is no SE when n=1.

Table 6.5 – Fold increase of cell area according to cortical area and genotype for node 3 and node 4.

	Node 3			Node 4		
genotype	outer	middle	inner	outer	middle	inner
IBM014	2.28	1.97	1.77	5.48	2.78	2.14
IBM086	1.56	1.32	1.23	3.19	2.35	2.24
IBM146	1.80	1.90	1.81	1.46	1.43	1.30
OhW128	2.24	2.17	1.74	3.73	3.23	2.54

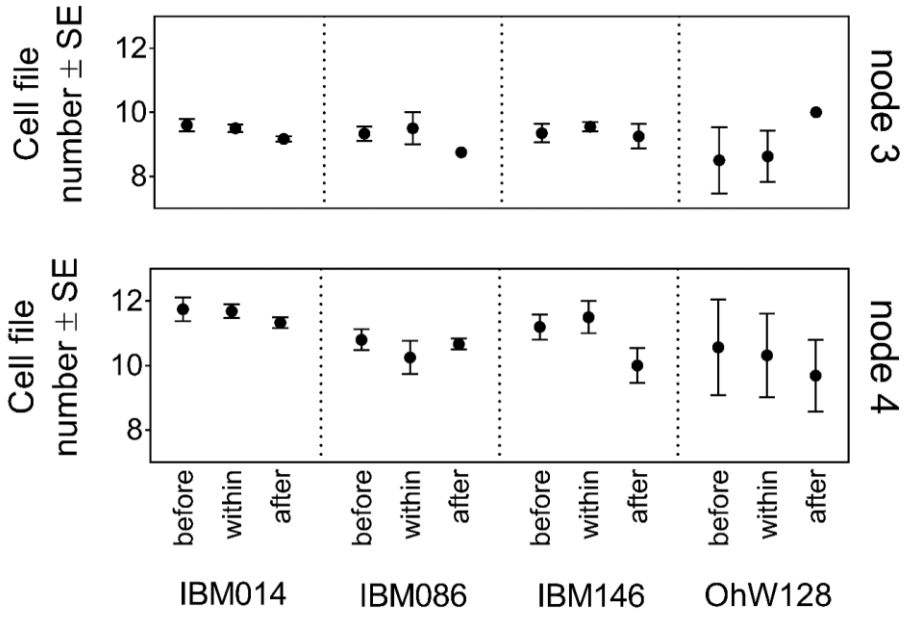

Figure 6.8 - Average cell file number ± SE for different nodes and genotypes along the root axis. No significant differences between locations were found. There is no SE when n=1 (node3; IBM086 and OhW128)

stable when crossing the compacted layer (Fig 6.8) Therefore, root thickening was due to increased cell area rather than increased cell file number.

6.4.2 Experiment 2: Ethylene caused thickening of roots

6.4.2.1 Node and genotype dependent root thickening due to ethylene

The application of ethylene increased the cortical area in some cases but did not affect stele area. Genotypes varied in ethylene responsiveness, for example node 3 roots of IBM014 had the greatest increase in cortical area in comparison with

node 3 roots of other genotypes (Fig. 6.9). Node 3 and node 4 differed in their reaction to ethylene application, for instance node 4 cortical area did not respond significantly to ethylene application for genotypes IBM014 and IBM146 while they did for node 3. IBM086 node 3 roots did not form significantly more cortex under ethylene while they did for node 4 roots. Control roots and roots treated with 1-MCP were indistinguishable (Fig. 6.9), as 1-MCP blocks the effect of ethylene it can be assumed that control roots were not responding to endogenous ethylene.

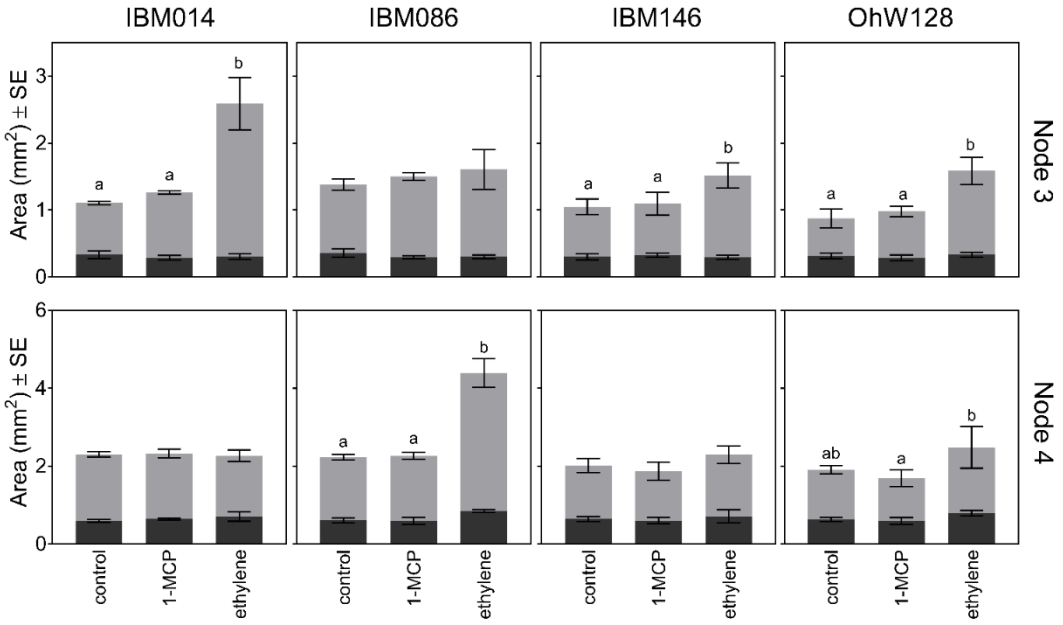

Figure 6.9 - Average cortical area (grey) and stele area (black) ± SE of root cross-sections under ethylene, 1-MCP and air treatments per node and genotype. Cortical area in light grey and stele are in dark grey. No significant differences were found in stele area. Lower case letters were used to identify differences in cortex areas within node and genotype according to Tukey's test ($P \leq 0.05$). Where no letters are shown, differences between treatments were non-significant.

6.4.3 Comparing soil and ethylene results

Results of independent impedance (experiment 1) and ethylene treatment (experiment 2) experiments were similar (Figs. 6.10, 6.11). Root cross-sectional area observed at the sectioning position before the compacted layer location (experiment 1) was similar to root cross-sectional area observed under control conditions in the ethylene experiment (experiment 2), across all genotypes and

node combinations (Fig. 6.10). Root cross-sectional areas under impeded conditions (within the compacted layer (experiment 1)) and with ethylene exposure (experiment 2) were the same with the exception of node 4 roots of IBM014 (Fig. 6.10). The smaller root cross-sectional area under ethylene can be partly explained by a cell file difference of approximately 2 cell files forthis genotype (Fig. S6.4).

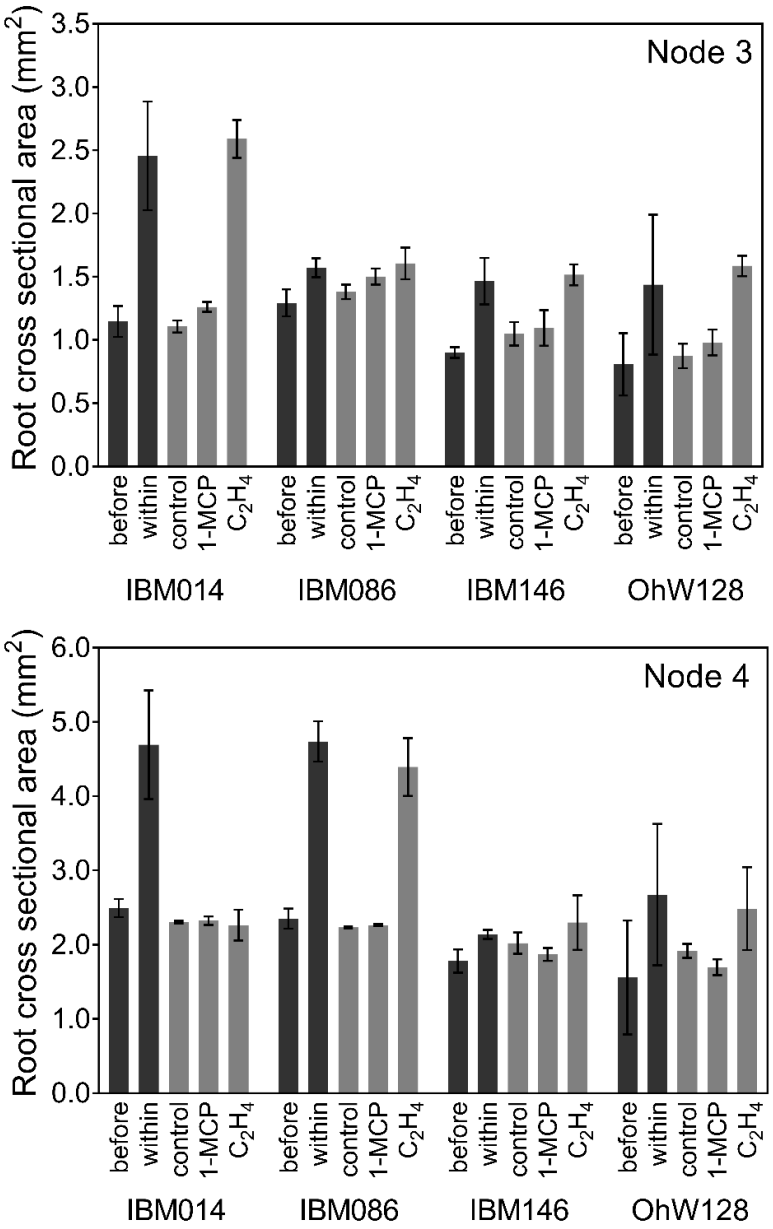

Figure 6.10 - Comparison of root cross-sectional area ± SE of experiment 1 (before and within compacted layer: black columns) and experiment 2 (control vs. ethylene vs. 1-MCP, grey columns) for the different genotypes and nodes. Letters show the differences between treatments assessed by Tukey comparisons within node-genotype combinations ($P \leq 0.05$). Cursive mean separation letters indicate when replicate numbers dropped for IBM086 to n=2.

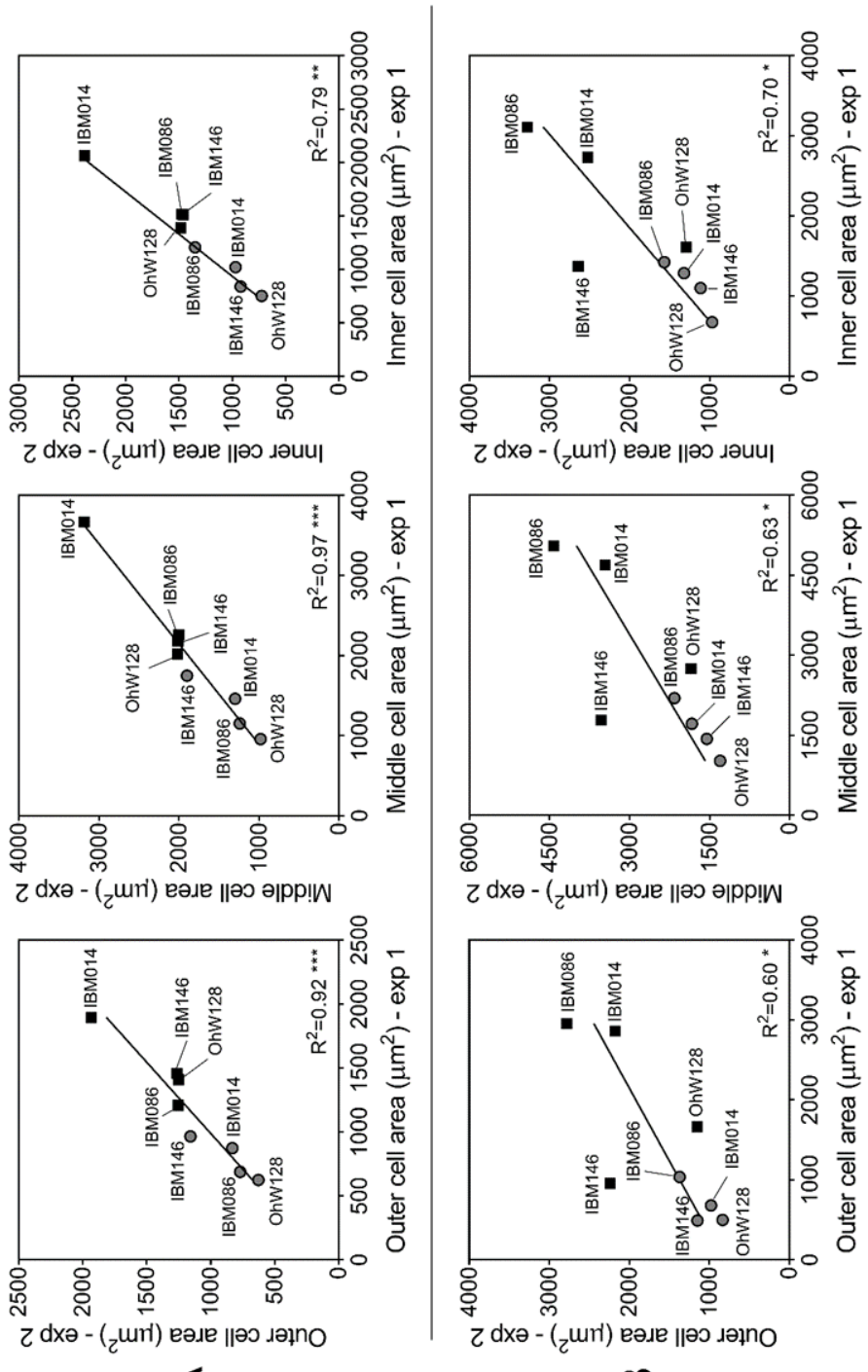

Figure 6.11 - Correlation between cell area data from different cortical regions of experiment 1 (pot trial in soil) and experiment 2 (grown hydroponically) for (A) node 3 and (B) node 4. Each point represents the average value obtained for a genotype and node. Grey circles depict values found for before (experiment 1) and control (experiment 2) combinations, while grey circles depict within (experiment 1) and ethylene (experiment 2) combinations.

When ethylene was applied, most roots thickened (Figs. 6.9, 6.10), with the following three exceptions: 1) genotype OhW128 had greater variance, which made the increase in root cross-sectional area non-significant for both nodes in soil, while for node 3 ethylene application did cause thickening, 2) For IBM086 no thickening was observed in response to ethylene for node 3. Node 4 however did thicken in both soil as well as ethylene exposure. However, root penetration for node 3 was difficult to assess as roots were often too shallow and hit the pot wall for this genotype before interacting with the compacted layer and 3) Node 4 roots of IBM014 thickened when grown in soil, while they did not thicken under ethylene application.

Cell areas increased in both experiments when plants encountered either impeded conditions or exogenous ethylene (Fig. 6.11, black squares versus grey circles). Average cell areas of genotypes grown in the hydroponics experiment were strongly correlated with areas of those grown in soil (Fig. 6.11). Genotype IBM014 had the greatest cell size in response to ethylene and within the compacted layer for node 3. For node 4 roots of IBM086 greater cell areas were attained in under growth in the compacted soil layer and in ethylene treatments.

6.5 Discussion

The initial hypothesis of this study was that cortical expansion of a root axis upon experiencing impedance is linked to ethylene and genotypes that are responsive to ethylene would radially thicken and show better penetration of a compacted soil layer. Root growth angle affected the ability of roots to reach the compacted layer. In contrast with the hypothesis genotypes that showed less radial expansion upon encountering compacted soil were better able to cross the compacted layer and attained greater rooting depth than genotypes with greater radial expansion (Fig. 6.3). Roots thickened through the expansion of the cortex more than the stele and cortical area increases were caused by an increase in cell size and not cell file number (Figs. 6.7, 6.8). Furthermore, ethylene may be related to genetic variation in radial thickening as most genotypes showed similar anatomical responses to mechanical impedance and conditions and exogenous ethylene application.

6.5.1 Root thickening was driven by cortical cell area expansion rather than increased cell file number

Radial expansion upon encountering the compacted layer was mainly due to cortical expansion and, to a lesser extent, expansion of the stele (Figs. 6.2, 6.6) as the root cortical area is overall greater than the stele area. Depending on genotype and node, stele area increased or remained unchanged under impedance (Fig. 6.6). Lupin roots that grew under impeded conditions maintain stele dimensions (Atwell, 1988; Hanbury and Atwell, 2005), while barley, maize, rice, pea and cotton roots showed increased stele diameters under impedance (Wilson *et al.*, 1977; Iijima *et al.*, 2007). As the stele tissue is completely enclosed by the cortical tissue, radial expansion might be more difficult due internal pressures between tissues restricting radial expansion. Alternatively the cortex could simply be more plastic than the stele in its response to its local environment. Huang *et al.* (1998) identified a cDNA clone (*pIIG1*) with higher expression in the cortical cells and protocambium of mechanically impeded maize roots illustrating that gene expression upon impedance can be localised in different root tissues. Functional consequences to drastic stele rearrangement could be important as xylem vessels might be affected as well (but presently not studied here but observed by Iijima *et al.*, 2007 on maize) with probable effects on water transport. Less change to stele tissue anatomy might therefore help maintain the tissue function.

Similarly to these results Iijima *et al.* (2007) showed that the cortical thickness of maize increased more than that the stele diameter in response to mechanical impedance. Cortical changes have been attributed to either increased cortical cell area (Atwell, 1988; Hanbury and Atwell, 2005; Veen, 1982) or a combination of increased cell area and increased cell file number (Colombi *et al.*, 2017b; Croser *et al*., 1999; Iijima *et al*., 2007). Cortical thickening was due to cell area increases, while cell file number remained stable along the root axis (Figs. 6.7, 6.8, 6.9) while published observations have used different plants to obtain root axes for their observations. This would introduce additional plant-to-plant uncertainty about cell file number changes. Additionally, studies have documented species differences (Iijima *et al.*, 2007; Colombi, 2016) rather than genotypic differences

in response to mechanical impedance. Genotypic differences have only been studied in wheat in a few cases (Colombi *et al.*, 2017b, 2019), while maize has been used even less (Chimungu *et al.,* 2015a).

The percentage of roots crossing the compacted layer from different nodal root whorls within the same genotype is not significantly different (Fig. 6.3C). Node 3 and node 4 roots have more similar characteristics than nodes formed further from each other; potentially, node 2 and node 6 roots may differ in the proportion of roots able to overcome impedance conditions. This could be due to the innate difference in root cross-sectional area, where thicker roots are predicted to experience less stress at the root tip and would experience smaller shear stresses over the root surface (Kirby and Bengough, 2002). Thicker roots are assumed to buckle less (Chimungu *et al.,* 2015a; Clark *et al.,* 2003). These other nodes in the current set-up could not be tested due to pot-size (nodes with thicker roots) and CT-scanner resolution limitations (nodes with thinner roots). Node 2 roots were hard to visualise and tended to encounter the pot wall before reaching the compacted layer, and allowing plant growth past node 4 would make evaluation difficult as columns become rootbound. Root cross-sectional area was not predictive for penetrability for node 3 and node 4. Older roots of wheat were studied by Colombi *et al.* (2017b), which has smaller diameter roots than maize. This different root system characteristic could mean that wheat and maize could have different ways of dealing with impedance. Smaller diameter roots, such as all root classes of wheat are able to explore the remaining porosity in a denser soil, while only laterals would be able to do so for maize (Cahn *et al.*, 1989; Yamaguchi and Tanaka, 1990). The thicker roots of maize might have a competitive advantage when soil is unstructured as there will be fewer cracks or biopores to explore or when porosity is further reduced so that even thinner roots would experience mechanical stress. In these cases thicker roots would be expected to experience less stress (Kirby and Bengough, 2002).

Why roots thicken by cell area expansion rather than increasing their cell file number merits further study. Cortical cell expansion might be more energy efficient. Different wheat genotypes grown under impeding conditions all thickened and under greater impedance, genotypes with greater cortical cell

diameters were more energy efficient (Colombi *et al*., 2019). A similar mechanism could form the basis for preferentially adjusting cell area instead of cell file number. If similar root cortical areas are composed of either greater number of cell files with smaller cells, or fewer cell files but with larger cells, the latter may entail less metabolic cost to the roots, because of reduced cell wall construction, and the reduced metabolic costs of larger cells, which have been proposed to have reduced cytoplasm per unit tissue volume than smaller cells (Lynch, 2013; Chimungu *et al.*, 2014b). Reduced metabolic costs assist with deeper rooting as energy can be used elsewhere in the plant including for greater soil exploration (Lynch and Wojciechowski, 2015; Lynch, 2015). In addition, a change in cellular area may be easier and quicker to achieve than a cell file number change which would entail meristematic changes.

Cortical cell areas differed depending on inner, middle or outer cortical region(Fig. 6.7) and expand differently (Table 5). For wheat and maize, greater outer cortical cell expansion has been reported in response to mechanical impedance (Wilson *et al.*, 1977; Veen, 1982). Expansion of outer cortical layers may be less limited as they experience less internal pressure from surrounding cells and only experience the mechanical resistance applied by direct contact of the soil (Bengough *et al.*, 2006; Veen, 1982). Outer cortical cells remained smaller than middle cortical cells (Fig. 6.7) and it has been suggested that several layers of smaller cells in the outer region of the cortex provide mechanical stability (Chimungu *et al.*, 2015a; Striker *et al.*, 2007). Why the different regions expand differentially remains unclear. If ethylene is mainly having effects on the cortex, it might be differentially perceived by the different cortical regions. The inner and middle cortex of maize primary roots has been observed to be more sensitive to exogenous ethylene then the outer cortex as microtubule distribution was disturbed more for these cells then for the outer 2-3 cell layers (Baluška *et al.*, 1993). Another possibility is that a gradient in ethylene exists across the cortex when there is little aerenchyma present.

6.5.2 Root thickening did not improve root penetration percentage through a compacted layer

Ethylene may well be involved in the radial thickening response as the genetic variation in ethylene-induced thickening was correlated with the genetic variation in impedance-induced thickening (Fig. 6.10). Impeded roots produce more ethylene than non-impeded controls (Moss *et al.*, 1988; Sarquis *et al.*, 1991; He *et al.,* 1996a). Root cross-sectional area measured on roots before the compacted layer location (experiment 1) and those under control conditions and 1-MCP treatment (experiment 2) were comparable (Fig. 6.10). 1-MCP will block ethylene perception by roots. It can therefore be assumed that thickness of roots growing through low levels of impedance (before and after the compacted layer) were not significantly influenced by ethylene. If the ability to cross the compacted layer was solely due to root diameter, all roots would need to radially expand to a certain diameter regardless of genotype or node. This was not the case for node 4 roots in the compacted layer where root cross-sectional area of IBM146 was significantly different from IBM014 and IBM086. These genotypes had similar root cross-sectional areas for node 4 roots before penetrating, but differed in root cross-sectional area in the compacted layer (Fig. S6.3). Genotypes that did not thicken in both experiments had greater root penetration percentage and grew deeper (Figs. 6.3, 6.4).

Ethylene regulates root extension and lateral root density (Moss *et al.*, 1988; Sarquis *et al.*, 1991; Borch *et al.*, 1999). Root thickening is associated with reduced elongation rates (Bengough and Mullins, 1991; Croser *et al.*, 2000) through the reduction of cell length and cell flux out of the meristem (Croser *et al.*, 1999). Ethylene itself reduces the number of meristematic cells which reduces meristem length (Barlow, 1976). Ethylene also reduces cell elongation and therefore reduces root elongation (Sarquis *et al*., 1991). This study suggests that roots that are ethylene insensitive can maintain root elongation under impeded conditions as cell elongation would be less restricted, enabling them to attain greater rooting depth allowing better access to water and nutrients. Positive effects have also been attributed to root thickening. For instance, thickening reduces the stress from the root tip (Kirby and Bengough, 2002) and thicker roots

buckle less (Clark *et al.*, 2008; Whiteley *et al.*, 1982). Ethylene also promotes root hair cell elongation (Pitts *et al.*, 2001), which could stabilise the root and help penetration (Haling *et al.*, 2013; Bengough *et al.*, 2016). Thickening of roots might be beneficial on small scales or for localised impeded conditions. In order for roots to penetrate harder soil clods/aggregates or to penetrate through a biopore wall, usually only a small distance of impedance needs to be overcome. However, the effect of thickening and reduced elongation rate clearly leads to reduced root length and soil exploration. This suggests that the negative effects of ethylene overrule the positive, especially when impedance persists in a thick layer of compacted soil.

Moss *et al.* (1988) found that a prolonged application of ethylene reduced primary root length further the longer it was applied. Under continued impeded conditions, ethylene, as a stress signal, could potentially inform the plant to alter its growth by for instance compensatory root growth mechanisms. The compacted layer in this research was designed to mimic the spatial abruptness of a plough pan, which could induce different anatomical responses then when a root axis has been experiencing impedance for a longer time. How continued impedance changes root anatomy and root architecture within a whole root system and how this differs from the current experimental system remains to be further investigated. Anatomical phenotypes recovered once the root had passed the compacted layer. Similarly, root elongation rates of barley were restored after 3 days when transferred from impeded conditions in ballotini to unimpeded growth in solution (Goss and Russell, 1977) and pea roots experienced reduced elongation rates for 48 hours after transferring to hydroponics after which elongation rate restored itself (Croser *et al.*, 2000). Assuming that under unimpeded conditions these roots can elongate more than 1 cm per day, the observed residual effect of impedance in soil was less pronounced than in other studies. Ethylene production rates can rapidly increase and decrease upon application of mechanical impedance (Sarquis *et al.*, 1991). The concentration of ethylene that roots are exposed to also plays a role as higher ethylene concentrations induce longer recovery time (Whalen and Feldman ,1988). Under the applied experimental conditions only a change in mechanical impedance of

0.35 MPa was present, smaller than in most other studies. It would therefore be reasonable to assume a short ethylene signal was present, after which roots quickly return to their original radial dimensions. It is also likely that roots will have experienced a range of physical stresses within the compacted layer, as the soil dried and then was re-wet, following watering. This might have significantly increased the degree of mechanical impedance when the soil was drier, and perhaps even let do transient hypoxia following re-watering.

This suggests that ethylene functions as a stop signal for root growth when axial roots become impeded. Dependent on specific conditions, the thickening effects could help overcome impedance but only for short distances, such as overcoming localised impeded conditions such as denser soil around a pore wall. When greater patches of impeded soil cause a prolonged production of ethylene, this will signal axial root growth to stop. Upon this signal root growth in the lesser impeded areas, or adjustments to above ground plant growth might become upregulated.

6.6 Conclusions

Root thickening is mainly caused by cortical expansion and less by changes to the stele. Previous studies have not considered a single root axis to investigate root anatomical changes along individual root axes in response to impeding soil conditions. No significant changes to the cell file number along a single root axis of maize were found when this axis grew through denser soil. Instead thickening of the cortex is caused by cell area expansion. Genotypic variation was identified for root thickening. Ethylene caused similar expansion of the cortex cells compared to the compacted layer. Root thickening was unrelated to the ability of the different genotypes to penetrate through a compacted soil layer and reach past the compacted layer. Genotypes that did not thicken, when encountering the compacted layer or under application of exogenous ethylene, had the highest penetration percentages and were able to grow deeper past the compacted layer. This was node and genotype dependent. As root thickening is associated with reduced elongation rates, prolonged exposure to ethylene could stop axial root

growth. Ethylene therefore could stop further root exploration when roots experience impedance.

Chapter 7 – General discussion and conclusions

7.1 General conclusions

The following key conclusions can be drawn from the research presented here:

- Nodal roots of some maize genotypes became obstructed when growing in compacted plots, while other genotypes are capable of growing through impeding conditions imposed by soil. These genotypes are better adapted to reach deeper when grown under impedance (Fig. 4.5).

- Genotypes with contrasting root system size (total coarse root length, large versus parsimonious) were equally capable of reaching deeper on compacted plots. The ability of a root system to grow deeper in a compacted soil is independent of the amount of roots formed (Fig. 4.8).

- Root thickening in response to impedance varied among genotypes for both field (Fig. 5.5) as well as pot trials (Fig. 6.2) and was negatively associated with rooting depth (Fig. 6.5).

- Root anatomy is associated with deeper rooting under compacted field conditions in a node-dependent manner. Root anatomy was more important for node 3 roots versus node 4 roots. Deeper rooting genotypes had reduced cell file number and greater middle cortical cell area for node 3 roots (Table 5.4). For node 4, greater aerenchyma area was related to deeper rooting (Table 5.4).

- The ability of roots to cross a compacted layer is not related to radial thickening. Genotypic variation for radial expansion is caused by increased in cortical cell area, while cortical cell number remains constant when the cortical area increases under impedance. The same genotypes tested showed similar response to ethylene applied in hydroponic experiments. Genotypes that did not increase in nodal root diameter in response to

ethylene were those that were better able to cross the compacted layer in the pot experiment (**Chapter 6**).

7.2 General discussion

7.2.1 Genotypic variability of roots in relation to growth under impeding conditions

This thesis has clearly shown that genotypic variability exists for the ability of roots to grow under impeding conditions. For example, in **Chapter 4** soil compaction influenced the root system distributions at both field sites and different rooting depths were reached for coarse (nodal) roots of different genotypes (Fig. 4.7). This implies that there is genotypic variation for nodal roots in their ability to grow through compacted soil. In general impedance reduces rooting depth and coarse roots are either capable of growing through impeding zones of soil or remain obstructed. Not just rooting depth, but also coarse root proportions were influenced by genotype at both field sites. The ability of the nodal roots to grow deeper under impeded conditions was not related to the amount of roots a genotype had (Fig. 4.7), instead we found that root anatomical traits of these genotypes were related to deeper rooting (Fig 5.8). Substantial genotypic variation for anatomical traits such as cortical cell file number, cell size and aerenchyma was present for the genotypes, which makes selection for root anatomy in response to impedance an important breeding target to consider.

Similar observations on genotypic variability were also made in the pot trial of **Chapter 6**, where different genotypes of maize interacted differently with a compacted layer (Fig. 6.2). Some genotypes radially expanded upon encountering the compacted layer, while others did not. The anatomical response was further linked to ethylene. How ethylene is exactly involved should be further investigated.

7.2.2 Nodal variability of root anatomy in relation to growth under impeding conditions

Different anatomical traits were associated with deeper rooting according to their nodes (Fig. 5.8, Table 5.4). Anatomical traits such as reduced cortical cell file number in combination with greater middle cortical area were positively associated with root depth in node 3, while increased aerenchyma was positively associated with root depth for node 4. Root anatomy had more influence on the rooting depth of the root system when associated with node 3 than with node 4 (Table 5.4). Node 4 roots of the four tested genotypes in Chapter 6 were better able to penetrate a compacted layer then node 3 roots as these roots showed less anatomical adjustment (Fig. 6.3). Node 3 roots from ethylene responsive genotypes expanded more under ethylene treatment and when encountering impedance. It can therefore be concluded that not only the anatomical phenotype of a root is important (**Chapter 5**), but also how these anatomical traits are changing when they encounter impedance as unchanging anatomy (less sensitive under ethylene) proved to be better (Figs. 6.2, 6.5, 6.7).

Root thickening in the field experiments was observed at the crown and obscured by allometry (Fig. 5.6). Roots that are thicker from the outset, such as those of the younger node 4, had less anatomical response to hard soil than those of node 3 (Table 5.4). In **Chapter 6** it was found that thickening of roots was node and genotype dependent and root radial expansion upon encountering impedance was present for both nodes. Even with a small subset of four genotypes used in the pot trial it was observed that node 4 roots were reaching deeper in comparison to node 3 roots. As different nodes react differently this could have consequences for the entire root system. For instance from **Chapter 4** it was clear that root system size did not influence the ability of roots growing on compacted plots, both large and parsimonious root systems were able to reach similar depths on compacted plots at both field sites (Fig. 4.7). Instead root traits identified in **Chapter 5** will enable deeper rooting. As each node of each genotype comes with their own unique anatomical response to impedance (Fig. 6.2) further research should consider root anatomy of maize within each node separately.

7.2.3 Thickening versus thicker roots

Thickening as well as non-thickening genotypes showed similar rooting depths on the compacted plots (Table 5.7), while genotypes that did not manifest radial thickening in the pot trial (Fig. 6.7) had greater rooting depths (Fig. 6.5). In both experiments where anatomy was investigated, the outcomes suggest that individual anatomy of a root may play a role in penetration of hard soil, while radial thickening is overall negative for penetration. On the other hand, greater root diameters would be capable of displacing larger particles and aggregates but when this is associated with radial expansion this is at the cost of elongation. As younger nodes are thicker it could be that these roots experience less impedance stress than the older nodes. Less thickening would occur for these younger nodes, which supports the view that non-plasticity for thickening would be better for growing through impedance. There is however a need to distinguish between thicker and thickening roots, which is not made in the current literature. This is not always easy, as allometric effects can be present (Fig. 5.6).

7.2.4 Successful growth strategies under impeded conditions

Root systems can be considered optimum when they provide the plant with sufficient nutrients and water for continued growth. Different genotypes showed either avoidance or adaptive strategies in our field trial when experiencing impedance as some genotypes had coarse roots that were able to overcome impedance, while other genotypes were forced to grow more shallow (Figs. 4.5, 4.7). As discussed a root system that is shallow risks rapid depletion of water and nutrients. Furthermore, compensatory mechanisms will make this worse, as more roots will explore a smaller soil volume. Therefore, root strategies that enable deeper rooting would be more successful.

Deeper rooting was assisted by the anatomical traits identified in **Chapter 5** which would enable a root system to grow with less metabolic costs, which enable the plant to invest resources elsewhere. In **Chapter 4** it was suggested that parsimonious root systems able to grow on compacted soil are better able to allocate resources elsewhere due to avoiding inter- or intra-root competition and lower maintenance and formation costs (Chapter 4). In **Chapter 6** we identified

that the radial expansion of a root axis was linked to cell area expansion rather than the production of additional cell files (Fig. 6.8), as producing and maintaining additional cells would require more energy of a root system. Regardless of whether radial expansion is beneficial or not, it could be that radial expansion by cell area increase is the most efficient way for a root to expand radially. A root system has therefore systems in place on different levels (from the amount of roots formed down to the level of anatomy) to reduce energy expenditure, which will promote growth overall. The fact that there is also nodal variation only contributes to the plant's ability to deal with adverse environments.

7.3 Further work

The main areas for continuation of this study are described below:

- Soil structure influences root growth as roots can make use of cracks and biopores as these impose less axial stress on roots. X-ray CT technology has already been used to quantify soil structure in detail and it would therefore be opportune to include a sampling strategy for soil structure in relation to root exploration for further studies.

- The expansion of the field trials and pot trials with additional genotypes would enable screening and further confirmation of the current findings. This could include additional nodes. Thinner nodes that arise earlier in maize could have different penetration capabilities than those that are formed latest. Root anatomy has been shown to differ with each node (although it scales to an extent), but the remaining nodal root anatomy has not yet been linked to growth under impeded conditions.

- Root distribution shifts were identified for the different genotypes in the field. Different distributions will influence resource acquisition, but details were not recorded. It would also be interesting to test phenotypes that contrast in their ability to grow deeper under impeded soil conditions for differences in nutrient and water acquisition.

- Mostly cortical phenes were investigated but should be expanded upon investigating stele phenes to provide a full record of maize anatomy in response to impedance. Also, other cortical traits could be included. For instance, we did not investigate the effect of the amount of cell wall formed by the different genotypes.

- It would be interesting to investigate the underlying kinematic machinery when roots are experiencing impedance and to investigate the kinematic changes a root undergoes when encountering impedance. Cell area and lengths adjust when roots radially expand in response to mechanical impedance. But the amount of cells produced by meristems of different nodes remains unexplored. It would be interesting to identify if those roots that are not responsive to ethylene and radially expand less when encountering a layer would or would not adjust cell production as this can also influence elongation rates.

- Root angle data has been investigated for different stresses, but less so in relation to impedance. Both root angle at incidence at the crown as well as when encountering a compacted layer should be further considered.

- The data generated so far could be included in heuristic models such as OpenSimRoot. These models should be expanded upon to include an impedance or penetration parameter to correctly estimate root elongation rates under impeding conditions.

- 2D images give an indication of what would be happening to cells in roots as we saw differential expansion according to the cortical region investigated. Further developments of sectioning methods, especially the LAT system, would enable 3D recording of cell volumes. Therefore, further work assessing cell volumes could explore the cortical differential response to impedance further. A potential outcome to either observing

stable, shrinking or enlarged cell volumes could have implications for modelling root growth as now a constant cell volume is assumed.

- This work gave an indication on how ethylene is involved as a stop signal for root growth. Assessing the hormonal signal of ethylene and how it subsequently alters roots in more detail would be interesting.

- Other beneficial phenes under impedance such as a sharper root tip shape, the presence of root hairs, etc. have been identified. How all these phenes can work together in a synergistic way merits further investigation. It is an unknown whether antagonistic relationships between these traits exist, if so these should be identified.

7.4 Concluding remarks

Maize roots experience mechanical impedance dependent on genotype and nodal position within the root system. Greater mechanical impedance will obstruct root growth. Those roots that are more ethylene sensitive will radially expand more. Radial expansion has been linked to reduced elongation rates, which will reduce root exploration. Not all roots react equally to impedance, therefore we suggest that a distinction between a thicker and a thickening root is to be made. Root anatomy, such as reduced cell file number in combination with greater middle cell area for node 3 or increased aerenchyma area for node 4, contributes to deeper rooting of root axis and plays a role in reaching deeper depths. These traits help penetration in contrast with this it was observed that the root system size did not contribute to the ability of roots to grow deeper. Parsimonious root systems were equally capable to reach as deep as larger root systems.

References

Abdalla, A.M., Hettiaratchi, D.R.P., Reece, A.R., 1969. The mechanics of root growth in granular media. Journal of Agricultural Engineering Research 14, 236–248.

Adcock, D., McNeill, A.M., McDonald, G.K., Armstrong, R.D., 2007. Subsoil constraints to crop production on neutral and alkaline soils in south-eastern Australia: a review of current knowledge and management strategies. Australian Journal of Experimental Agriculture 47, 1245-1261.

Aggarwal, P., Choudhary, K.K., Singh, A.K., Chakraborty, D., 2006. Variation in soil strength and rooting characteristics of wheat in relation to soil management. Geoderma 136, 353–363.

Ahmed, M.A., Zarebanadkouki, M., Meunier, F., Javaux, M., Kaestner, A., Carminati, A., 2017. Root type matters: Measurement of water uptake by seminal, crown, and lateral roots in maize. Journal of Experimental Botany 69, 1199–1206.

Alameda, D., Anten, N.P.R., Villar, R., 2012. Soil compaction effects on growth and root traits of tobacco depend on light, water regime and mechanical stress. Soil and Tillage Research 120, 121–129.

Alameda, D., Villar, R., 2012. Linking root traits to plant physiology and growth in *Fraxinus angustifolia* Vahl. seedlings under soil compaction conditions. Environmental and Experimental Botany 79, 49–57.

Araki, H., Hirayama, M., Hirasawa, H., Iijima, M., 2000. Which roots penetrate the deepest in rice and maize root systems? Plant Production Science 3, 281–288.

Athmann, M., 2019. Comparing macropore exploration by faba bean, wheat, barley and oilseed rape roots using in situ endoscopy. Journal of Soil Science and Plant Nutrition. doi: 10.1007/s42729-019-00069-0.

Atkinson, J.A., Rasmussen, A., Traini, R., Voss, U., Sturrock, C., Mooney, S.J., Wells, D.M., Bennett, M.J., 2014. Branching out in roots: Uncovering form, function, and regulation. Plant Physiology 166, 538–550.

Atkinson, J.A., Wells, D.M., 2017. An updated protocol for high throughput plant tissue sectioning. Frontiers in Plant Science, 8, 1-8.

Atwell, B.J., 1988. Physiological responses of lupin roots to soil compaction. Plant and Soil 111, 277–281.

Atwell, B.J., 1990. The effect of soil compaction on wheat during early tillering: I. Growth, development and root structure. New Phytologist 115, 29–35.

Atwell, B.J., 1993. Response of roots to mechanical impedance. Environmental and Experimental Botany 33, 27–40.

Babalola, O., Lal, R., 1977. Subsoil and gravel horizon and maize root growth: II Effects of gravel size, inter-gravel texture and natural gravel horizon. Plant and Soil 46, 347–357.

Baluška, F., Brailsford, R.W., Hauskrecht, M., Jackson, M.B., Barlow, P.W., 1993. Cellular dimorphism in the maize root cortex: Involvement of microtubules, ethylene and gibberellin in the differentiation of cellular behaviour in postmitotic growth zones. Botanica Acta 106, 394-403.

Baluška, F., Barlow, P.W., Kubica, Š., 1994. Importance of the post-mitotic isodiametric growth (PIG) region for growth and development of roots. Plant and Soil 167, 31–41.

Barlow, P.W., 1976. The effect of ethylene on root meristems of *Pisum sativum* and *Zea mays*. Planta 131, 235-243.

Barraclough, P.B., Weir, A.H., 1988. Effects of a compacted subsoil layer on root and shoot growth, water use and nutrient uptake of winter wheat. The Journal of Agricultural Science 110, 207–216.

Batey, T., 2009. Soil compaction and soil management - A review. Soil Use and Management 25, 335–345.

Batey, T., McKenzie, D.C., 2006. Soil compaction: Identification directly in the field. Soil Use and Management 22, 123–131.

Bengough, A.G., McKenzie, B.M., 1997. Sloughing of root cap cells decreases the frictional resistance to maize (*Zea mays* L.) root growth. Journal of Experimental Botany 48, 885-893.

Bengough, A., Mullins, C., 1990. Mechanical impedance to root growth: A review of experimental techniques and root growth responses. Journal of Soil Science. 41, 341–358.

Bengough, A.G., Mullins, C.E., 1991. Penetrometer resistance, root penetration resistance and root elongation rate in two sandy loam soils. Plant and Soil 131, 59–66.

Bengough, A.G., Young, I.M., 1993. Root elongation of seedling peas through layered soil of different penetration resistances. Plant and Soil 149, 129–139.

Bengough, A.G., Croser, C., Pritchard, J., 1997. A biophysical analysis of root growth under mechanical stress. Plant and Soil 189, 155–164.

Bengough, A.G., Bransby, M.F., Hans, J., McKenna, S.J., Roberts, T.J., Valentine, T.A., 2006. Root responses to soil physical conditions; growth dynamics from field to cell. Journal of Experimental Botany 57, 437–447.

Bengough, A.G., McKenzie, B.M., Hallett, P.D., Valentine, T.A., 2011. Root elongation, water stress, and mechanical impedance: A review of limiting stresses and beneficial root tip traits. Journal of Experimental Botany 62, 59–68.

Bengough, G.A., Loades, K., McKenzie, B.M., 2016. Root hairs aid soil penetration by anchoring the root surface to pore walls. Journal of Experimental Botany 67, 1071–1078.

Bennie, A.T.P., 1996. Growth and mechanical impedance. In: Waisel, Y; Eshel, A. Kafkafi, U. (Eds.) Plant Roots: The Hidden Half. Marcel Dekker, New York, pp. 453–470.

Bingham, I.J., Bengough, A.G., 2003. Morphological plasticity of wheat and barley roots in response to spatial variation in soil strength. Plant and Soil 250, 273–282.

Boeuf-Tremblay, V., Plantureux, S., Guckert, A., 1995. Influence of mechanical impedance on root exudation of maize seedlings at two development stages. Plant and Soil 279–287.

Borch, K., Bouma, T.J., Lynch, J.P., Brown, K.M., 1999. Ethylene: A regulator of root architectural responses to soil phosphorus availability. Plant Cell and Environment 22, 425–431.

Botwright Acuña, T.L., Wade, L.J., 2005. Root penetration ability of wheat through thin wax-layers under drought and well-watered conditions. Aust. J. Agric. Res. 56, 1235–1244.

Bramley, H., Turner, N.C., Turner, D.W., Tyerman, S.D., 2009. Roles of morphology, anatomy, and aquaporins in determining contrasting hydraulic behavior of roots. Plant Physiology 150, 348–364.

Brereton, J.C., McGowan, M., Dawkins, T.C., 1986. The sensitivity of barley, field beans and sugar beet to soil compaction. Field Crops Research 13, 223–237.

Burton, A.L., Brown, K.M., Lynch, J.P., 2013. Phenotypic diversity of root anatomical and architectural traits in *Zea* species. Crop Science 53, 1042–1055.

Cahn, M.D., Zobel, R.W., Bouldin, D.R., 1989. Relationship between root elongation rate and diameter and duration of growth of lateral roots of maize. Plant and Soil 119, 271–279.

Cairns, J.E., Audebert, A., Townend, J., Price, A. H., Mullins, C.E., 2004. Effect of soil mechanical impedance on root growth of two rice varieties under field drought stress. Plant and Soil 267, 309–318.

Carminati, A., Passioura, J.B., Zarebanadkouki, M., Ahmed, M.A., Ryan, P.R., Watt, M., Delhaize, E., 2017. Root hairs enable high transpiration rates in drying soils. New Phytologist 216, 771-781.

Chandra Babu, R., Shashidar, H.E., Lilley, J.M., Thanh, N.D., Ray, J.D., Sadasivam, S., Sarkarung, S., O'Toole, J.C., Nguyen, H.T., 2001. Variation in root penetration ability, osmotic adjustment and dehydration tolerance among accessions of rice adapted to rainfed lowland and upland ecosystems. Plant Breeding 120, 233–238.

Chen, G., Weil, R.R., 2011. Root growth and yield of maize as affected by soil compaction and cover crops. Soil and Tillage Research 117, 17–27.

Chen, G., Weil, R.R., Hill, R.L., 2014a. Effects of compaction and cover crops on soil least limiting water range and air permeability. Soil and Tillage Research 136, 61–69.

Chen, Y.L., Palta, J., Clements, J., Buirchell, B., Siddique, K.H.M., Rengel, Z., 2014b. Root architecture alteration of narrow-leafed lupin and wheat in response to soil compaction. Field Crops Research 165, 61–70.

Chimungu, J.G., Brown, K.M., Lynch, J.P., 2014a. Reduced root cortical cell file number improves drought tolerance in maize. Plant Physiology 166, 1943–1955.

Chimungu, J.G., Brown, K.M., Lynch, J.P., 2014b. Large root cortical cell size improves drought tolerance in maize. Plant Physiology 166, 2166–2178.

Chimungu, J.G., Loades, K.W., Lynch, J.P., 2015a. Root anatomical phenes predict root penetration ability and biomechanical properties in maize (*Zea mays*). Journal of Experimental Botany 66, 3151–3162.

Chimungu, J.G., Maliro, M.F.A., Nalivata, P.C., Kanyama-Phiri, G., Brown, K.M., Lynch, J.P., 2015b. Utility of root cortical aerenchyma under water limited conditions in tropical maize (*Zea mays* L.). Field Crops Research 171, 86–98.

Chochois, V., Vogel, J.P., Rebetzke, G.J., Watt, M., 2015. Variation in adult plant phenotypes and partitioning among seed and stem-borne roots across *Brachypodium distachyon* accessions to exploit in breeding cereals for well-watered and drought environments . Plant Physiology 168, 953–967.

Clark, D.G., Gubrium, E.K., Barrett, J.E., Terril, A.N., Klee, H.J., 1999. Root formation in ethylene insensitive plants. Plant Physiology 121, 53-60.

Clark, L.J., Aphale, S.L., Barraclough, P.B., 2000. Screening the ability of rice roots to overcome the mechanical impedance of wax layers: Importance of test conditions and measurement criteria. Plant and Soil 219, 187–196.

Clark, L.J., Whalley, W.R., Barraclough, P.B., 2001. Partial mechanical impedance can increase the turgor of seedling pea roots. Journal of Experimental Botany 52, 167–171.

Clark, L.J., Cope, R.E., Whalley, W.R., Barraclough, P.B., Wade, L.J., 2002. Root penetration of strong soil in rainfed lowland rice: Comparison of laboratory screens with field performance. Field Crops Research 76, 189–198.

Clark, L.J., Whalley, W.R., Barraclough, P.B., 2003. How do roots penetrate strong soil? Plant and Soil 255, 93–104.

Clark, L.J., Price, A.H., Steele, K.A., Whalley, W.R., 2008. Evidence from near-isogenic lines that root penetration increases with root diameter and bending stiffness in rice. Functional Plant Biology 35, 1163–1171.

Coelho Filho, M.A., Colebrook, E.H., Lloyd, D.P.A., Webster, C.P., Mooney, S.J., Phillips, A.L., Hedden, P., Whalley, W.R., 2013. The involvement of gibberellin signalling in the effect of soil resistance to root penetration on leaf elongation and tiller number in wheat. Plant and Soil 371, 81–94.

Colmer, T.D., 2003. Long-distance transport of gases in plants: a perspective on internal aeration and radial oxygen loss from roots. Plant, Cell and Environment 26, 17–36.

Colombi, T., Walter, A., 2016. Root responses of triticale and soybean to soil compaction in the field are reproducible under controlled conditions. Functional Plant Biology 43, 114–128.

Colombi, T., Braun, S., Keller, T., Walter, A., 2017a. Artificial macropores attract crop roots and enhance plant productivity on compacted soils. Science of the Total Environment 574, 1283–1293.

Colombi, T., Kirchgessner, N., Walter, A., Keller, T., 2017b. Root tip shape governs root elongation rate under increased soil strength. Plant Physiology 174, 2289–2301.

Colombi, T., Torres, L.C., Walter, A., Keller, T., 2018. Feedbacks between soil penetration resistance, root architecture and water uptake limit water accessibility and crop

growth – A vicious circle. Science of the Total Environment 626, 1026–1035.

Colombi, T., Herrmann, A.M., Vallenback, P., Keller, T., 2019. Cortical cell diameter is key to energy costs of root growth in wheat. Plant Physiology 180, 2049-2060.

Coudert, Y., Périn, C., Courtois, B., Khong, N.G., Gantet, P., 2010. Genetic control of root development in rice, the model cereal. Trends in Plant Science 15, 219–226.

Cribari-Neto, F., Zeileis, A., 2015. Beta regression in R . Journal of Statistical Software 34, Issue 2.

Croser, C., Bengough, A.G., Pritchard, J., 1999. The effect of mechanical impedance on root growth in pea (*Pisum sativum*). I. Rates of cell flux, mitosis, and strain during recovery. Physiologia Plantarum 107, 277–286.

Croser, C., Bengough, A.G., Pritchard, J., 2000. The effect of mechanical impedance on root growth in pea (*Pisum sativum*). II. Cell expansion and wall rheology during recovery. P Physiologia Plantarum hysiol. Plant. 109, 150–159.

Dahleen, L.S., Tyagi, N., Bregitzer, P., Brown, R.H., Morgan, W.C., 2012. Developing tools for investigating the multiple roles of ethylene: Identification and mapping genes for ethylene biosynthesis and reception in barley. Molecular Genetics and Genomics 287, 793–802.

Day, P.R., 1965. Particle fractionation and particle size analysis. In: Methods of soil analysis, part 1. Black, C.A., (Eds.). American Society of Agronomy and Soil Science Society of America, Madison, WI, USA, 545-567.

Deacon, J.W., Drew, M.C., Darling, A., 1986. Progressive cortical senescence in formation of lysigenous gas space (aerenchyma) distinguished by nuclear staining in adventitious roots of *Zea mays*. Annals of Botany 58, 719-727.

Dexter, A.R., Hewitt, J.S., 1978. The deflection of plant roots. Journal of Agricultural Engineering Research 23, 17–22.

Dong, W., Fu, Q., Wang, Q. jiu, Cao, C., 2017. Effect of plough pans on the growth of soybean roots in the black-soil region of northeastern China. Journal of Integrative Agriculture 16, 2191–2196.

Drew, M.C., He, C., Morgan, P.W., 2000. Programmed cell death and aerenchyma formation in roots. Trends in Plant Science 5, 123–127.

Ehlers, W., Köpke, U., Hesse, F., Böhm, W., 1983. Penetration resistance and root growth of oats in tilled and untilled loess soil. Soil and Tillage Research 3, 261–275.

Evans, D.E., 2004. Aerenchyma formation. New Phytologist 161, 35–49.

Fan, M., Zhu, J., Richards, C., Brown, K.M., Lynch, J.P., 2003. Physiological roles for aerenchyma in phosphorus-stressed roots. Functional Plant Biology 30, 493-506.

FAO, 2016. Save and grow in practise: maize, rice, wheat. A guide to sustainable cereal production, Food and Agriculture Organization of the United Nations, Rome, Italy, 1-124.

Galindo-Castañeda, T., Brown, K.M., Lynch, J.P., 2018. Reduced root cortical burden

improves growth and grain yield under low phosphorus availability in maize. Plant, Cell and Environment 41, 1579–1592.

Gao, W., Watts, C.W., Ren, T., Whalley, W.R., 2012. The effects of compaction and soil drying on penetrometer resistance. Soil and Tillage Research 125, 14–22.

Gao, W., Hodgkinson, L., Jin, K., Watts, C.W., Ashton, R.W., Shen, J., Ren, T., Dodd, I.C., Binley, A., Phillips, A.L., Hedden, P., Hawkesford, M.J., Whalley, W.R., 2016. Deep roots and soil structure. Plant Cell and Environment 39, 1662–1668.

Gao, Y., Lynch, J.P., 2016. Reduced crown root number improves water acquisition under water deficit stress in maize (*Zea mays* L.). Journal of Experimental Botany 67, 4545–4557.

Ge, Z., Rubio, G., Lynch, J.P., 2000. The importance of root gravitropism for inter-root competition and phosphorus acquisition efficiency: results from a geometric simulation model. Plant and Soil 218, 159–71.

Glazier, D.S., 2009. Metabolic level and size scaling of rates of respiration and growth in unicellular organisms. Functional Ecology 23, 963-968.

Godfray, H.C.J., Reddington, J.R., Crute, I., Haddad, L., Lawrence, D., Muir, J.F., Pretty, J., Robinson, S., Thomas, S.M., Toulmin, C., 2010. Food security: The challenge of the present. Science 327, 812–818.

Gong, F., Wu, X., Zhang, H., Chen, Y., Wang, W., 2015. Making better maize plants for sustainable grain production in a changing climate. Frontiers in Plant Science 6, 1–6.

Goss, M.J., 1977. Effects of mechanical impedance on root growth in barley (*Hordeum vulgare L.*) I. Effects on the elongation and branching of seminal root axes. Journal of Expirmental Botany 28, 1216–1227.

Goss, M.J., Scott Russell, R., 1977. Effects of mechanical impedance on root growth in barley, *Hordeum vulgare* L. III. Observations on the mechanism of response. Journal of Experimental Botany 28, 1216–1227.

Gregory, P.J., 2006. Roots and the architecture of root systems, in: Plant roots: Growth, activity and interaction with soils. Blackwell Publishing, Oxford, UK, pp. 18–44.

Gregory, P.J., Bengough, A.G., Grinev, D., Schmidt, S., Thomas, W.T.B., Wojciechowski, T., Young, I.M., 2009. Root phenomics of crops: Opportunities and challenges. Functional Plant Biology 36, 922–929.

Grzesiak, M.T., 2009. Impact of soil compaction on root architecture, leaf water status, gas exchange and growth of maize and triticale seedlings. Plant Root 3, 10–16.

Grzesiak, S., Grzesiak, M.T., Hura, T., Marcińska, I., Rzepka, A., 2013. Changes in root system structure, leaf water potential and gas exchange of maize and triticale seedlings affected by soil compaction. Environmental and Experimental Botany 88, 2–10.

Grzesiak, M.T., Ostrowska, A., Hura, K., Rut, G., Janowiak, F., Rzepka, A., Hura, T., Grzesiak, S., 2014. Interspecific differences in root architecture among maize and triticale genotypes grown under drought, waterlogging and soil compaction. Acta Physiologiae Plantarum 36, 3249–3261.

Gunawardena, A.H.L.A.N., Pearce, D.M., Jackson, M.B., Hawes, C.R., Evans, D.E., 2001. Characterisation of programmed cell death during aerenchyma formation induced by ethylene or hypoxia in roots of maize (*Zea mays* L.). Planta 212, 205–214.

Guo, H., York, L.M., 2019. Maize with fewer nodal roots allocates mass to more lateral and deep roots that improve nitrogen uptake and shoot growth. Journal of Experimental Botany 70, 5299-5309.

Håkansson, I., Lipiec, J., 2000. A review of the usefulness of relative bulk density values in studies of soil structure and compaction. Soil and Tillage Research 53, 71–85.

Haling, R.E., Brown, L.K., Bengough, A.G., Young, I.M., Hallett, P.D., White, P.J., George, T.S., 2013. Root hairs improve root penetration, root-soil contact, and phosphorus acquisition in soils of different strength. Journal of Expirmental Botany 64, 3711–3721.

Haling, R.E., Brown, L.K., Bengough, A.G., Valentine, T.A., White, P.J., Young, I.M., George, T.S., 2014. Root hair length and rhizosheath mass depend on soil porosity, strength and water content in barley genotypes. Planta 239, 643–651.

Hall, B., Lanba, A., Lynch, J.P., 2019. Three-dimensional analysis of biological systems via a novel laser ablation technique. Journal of Laser Applications 31, https://doi.org/10.2351/1.5096089.

Hamza, M.A., Anderson, W.K., 2005. Soil compaction in cropping systems: A review of the nature, causes and possible solutions. Soil and Tillage Research 82, 121–145.

Han, E., Kautz, T., Perkons, U., Uteau, D., Peth, S., Huang, N., Horn, R., Köpke, U., 2015. Root growth dynamics inside and outside of soil biopores as affected by crop sequence determined with the profile wall method. Biology and Fertility of Soils 51, 847–856.

Hanbury, C.D., Atwell, B.J., 2005. Growth dynamics of mechanically impeded lupin roots: does altered morphology induce hypoxia? Annals of Botany 96, 913–924.

Hatano, R., Iwanaga, K., Okajima, H., Sakuma, T., 1988. Relationship between the distribution of soil macropores and root elongation. Soil Science and Plant Nutrition 34, 535–546.

He, C., Finlayson, S. a., Drew, M.C., Jordan, W.R., Morgan, P.W., 1996a. Ethylene biosynthesis during aerenchyma formation in roots of maize subjected to mechanical impedance and hypoxia. Plant Physiology 112, 1679–1685.

He, C., Morgan, P., Drew, M., 1996b. Transduction of an ethylene signal is required for cell death and lysis in the root cortex of maize during aerenchyma formation induced by hypoxia. Plant Physiology 112, 463–472.

Helliwel, J.R., Sturrock, C.J., Grayling, K.M., Tracy, S.R., Flavel, R.J., Young, I.M., Whalley, W.R., Mooney, S.J., 2013. Applications of X-ray computed tomography for examining biophysical interactions and structural development in soil systems: a review. European Journal of Soil Science 64, 279-297.

Helliwell, J.R., Sturrock, C.J., Miller, A.J., Whalley, W.R., Mooney, S.J., 2019. The role of plant species and soil condition in the physical development of the rhizosphere. Plant, Cell and Environment 42, 1974-1986.

Hettiaratchi, D.R.P., 1990. Soil compaction and plant root growth. Philosophical

Transactons of the Royal Society of London 329, 343–355.

Hochholdinger, F., Woll, K., Sauer, M., Dembinsky, D., 2004. Genetic dissection of root formation in maize (*Zea mays*) reveals root-type specific developmental programmes. Annals of Botany 93, 359–368.

Horn, R., Domzal, H., Slowihnka-Jurkiewicz, A., van Ouwerkerk, C., 1995. Soil compaction processes and their effects on the structure of arable soils and the environment. Soil and Tillage Research 35, 23–36.

Hu, B., Henry, A., Brown, K.M., Lynch, J.P., 2014. Root cortical aerenchyma inhibits radial nutrient transport in maize (*Zea mays*). Annals of Botany. 113, 181–189.

Huang, Y., Jordan, W.R., Wing, R.A., Morgan, P.W., 1998. Gene expression induced by physical impedance in maize roots. Plant Molecular Biology 73, 921-930.

Hund, A., Ruta, N., Liedgens, M., 2009. Rooting depth and water use efficiency of tropical maize inbred lines, differing in drought tolerance. Plant and Soil 318, 311–325.

Iijima, M., Kono, Y., 1991. Interspecific differences of the root system structures of four cereal species as affected by soil compaction. Japanese Journal Crop Science 60, 130–138.

Iijima, M., Kono, Y., Yamauchi, A., Pardales, J.R., 1991. Effects of soil compaction on the development of rice and maize root systems. Environmental and Expirmental Botany 31, 333-342.

Iijima, M., Griffiths, B., Bengough, A.G., 2000. Sloughing of cap cells and carbon exudation from maize seedling roots in compacted sand. New Phytologist 145, 477–482.

Iijima, M., Barlow, P.W., Bengough, A.G., 2003a. Root cap structure and cell production rates of maize (*Zea mays*) roots in compacted sand. New Phytologist 160, 127–134.

Iijima, M., Higuchi, T., Barlow, P.W., Bengough, A.G., 2003b. Root cap removal increases root penetration resistance in maize (*Zea mays* L.). Journal of Experimental Botany 54, 2105–2109.

Iijima, M., Higuchi, T., Barlow, P.W., 2004. Contribution of root cap mucilage and presence of an intact root cap in maize (*Zea mays*) to the reduction of soil mechanical impedance. Annals of Botany 94, 473–477.

Iijima, M., Kato, J., Taniguchi, A., 2007. Combined soil physical stress of soil drying, anaerobiosis and mechanical impedance to seedling root growth of four crop species. Plant Production Science 10, 451–459.

Ishaq, M., Ibrahim, M., Hassan, A., Saeed, M., Lal, R., 2001. Subsoil compaction effects on crops in Punjab, Pakistan: II. Root growth and nutrient uptake of wheat and sorghum. Soil and Tillage Research 60, 153–161.

Jaramillo, R.E., Nord, E.A., Chimungu, J.G., Brown, K.M., Lynch, J.P., 2013. Root cortical burden influences drought tolerance in maize. Annals of Botany 112, 429–437.

Jia, X., Liu, P., Lynch, J.P., 2018. Greater lateral root branching density in maize improves phosphorus acquistion from low phosphorus soil. Journal of Experimental Botany 69,

4961-4790.

Jin, K., Shen, J., Ashton, R.W., Dodd, I.C., Parry, M.A.J., Whalley, W.R., 2013. How do roots elongate in a structured soil? J.ournal of Experimenatl Botany 64, 4761–4777.

Jin, K., White, P.J., Whalley, W.R., Shen, J., Shi, L., 2017. Shaping an optimal soil by root–soil interaction. Trends in Plant Science 22, 823–829.

Karahara, I., Umemura, K., Soga, Y., Akai, Y., Bando, T., Ito, Y., Tamaoki, D., Uesugi, K., Abe, J., Yamauchi, D., Mineyuki, Y., 2012. Demonstration of osmotically dependent promotion of aerenchyma formation at different levels in the primary roots of rice using a "sandwich" method and X-ray computed tomography. Annals of Botany 110, 503–509.

Kawai, M., Samarajeewa, P.K., Barrero, R.A., Nishiguchi, M., Uchimiya, H., 1998. Cellular dissection of the degradation pattern of cortical cell death during aerenchyma formation of rice roots. Planta 204, 277–287.

Kays, S.J., Nicklow, C.W., Simons, D.H., 1974. Ethylene in relation to the response of roots to physical impedance. Plant and Soil 40, 565–571.

Kirby, J.M., Bengough, A.G., 2002. Influence of soil strength on root growth: experiments and analysis using a critical-state model. European Journal of Soil Science 53, 119–128.

Konishi, S., Kitagawa, G., 2008. Information criteria and statistical modelling. Springer, New York, USA. 1-273.

Konôpka, B., Pagès, L., Doussan, C.W., 2008. Impact of soil compaction heterogeneity and moisture on maize (*Zea mays* L .) root and shoot development. Plant, Soil and Environment 54, 509–519.

Konôpka, B., Pagès, L., Doussan, C., 2009. Soil compaction modifies morphological characteristics of seminal maize roots. Plant, Soil and Environment 55, 1–10.

Kubo, K., Iwama, K., Yanagisawa, A., Watanabe, Y., Terauchi, T., Jitsuyama, Y., Mikuma, T., 2006. Genotypic variation in the ability of root to penetrate hard soil layers among Japanese wheat cultivars. Plant Production Science 9, 47-55.

Kuchenbuch, R.O., Barber, S.A., 1988. Significance of temperature and precipitation for maize root distribution in the field. Plant and Soil 106, 9–14.

Kuncoro, P.H., Koga, K., Satta, N., Muto, Y., 2014. A study on the effect of compaction on transport properties of soil gas and water. II: Soil pore structure indices. Soil and Tillage Research 143, 180–187.

Laboski, C.A.M., Dowdy, R.H., Allmaras, R.R., Lamb, J.A., 1998. Soil strength and water content influences on corn root distribution in a sandy soil. Plant and Soil 203, 239–247.

Lenochová, Z., Soukup, A., Votrubová, O., 2009. Aerenchyma formation in roots. Biologia Plantarum 53, 263-270.

Lilley, J.M., Kirkegaard, J.A., 2016. Farming system context drives the value of deep wheat roots in semi-arid environments. Journal of Experimenal Botany 67, 3665–3681.

Lin, L.R., He, Y.B., Chen, J.Z., 2016. The influence of soil drying- and tillage-induced penetration resistance on maize root growth in a clayey soil. Journal of Integrated Agriculture 15, 1112–1120.

Lipiec, J., Hatano, R., 2003. Quantification of compaction effects on soil physical properties and crop growth. Geoderma 116, 107–136.

Lipiec, J., Horn, R., Pietrusiewicz, J., Siczek, A., 2012. Effects of soil compaction on root elongation and anatomy of different cereal plant species. Soil and Tillage Research 121, 74–81.

Loades, K.W., Bengough, A.G., Bransby, M.F., Hallett, P.D., 2013. Biomechanics of nodal, seminal and lateral roots of barley: Effects of diameter, waterlogging and mechanical impedance. Plant and Soil 370, 407–418.

Lobell, D.B., Schlenker, W., Costa-Roberts, J., 2011. Climate trends and global crop production since 1980. Science 333, 616–620.

Logsdon, S.D., Parker, J.C., Reneau, R.B., 1987. Root growth as influenced by aggregate size. Plant and Soil 99, 267–275.

Lynch, J.P, 1995. Root architecture and plant productivity. Plant Physiology 109, 7–13.

Lynch, J.P., 2003. Rhizoeconomics: Carbon costs of phosphorus acquisition. Plant and Soil 269, 45-56

Lynch, J.P., 2011. Root phenes for enhanced soil exploration and phosphorus acquisition: Tools for future crops. Plant Physiology 156, 1041–1049.

Lynch, J.P., 2013. Steep, cheap and deep: An ideotype to optimize water and N acquisition by maize root systems. Annals of Botany 112, 347–357.

Lynch, J.P., 2015. Root phenes that reduce the metabolic costs of soil exploration: Opportunities for 21st century agriculture. Plant, Cell and Environment 38, 1775–1784.

Lynch, J.P., 2018. Rightsizing root phenotypes for drought resistance. Journal of Experimenatl Botany 69, 327-3292.

Lynch, J.P., 2019. Root phenotypes for improved nutrient capture: an underexploited opportunity for global agriculture, New Phytologist 223, 548-564.

Lynch, J.P., Brown, K.M., 2001. Topsoil foraging - An architectural adaptation of plants to low phosphorus availability. Plant and Soil 237, 225–237.

Lynch, J.P., Brown, K.M., 2012. New roots for agriculture: Exploiting the root phenome. Philosophical Transcrpts of the Royal Society of Biological Sciences 367, 1598–1604.

Lynch, J.P., Wojciechowski, T., 2015. Opportunities and challenges in the subsoil: pathways to deeper rooted crops. Journal of Experimental Botany 66, 2199–2210.

Lynch, J.P., Chimungu, J.G., Brown K.M., 2014. Root anatomical phenes associated with water acquisition from drying soil: Targets for crop improvement. Journal of Expirmental Botany 65, 6155-6166.

Martino, D.L., Shaykewich, C.F., 2011. Root penetration profiles of wheat and barley as

affected by soil penetration resistance in field conditions. Canadian Journal of Soil Science 74, 193–200.

Materechera, S.A., Dexter, A.R., Alston, A.M., 1991. Penetration of very strong soils by seedling roots of different plant species. Plant and Soil 135, 31–41.

Materechera, S.A., Alston, A.M., Kirby, J.M., Dexter, A.R., 1993. Field evaluation of laboratory techniques for predicting the ability of roots to penetrate strong soil and of the influence of roots on water sorptivity. Plant and Soil 149, 149–158.

McCully, M.E., 1999. Roots in soil: Unearthing the complexities of roots and their rhizospheres. Annual Review of Plant Physiology and Plant Molecular Biology 50, 695–718.

Merotto, A.J., Mundstock, C.M., 1999. Wheat root growth as affected by soil strength. Revista Brasileira de Ciencia Do Solo 23, 197–202.

Miles, J., Shevlin, M., 2001. Applying regression and correlation. A guide for students and researchers. Sage Publications Ltd., London, UK, 1-254.

Misra, R.K., 1997. Maximum axial growth pressures of the lateral roots of pea and eucalypt. Plant and Soil 188, 161–170.

Montagu, K.D., Conroy, J.P., Atwell, B.J., 2001. The position of localized soil compaction determines root and subsequent shoot growth responses. Journal of Experimental Botany 52, 2127–2133.

Mooney, S.J., 2002. Three-dimensional visualization and quantification of soil macroporosity and water flow patterns using computed tomography. Soil Use and Management 18, 12-151.

Mooney, S.J., Pridmore, T.P., Helliwel, J., Bennett, M.J., 2012. Developing X-ray Computed Tomography to non-invasively image 3-D root systems architecture in soil. Plant and Soil 352, 1-22.

Moss, G.I., Hall, K.C., Jackson, M.B., 1988. Ethylene and the responses of roots of maize (*Zea mays* L.) to physical impedance. New Phytologist 109, 303–311.

Mullins, C.E., Young, I.M., Bengough, A.G., Ley, G.J., 1987. Hard-setting soils. Soil Use Management. 3, 79–83.

Nagarajah, S., 1987. Effects of soil texture on the rooting patterns of thompson seedless vines on own roots and on ramsey rootstock in irrigated vineyards. American Journal of Enology and Viticulture 38, 54–59.

Nagel, K.A., Putz, A., Gilmer, F., Heinz, K., Fischbach, A., Pfeifer, J., Faget, M., Blossfeld, S., Ernst, M., Dimaki, C., Kastenholz, B., Kleinert, A.-K., Galinski, A., Scharr, H., Fiorani, F., Schurr, U., 2012. GROWSCREEN-Rhizo is a novel phenotyping robot enabling simultaneous measurements of root and shoot growth for plants grown in soil-filled rhizotrons. Functional Plant Biology 39, 891-904.

Nakhforoosh, A., Grausgruber, H., Kaul, H.P., Bodner, G., 2014. Wheat root diversity and root functional characterization. Plant and Soil 380, 211–229.

Nosalewicz, A., Lipiec, J., 2014. The effect of compacted soil layers on vertical root

distribution and water uptake by wheat. Plant and Soil 375, 229–240.

Oldeman, L.R., Hakkeling, R.T.A, Sombroek, W.G., 1991. World map of the status of human-induced soil degradation: An explanatory note. ISRIC, UN Envirionment Programme, Wageningen, The Netherlands, 1-35.

Padgham, J., 2009. Agricultural development under a changing climate: Opportunities and challenges for adaptation, The World Bank, Washington, USA, 1-198.

Pajor, R., Fleming, A., Osborne, C.P., Rolfe, S.A., Sturrock, C.J., Mooney, S.J., 2013. Seeing space: visualisation and quantification of plant leaf structure using X-ray micro-computed tomography. Journal of Experimental Botany 64, 385-390.

Panayiotopoulos, K.P., Papadopoulou, C.P., Hatjiioannidou, A., 1994. Compaction and penetration resistance of an Alfisol and Entisol and their influence on root growth of maize seedlings. Soil and Tillage Research 31, 323–337.

Pankhurst, C.E., Pierret, A., Hawke, B.G., Kirby, J.M., 2002. Microbiological and chemical properties of soil associated with macropores at different depths in a red-duplex soil in NSW Australia. Plant and Soil 238, 11–20.

Passioura, J.B., 2002. Soil conditions and plant growth. Plant, Cell and Environment 25, 311–318.

Pauluzzi, G., Divol, F., Puig, J., Guiderdoni, E., Dievart, A., Périn, C., 2012. Surfing along the root ground tissue gene network. Developmental Biology 365, 14–22.

Pfeifer, J., Faget, M., Walter, A., Blossfeld, S., Fiorani, F., Schurr, U., Nagel, K.A., 2014. Spring barley shows dynamic compensatory root and shoot growth responses when exposed to localised soil compaction and fertilisation. Functional Plant Biology 41, 581–597.

Pitts, J.R., Cernac, A., Estelle, M. 1998. Auxin and ethylene promote root hair elongation in Arabidopsis. The Plant Journal 16, 553-560.

Postma, J.A., Lynch, J.P., 2011. Root cortical aerenchyma enhances the growth of maize on soils with suboptimal availability of nitrogen, phosphorus, and potassium. Plant Physiology 156, 1190–1201.

Postma, J.A., Lynch, J.P., 2012. Complementarity in root architecture for nutrient uptake in ancient maize/bean and maize/bean/squash polycultures. Annals of Botany 110, 521–534

Postma, J.A., Jaramillo R., Lynch, J.P., 2013. Towards modeling the function of root traits for enhancing water acquisition by crops. In: Ahuja L.R., Reddy V.R. Saseendran S.A., Yu, Q. (Eds.) Advances in agricultural systems modelling: Response of crops to limited water: Understanding and modeling water stress effects on plant growth processes. ASA, CSSA, SSSA, Madison, USA, pp 251- 275.

Postma, J.A., Dathe, A., Lynch, J.P., 2014. The optimal lateral root branching density for maize depends on nitrogen and phosphorus availability. Plant Physiology 166, 590–602.

Potocka, I., Szymanowska-Pułka, J., 2018. Morphological responses of plant roots to mechanical stress. Annals of Botany 122, 711–723.

Potocka, I., Szymanowska-Pułka, J., Karczewski, J., Nakielski, J., 2011. Effect of mechanical stress on Zea root apex. I. Mechanical stress leads to the switch from closed to open meristem organization. Journal of Experimental Botany 62, 4583–4593.

Pritchard, J., 1994. The control of cell expansion in roots. New Phytologist 127, 3–26.

R Core Team, 2018. R: A language and environment for statistical computing (software).

Raper, R., 2005. Agricultural traffic impacts on soil. Journal of Terramechanics 42, 259–280.

Rich, S.M., Watt, M., 2013. Soil conditions and cereal root system architecture: Review and considerations for linking Darwin and Weaver. Journal of Experimental Botany 64, 1193–1208.

Rivera, M., Polanía, J., Ricaurte, J., Borrero, G., Beebe, S., Rao, I., 2019. Soil compaction induced changes in morpho-physiological characteristics of common bean. Journal of Soil Science and Plant Nutrition 19, 217-227.

Rubio, G., Walk, T., Ge, Z., Yan, X., Liao, H., Lynch, J.P., 2001. Root gravitropism and below-ground competition among neighbouring plants: A modelling approach. Ann. Bot. 88, 929–940.

Rizzo, G. Rattalino Edreira J.I., Archontoulis, S.V., Yang, H.S., Grassini, P., 2018. Do shallow water tables contribute to high and stable maize yields in the US corn belt? Global Food Security 18, 27-34.

Rowell, D.L., 1994. Soil Science: Methods and applications, Longman Scientific and Technical, UK, 1-349.

Saengwilai, P., Tian, X., Lynch, J.P., 2014a. Low crown root number enhances nitrogen acquisition from low-nitrogen soils in maize. Plant Physiology 166, 581–589.

Saengwilai, P., Nord, E.A., Chimungu, J.G., Brown, K.M., Lynch, J.P., 2014b. Root cortical aerenchyma enhances nitrogen acquisition from low-nitrogen soils in maize. Plant Physiology 166, 726–735.

Sarquis, J.I., Jordan, W.R., Morgan, P.W., 1991. Ethylene evolution from maize (*Zea Mays* L.) seedling roots and shoots in response to mechanical impedance. Plant Physiology 96, 1171–1177.

Schenk, J.H., Jackson, R.B., 2002. The global biogeography of roots. Ecolgical Monographs 72, 311–328.

Schindelin, J., Arganda-Carreras, I., Frise, E., Kaynig, V., Longair, M., Pietzsch, T., Preibisch, S., Rueden, C., Saalfeld, S., Schmid, B., Tinevez, J.Y., White, D.J., Hartenstein, V., Eliceiri, K., Tomancak, P., Cardona, A., 2012. Fiji: an open-source platform for biological-image analysis. Nature Methods 9, 676–682.

Schmidt, S., 2011. Root responses to soil physical conditions and the role of root-particle contact. PhD thesis, University of Abertay Dundee, UK, 1-216.

Schmidt, S., Gregory, P.J., Grinev, D. V., Bengough, A.G., 2013. Root elongation rate is correlated with the length of the bare root apex of maize and lupin roots despite

contrasting responses of root growth to compact and dry soils. Plant and Soil 372, 609–618.

Schneider, H.M., Wojciechowski, T., Postma, J.A., Brown, K.M., Lücke, A., Zeisler, V., Schreiber, L., Lynch, J.P., 2017. Root cortical senescence decreases root respiration, nutrient content and radial water and nutrient transport in barley. Plant Cell and Environment 40, 1392–1408.

Schneider, H.M., Lynch, J.P., 2018. Functional implications of root cortical senescence for soil resource capture. Plant and Soil 423, 13-26.

Scholefield, D., Hall, D.M., 1985. Constricted growth of grass roots through rigid pores. Plant and Soil 85, 153–1162.

Shierlaw, J., Alston, A.M., 1984. Effect of soil compaction on root growth and uptake of phosphorus. Plant and Soil 77, 15–28.

Shishkova, S., Rost, T.L., Dubrovsky, J.G., 2008. Determinate root growth and meristem maintenance in angiosperms. Annals of Botany 101, 319–340.

Simojoki, A., Jaakkola, A., Alakukku, L., 1991. Effect of compaction on soil air in a pot experiment and in the field. Soil and Tillage Research 19, 175–186.

Steinemann, S., Zeng, Z., McKay, A., Heuer, S., Langridge, P., Huang, C.Y., 2015. Dynamic root responses to drought and rewatering in two wheat (*Triticum aestivum*) genotypes. Plant and Soil 391, 139–152.

Stirzaker, R.J., Passioura, J.B., Wilms, Y., 1996. Soil structure and plant growth: Impact of bulk density and biopores. Plant and Soil 186, 151-162.

Striker, G.G., Insausti, P., Grimoldi, A.A., León, R.J.C., 2006. Root strength and trampling tolerance in the grass Paspalum dilatatum and the dicot Lotus glaber in flooded soil. Functional Ecology 20, 4–10.

Striker, G.G., Insausti, P., Grimoldi, A.A., Vega, A.S., 2007. Trade-off between root porosity and mechanical strength in species with different types of aerenchyma. Plant, Cell and Environment 30, 580–589.

Strock, C.F., Morrow de la Riva, L., Lynch, J.P., 2018. Reduction in root secondary growth as a strategy for phosphorus acquisition. Plant Physiology 176, 691-703.

Strock, C.F., Schneider, H.M., Galindo-Castañeda, T., Hall, B.T., Van Gansbeke, B., Mather, D.E., Roth, M.G., Chilvers, M.I., Guo, M.I., Brown, K., Lynch, J.P., 2019. Laser ablation tomography for visualisation of root colonization by edaphic organisms. Journal of Experimental Botany, 19, 5327-5342.

Szatanik-Kloc, A., Horn, R., Lipiec, J., Siczek, A., Szerement, J., 2018. Soil compaction-induced changes of physicochemical properties of cereal roots. Soil and Tillage Research 175, 226–233.

Tanimoto, M., Roberts, K., Dolan, L., 1995 Ethylene is a positive regulator of root hair development in Arabidopsis thaliana. The Plant Journal 8, 943–948.

Tardieu, F., Pellerin, S., 1990. Trajectory of the nodal roots of maize in fields with low mechanical constraints. Plant and Soil 124, 39-45.

To, J., Kay, B.D., 2005. Variation in penetrometer resistance with soil properties: The contribution of effective stress and implications for pedotransfer functions. Geoderma 126, 261–276.

Trachsel, S., Kaeppler, S.M., Brown, K.M., Lynch, J.P., 2011. Shovelomics: High throughput phenotyping of maize (*Zea mays* L.) root architecture in the field. Plant and Soil 341, 75-87.

Trachsel, S., Kaeppler, S.M., Brown, K.M., Lynch, J.P., 2013. Maize root growth angle becomes steeper under low N conditions. Field Crops Research 140, 18-31.

Tracy, S.R., Roberts, J.A., Black, C.R., McNeill, A., Davidson, R., Mooney, S.J., 2010. The X-factor: visualizing undisturbed root architecture in soils using X-ray computed tomography. Journal of Experimental Botany, 61, 311-313.

Tracy, S.R., Black, C.R., Roberts, J.A., Mooney, S.J., 2011. Soil compaction: A review of past and present techniques for investigating effects on root growth. J. Sci. Food Agric. 91 Tracy, S.R., Black, C.R., Roberts, J.A., Mooney, S.J., 2011. Soil compaction: A review of past and present techniques for investigating effects on root growth. Journal of the Science of Food and Agriculture 91, 1528–1537.

Tracy, S.R., Black, C.R., Roberts, J.A., Sturrock, C., Mairhofer, S., Craigon, J., Mooney, S.J., 2012. Quantifying the impact of soil compaction on root system architecture in tomato (*Solanum lycopersicum*) by X-ray micro-computed tomography. Annals of Botany 110, 511–519.

Tracy, S.R., Black, C.R., Roberts, J.A., Mooney, S.J., 2013. Exploring the interacting effect of soil texture and bulk density on root system development in tomato (Solanum lycopersicum L.). Environmental and Experimental Botany 91, 38–47.

Usowicz, B., Lipiec, J., 2017. Spatial variability of soil properties and cereal yield in a cultivated field on sandy soil. Soil and Tillage Research 174, 241–250.

Valentine, T.A., Hallett, P.D., Binnie, K., Young, M.W., Squire, G.R., Hawes, C., Bengough, A.G., 2012. Soil strength and macropore volume limit root elongation rates in many UK agricultural soils. Annals of Botany 110, 259–270.

Van Noordwijk, M., Brouwer, S., 1993. Gas-filled root porosity in response to temporary low oxygen supply in different growth stages. Plant and Soil 152, 187-199.

van Ouwerkerk, C., Soane, 1994. Conclusions and recommendations for further research on soil compaction and crop production, in: Soane, B.D., van Ouwerkerk, C. (Eds.), Soil Compaction in Crop Productions. Elsevier Science B.V., Haren, pp. 627–642.

Varney, G.T., Canny, M.J., Wang, X.L., McCully, M.E., 1991. The branch roots of *Zea*. I. First order branches, their number, sizes and division into classes. Annals of Botany 67, 357–364.

Vaz, C.M.P., Manieri, J.M., de Maria, I.C., Tuller, M., 2011. Modeling and correction of soil penetration resistance for varying soil water content. Geoderma 166, 92–101.

Veen BW., 1982. The influence of mechanical impedance on the growth of maize roots. Plant and Soil 66, 101–109.

Veen, B.W., Boone, F.R., 1990. The influence of mechanical resistance and soil water on

the growth of seminal roots of maize. Soil and Tillage Research 16, 219–226.

Veen, B.W., Van Noordwijk, M., De Willigen, P., Boone, F.R., Kooistra, M.J. 1992. Root-soil contact of maize, as measured by thin-section technique. Plant and Soil 139, 131-138.

Vischer N, Nastase S., 2009. ObjectJ: Non-destructive marking and linked results in imageJ. https://sils.fnwi.uva.nl/bcb/objectj/index.html.

Vollsnes, A. V., Futsaether, C.M., Bengough, A.G., 2010. Quantifying rhizosphere particle movement around mutant maize roots using time-lapse imaging and particle image velocimetry. European Journal of Soil Science 61, 926–939.

Whalen, M.C, Feldman, L.J., 1988. The effect of ethylene on root growth of *Zea mays* seedlings. Canadian Journal of Botany 66, 719-723.

Whalley, W.R., Leeds-Harrison, P.B., Clark, L.J., Gowing, D.J.G., 2005. Use of effective stress to predict the penetrometer resistance of unsaturated agricultural soils. Soil and Tillage Research 84, 18–27.

Whalley, W.R., Watts, C.W., Gregory, A.S., Mooney, S.J., Clark, L.J., Whitmore, A.P., 2008. The effect of soil strength on the yield of wheat. Plant and Soil 306, 237–247.

Whalley, W.R., Dodd, I.C., Watts, C.W., Webster, C.P., Phillips, A.L., Andralojc, J., White, R.P., Davies, W.J., Parry, M.A.J., 2013. Genotypic variation in the ability of wheat roots to penetrate wax layers. Plant and Soil 364, 171-179.

White, R.E., 2006. Principles and practice of soil science: The soil as a natural resource. 4th Edition. Blackwell Science Ltd, UK, 1-363.

White, R.G., Kirkegaard, J.A., 2010. The distribution and abundance of wheat roots in a dense, structured subsoil - Implications for water uptake. Plant, Cell and Environment 33, 133–148.

White, P.J., George, T.S., Gregory, P.J., Bengough, A.G., Hallett, P.D., McKenzie, B.M., 2013. Matching roots to their environment. Annals of Botany 112, 207–222.

Whiteley, G.M., Hewitt, J.S., Dexter, A.R., 1982. The buckling of plant roots. Physiologia Plantarum 54, 333–342.

Whiteley, G.M., Dexter, A.R., 1984. Displacement of soil aggregates by elongating roots and emerging shoots of crop plants. Plant and Soil 77, 131–140.

Whitmore, A.P., Whalley, W.R., 2009. Physical effects of soil drying on roots and crop growth. Journal of Experimental Botany 60, 2845–2857.

Wilson, A.J., Robards, A.W., Goss, M.J., 1977. Effects of mechanical impedance on root growth in barley, Hordeum vulgare L. II. Effects on cell development in seminal roots. Journal of Expirmental Botany 28, 1216–1227.

Wu, J., Pagès, L., Wu, Q., Yang, B., Guo Y., 2015. Three-dimensional architecture of axile roots of field-grown maize. Plant and Soil 387, 363-377.

Wu, Q., Pagès, L., Wu, J., 2016. Relationships between root diameter, root length and root branching along lateral roots in adult, field-grown maize. Annals of Botany 117, 379–390.

Yamaguchi, J., Tanaka, A., 1990. Quantitative observation on the root system of various crops growing in the field. Soil Science and Plant Nutrition 36, 483–493.

Yamauchi, T., Shimamura, S., Nakazono, M., Mochizuki, T., 2013. Aerenchyma formation in crop species: A review. Field Crops Research 152, 8-16.

Yang, J.T., Schneider, H.M., Brown, K.M., Lynch, J.P., 2019. Genotypic variation and nitrogen stress effects on root anatomy in maize are node specific. Journal of Experimental Botany, 19, 5311-5325.

York, L.M., Nord, E.A., Lynch, J.P., 2013. Integration of root phenes for soil resource acquisition. Frontiers in Plant Science 4, doi: 10.3389/fpls.2013.00355.

York, L.M., Galindo-Castañeda, T., Schussler, J.R., Lynch J.P., 2015. Evolution of US maize (*Zea mays* L.) root architectural and anatomical phenes over the past 100 years corresponds to increased tolerance of nitrogen stress. Journal of Experimental Botany 66, 2347-2358.

York, L.M., Silberbush, M., Lynch, J.P., 2016. Spatiotemporal variation of nitrate uptake kinetics within the maize (*Zea mays* L.) root system is associated with greater nitrate uptake and interactions with architectural phenes. Journal of Experimental Botany 67, 3763–3775.

Yu, L.-X., Ray, J.D., O'Toole, J.C., Nguyen, H.T., 1995. Use of wax-petrolatum layers for screening rice root penetration. Crop Science 35, 684–687.

Yu P., Gutjahr, C., Li, C., Hochholdinger, F., 2016. Genetic control of lateral root formation in cerals. Trends in Plant Science 21, 951-961.

Zacarias, L., Reid, M.S., 1992. Inhibition of ethylene action prevents root penetration through compressed media in tomato (*Lycopersicon esculentum*) seedlings. Physologia Plantarum 86, 301–307.

Zhan, A., Lynch, J.P., 2015. Reduced frequency of lateral branching improves N capture from low-N soils in maize. Journal of Experimental Botany 66, 2055-2065.

Zhan, A., Schneider, H., Lynch, J.P., 2015. Reduced lateral root branching density improves drought tolerance in maize. Plant Physiology 168, 1603–1615.

Zhang ,Y.J,. Lynch, J.P., Brown, K.M., 2003. Ethylene and phosphorus availability have interacting yet distinct effects on root hair development. Journal of Experimental Botany 54, 2351–2361.

Zhu, J., Brown, K.M., Lynch, J.P., 2010. Root cortical aerenchyma improves the drought tolerance of maize (*Zea mays* L.). Plant, Cell and Environment 33, 740–749.

Appendices

Supplementary figures

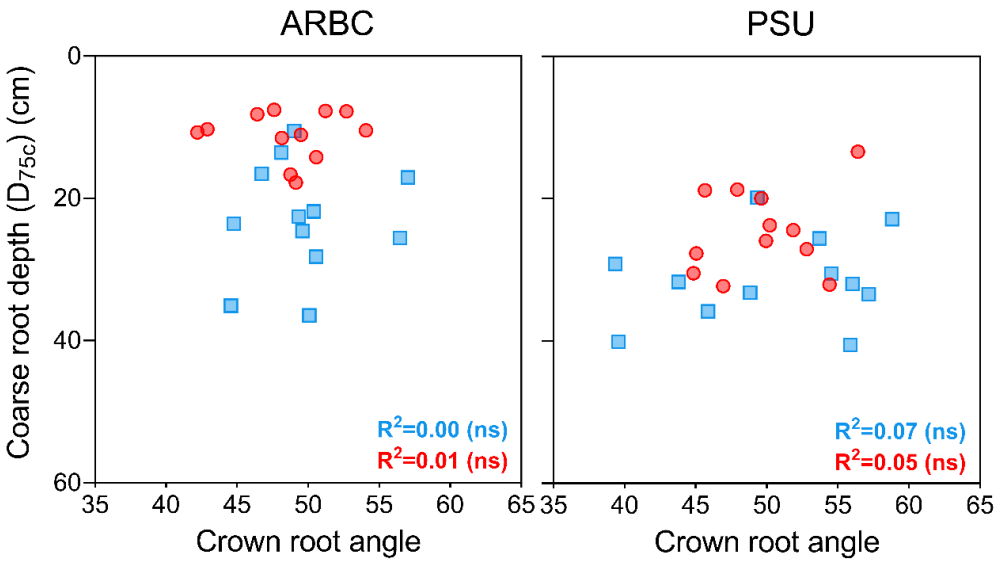

Figure S4.1 – Relationship between crown root angle and coarse rooting depth for ARBC and PSU field sites.

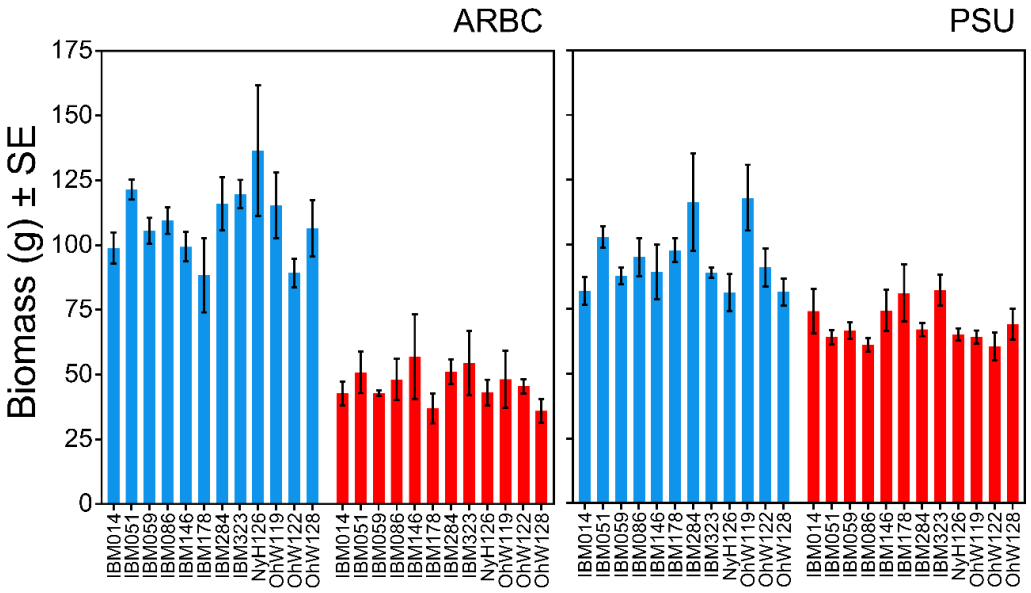

Figure S4.2 – Biomass ± SE at both field sites under compacted (red) and non-compacted (blue) conditions for each genotype.

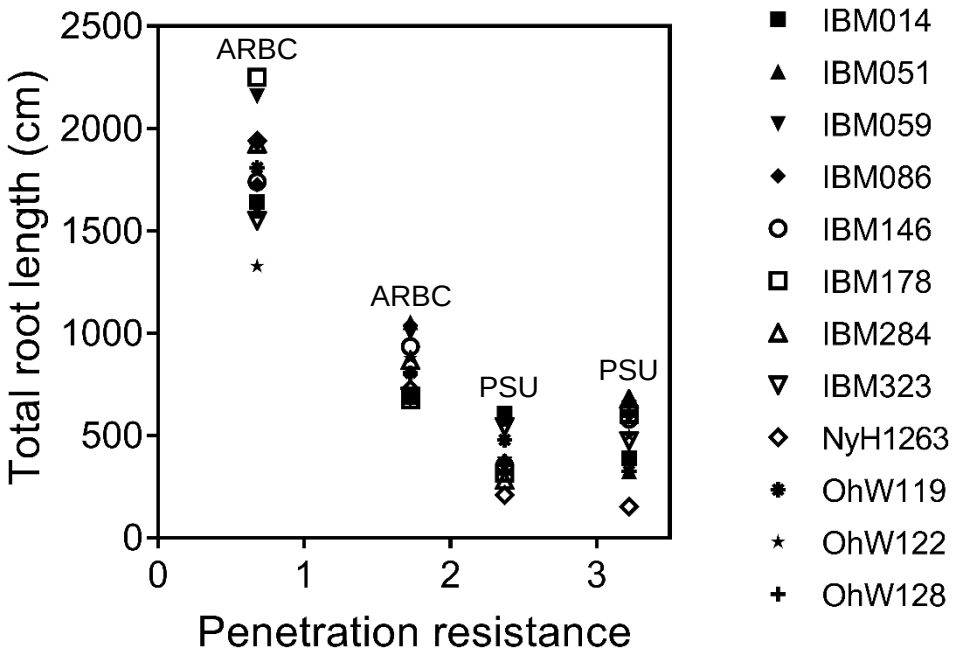

Fig S4.3 – The total root length measured in a 60 cm core of 12 genotypes versus the averaged penetration resistance (MPa) of the two field site and two compaction treatment combinations.

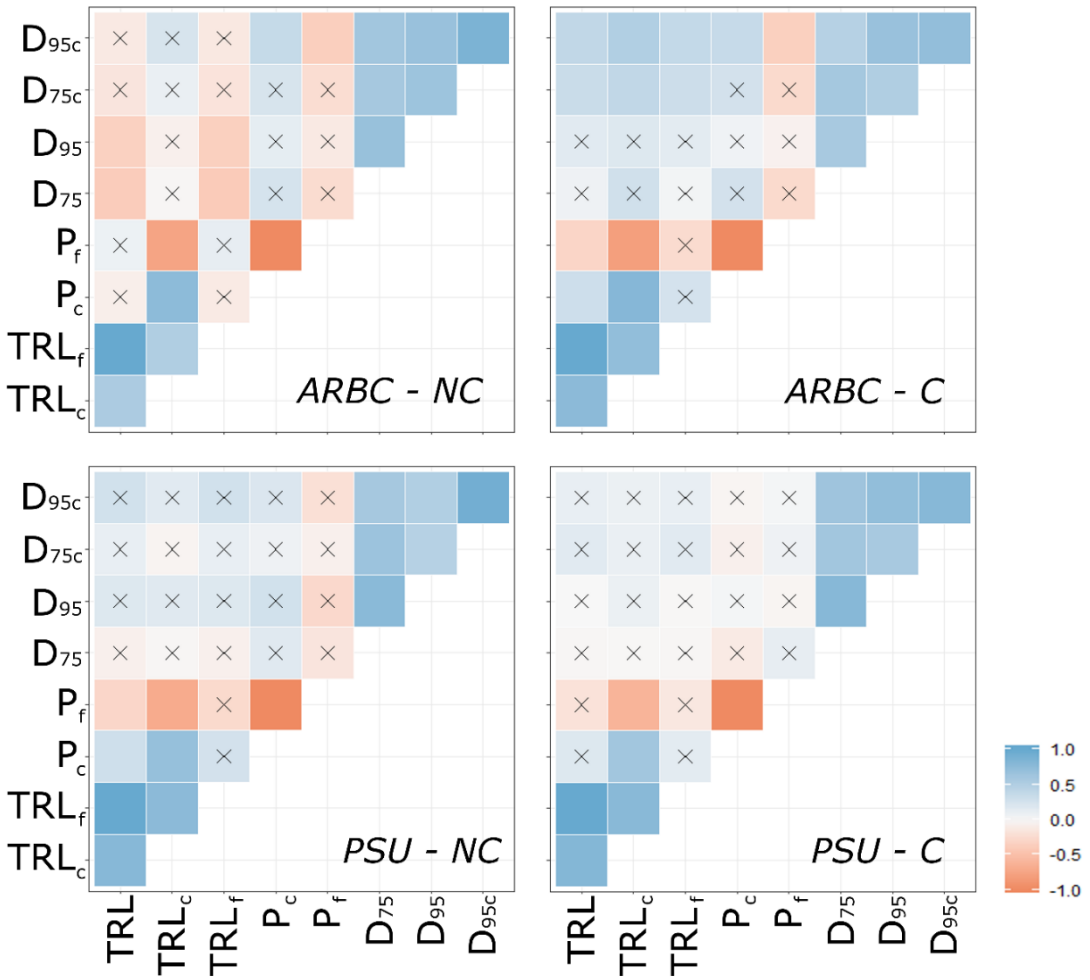

Figure S4.4 – Correlation plots between tested variables averaged over all genotypes across field sites (ARBC or PSU) and compacted (C) or non-compacted plots (NC) combinations. The correlation coefficient is visualised by the scale bar, negative correlations are orange and positive correlations are blue. A cross represents a non-significant correlation at significance $p \leq 0.05$.

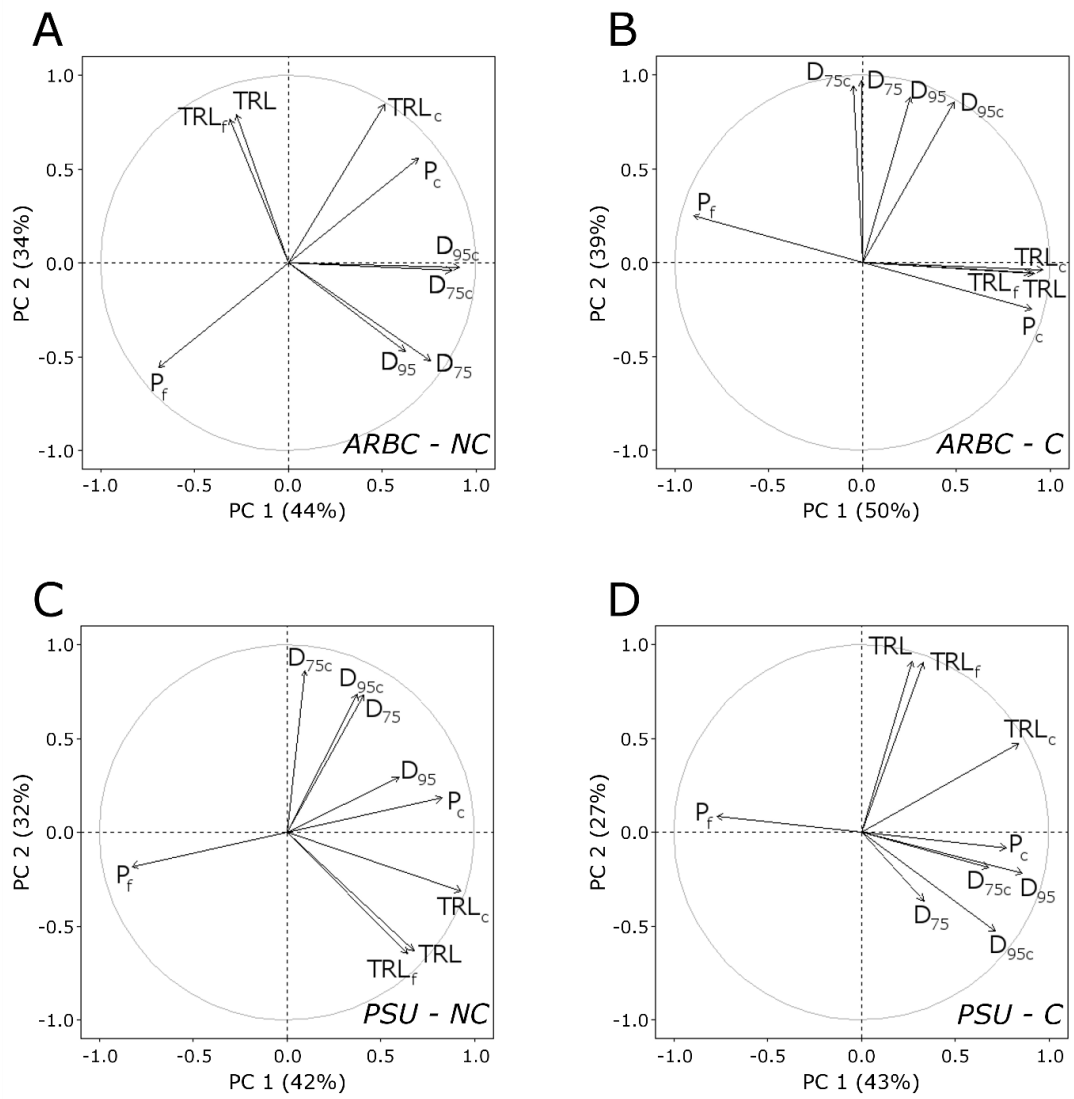

Figure S4.5 – Principal component analysis per field site (ARBC or PSU) – compaction treatment (C – compacted; NC – non-compacted) combination illustrating relationships between coring variables within respective environmental conditions.

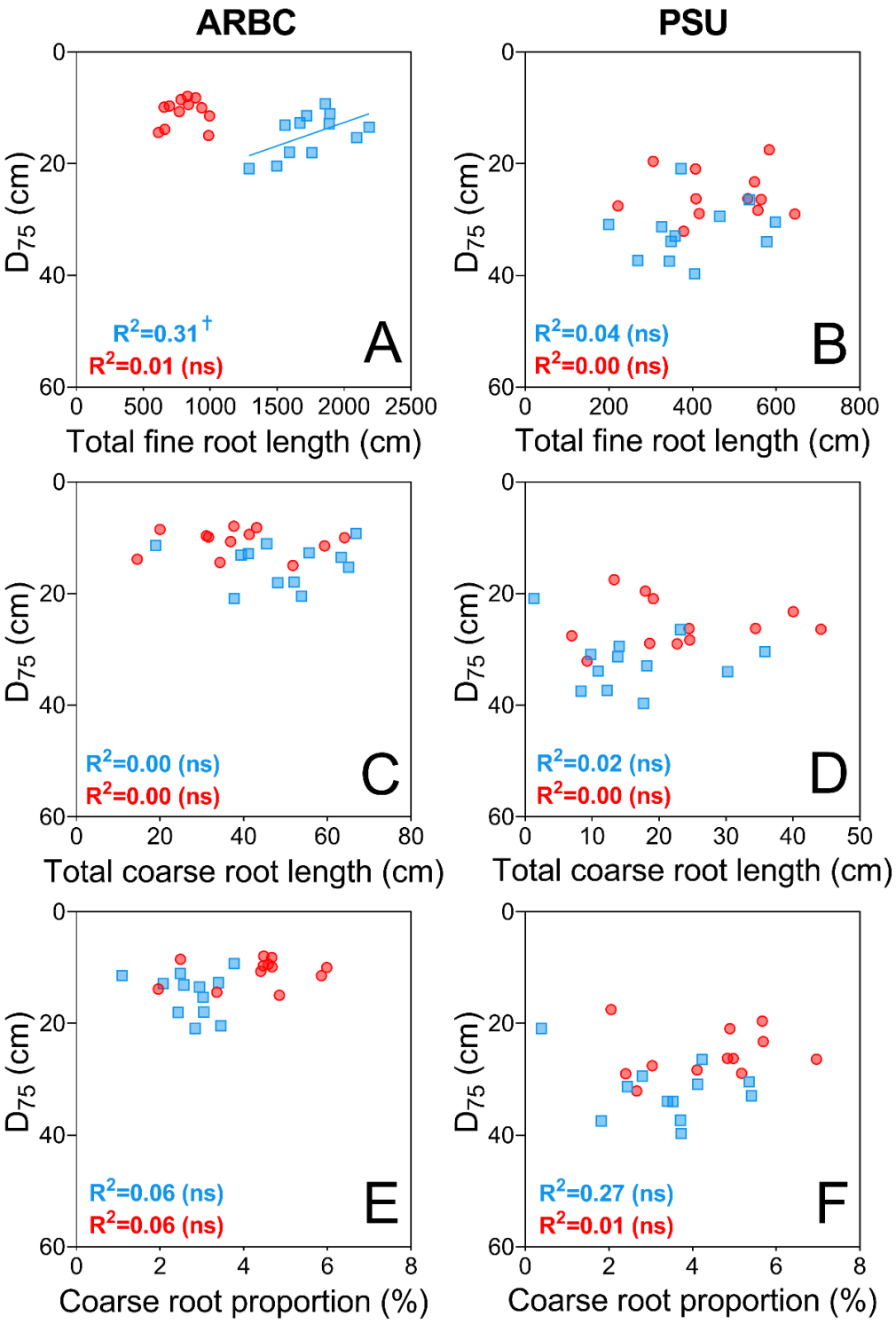

Figure S4.6 – Relationships between total rooting depth (D_{75}) and other coring variables across field sites and compaction treatments. Linear regression was used for A-D and beta-regression for E-F due to proportional data. Panels A,C and E represent field site ARBC and panels B, D and F represent field site PSU. Non-compacted data in blue, compacted data in red. One significant relationship was detected at significance level † $p \leq 0.10$, other relationships were non-significant (ns).

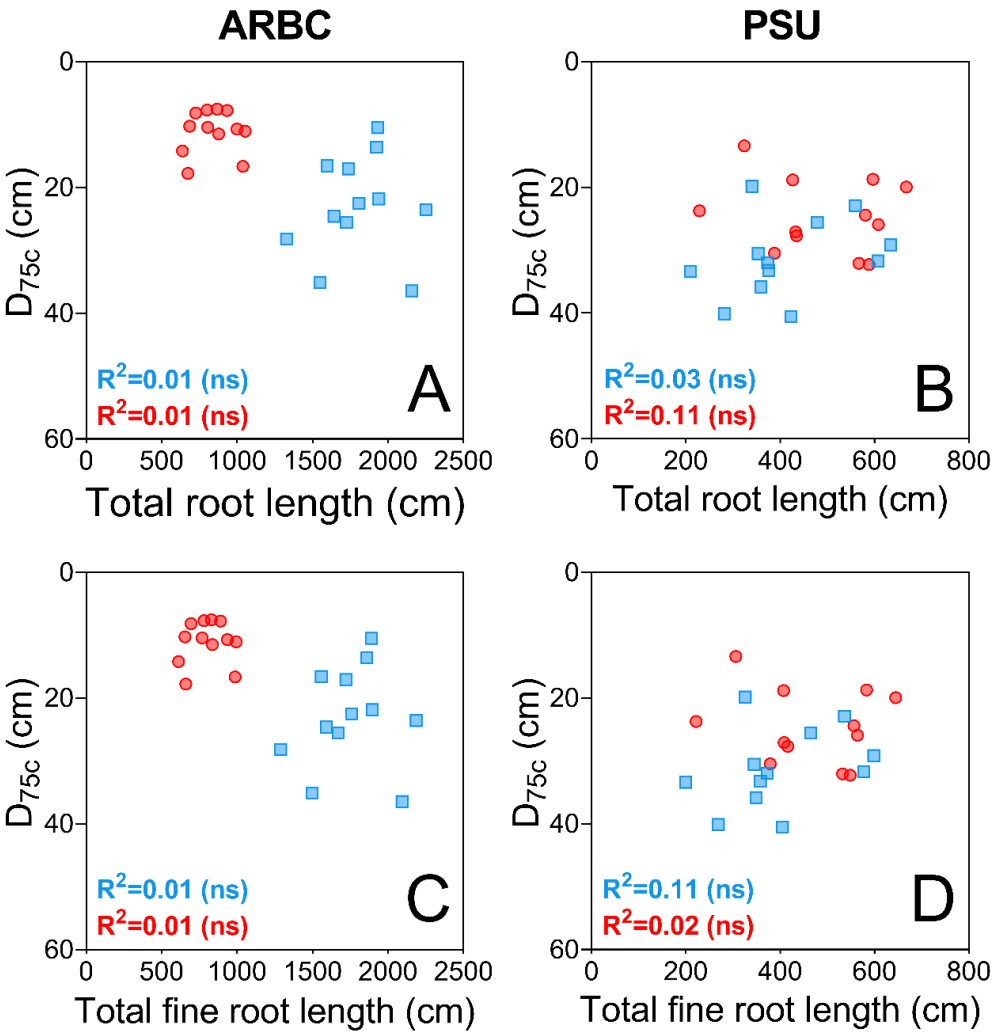

Figure S4.7 – Relationships between total rooting depth (D_{75c}) and other coring variables across field sites and compaction treatments. Panels A and C represent field site ARBC and panels B and D field site PSU. Non-compacted data in blue, compacted data in red. No significant (ns) linear relationships were detected.

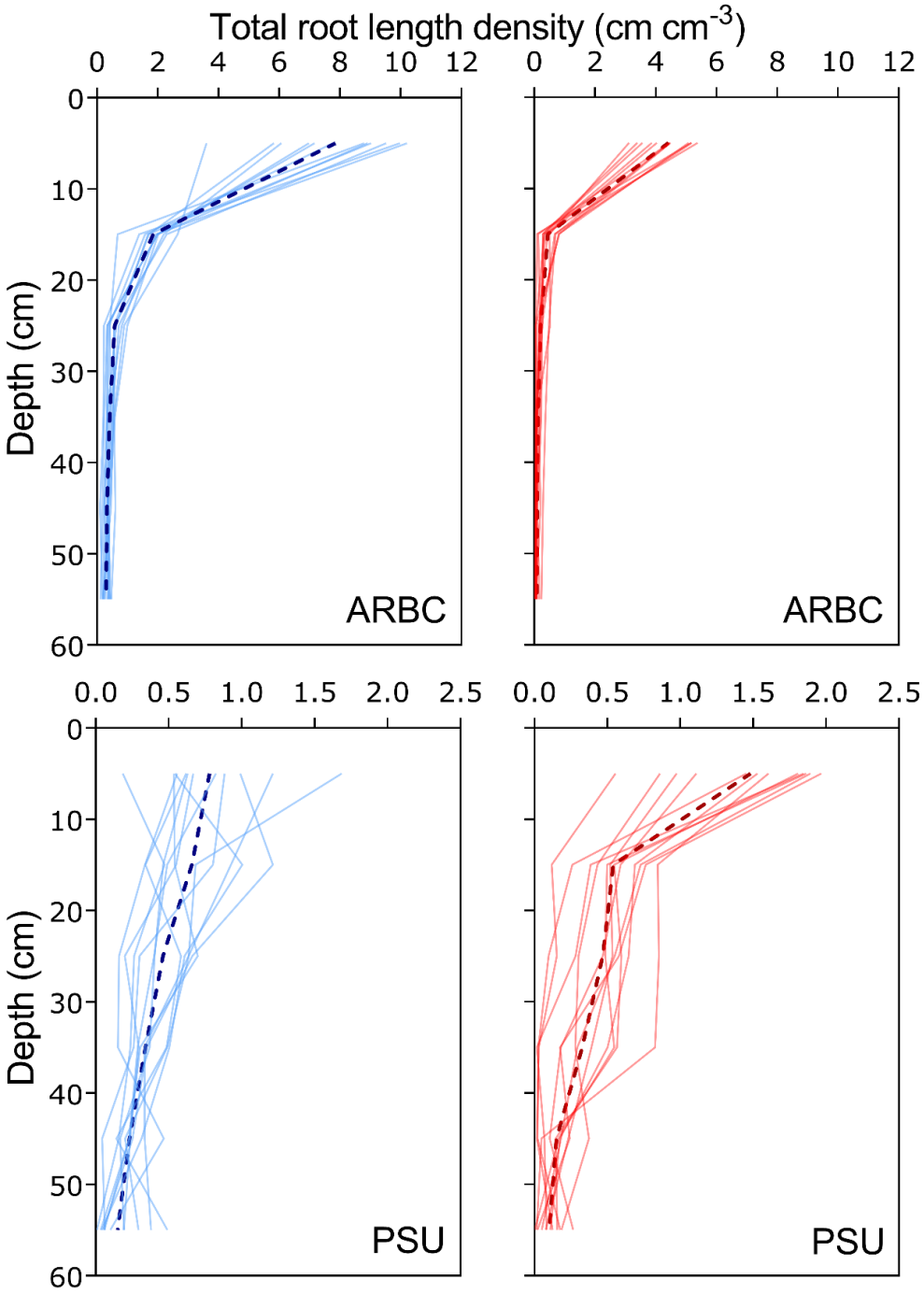

Figure S4.8 – Genotypic variation in total root length density (cm cm^{-3}) per depth increment across two field sites and two compaction treatments. Non-compacted data in blue and compacted data in red. The striped line are the averages across all genotypes, lighter coloured lines are the average for individual genotypes tested.

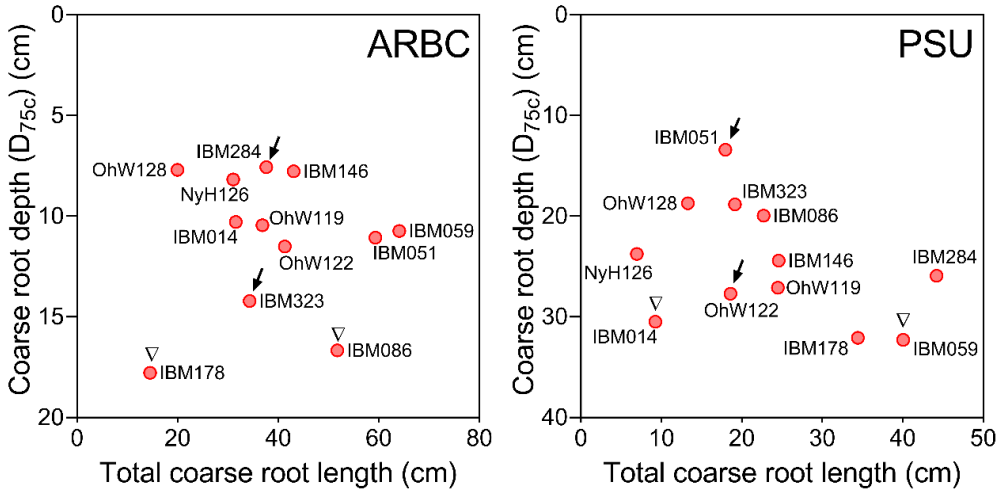

Figure S4.9 – Selection of genotypes to be compared based on their coarse rooting depth and coarse total root length. Genotypes indicated with an arrow were selected on the bases of similar coarse root length but different coarse rooting depths (shallow versus deep) and genotypes indicated with a triangle were selected on the basis of similar coarse rooting depth but are different according to total coarse root length (few versus many roots for deeper rooting genotypes).

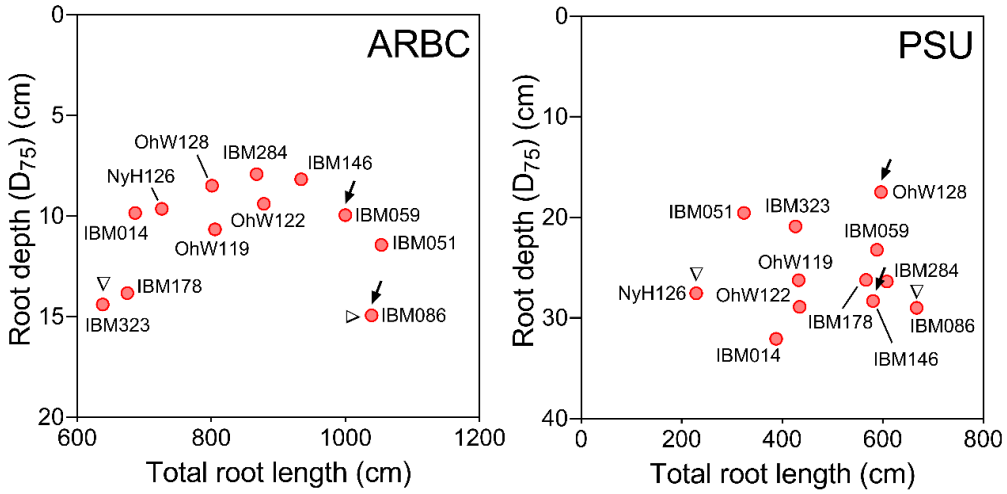

Figure S4.10 – Selection of genotypes to be compared based on their total rooting depth and total root length. Genotypes indicated with an arrow were selected on the bases of similar coarse root length but different coarse rooting depths (shallow versus deep) and genotypes indicated with a triangle were selected on the basis of similar coarse rooting depth but are different according to total coarse root length (few versus many roots for deeper rooting genotypes).

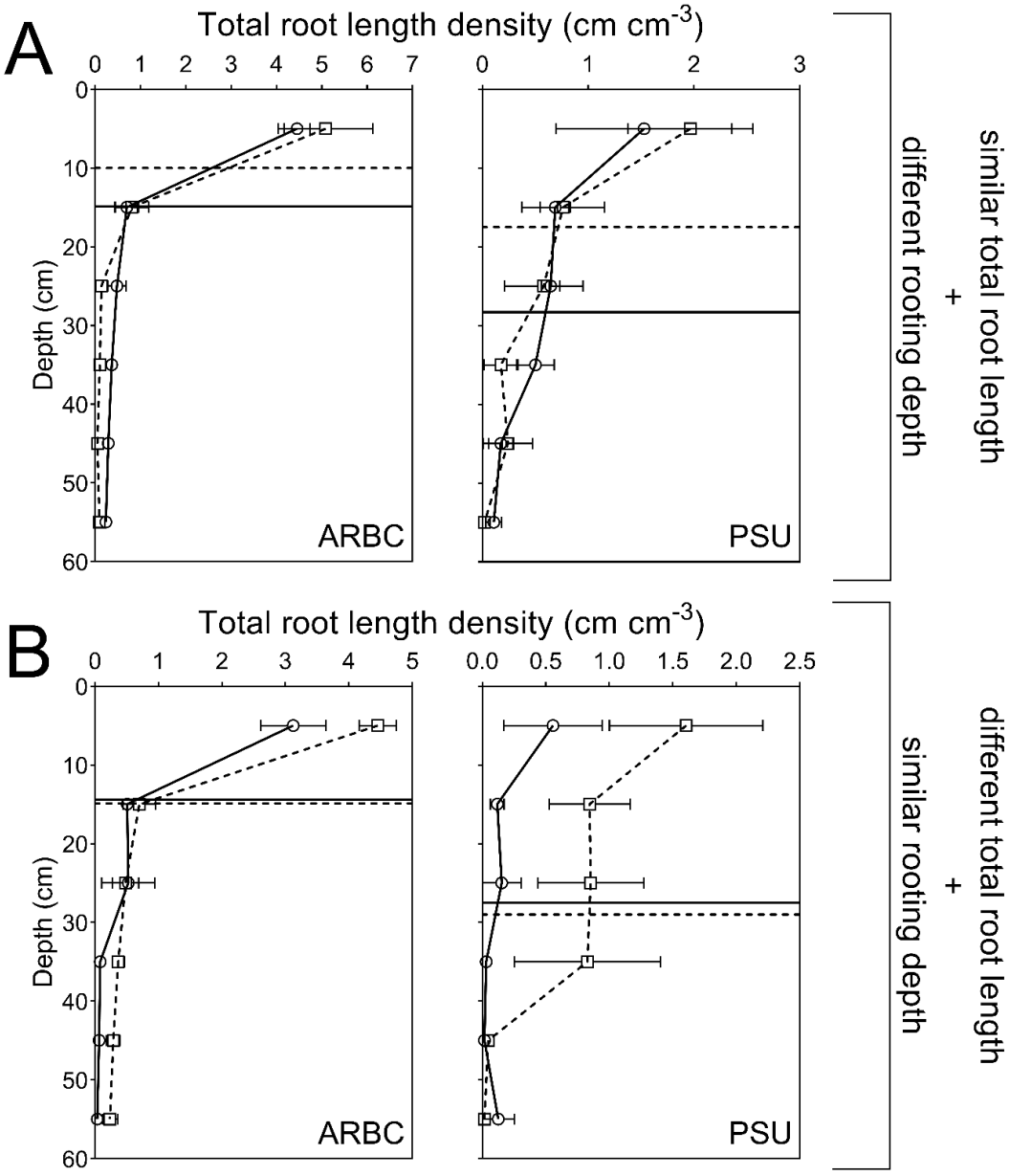

Figure S4.11 - Total root length densities (cm cm^{-3}) ± SE distributions with soil depth on compacted plots comparing (A) two genotypes per field season with similar total coarse root length but with different associated rooting depths and (B) two genotypes with similar rooting depths but with different total coarse root lengths. For (A) solid lines stands for the deeper rooting genotype and associated D_{75}, while the striped line stands for the shallower rooting genotypes and associated D_{75}. For (B), the solid line is used for the genotype that produces less roots but reaches equally deep then the genotype that produces more roots (striped lines).

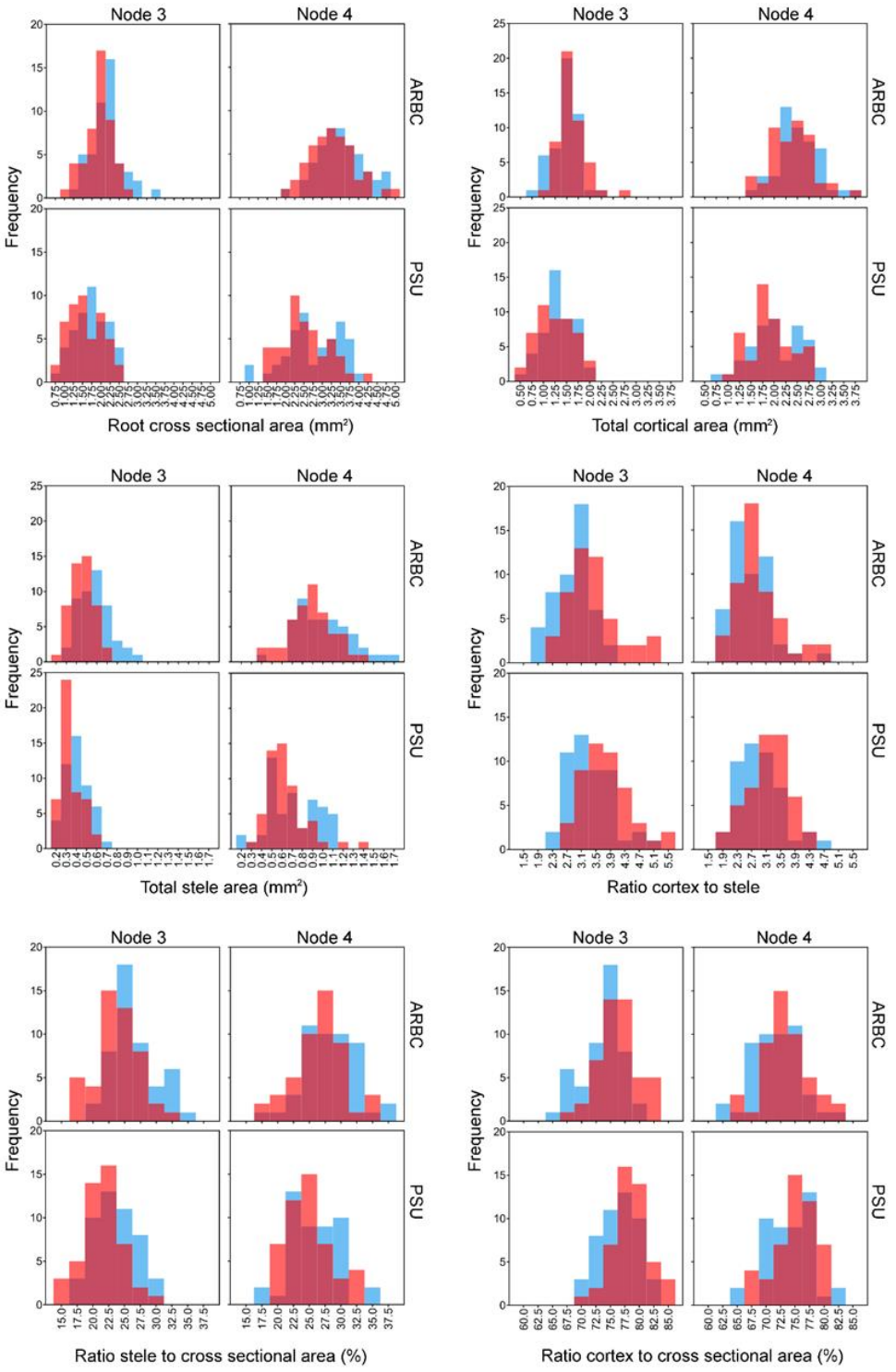

Figure S5.1 - Histograms for each anatomical trait measured within for each field site and node. Compacted data in red, non-compacted data in blue (page 1/3).

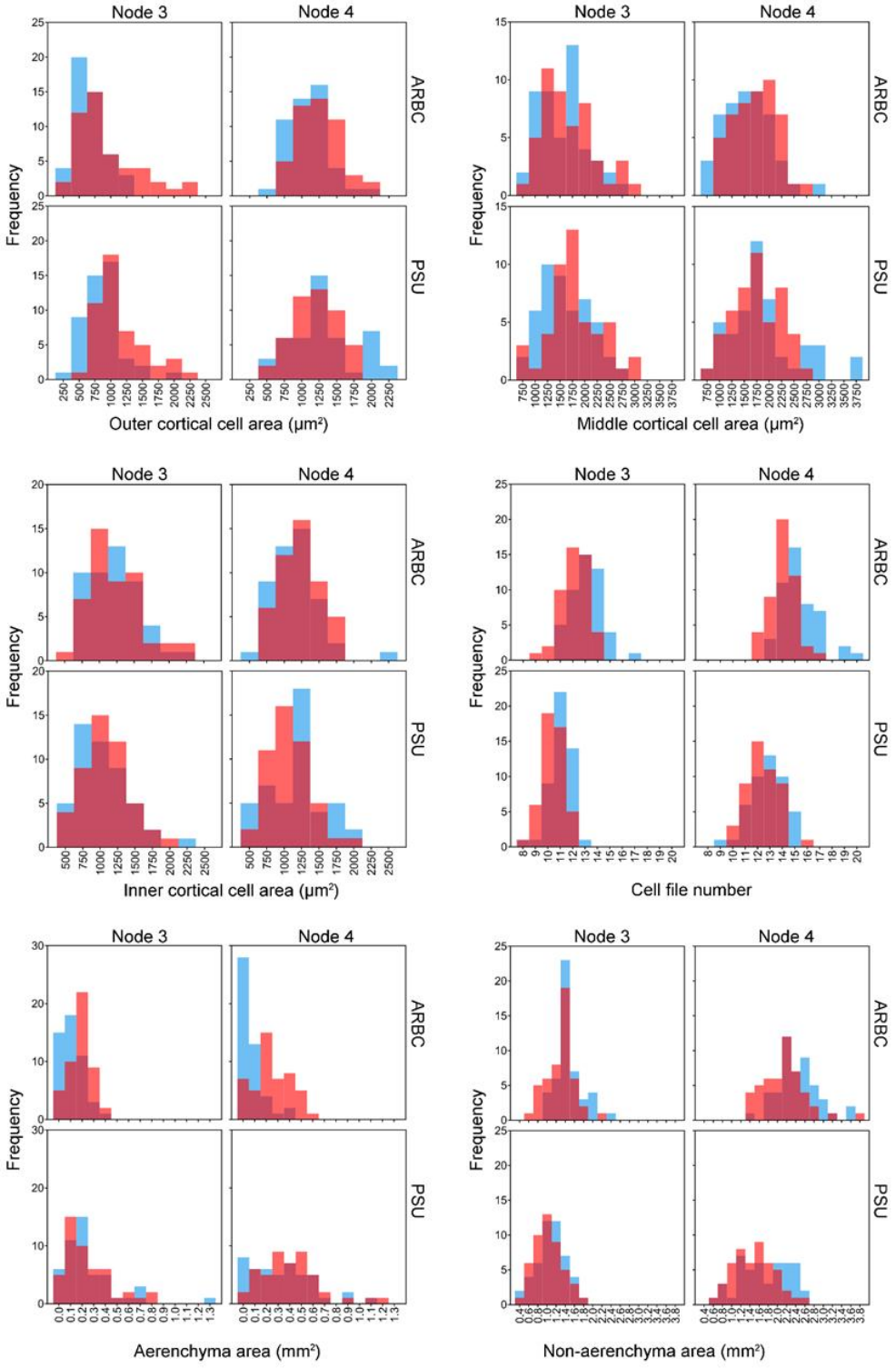

Figure S5.1 – continued (page 2/3).

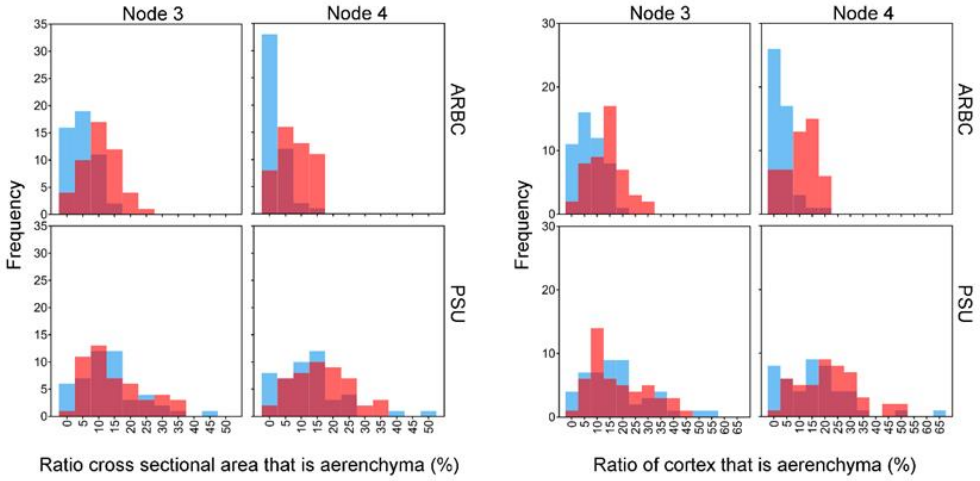

Figure S5.1 – continued (page 3/3).

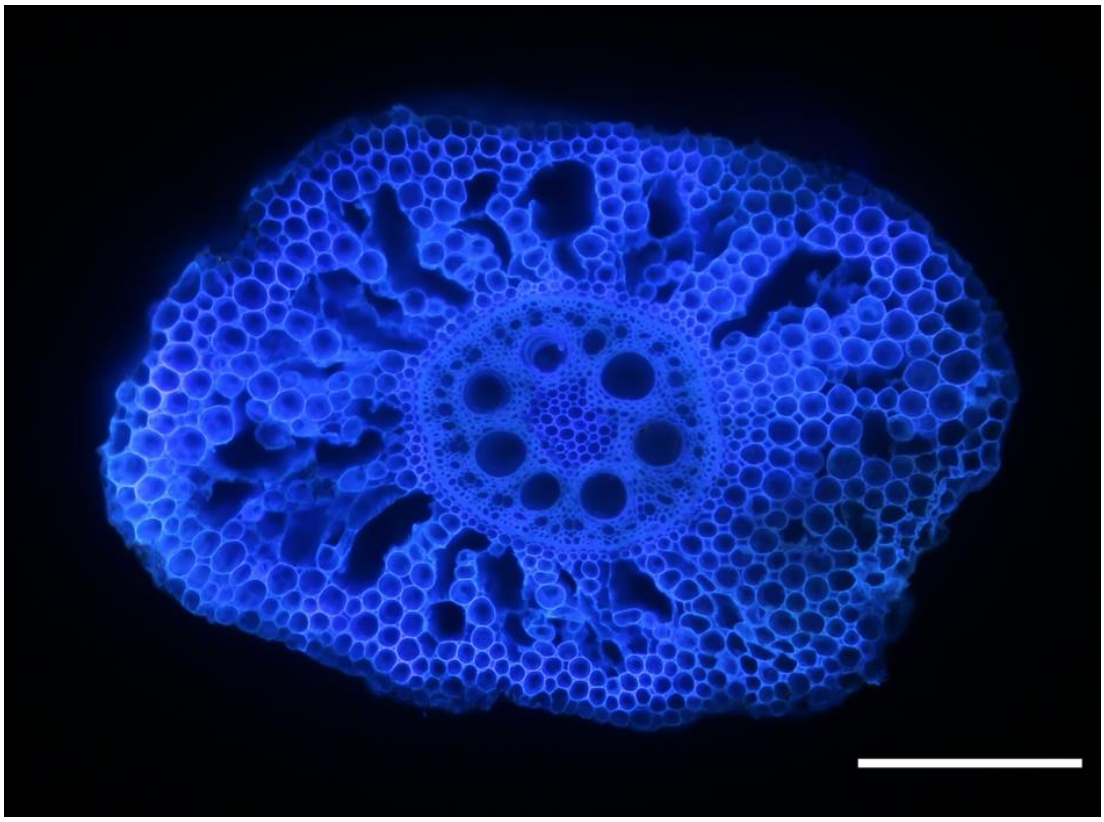

Figure S5.2 - Example of irregularly shaped root section of a root grown under compacted conditions. Root taken from node 3, scale bar at 500 µm.

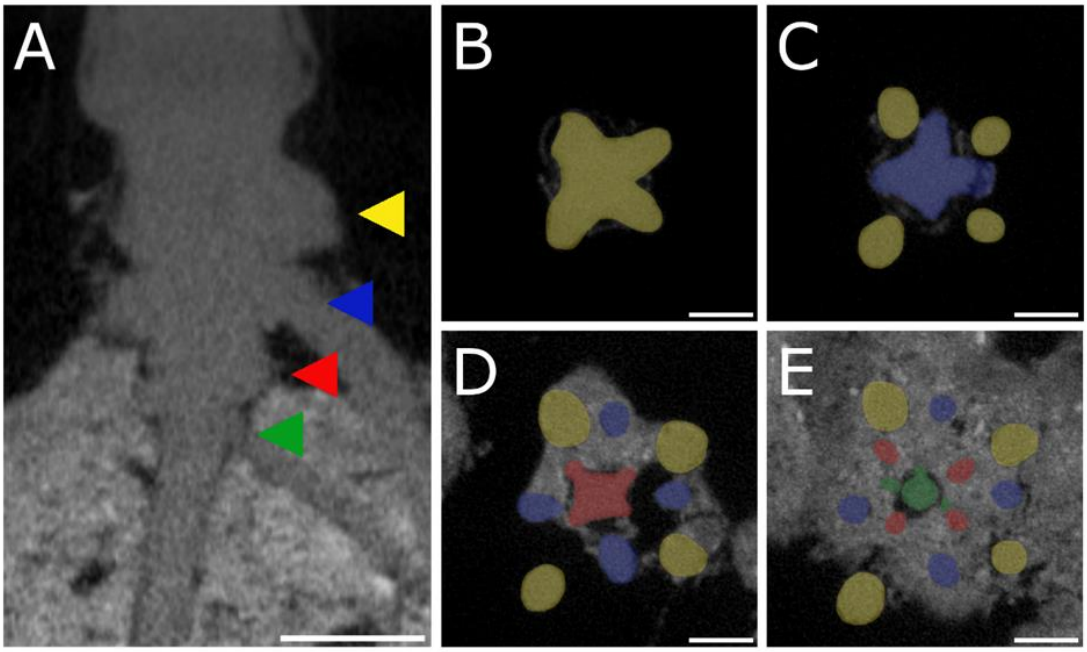

Figure S6.1 - Node identification on 2 dimensional planes during image processing of X-ray CT scans. (A) shows a xy-projection at the root base. (B-E) show different yz-projections moving from the top of the column down. Different nodes are indicated by the different colours (green – node 1, red – node 2, blue – node 3, yellow – node 4). Scale bars are set at 1 cm.

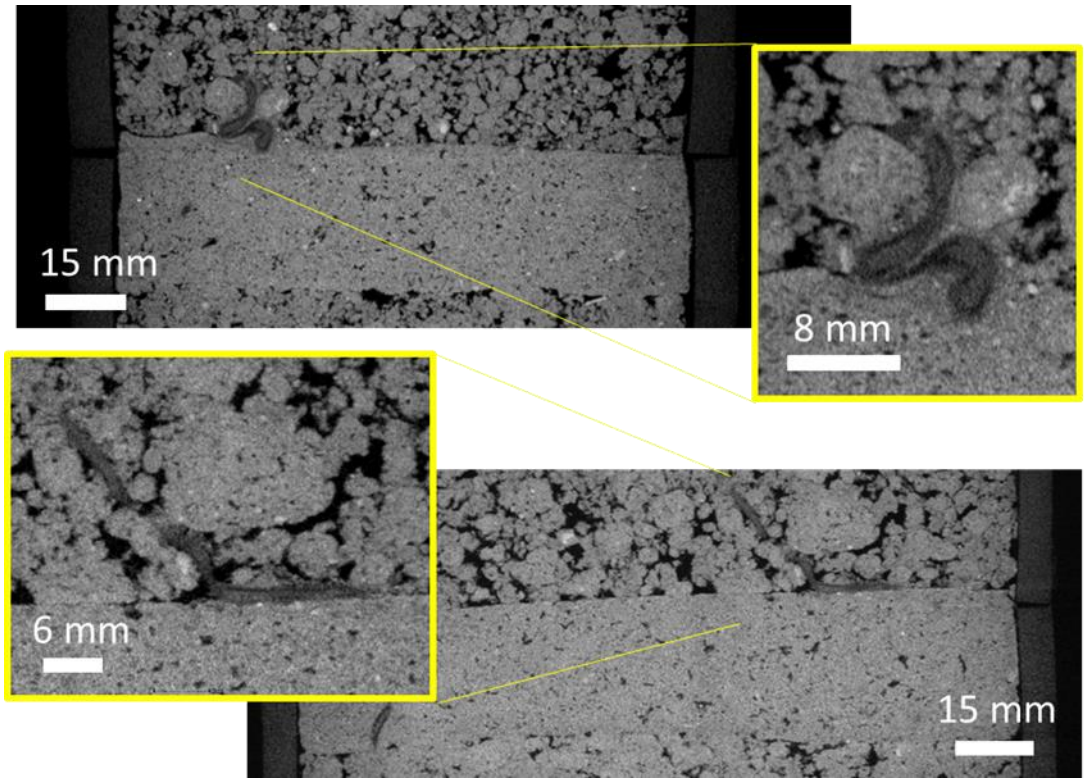

Figure S6.2 - Nodal roots of maize can buckle (top panel) or deflect (bottom panel) when encountering a dense layer

Figure S6.3 -– Root cross-sectional area for both nodes and four genotypes before, within and after the compacted layer. Differences between nodes (capital letters, P ≤ 0.001) and between genotypes within respective nodes (lower case letters, P ≤ 0.05) were calculated by Tukey comparisons. Genotypes indicated by * had a limited amount of sections due to limited amount of roots able to cross the compacted layer. Where no letters are shown, no significant differences were found between nodes or genotypes within nodes.

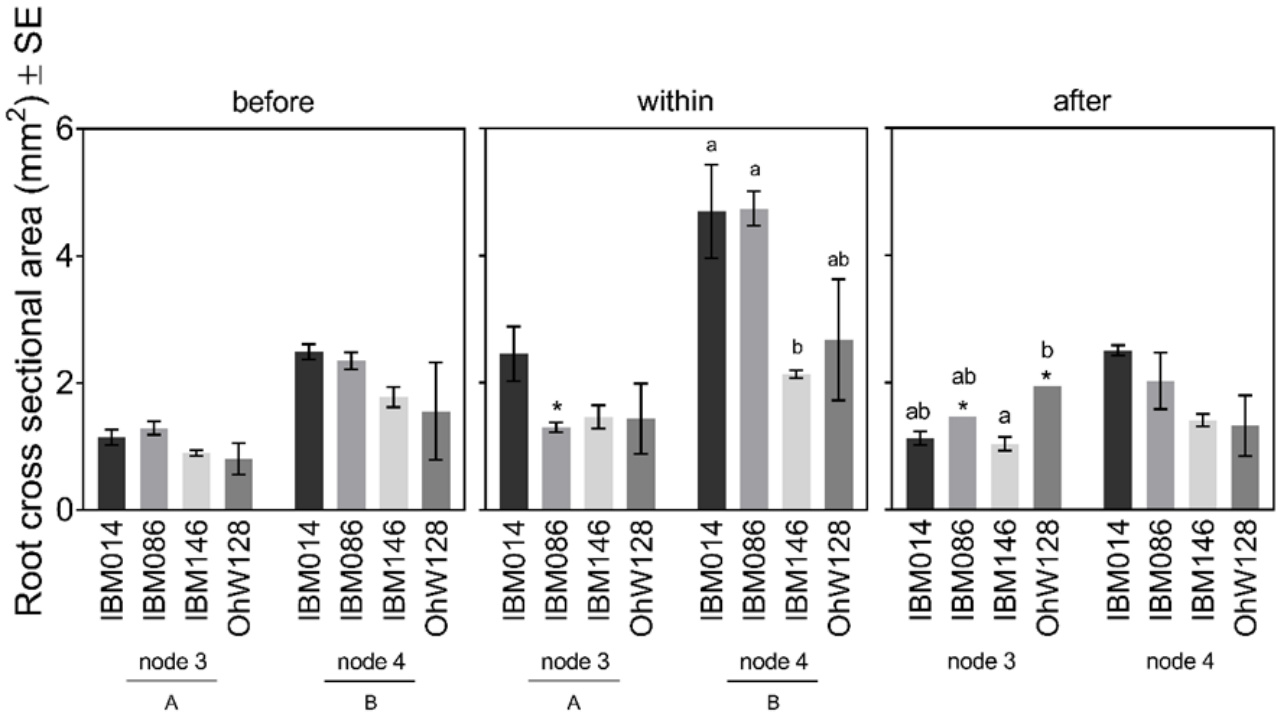

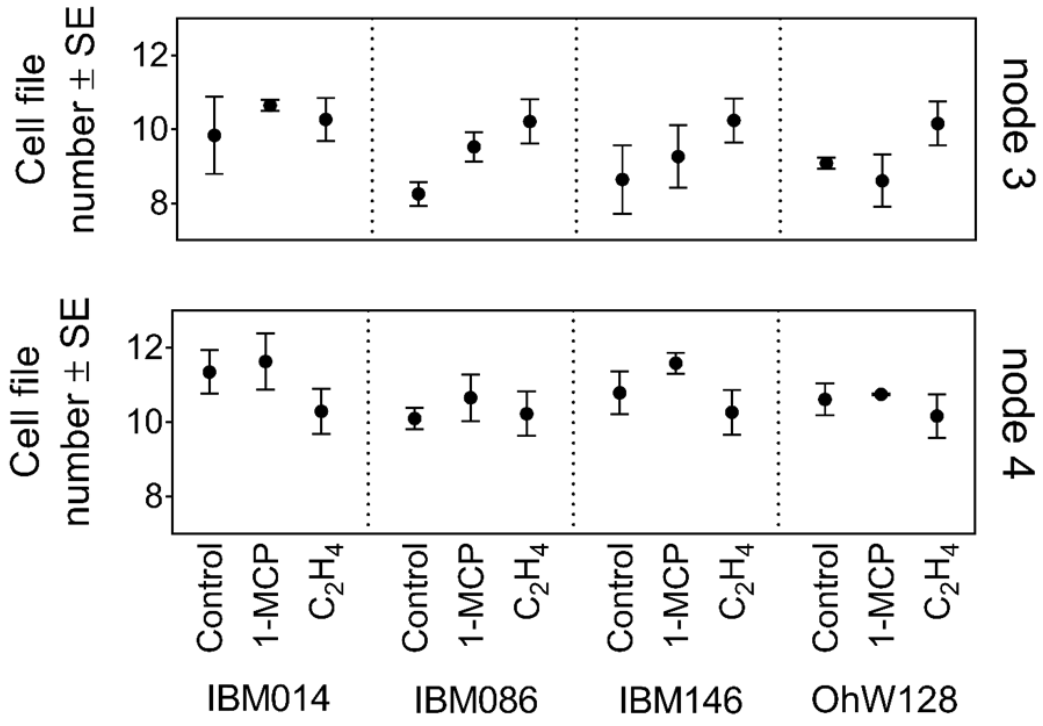

Figure S6.4 - Average cell file number ± SE for different nodes and genotypes under ethylene treatment. No significant differences were found between treatments within each genotype-node combination. For some observations the standard error was so small it could not be visualised.

Supplementary tables

Table S4.1 – Average bulk density ± SE over the soil profile at the two different field sites.

		Compacted	Non-compacted
	Depth	**Average bulk density (g/cm^3)**	**Average bulk density (g/cm^3)**
ARBC	**0-10**	1.65 ± 0.02	1.33 ± 0.03
	10-20	1.70 ± 0.02	1.52 ± 0.02
	20-30	1.66 ± 0.05	1.61 ± 0.02
	30-40	1.53 ± 0.06	1.43 ± 0.05
	40-50	1.48 ± 0.06	1.55 ± 0.10
PSU	**0-10**	1.29 ± 0.05	1.18 ± 0.07
	10-20	1.35 ± 0.02	1.18 ± 0.02
	20-30	1.30 ± 0.05	1.17 ± 0.05
	30-40	1.37 ± 0.04	1.26 ± 0.05
	40-50	1.41 ± 0.05	1.31± 0.08

Table S4.2 – Volumetric moisture content (v/v) with depth for the two different field sites.

	Depth	Compacted	Non-compacted
ARBC	0-10	31.7%	27.5%
	10-20	31.5%	28.4%
	20-30	27.6%	28.5%
	30-40	26.8%	30.6%
	40-50	26.5%	32.1%
PSU	0-10	19.5%	19.0%
	10-20	22.4%	20.9%
	20-30	23.1%	22.2%
	30-40	23.8%	23.1%
	40-50	23.7%	24.1%

Table S4.3 – Field applications during the field season

	Field applications					
	Irrigation		Fertilizers		Pesticides	
ARBC	18/06/2016	0.94 mm	04/06/2016	ProSol (15 gallons/acre)	17/06/2016	Atrazine and S-metolachlor
	21/06/2016	0.60 mm	14/06/2016	ProSol (12.5 gallons/acre)	14/06/2016	Copper, Azoxystrobin and Chlorantraniliprole
	22/06/2016	1.20 mm	15/06/2016	UAN (38.3 lbs/acre)	23/06/2016	Chlorantraniliprole
	23/06/2016	0.32 mm	16/06/2016	ProSol (12.5 gallons/acre)		
	25/06/2016	1.60 mm				
	28/06/2016	0.30 mm				
	04/06/2016	0.24 mm				
	06/06/2016	0.20 mm				
	08/06/2016	0.50 mm				
	10/06/2016	0.72 mm				
	17/06/2016	0.75 mm				
	20/06/2016	0.50 mm				
	24/06/2016	0.50 mm				
	27/06/2016	0.50 mm				
	09/08/2016	0.50 mm				
PSU	*No irrigation applied as moisture content remained stable during growing season*		urea Nitrogen (200 lbs/acre) applied prior to planting		*No pesticides were applied*	

Table S4.4 – F-values of the analysis of covariance for the relationship between D75 and D75c grouped by compaction. Level of significance $p < 0.05$.

$D_{75} \sim D_{75c}$ + Treatment

	ARBC	PSU
Compaction	0.09	3.56
D_{75c}	22.29 *	8.59 *
Compaction x D_{75c}	2.54	2E-03

Table S5.1 – Avergage brace and crown root angle for the twelve tested genoytpes at the two different field sites

		Crown roots		Brace roots	
		Non-compacted	Compacted	Non-compacted	Compacted
	Genotype	Average root angle (°) ± SE	Average root angle (°) ± SE	Average root angle (°) ± SE	Average root angle (°) ± SE
ARBC	IBM014	50 ± 4	43 ± 4	45 ± 4	53 ± 2
	IBM051	47 ± 3	49 ± 2	57 ± 3	48 ± 2
	IBM059	50 ± 3	42 ± 3	45 ± 3	46 ± 3
	IBM086	56 ± 3	49 ± 4	50 ± 2	50 ± 3
	IBM146	57 ± 2	53 ± 3	58 ± 3	53 ± 3
	IBM178	45 ± 3	49 ± 1	48 ± 3	50 ± 2
	IBM284	48 ± 3	48 ± 3	49 ± 2	49 ± 2
	IBM323	45 ± 2	51 ± 3	41 ± 3	49 ± 2
	NyH126	50 ± 3	46 ± 3	42 ± 2	48 ± 3
	OHW119	49 ± 3	54 ± 1	54 ± 3	54 ± 3
	OHW122	51 ± 4	48 ± 1	52 ± 3	55 ± 3
	OHW128	49 ± 3	51 ± 2	49 ± 3	53 ± 2
PSU	IBM014	44 ± 4	45 ± 4	47 ± 5	45 ± 6
	IBM051	54 ± 2	53 ± 3	45 ± 3	51 ± 4
	IBM059	59 ± 3	45 ± 3	34 ± 5	31 ± 3
	IBM086	56 ± 3	48 ± 3	42 ± 3	44 ± 4
	IBM146	49 ± 3	56 ± 4	48 ± 3	48 ± 2
	IBM178	46 ± 3	47 ± 5	45 ± 4	52 ± 8
	IBM284	49 ± 4	50 ± 5	38 ± 5	37 ± 3
	IBM323	55 ± 2	52 ± 4	33 ± 2	37 ± 2
	NyH126	56 ± 4	54 ± 3	47 ± 3	37 ± 2
	OHW119	40 ± 4	50 ± 4	50 ± 3	57 ± 3
	OHW122	39 ± 6	46 ± 5	45 ± 5	61 ± 5
	OHW128	57 ± 2	50 ± 5	43 ± 6	52 ± 11

Table S5.2 - General linear model summary of the effect of factors season, compaction, genotype, node and thickening on rooting depth D_{75} of selected thickening and non-thickening genotypes. *** level of significance at $p \leq 0.001$.

	Estimate	SE	t-value	p-value	
(Intercept)	0.07	0.02	3.47	6.52E-04	***
Field site	-0.03	4.00E-03	-6.86	1.17E-10	***
Compaction treatment	-0.02	4.00E-03	-4.44	1.59E-05	***
Node	-0.01	3.00E-03	-1.50	1.35E-01	
Genotype	2.00E-03	3.00E-03	0.49	6.27E-01	
Thickening	-0.05	0.12	-0.40	6.92E-01	

Table S5.3 – Summary of ANCOVA for the effect of field site, compaction treatment and thickening on rooting depth D_{75}. *** level of significance at $p \leq 0.001$ and * level of significance at $p \leq 0.05$.

	F-value	p-value	
(Intercept)	5288.64	<2.2E-16	***
Field site	84.650	<2.2E-16	***
Compaction treatment	42.76	6.81E-10	***
Thickening	1.30	0.26	
Field site:Compaction Treatment	5.62	0.02	*
Field site:Thickening	5.77	0.02	*
Compaction treatment:Thickening	1.71	0.19	
Field site:Compaction treatment:Thickening	0.76	0.38	

Table S5.4 –Pearson correlations for anatomical traits and D_{75}. *** level of significance at $p \leq 0.001$, ** level of significance at $p \leq 0.01$ and * level of significance at $p \leq 0.05$. (A) for correlations within node 3 and (B) for correlations within node 4. Abbreviations for anatomical traits can be found in Table 5.1.

A

	RXSA	TSA	TCA	TCA/TSA	TCA/RCSA	TSA/RCSA	CF	IN	MID	OUT	AA	AA/TCA	AA/RCSA	nonAA	D75
RXSA	1														
TSA	0.84 **	1													
TCA	0.98 **	0.71 **	1												
TCA/TSA	-0.05	-0.55 **	0.14	1											
TCA/RCSA	-0.09	-0.59 **	0.11	0.97 **	1										
TSA/RCSA	0.09	0.59 **	-0.11	-0.97 **	-1	1									
CF	0.46 **	0.49 **	0.42 **	-0.21 *	-0.21	0.21	1								
IN	0.48 **	0.17	0.55 **	0.43 **	0.41 **	-0.41 **	-0.02	1							
MID	0.45 **	0.05	0.56 **	0.55 **	0.55 **	-0.55 **	-0.24 *	0.77 **	1						
OUT	0.1	-0.29 **	0.24 *	0.67 **	0.65 **	-0.65 **	-0.4 **	0.6 **	0.78 **	1					
AA	0.3 **	0.13	0.34 **	0.12	0.13	-0.13	-0.1	0.18	0.43 **	0.27 *	1				
AA/TCA	-0.03	-0.1	0	0.05	0.08	-0.08	-0.2	0.02	0.25 *	0.19	0.89 **	1			
AA/RCSA	-0.03	-0.13	0.01	0.12	0.15	-0.15	-0.22	0.05	0.28 **	0.23 *	0.9 ***	1 **	1		
nonAA	0.88 **	0.68 **	0.88 **	0.08	0.04	-0.04	0.49 **	0.49 **	0.36 **	0.11	-0.15	-0.45 **	-0.44 **	1	
D75	-0.08	-0.15	-0.05	0.11	0.17	-0.17	-0.4 **	0.01	0.3 *	0.23 *	0.24 *	0.2	0.21 *	-0.17	1

B

	RXSA	TSA	TCA	TCA/TSA	TCA/RCSA	TSA/RCSA	CF	IN	MID	OUT	AA	AA/TCA	AA/RCSA	nonAA	D75
RXSA	1														
TSA	0.88 **	1													
TCA	0.98 **	0.75 **	1												
TCA/TSA	-0.2	-0.61 **	0	1											
TCA/RCSA	-0.19	-0.63 **	0.02	0.97 **	1										
TSA/RCSA	0.19	0.63 **	-0.02	-0.97 **	-1 **	1									
CF	0.55 **	0.57 **	0.49 **	-0.23 *	-0.27	0.27 *	1								
IN	0.57 **	0.29 *	0.65 **	0.32 *	0.33 *	-0.33 *	0.1	1							
MID	0.43 **	0.08	0.56 **	0.5 **	0.54 **	-0.54 **	-0.18	0.79 **	1						
OUT	0.12	-0.21 *	0.26 *	0.66 **	0.65 **	-0.65 **	-0.3 *	0.51 **	0.68 **	1					
AA	0	-0.12	0.06	0.22 *	0.24 *	-0.24 *	-0.22 *	-0.02	0.31 *	0.14	1				
AA/TCA	-0.32 *	-0.34 *	-0.28 *	0.14	0.17	-0.17	-0.41 **	-0.26 *	0.07	0.01	0.88 **	1			
AA/RCSA	-0.33 *	-0.38 **	-0.28 *	0.2	0.23 *	-0.23 *	-0.43 **	-0.24 *	0.11	0.06	0.88 **	1 **	1		
nonAA	0.91 **	0.75 **	0.91 **	-0.08	-0.07	0.07	0.55 **	0.62 **	0.4 **	0.2	-0.35 **	-0.62 **	-0.62 **	1	
D75	-0.22 *	-0.28 *	-0.18	0.11	0.15	-0.15	-0.26 *	-0.12	0.14	0.08	0.28 *	0.33 *	0.33 *	-0.26 *	1

Table S5.5 - Summary of stepwise multiple regression models for node 3. *** level of significance at p ≤ 0.001, ** level of significance at p ≤ 0.01 and * level of significance at p ≤ 0.05.

Multiple linear regression including all preselected traits:
These preselected traits are across tissues (AA, AA/RCSA) and cellular traits (CF, MID, OUT)

Model 1: D_{75} ~ CF + MID + OUT + AA + AA/RCSA

	Estimate	SE	t-value	p-value	
(Intercept)	51.49	13.26	3.88	2.09E-04	***
CF	-3.70	1.00	-3.71	3.75E-04	***
MID	0.01	0.00	1.52	0.13	
OUT	0.00	0.00	-1.12	0.27	
AA	17.38	18.94	0.92	0.36	
AA/RCSA	-18.44	36.10	-0.51	0.61	
Multiple R^2	0.24				
Adjusted R^2	0.19				
p-value	4.85E-03	***			

Stepwise linear regression of model including all preselected traits:

Model 2: D_{75} ~ CF + MID

	Estimate	SE	t-value	p-value	
(Intercept)	43.96	11.36	3.87	2.14E-04	***
CF	-3.13	0.89	-3.52	6.93E-03	***
MID	4.67E-03	2.22E-03	2.10	0.04	*
Multiple R^2	0.20				
Adjusted R^2	0.19				
p-value	6.65E-05	***			

Multiple linear regression including preselected tissue traits:

Model 3: D_{75} ~ AA + AA/RCSA

	Estimate	SE	t-value	p-value	
(Intercept)	13.92	2.33	5.98	5.30E-08	***
AA	15.90	17.24	0.92	0.36	
AA/RCSA	2.28	34.76	0.07	0.95	
Multiple R^2	0.06				
Adjusted R^2	0.03				
p-value	9.16E-02				

Stepwise linear regression of model including preselected tissue traits:

Model 4: D_{75} ~ AA

	Estimate	SE	t-value	p-value	
(Intercept)	13.98	2.09	6.70	2.17E-09	***
AA	16.92	7.59	2.23	2.84E-02	*
Multiple R^2	0.06				
Adjusted R^2	0.04				
p-value	2.84E-02	*			

Multiple linear regression including preselected cellular traits:

Model 5: D_{75} ~ CF + MID + OUT

	Estimate	SE	t-value	p-value	
(Intercept)	48.79	11.85	4.12	8.97E-05	***
CF	-3.58	0.94	-3.79	2.82E-04	***
MID	0.01	3.43E-03	2.40	1.86E-02	*
OUT	-0.01	4.35E-03	-1.36	0.18	
Multiple R^2	0.22				
Adjusted R^2	0.19				
p-value	1.08E-04	***			

Stepwise linear regression of model including preselected cellular traits:

Model 6: D_{75} ~ CF + MID

See model 2 for summary

Table S5.6 - Summary of stepwise multiple regression models for node 3. *** level of significance at p ≤ 0.001, ** level of significance at p ≤ 0.01 and * level of significance at p ≤ 0.05.

Multiple linear regression including all preselected traits:

These preselected traits are across tissues (RCSA, TSA, AA, AA/TCA and AA/RCSA) and just one cellular trait (CF)

Model 1: D_{75} ~ RCSA + TSA + CF + AA + AA/TCA + AA/RCSA + nonAA

	Estimate	SE	t-value	p-value	
(Intercept)	33.46	15.10	2.22	2.96E-02	*
RCSA	-4.73	32.82	-0.14	0.89	
TSA	-15.35	42.22	-0.36	0.72	
CF	-1.06	1.12	-0.95	0.35	
AA	17.25	30.31	0.57	0.57	
AA/TCA	250.59	232.89	1.08	0.29	
AA/RCSA	-326.05	325.73	-1.00	0.32	
nonAA	9.18	30.13	0.31	0.76	
Multiple R^2	0.18				
Adjusted R^2	0.10				
p-value	2.73E-02	*			

Stepwise linear regression of model including all preselected traits:

Model 2: D_{75} ~ TSA + AA/RCSA

	Estimate	SE	t-value	p-value	
(Intercept)	20.11	4.95	4.06	1.09E-04	***
TSA	-9.00	5.18	-1.74	8.61E-02	
AA/TCA	27.46	11.12	2.47	1.56E-02	*
Multiple R^2	0.14				
Adjusted R^2	0.12				
p-value	1.83E-03	**			

Multiple linear regression including preselected tissue traits:

Model 3: D_{75} ~ RCSA + TSA + AA + AA/TCA + AA/RCSA + nonAA

	Estimate	SE	t-value	p-value	
(Intercept)	21.05	7.51	2.80	6.32E-03	**
RCSA	-8.82	32.52	-0.27	0.79	
TSA	-11.41	41.98	-0.27	0.79	
AA	18.23	30.27	0.60	0.55	
AA/TCA	207.08	228.17	0.91	0.37	
AA/RCSA	-256.91	317.24	-0.81	0.42	
nonAA	12.46	29.91	0.42	0.68	
Multiple R^2	0.17				
Adjusted R^2	0.10				
p-value	2.07E-02	*			

Stepwise linear regression of model including preselected tissue traits:

Model 4: D_{75} ~ TSA + AA/RCSA

See model 2 for summary

Multiple linear regression including preselected cellular traits:

Model 5: D_{75} ~ CF

	Estimate	SE	t-value	p-value	
(Intercept)	46.00	11.36	4.05	1.13E-04	***
CF	-2.18	0.87	-2.50	1.44E-02	*
Multiple R^2	0.07				
Adjusted R^2	0.06				
p-value	1.44E-02	*			

Table S6.1 – ANOVA results for anatomical traits. Each table shows all the main effect results regardless of significance, interatction terms were discarded if proven insignificant.

Root cross-sectional area			
Factor	F-value	p-value	
Node	44.51	2.65E-09	***
Genotype	9.90	1.19E-05	***
Sectioning position	23.07	1.08E-08	***
Node:Sectioning position	3.33	4.06E-02	*

Total cortical area			
Factor	F-value	p-value	
Node	29.66	5.15E-07	***
Genotype	9.29	2.30E-05	***
Sectioning position	22.15	1.96E-08	***
Node:Sectioning position	3.44	3.66E-02	*

Total stele area			
Factor	F-value	p-value	
Node	56.62	5.07E-11	***
Genotype	7.57	1.52E-04	***
Sectioning position	12.32	2.01E-05	***

Cell area			
Factor	F-value	p-value	
Node	8.38	4.13E-03	**
Genotype	18.25	1.01E-10	***
Sectioning position	60.64	<2.2E-16	***
Cortical region	36.18	1.69E-14	***
Node:Genotype	4.65	3.50E-03	**
Node:Sectioning postion	5.86	3.27E-03	**
Genotype:Sectioning position	4.13	5.71E-04	***
Sectioning position:Region	2.69	3.16E-02	*
Node:Genotype:Sectioning position	2.64	1.69E-02	*

Cell file number			
Factor	F-value	p-value	
Node	42.81	4.32E-09	***
Genotype	3.32	2.37E-02	*
Sectioning position	1.29	2.82E-01	